Studies on Catalytic Cyclization of 1,6-Diynes *via* Bifunctional Ruthenium Carbene Complexes

二官能性ルテニウムカルベン錯体を活用した **1,6**-ジインの
触媒的環化反応の研究

YAMASHITA Ken

山下　健

2012

Studies on Catalytic Cyclization of 1,6-Diynes *via* Bifunctional Ruthenium Carbene Complexes

二官能性ルテニウムカルベン錯体を活用した 1,6-ジインの触媒的環化反応の研究

Table of Contents

Chapter 1

General Introduction

1. Control of Reactivities of Carbenes by Transition Metal Complexes

The usefulness of carbene species in organic synthesis is originated from their versatile reactivity. In addition, as might be expected for unusual divalent carbon center, carbenes are unstable and highly reactive. A severe drawback that comes with the high reactivity is low chemo- and regio-selectivities in their reactions. Taking an example of insertion of methylene to C–H bond, the reaction is too unselective to find an application in organic synthesis. Methylene species generated from photochemical degradation of diazomethane (**1**) inserts to various C–H bonds at random. In the reaction with cyclohexene, 1-methylcyclohexene (**2**), 2-methylcyclohexene (**3**) and 3-methylcyclohexene (**4**) are formed in an almost statistical ratio of 2:5:5 accompanied by considerable amount of bicyclo[4.1.0]heptane (**5**). The methylene failed to distinguish vinyl, allyl and aliphatic C–H (Scheme 1).[1]

Scheme 1. Unselective C–H insertion of a free carbene.

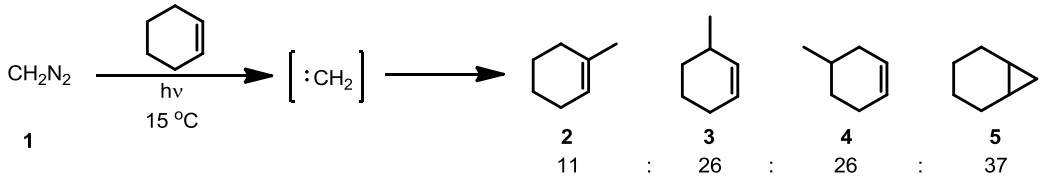

It is true that diazo compounds itself were conveniently used to α,α-substitution, e.g. for the production of α,α-carbonyl compounds. However, abovementioned low regioselectivity was a major obstacle in applying the carbene chemistry for C–C bond formation.

There's no question that the true synthetic value of carbene chemistry became evident in combination with organometallic chemistry. Typically, the combination of diazo ester and a series of dirhodium complexes have converted this concept into tangible form in the realm of viable synthetic applications. For a good example, Davies and co-workers have presented a usefulness of dirhodium complex-catalyzed asymmetric C–H insertion of a carbene for intermolecular C–C bond formation.[2] As the rhodium-catalyzed insertion of the carbene is partially a hydride-abstracting event, the reaction favorably occurs at a position adjacent to a hetero atom which can stabilize a developing positive charge. With a dirhodium complex

Rh_2(*S*-biDOSP)$_2$ (**6**) bearing a proline-derived carboxylate ligand, phenyldiazo acetate and *N*-Boc pyperidine afforded (*R*,*R'*)-(+)-methylphenidate (**7**), which is a well known drug for ADHD, Ritalin, in 86% *ee* (Scheme 2).

Scheme 2. Example of a highly controlled C–H insertion of carbene: chiral rhodium complex-catalyzed asymmetric and regioselective C–H insertion.

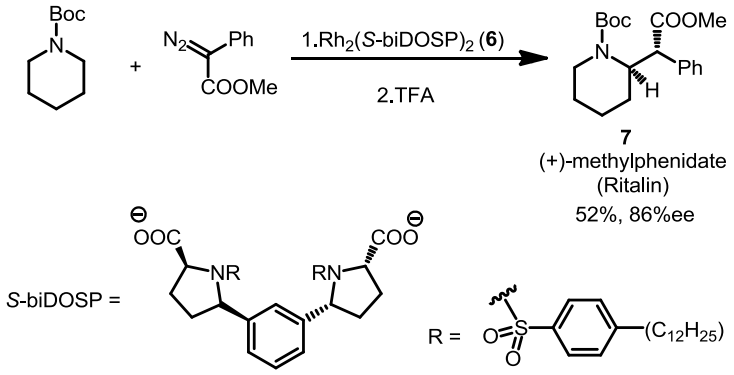

As described above, electronic and steric modulation of the carbene intermediate enabled the control of the regio- and stereo-selectivity. However, the merits derived from the combination of carbene and transition metal catalysts are not limited to these two selectivities. Great advances have been made by investigating the reactivity of isolable carbenoid complexes.

When a heteroatom with a donatable lone pair, typically N or O, is connected to a carbene carbon, the carbene favors triplet electron configuration due to the resonance stabilization. Generally, the carbenes of this class have affinity for low valent but low electron density transition metal centers. In the complex, both σ-electron donation from the carbene carbon to the metal center and π-back donation from the metal center to the carbon constitute the binding. However, the contribution of former is larger, and the π-electron is polarized to the low-energy d-orbital on the metal center.[3] This polarization pattern makes the carbene carbon an electrophilic center (Fischer carbene). Since the first report of the isolation of a Fischer-type carbene complexes, this electrophilic nature has been widely utilized. Most representatively, methoxocarbene complexes can be used as an ester surrogate (Scheme 3).[4]

Scheme 3. Example of a use of Fischer-type methoxocarbene complex as an ester surrogate.

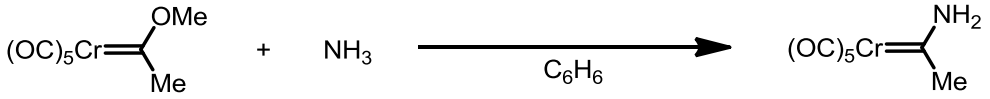

On the other hand, when the carbene species do not possess a stabilizing group, they tend to take triplet electronic state. In general, such triplet carbene species are associated with early transition metal centers with very high oxidation numbers and few valence electrons (typically d^0). In these so-called Schrock carbene complexes, π-electrons are almost equally distributed to the metal center and the carbon. Hence, contrarily to Fischer carbenes, Shcrock carbene complexes tend to exhibit nucleophilicity on the carbon atom.

In addition to these two classes, non-heteroatom stabilized carbenes can bound to low oxidation state transition metals. In general these complexes partially fit the definitions of both classes, and in fact, show border-line reactivity. For instance, Casey and co-workers have prepared an amphiphilic rhenium carbene complex.[5] A tethered alkylidene complex **8** has a low valent Re center and seems to fit the criteria of Fischer-type carbene complex. In fact, trimethylphosphine adds to the carbene carbon. On the other hand, **8** also reacted with Brønsted acid, such as hydrochloric acid, to cleanly afford a Re(III) alkyl complex (Scheme 4).

Scheme 4. Reactions of amphiphilic Re–carbene complex with a nucleophile or an electrophile.

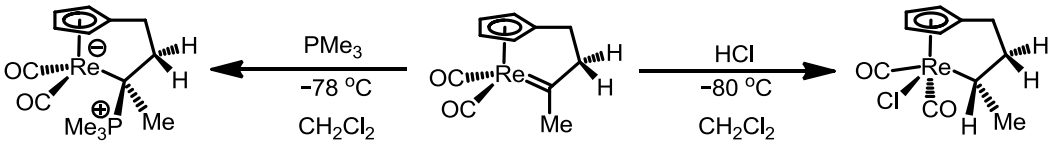

In a carbene complex, various factors could be diversified, which include the central metal, steric and electronic effects of spectator ligands and stabilizing group on the carbene carbon. This enables a tuning of reactivities of carbene complexes. As a result, numerous new reaction

patterns of carbene complexes were invented, and these complexes are no longer simply well-controlled surrogates for free carbenes. One of the best examples of the synthetic applications of the carbene species resulting from the synergy with transition metal complexes can be seen in the chemistry of olefin metathesis.

2. Affinity of Transition Metals for Carbenes

A reactivity common to various sort of carbene complexes is the catalytic activity toward olefin metathesis and related reactions. Although synthetically useful olefin metathesis reactions are performed by using ruthenium alkylidene complexes coordinated by strongly electron-donating ligands (Grubbs' complexes) or molybdenum or tungsten alkylidene complexes modified with imine ligands (Schrock's complex), initial mechanistic studies of the olefin metathesis reactions were performed with *in situ* prepared unknown active species[9b-d] or structurally-well defined Fischer-type complexes[9a].

The prototype of olefin metathesis reaction was reported in 1964 by Banks, Natta and their respective co-workers.[6,7] In Banks' example, heterogeneous catalyst based on $CoO\text{-}MoO_3/Al_2O_3$ was used for the disproportionation of olefins. Natta performed ring opening metathesis polymerization of cyclopentenes with the catalysts $MoCl_6$- or WCl_3-$AlEt_3$. In neither report, reaction mechanism was studied. In the early stage of the olefin metathesis reaction studies, "pairwise mechanism" was favored by those who are concerned (Scheme 5).

Scheme 5. The "pairwise mechanism" proposed for olefin metathesis.

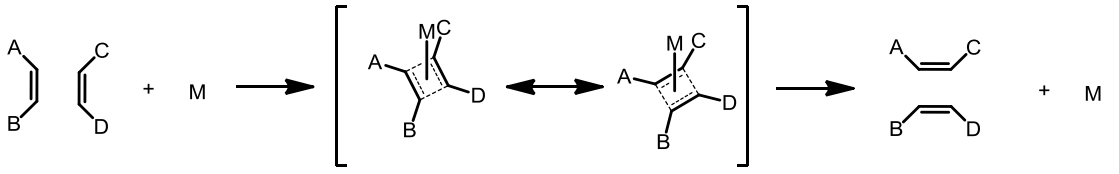

In 1971, Chauvin and co-workers reported a mechanistic elucidation of olefin metathesis, by studying the reaction between cyclopentenes and 2-pentene catalyzed by a homogeneous catalyst prepared from $WOCl_4$, and $Sn(n\text{-}Bu)_4$ or $AlEt_2Cl$. [8] When the combination of these C_5

components were treated under the catalytic condition, in addition to C_9, C_{10} and C_{11} metathesis products, telomerization products triad C_{5n+4}, C_{5n+5}, C_{5n+6} were observed. Almost constant ratios of C_{5n+4} : C_{5n+5} : C_{5n+6} = 1 : 2 : 1 were observed for n = 1 to 4 (Scheme 6). This result indicates that the 2-pentene participates in the telomerization reaction in a same manner as the metathesis reaction, and the telomerization products were not derived from the initial product of the metathesis. This situation means that the alkylidene parts originating from an olefin moiety reside on the metal center. These observations resulted in a establishment of the mechanism of olefin metathesis reaction as "carbene/metallacyclobutane" path, in which [2+2] cycloaddition between the carbene and an alkene, and a following ring opening afford the metathesis product (Chauvin mechanism). This mechanism was later confirmed with additional experiment by other groups.[9]

Scheme 6. Metathesis and telomerization of cyclopentene with 2-pentene.

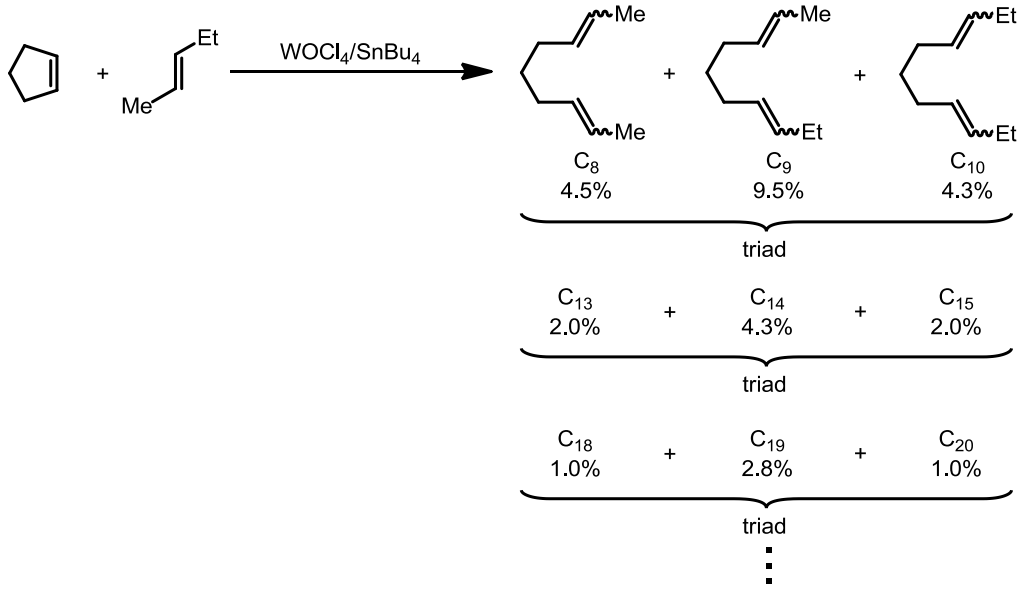

The Chauvin mechanism of olefin metathesis is closely related to transition metal-catalyzed cyclopropanation reactions. Following the [2+2] cycloaddition of the metal-carbene moiety and an olefin component, reductive elimination of the transition metal center will afford a cyclopropane product. Although vast majority of transition metal-catalyzed cyclopropanation reaction reactions[10] and Simons-Smith reaction[11] are thought to proceed through a concerted

carbene transfer mechanism, several Pd- or Ru-catalyzed [12, 13] or Fe–carbene-mediated reactions [14] are proposed to proceed through a step-wise mechanism which involves metallacyclobutane intermediates. In fact, in some cases, metallacyclobutane intermediates were isolated and reveled to afford cyclopropane production as a result of reductive elimination.[15] On the other hand, the ring opening of the metallacyclobutane intermediates *via* the cleavages of C–C and C–metal bond results in the formation of a pair-exchanged olefin and the regeneration of the carbene complex.

The fact that various transition metal carbenoid species are efficiently regenerated in the olefin metathesis reaction suggests that a transition metal center with an appropriate coordination environment shows strong affinity for carbene carbons. This general propensity of transition metal complexes to form carbenoid species is meaningful in terms of catalytic chemistry. This is because, the affinity enables the complexes to generate metal carbenoid species from intrinsically carbenic molecules under a catalytic condition, rather than from precursors that has explicitly carbenic nature such as diazo compounds.

3. Transition Metal-Induced Generation of Carbenic Species from Alkynes and Their Reactivities

The most straightforward method for the generation of metal carbenoid species is the carbene transfer from diazomethane. Transition metal–carbene species produced from diazo compounds are assumed or even isolated as catalytic intermediates. As an intermediate of cyclopropanation reactions of alkene by diazo compounds, ruthenium– or dirhodium–carbene complexes have been isolated.[16] In addition, commercially available Grubbs' catalyst are prepared *via* the substitution of a phosphine ligand in a ruthenium complex [$RuCl_2(PPh_3)_3$] by a benzylidene species transferred from phenyldiazomethane.[17]

Alkynes are frequently used as carbene sources. Originally, terminal alkynes can generate free vinylidene species through a tautomerization. For instance, in the synthesis of an isomer of a sesquiterpene Ptychanolide (**10**), Dreiding has effectively applied an alkynyl ketone cyclization that involves thermally generated vinylidene intermediate **9** (Scheme 7).[18] Although this was a sophisticated methodology for the annulation of five-membered ring, the

thermodynamic inferiority of the vinylidene intermediates makes the reaction condition very harsh (flash pyrolysis, 620 °C).

Scheme 7. Thermal generation of vinylidene intermediate and intramolecular C–H insertion.

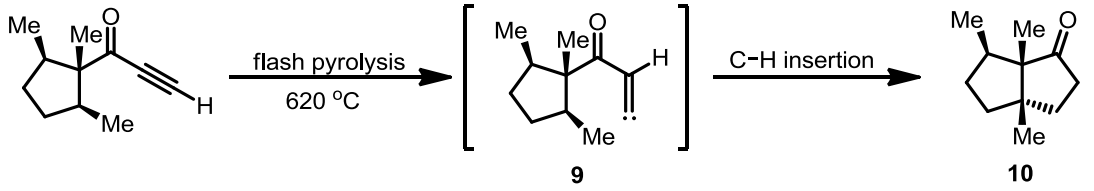

9 **10**

In the presence of an appropriate transition metal complex, formation of a vinylidene equivalent from an alkyne is dramatically eased. In the 1970s, preparations of several η^1-vinylidene complexes were reported. Among them, the first synthesis of a vinylidene complex **11**, albeit in a low yield, from an alkyne precursor was achieved by Antonova and co-workers by using [$CpMn(CO)_2$] as a transition metal component (eq 1, Scheme 8).[19a,b] Following this study, Bruce[19c] and Davison[19d] reported the formation of iron–vinylidene complexes **12** and **13,** and a ruthenium–vinylidene complex **14** from cyclopentadienyliron acetylide or from the combination of terminal alkyne and divalent [CpRu] complex respectively (eq 2 and 3).

Scheme 8. Formation of transition metal–vinylidene complexes from alkynes.

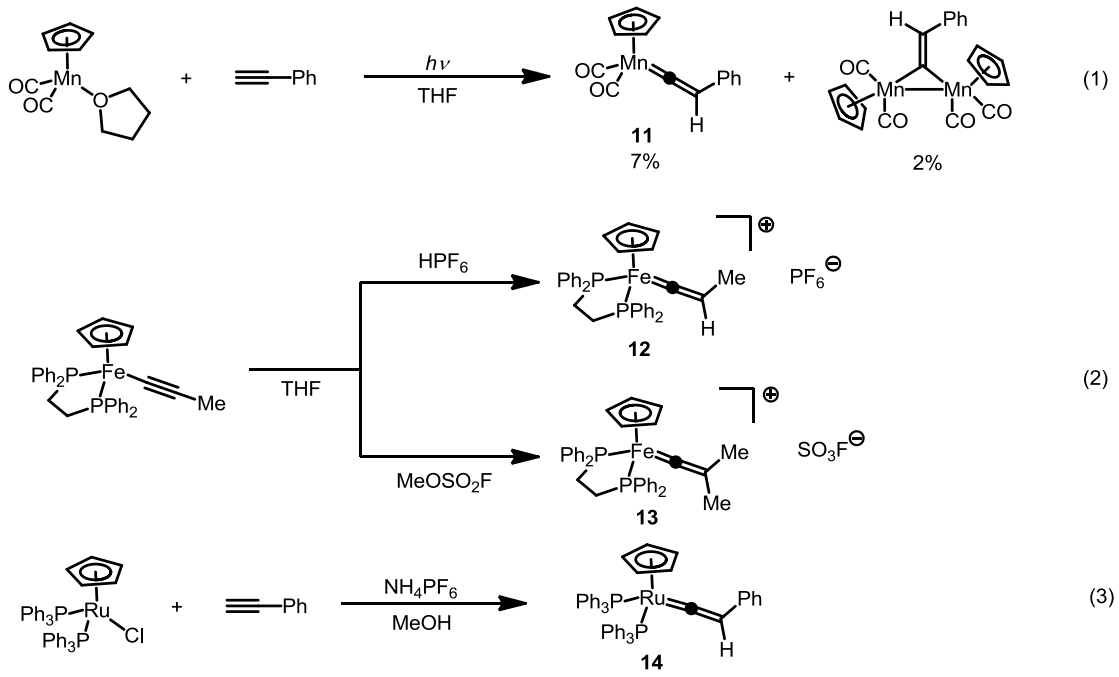

Other than these, η^1-vinylidenes coordinated to group IV–IX metals have been isolated and structurally elucidated.[20]

The pronounced reactivity common to vinylidene complexes is electrophilicity on the α-carbon. For example, aforementioned iron-vinylidene complex **13** accepts hydride on the carbene carbon to form a vinyl complex **15** (Scheme 9).

Scheme 9. Electrophilic reactivity of a vinylidene complex.

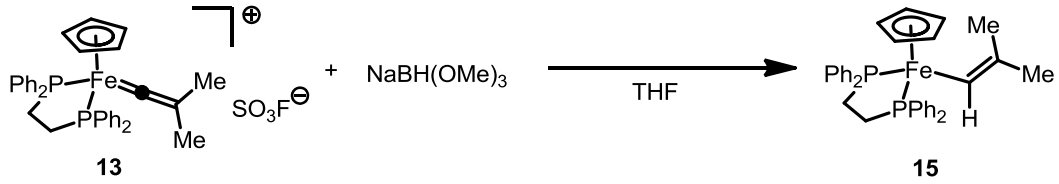

For catalytic applications, vinylidene complexes having a ruthenium or group VI metal center are overwhelmingly important. They are frequently utilized in combination with nucleophiles. Although a broad range of nucleophiles including carbon nucleophiles[21], carbonyl

oxygen[22], epoxides[23], nitrogen nucleophiles[24], thiols[25] and phosphines[26] have been utilized, hydroxylic or carboxylic nucleophiles are well studied.

Dixneuf and co-workers have disclosed that $RuCl_3$ catalyzes the addition of a carboxylic acid to s terminal alkyne in anti-Markovnikov manner (Scheme 10).[27] The reaction mechanism has not been fully elucidated, but intermediacy of vinylidene complex can account for the regioselectivity. The carboxylate anion attacks an electrophilic carbene carbon of the vinylidene intermediate **18**, and following protonation of the vinyl complex and a reductive elimination affords the vinyl ester **16**.

Scheme 10. Ruthenium-catalyzed anti-Markovnikov addition of a carboxylic acid to a terminal alkyne.

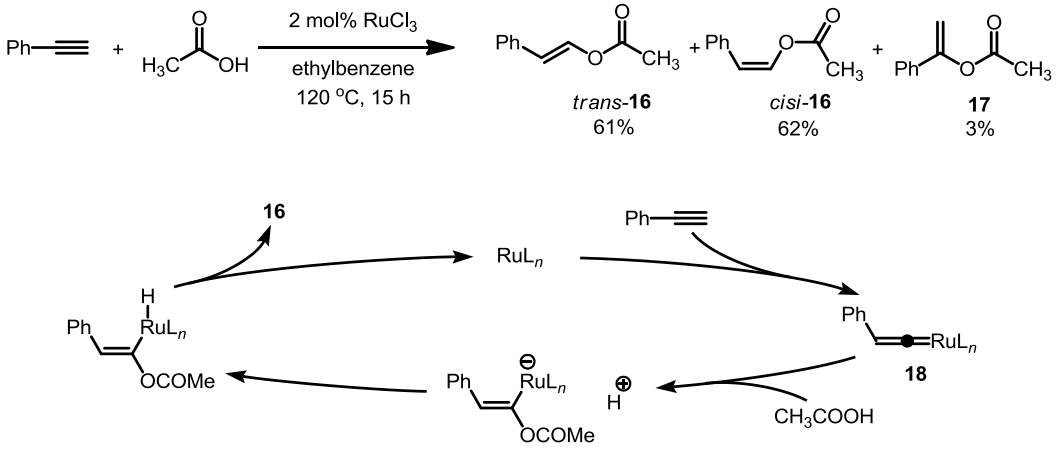

Similarly, hydration of a terminal alkyne takes place to afford an aldehyde product **19** (Scheme 11).[28] Though computationally predicted mechanism is slightly different from the carboxylation reaction,[29] it involves the vinylidene intermediate **20**. **20** was presumed to arise from a vinyl complex *via* α-hydrogen elimination. The vinyl complex is formed through protonation of π-bound alkyne by water. The nucleophilic attack on the carbene carbon gives rise to a vinyl alcohol intermediate. Following tautomerization and reductive elimination produces the aldehyde product **19**.

Scheme 11. Hydration of terminal alkyne *via* a vinylidene intermediate.

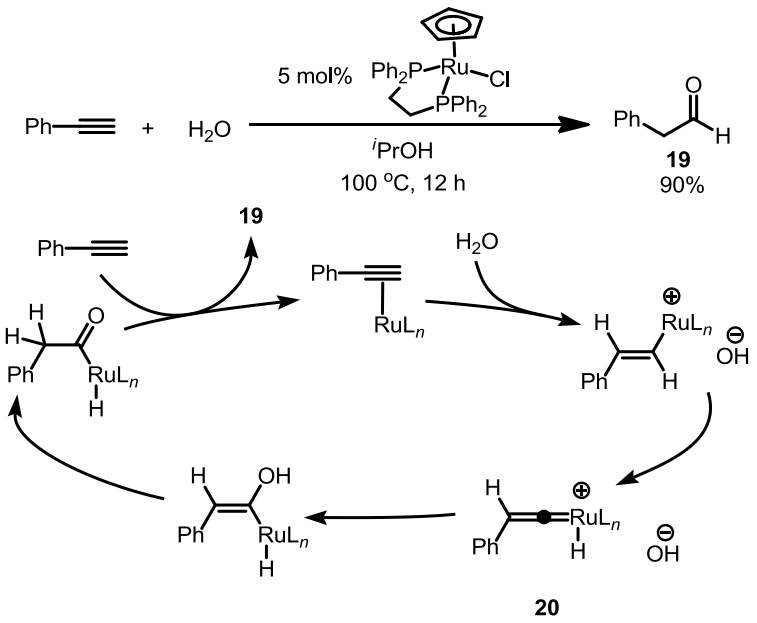

On the other hand, when the vinylidene complexes are treated with alcohol, Fischer-type carbenes are formed (Scheme 12). In an intermolecular reaction with methanol, a ruthenium vinylidene complex **14** is transformed into an alkoxycarbene complex **21** (eq 4).[30] *In situ* generated vinylidene complexes from group VI carbonyl complexes and homopropargyl alcohol undergo *endo*-cyclization to afford tetrahydrofuranylidene complexes **22** and **23** (eq 5).[31] The stability of the Fischer-type complexes is an obstacle to catalytic reaction.

Scheme 12. Formation of Fischer-type carbene complexes *via* the nucleophilic addition of alcohols to vinylidenes.

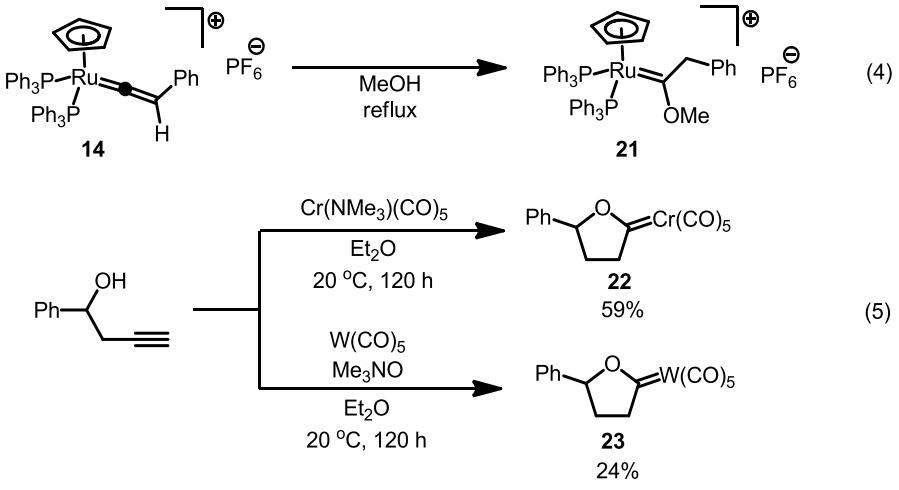

This is in contrast to the reactivity of related class of carbene complexes, the allenylidenes. Nishibayashi *et al.* has developed a series of propargylic substitution reactions catalyzed by thiolate-bridged binuclear ruthenium complex **24** (Scheme 13).[32] In a proposed mechanism the reaction is initiated by the formation of a vinylidene complex **27** from the ruthenium center and a propargyl alcohol **25**, and the following dehydration gives rise to an allenylidene intermediate **28**. In the allenylidene intermediate, α- and γ-carbon has electrophilicity, and β-carbon has nucleophilicity. Nucleophiles preferentially attack on the γ-carbon in this case. Thus-formed vinylidene intermediate **29** is in equilibrium with a η^2-alkyne complex **30**, and ligand exchange with a substrate propargyl alcohol gives the substitution product **26**.

Scheme 13. Propargylic substitution reaction catalyzed by thiolate-bridged binuclear ruthenium complex.

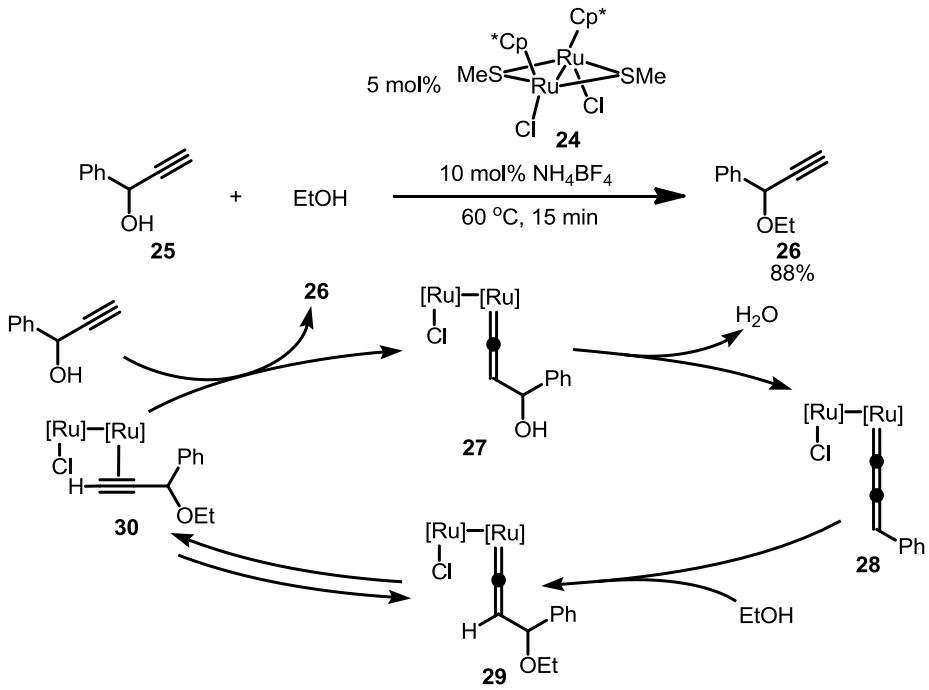

Demetallation from the Fischer-type carbene complexes is expected to promote the catalytic cycle. In the case of the group VI metal complex, molybdenum carbonyl in combination with triethylamine catalyzes the cyclization of the homopropargylic alcohol (Scheme 14). In a putative mechanism, the tertiary amine isomerizes the Fischer carbene complex **32** to a vinyl hydrido complex **33** by deprotonating a methylene adjacent to the carbene carbon. The

following reductive elimination affords the cyclyzed product **31**.

Scheme 14. Endo cyclization of a homopropargyl alcohols catalyzed by $[Mo(CO)_5]$–NEt_3.

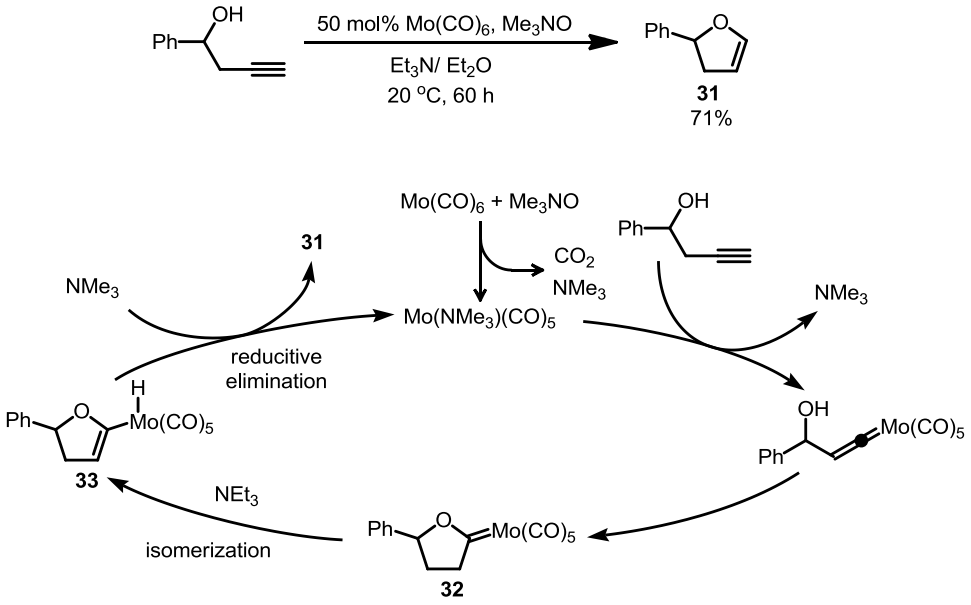

As for CpRu(II) complexes, Trost and co-workers have developed two solutions to avoid a catalytic dead-end (Scheme 15). To quench the carbenic character, the reversal process of the formation of Fischer carbene complex formation may be effective (eq 6). Another feasible strategy is to substitute the transition metal with a species which has a stronger affinity for the carbene carbon (eq 7). In this case, coexistence of electron donating and accepting character (push-pull reactivity) on the incoming group will facilitate the transformation.

Scheme 15. Transformations to impair the stable Fischer-carbene character.

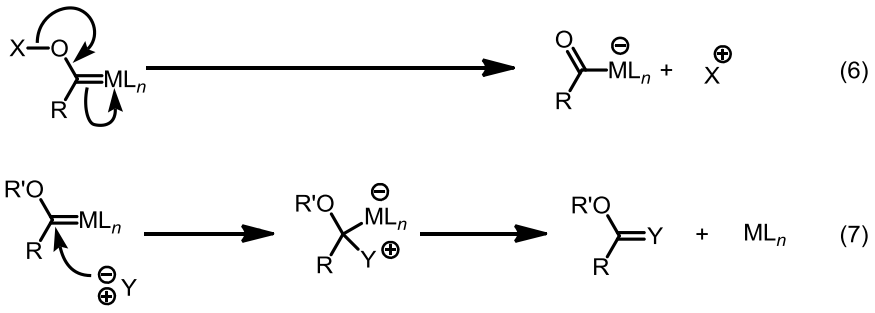

Allyl alcohols could be used to realize the former transformation (Scheme 16).[33] When a terminal alkyne is treated with an excess amount of allyl alcohol in the presence of $CpRuCl(PPh_3)_2$ (**34**), Fischer-type intermediate **36** is formed. Subsequently, C(allyl)−O bond in **36** cleaves to generate an acyl complex. The reductive elimination of π-allyl and acyl units afford a β,γ-unsaturated ketone **35**.

Scheme 16. Ruthenium-catalyzed coupling of a terminal alkyne and an ally alcohol.

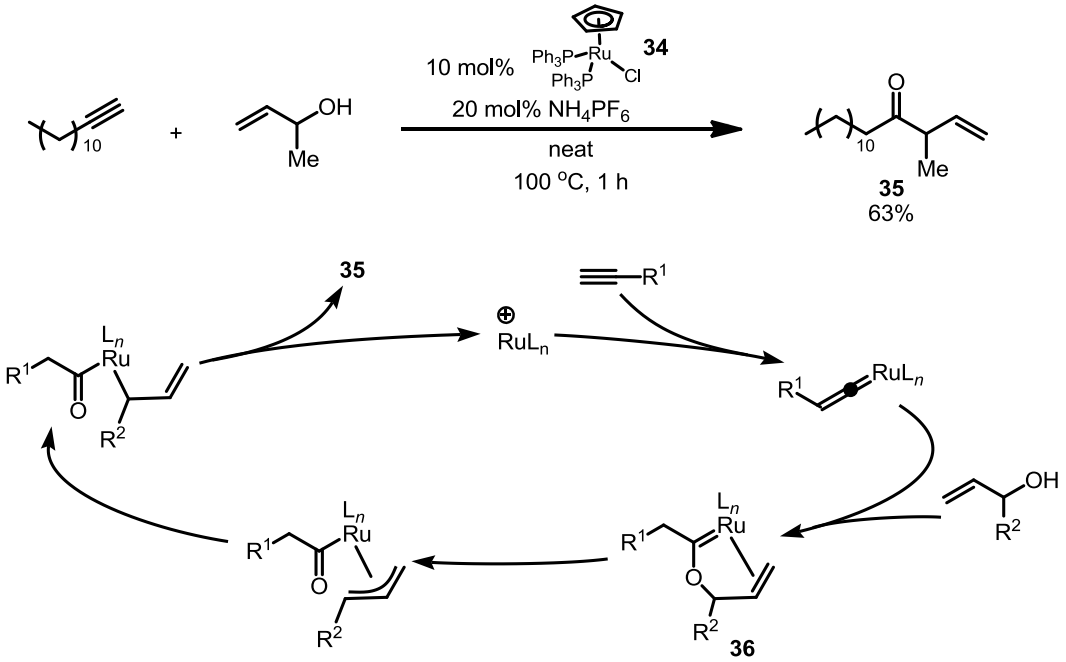

As the strategy depicted in the eq 7 in Scheme 15, oxidative demetallation can be combined with *endo*-cyclization of homopropargyl alcohol **37**. As a result, γ-butyrolactone **39** is formed (Scheme 17).[34]

Scheme 17. Ruthenium-catalyzed *endo*-cyclization of a homopropargyl alcohol and oxidation by *N*-hydroxysuccinimide to produce a γ-butyrolactone.

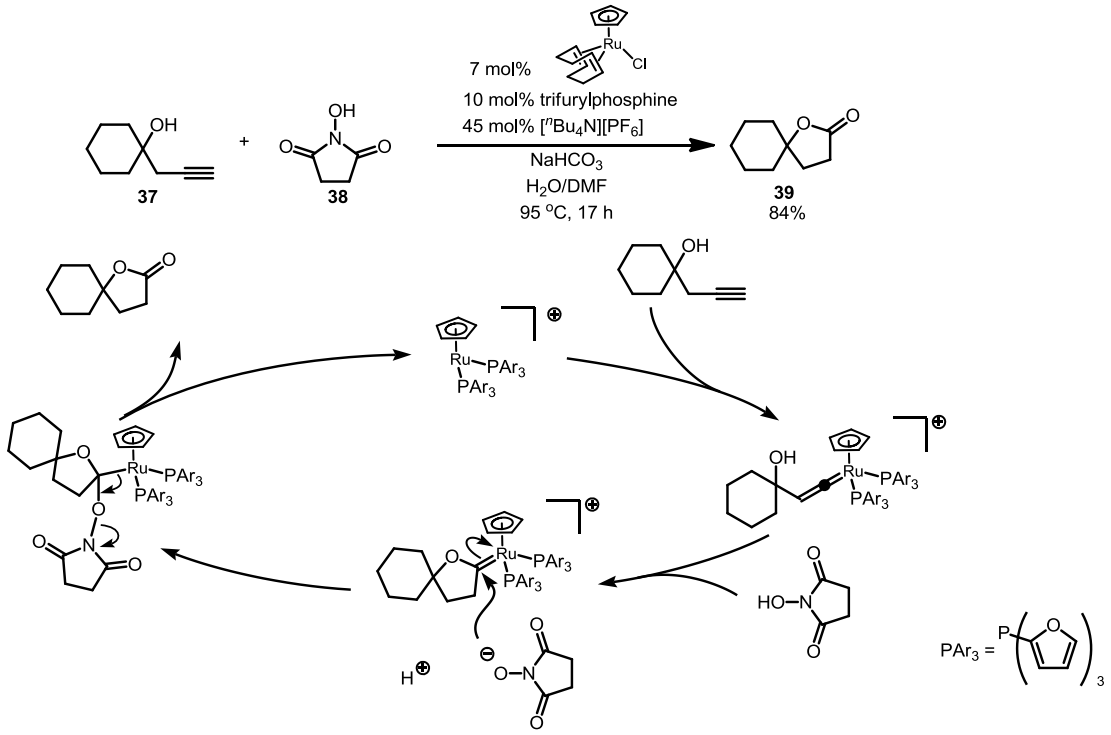

In this case, *N*-hydroxysuccinimide (**38**) acts as both electron donor and accepter. This reactivity is same as that of dimethylsulfoxide (DMSO) in Kornblum-type oxidations.[35] In fact, DMSO has been used as an oxidizing agent toward an electrophilic carbene complex (Scheme 18).[36] However, catalytic reaction that proceeds through oxidation of carbene intermediate is quite rare.

Scheme 18. Oxidation of a Fischer-type carbene by dimethylsulfoxide.

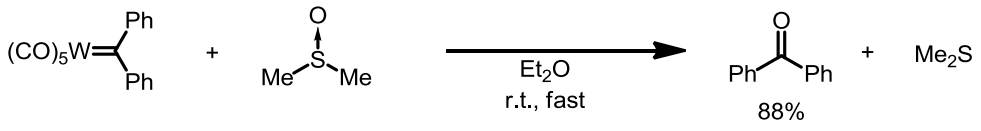

The linear unsaturated carbenes such as vinylidenes or allenylidenes are monofunctional carbene species. Meanwhile, activation of an alkyne moiety leading to a bifunctional carbene-like species is also possible. When two electron pairs of an alkyne localize on each carbons, biscarbenic character appears (Scheme 19). If a transition metal complex has a high affinity for a carbene species, an active species which serves as 1,2-biscarbene synthon **40** is expected be formed.

Scheme 19. Virtual biscarbenic nature of alkyne induced by a transition metal complex.

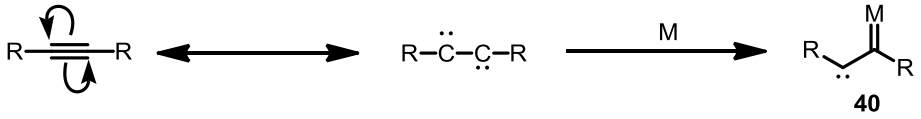

Activation of alkynes in this manner was achieved by using Ru, Pd, Pt or Au. In many cases, the generated carbenes was trapped by alkenes intramolecularly or intermolecularly.

In a mechanistic study of a palladium-catalyze cycloisomerization of enynes, Trost and co-workers found that a divalent palladium complex promotes the intramolecular cyclopropanation between an alkyne carbon and olefin moiety of a dienyne (Scheme 20).[37] The supposed palladium vinylalkylidene complex **41** was trapped by an external alkene to form a cyclopentene **42**.

Scheme 20. Palladium catalyzed intramolecular cyclopropanation.

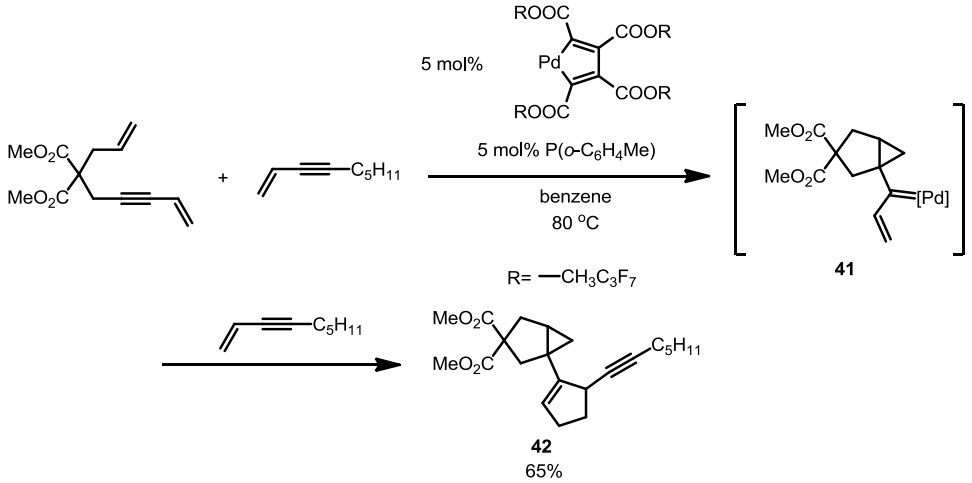

Even more impressive avatar of the 1,2-biscarbenic character of transition metal-activated alkyne was exhibited by Murai and co-workers (Scheme 21).[38] In their work, divalent ruthenium complex activates an alkyne moiety, and not only the first intermediate, but also the second intermediate was captured by olefins to afford the double cyclopropanation product **43**.

Scheme 21. Ruthenium-catalyzed double cyclopropanation of dienynes.

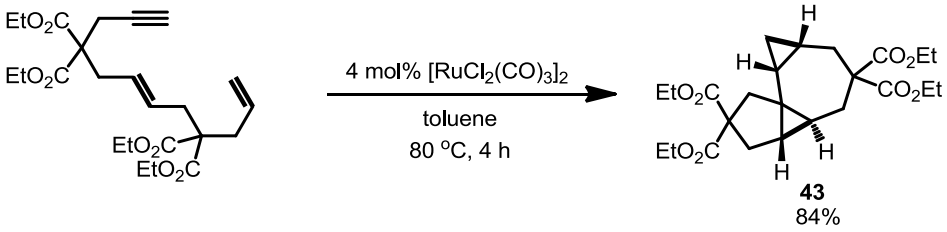

The transition metal-induced biscarbenic species enables synthetically useful transformations. In recent years, gold complexes are frequently used as soft and carbophilic Lewis acid. Hashmi and co-workers has developed a gold-catalyzed phenol synthesis from an alkynyl furan **44** (Scheme 22). The reaction starts with a cyclopropanation of furane by the gold-activated alkyne to generate **46**. A gold–carbene species **47** is assumed as an intermediate, and following electrocyclization afford the phenol product **45**.

Scheme 22. Gold-catalyzed phenyl synthesis form alkynyl furans.

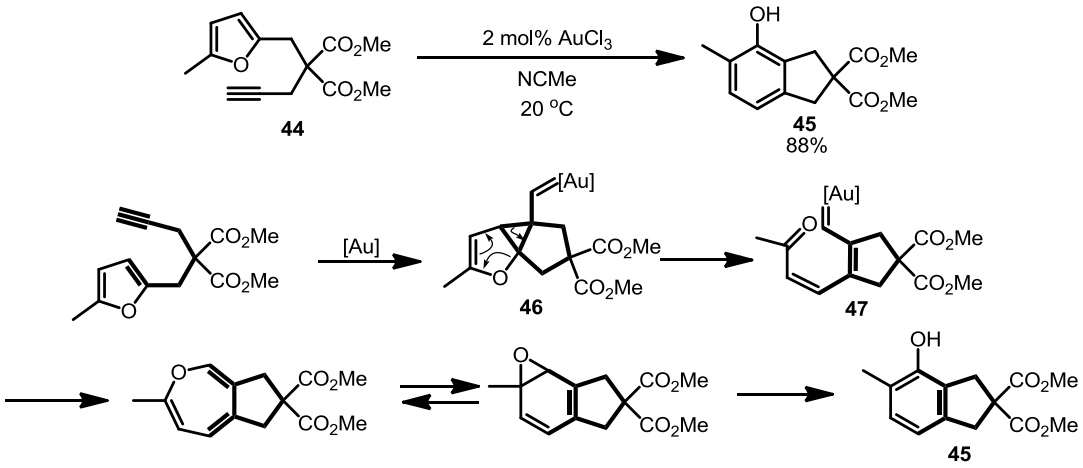

The nature of the Au−carbene species is investigated by Fürstner, Toste and their co-worker.[39] It was strongly advocated that the real picture of the transition metal-induced manifestation of carbene-like reactivity on an alkyne is different from the illustration in Scheme 19. The formation of cyclopropyl gold carbene intermediate was suggested to proceed through an ionic and stepwise mechanism (eq 8, Scheme 23) rather than a classical concerted mechanism. In this sequence, in analogy with transition metal catalyzed nucleophilic addition to alkenes,[40] the slippage of gold atom along the alkyne is the key step in the activation of the alkyne.[39a]

The special case of the activation of alkynes by carbophilic Lewis acid is envisioned when two alkynes are simultaneously activated on a transition metal center in a similar fashion. When adequate electron back-donating ability exists on the transition metal center, formation of a five-membered metallacycle is expected (eq 9).

Scheme 23. Activation of alkynes by through a slippage of transition metal along the C–C bond.

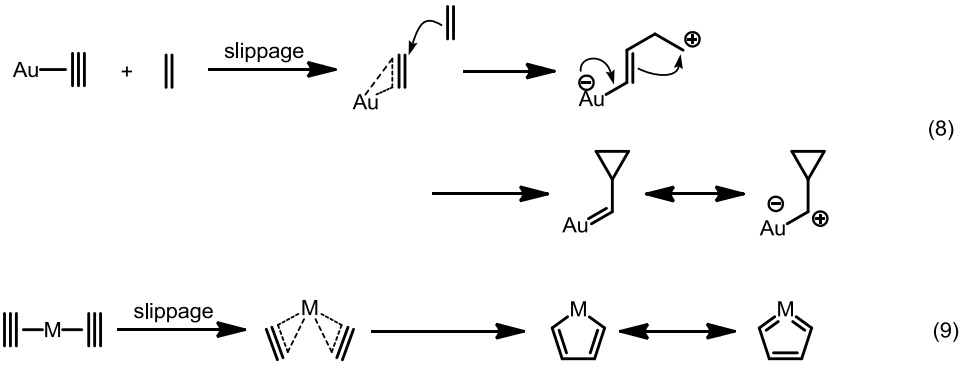

4. Ruthenacyclopentatrienes

Singleton and co-workers have discovered that a half sandwich complex of a divalent ruthenium CpRuBr(cod) (**49**) and two monoynes undergo oxidative cyclization (Scheme 24).[41] In the newly formed ruthenacycle complex **50**, Ru–C was 1.94 Å, which was close to the bond length of ruthenium alkylidene double bonds (1.83–1.91 Å). In addition, in ^{13}C NMR spectrum, the resonance corresponding to α-carbon appeared unusually low δ = 271.1 ppm, suggestive of a strong ring current of the ruthenacycle. These facts indicate that the resonance structure **50b**

rather than **50a** has greater contribution to the property of the ruthenacycle. So, the produced ruthenacycle is best described as a ruthenacyclopentatriene.

Scheme 24. Oxidative cycloaddition of a [CpRuBr] fragment and two alkynes.

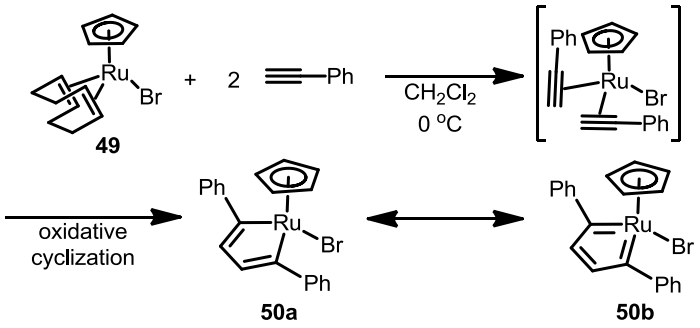

Direct evidence of the carbenic nature of the Ru–C bond in the ruthenacyclopentatriene was discovered, i.e. the two α-carbons served as carbene sources for double cyclopropanation (Table 1).[42] In the presence of Cp*RuCl(cod) (**51a**), when a 1,6-diyne was treated with norbornene, a small amount of tandem cyclopropanation product **55** was detected besides a [2+2+2] cycloaddition product **54** (entry 1). Interestingly the ratio of both products switched almost completely when the Cp analogue **51h** was used (entry 2). An η^5-indenyl complex (Ind)RuCl(PPh_3)$_2$ (**52**) exhibited higher selectivity for the cyclopropanation. This tendency is attributed to the indenyl or Cp ligands' increased propensity for $\eta^5 \rightarrow \eta^3$ haptotropic shift. The ring slippage and the resultant decreased electron donation is supposed to help the ruthenacyclopentatriene intermediate to sustain the carbenic character by adhering to 18-electron rule on the occasion of incorporating the alkene substrate.

Table 1. [Cp'RuCl]-catalyzed double cyclopropanation reaction of diynes and norbornenes.

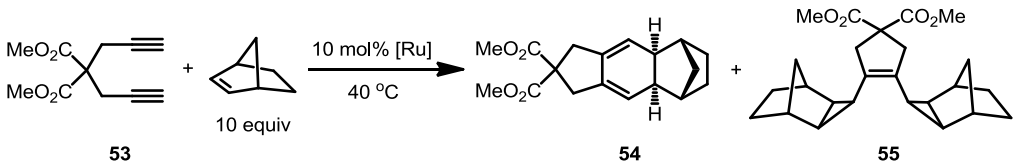

entry	[Ru]	solvent	time [h]	**54** yield [%]	**55** yield [%]
1	Cp*RuCl(cod) (**51a**)	CH_2Cl_2 (reflux)	17	47	15
2	CpRuCl(cod) (**51h**)	CH_2Cl_2 (reflux)	72	10	47
3	IndRuCl(PPh_3)$_2$ (**52**)	$ClCH_2CH_2Cl$	24	10	78

The applications of the ruthenacyclopentatrienes has been extensively studied by multiple groups and applied for useful catalytic reactions. Among them, Yamamoto and co-workers has developed a series of catalytic [2+2+2] cycloaddition reactions between diynes and carbon–carbon or carbon–hetero atom unsaturated compounds that afford six-membered carbo- or hetero-cycles (Scheme 25). In combination with alkenes or alkynes, diynes afford 1,2-cyclohexadienes or arenes. In the presence of nitriles or isocyanates, pyridines or pyridones are formed. The catalytic system is tolerable toward sulfur-containing compounds, and also incorporates isothiocyanate or sulfur disulfide.

Scheme 25. [Cp*RuCl]-catalyzed [2+2+2] cycloaddition of a diyne and various unsaturated substrates.

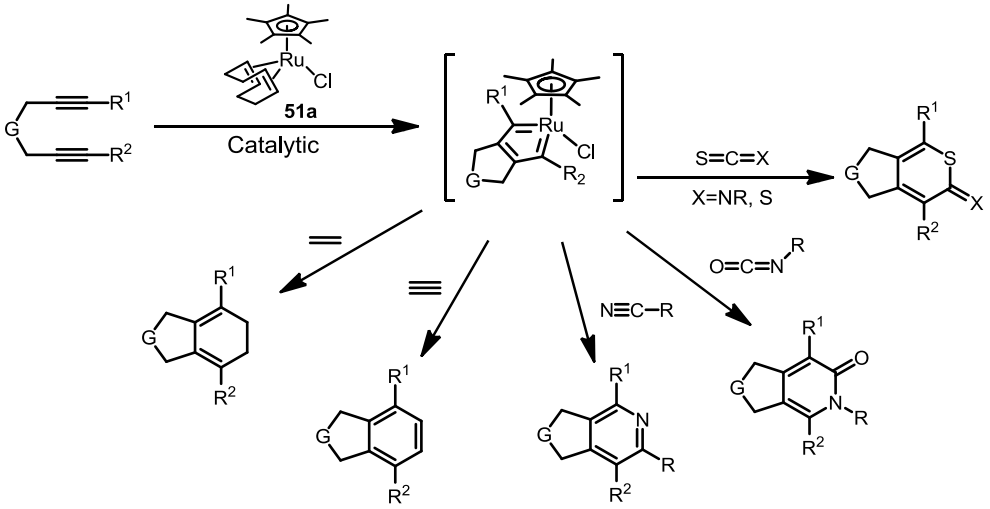

With regard to cyclotrimerization of alkynes, it was found that in the presence of 1 mol% of Cp*RuCl(cod) (**51a**), an dissymmetric diyne and terminal monoyne underwent [2+2+2] cycloaddition to afford arene products in favor of *meta*-**56** in a good yield and regioselectivity (Scheme 26).[43]

Scheme 26. [Cp*RuCl]-catalyzed [2+2+2] cycloaddition between a diyne and monoyne.

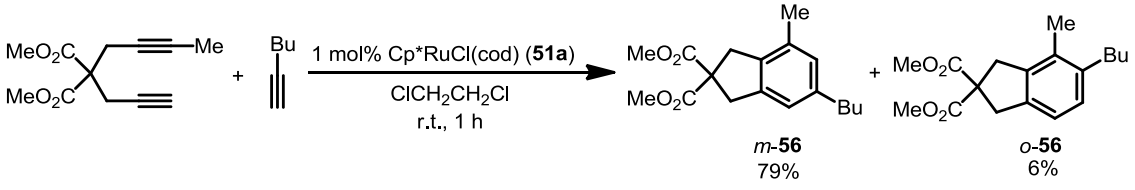

Since the pioneering work by Reppe,[44] various transition metal complexes have been used for cyclotrimerization of alkynes. Except for stepwise ring-closing metathesis strategy,[45] most of transition metal-catalyzed cyclotrimerization reactions involve five-membered metallacycles. Most commonly, the five-membered metallacycle intermediates are considered as metallacyclopentadienes rather than metallacyclopentatrienes, and the incorporation of the third alkyne component is thought to take place as a direct insertion to a metal–carbon bond (path A, Scheme 27) or Diels–Alder-type [4+2] cycloaddition (Scheme 27).[46] For example, in the case of group IX metal-catalyzed cycloisomerization, a series of DFT studies imply that the reactions precede through the path A.[47]

Scheme 27. Three possible mechanisms for the incorporation of the third alkyne component by metallacycle intermediates in alkyne cyclotrimerization reaction.

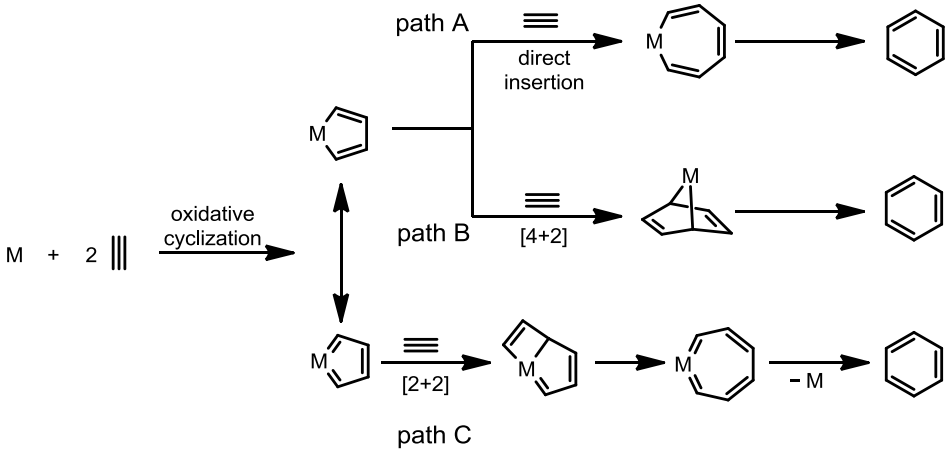

On the other hand, as might be expected for carbene complexes, the incorporation of the third alkyne by the ruthenacyclopentatrienes takes place as [2+2] cycloaddition and following ring expansion (path C), which is a key step in enyne metathesis. Yamamoto and Kirchner independently confirmed the feasibility of this mechanism by means of DFT calculation.[48] It was found that an isolable bicyclic ruthenacyclopentatriene complex **58** could be obtained from the complex Cp*RuCl(cod) (**51a**) and a α,ω-diyne **57** bearing phenyl substituents on both terminals. Thus obtained **58** was fully characterized by spectroscopies and X-ray crystallography.[48a] The complex reacted with acetylene (1 atm) to afford a [2+2+2]

cycloaddition product **59** (Scheme 28).[48a] With this results, the intermediacy of the ruthenacyclopentatriene in the catalytic cycle was established.

Scheme 28. Formation of an isolable bicyclic ruthenacyclopentatriene and its reaction with acetylene.

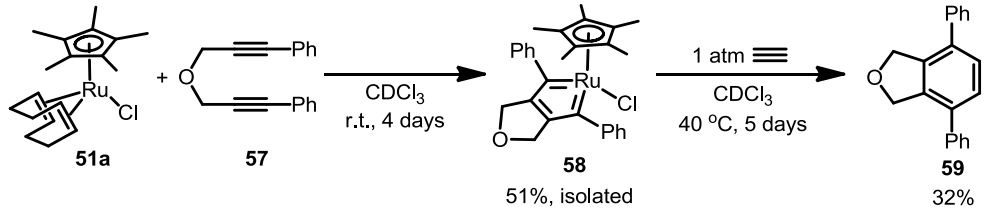

In a simplified model (Scheme 29), DFT study revealed that the oxidative cyclization of the two alkynes and the divalent ruthenium center is the rate-limiting step (**TS-AB**). After the formation of the ruthenacyclopentatriene intermediate, the [2+2] cycloaddition of third alkyne component and the Ru–C double bond occurred with no barrier (**TS-CD**), and the Diels-Alder-type [4+2] transition state was energetically unfavorable (**TS-CE**).

Scheme 29. Computational model of ruthenium-catalyzed cycloaddition of alkynes.

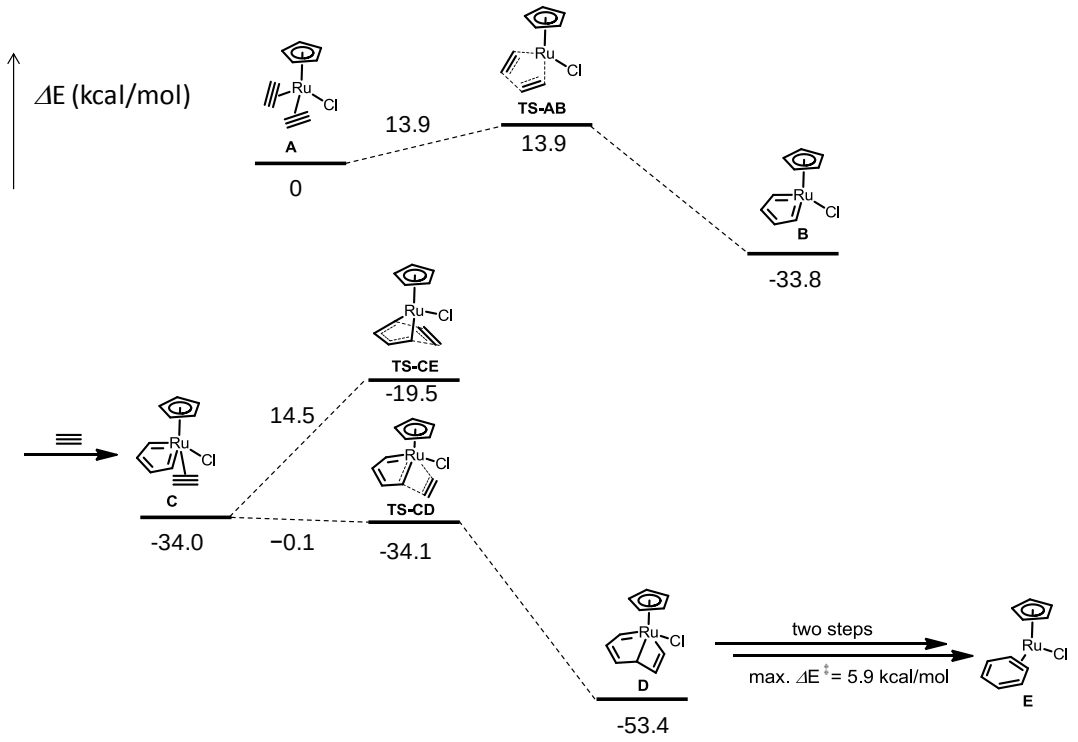

One of the important features of the ruthenium-catalyzed [2+2+2] cycloaddition reaction is its functional group tolerability. The reaction tolerates functional groups such as esters, ketones, acetals, amines and amides (Scheme 30).

Scheme 30. [Cp*RuCl]-catalyzed [2+2+2] cycloadditions of hexyne and diynes bearing various functional groups.

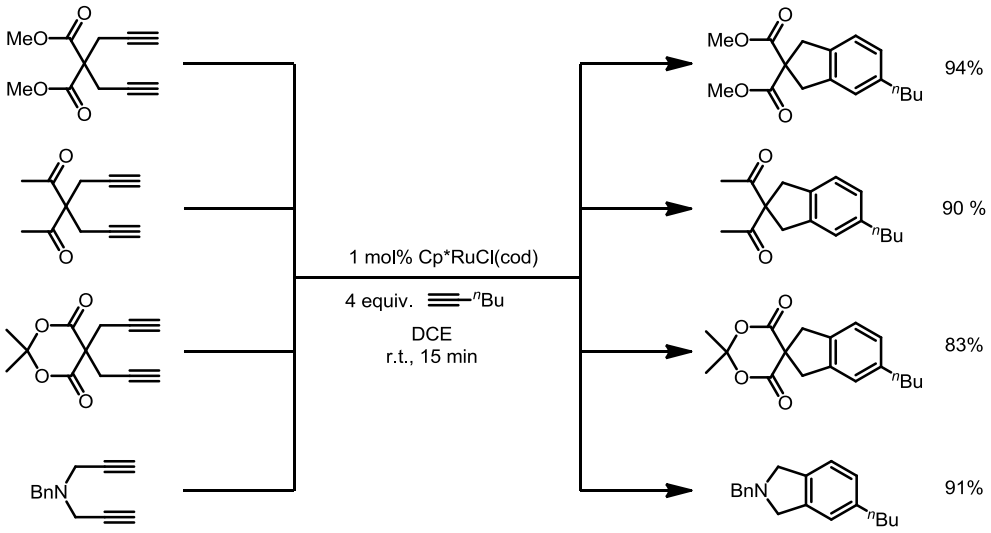

Most impressively, diynes with C^{sp}–I bonds, which is vulnerable to oxidative addition of low valent transition metal complexes[49], can be used as substrate to afford *p*-diiodobenzenes **61a-e** (Scheme 31).

Scheme 31. [Cp*RuCl]-catalyzed [2+2+2] cycloaddition reactions employing diiodoalkynes.

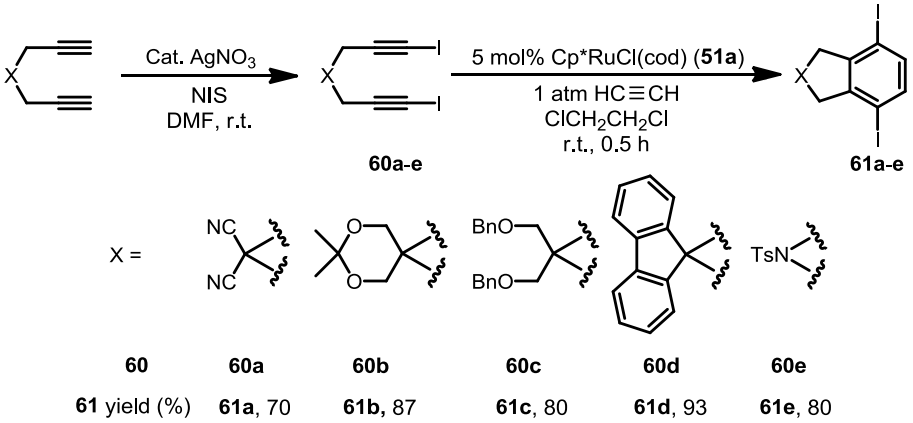

Halobenzenes, including iodobenzenes, are preferable substrates for a series of palladium-catalyzed cross coupling processes, and are useful building blocks in organic synthesis. In addition, the tolerability of the [Cp*RuCl] toward he C^{sp}–halogen compounds are effectively utilized for the synthesis of marine-derived chlorinated natural compounds sporolide B (**63**) by using a chloroalkyne **62** as a component.[50]

Scheme 32. Utilization of the [Cp*RuCl]-catalyzed [2+2+2] cycloaddition of chloroalkyne in the synthesis of sporolide B.

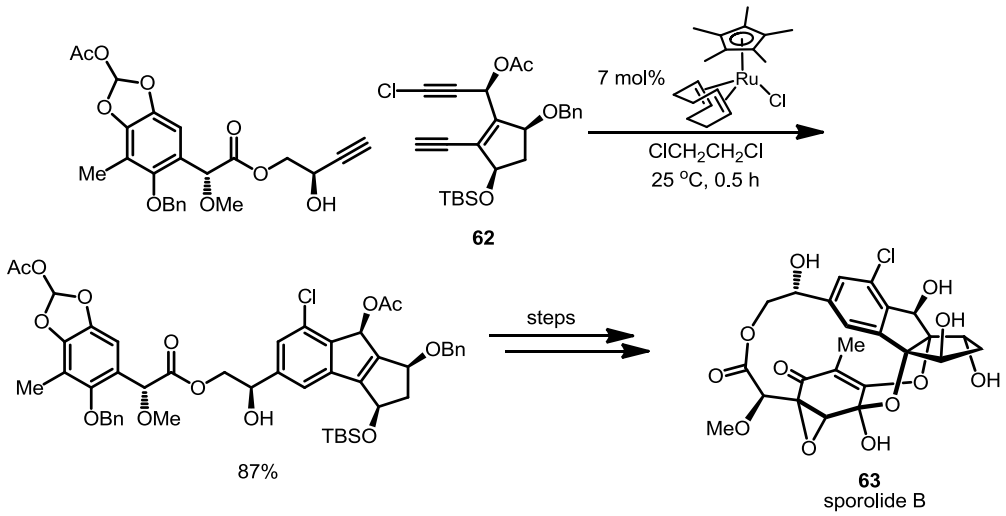

Although the ruthenium-catalyzed [2+2+2] cycloadditions are synthetically useful, there is a severe drawback that accompanies the use of haloalkynes. While 1 mol% of catalyst was sufficient to accomplish the cyclotrimerization of less sterically demanding 1,6-diynes and monoyne (e.g. Scheme 26), required catalyst loading significantly increases when the diynes had bulky halogen atoms on their terminal. Especially when the monoyne component was also substituted with bulky group, e.g. tolan, as much as 15 mol% of catalyst was required (Scheme 33).

Scheme 33. [2+2+2] cycloaddition adopting tolan as internal alkyne.

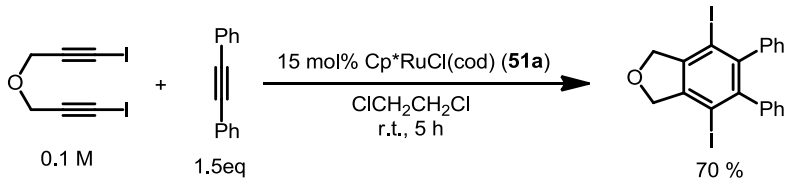

As the pentamethylcyclopentadienyl ligand is bulky, and strictly limits the available space around the metal center, elimination of methyl groups from the ligand is expected to improve the catalytic performance. However, in addition to the steric effects, electronic effect of the ligand should also be considered. A methyl group is inductively electron donating, so the substitution pattern on the cyclopentadienyl ligand will affect the electron density on the ruthenium center. Since the proposed rate-limiting step is oxidative cyclization involving a Ru(II) and two alkyne moieties, the increased electron density on the ruthenium center is expected to accelerate the catalytic cycle. In this manner, the author envisioned that the substituents on the cyclopentadienyl ligand exert at least two contradictory effects. However, studies on the influence of steric and electronic effects on Cp'Ru(II) complexes have scarcely been done.

Not only are the affinity to unsaturated compounds, but also both electrophilic and nucleophilic reactivities are the important carbenic nature of the ruthenacyclopentatrienes. Kirchner and co-workers have found that a cationic complex $[CpRu(PMe_3)(NCMe)_2](PF_6)$ (**64**) reacts with 1,6-diyne or various monoynes to form an allyl carbene complex **65**.[51]

Scheme 34. Formation of ruthenium allylcarbene complexes from from divalent $[CpRu(PR_3)^+]$ and 1,6-heptadiyne.

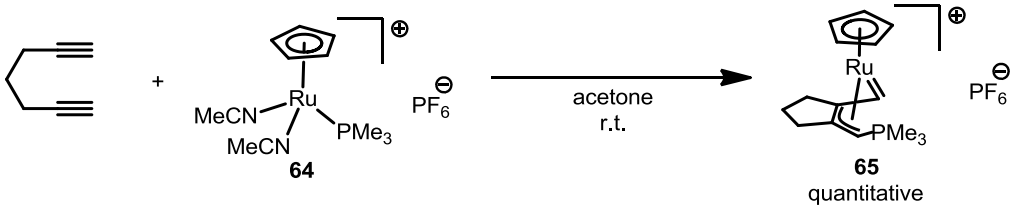

Dinjus and co-workers proved the intermediacy of a ruthenacyclopentatriene complex in this reaction (Scheme 35).[52] In their report, treatment of an isolated neutral ruthenacyclopentatriene **66** with trimethylphosphine resulted in the dissociation of a chlorine ligand and the formation of cationic ally carbene complex **67** similar to Kirchner's complex **65**. Interestingly, when trimethylphosphite in place of the phosphine was used, Arbuzov-type reaction took place to give dimethylphosphate analogue **68**.

Scheme 35. Kirchner-type reaction adopting a neutral ruthenacyclopentatriene **66**.

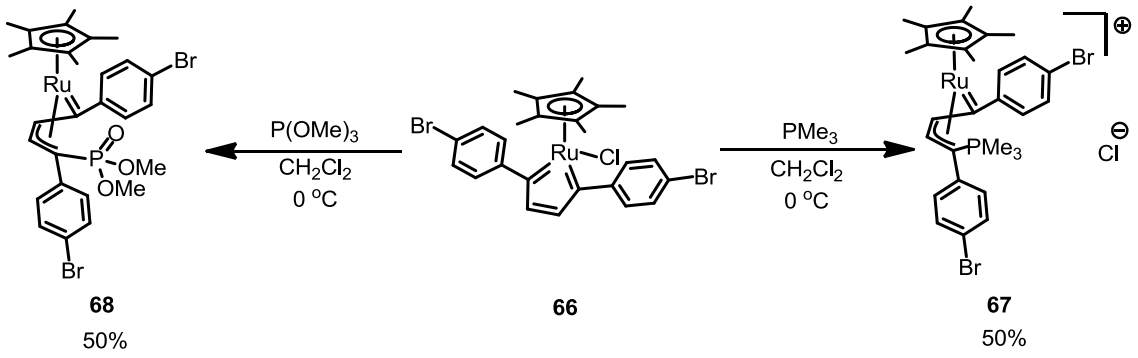

Also DFT study confirmed that the reaction proceed through a ruthenacyclopentatriene.[51b] The P–C bond formation can be regarded as 1,2-migration of the phosphine ligand (Scheme 36).

Scheme 36. 1,2-migration of a phosphine ligand in a ruthenacyclopentatriene.

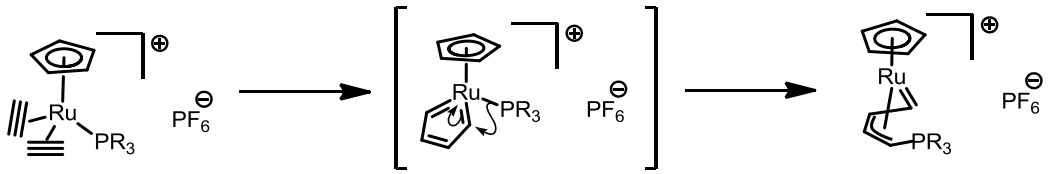

The electrophilicity of the ruthenacyclopentatriene is of great use in catalytic chemistry. When the oxygen nucleophile is used, the coupling of alkynes and the nucleophiles mediated by the ruthenium catalytic intermediate can be carried.

Trost and co-workers have developed a ruthenium-catalyzed dimerization/isomerization of propargyl alcohols (Scheme 37).[53] In a proposed mechanism, the substrate propargyl alcohol **69** and cationic ruthenium complex **70b** form a ruthenacycle intermediate **72** in a head-to-head fashion (in the original report, this ruthenacycle was regarded as a ruthenacyclopentadiene). With the aid of proton, one hydroxyl group is eliminated to generate dicationic and carbenic α-propylidene ruthenacyclopentadiene **73**. The nucleophilic attack of the water molecule to the carbenic carbon followed by deprotonation, proton transfer and reductive elimination affords the product **71**. Although the electrophilic species is not a ruthenacyclopentatriene, electrophilicity of cationic ruthenium carbene complex is effectively utilized.

Scheme 37. [CpRu$^+$]-catalyzed isomerization/dimerization of propargyl alcohol.

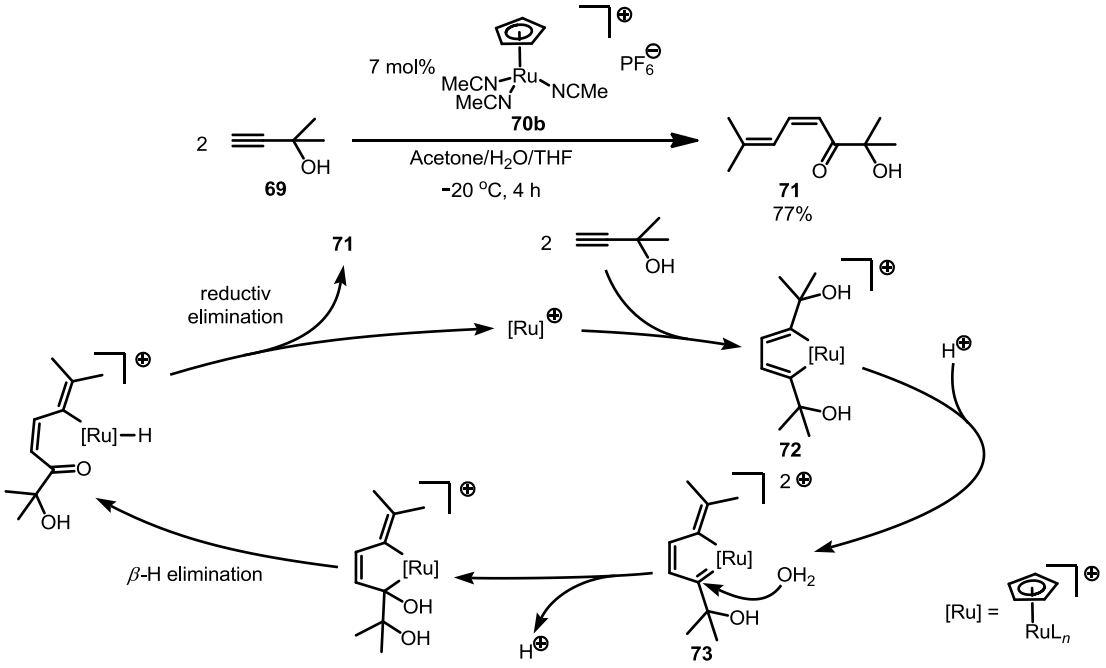

When an alkyne substrate other than propargyl alcohol is subjected to the same condition together with an external oxygen nucleophile, the very ruthenacyclopentatriene complex (**76**) serves as the electrophile (Scheme 38).[54] After the nucleophilic attack of water to the cationic ruthenacyclopentatriene intermediate **76**, concomitantly produced proton promote the decomposition of hydroxylic intermediate **77** to afford cyclic enone **74**. The use of alcohol instead of water gives cyclic diene **75**.

Scheme 38. [CpRu$^+$]-catalyzed hydrative and alkoxylative cyclization of 1,6-diynes.

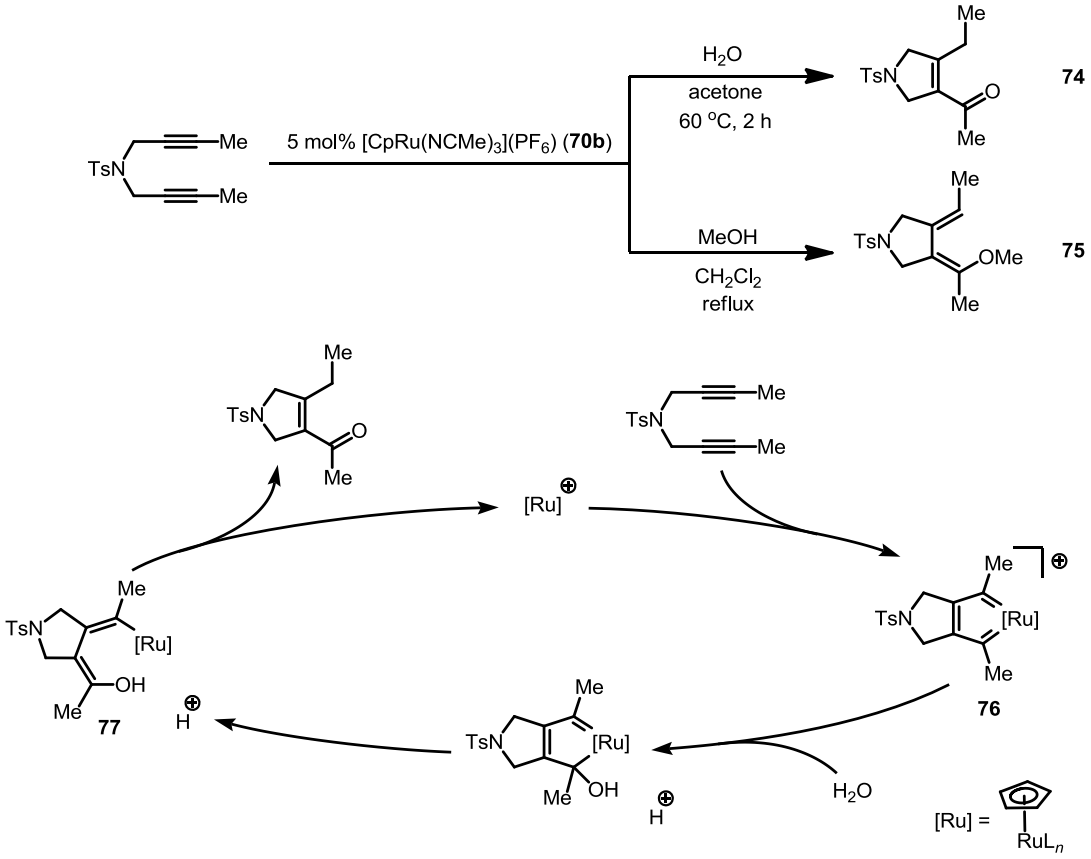

Related ruthenium catalyzed hydrative dimerization of monoynes to form linear ketone **78** was reported by Dixneuf *et al.* The reaction condition resembles the that of Trost's reaction and cationic [Cp*Ru(NCMe)](PF$_6$) (**70a**) was adopted as the catalyst. However, as a notable difference, sulfonic acid co-catalyst was required to promote the reaction.[55a] The acid is supposed to protonate the monocationic ruthenacyclopentatriene intermediate to form a dicationic species **79**.

Scheme 39. [Cp*Ru$^+$]- and acid-catalyzed hydrative head–to–head dimerization of arylmonoynes.

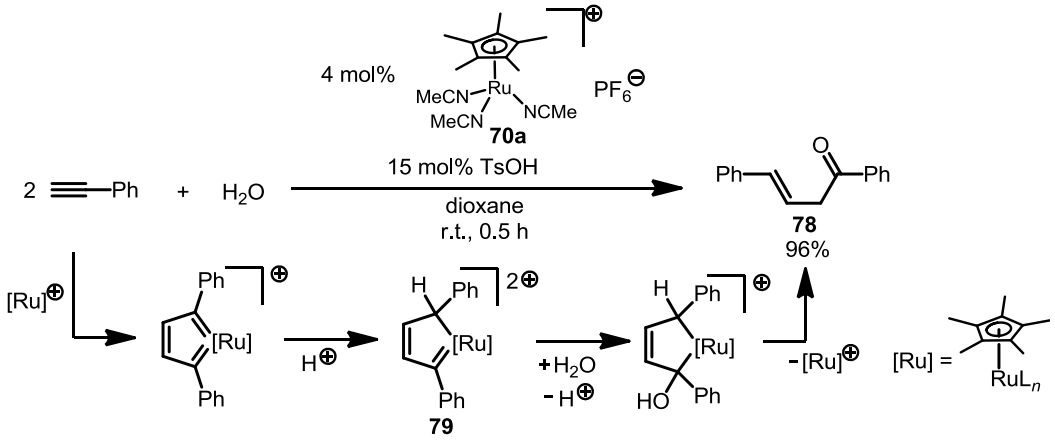

In the study of alkoxylative head-to-head dimerization of aryl alkynes (Scheme 40), importance of positive charge of the catalyst precursor was disclosed.[55b] The neutral complex Cp*RuCl(cod) (**51a**) did not promote the reaction at all, even though its ability to form a ruthenacyclopentatriene with two molecules of aryl diynes have been recognized.[56a] Accordingly, cationic precursor **70a** was employed also here to yield the dienyl ether **80**. The produced dienyl ether was hydrolyzed and oxidized to transform into 2,5-diarylfurans **81**.

Scheme 40. Alkoxylative head–to–head dimerization of aryl monoynes and one pot hydrolysis/oxidation to form 2,5-diarylfurans.

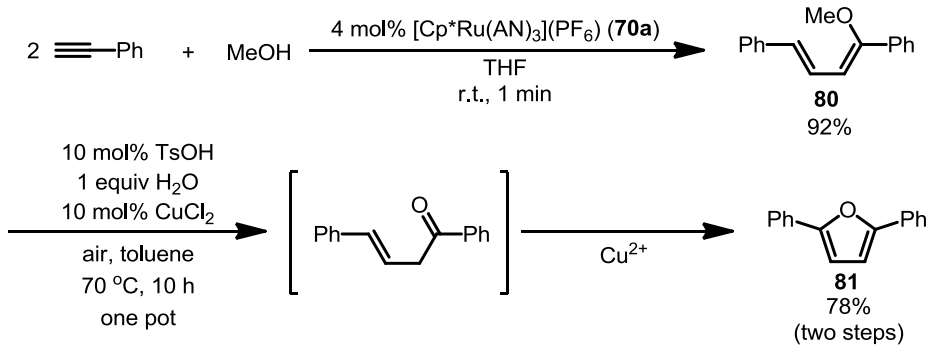

With respect to proposed reaction mechanisms of alcohol incorporation, there is a substantial difference between the reports by Trost and the one by Dixneuf. At any rate, two examples are consistent with each other in that the positive charge of the ruthenacyclopentatriene intermediate facilitates the nucleophilic attack of oxygen nucleophiles. Nevertheless, in the latter proposal, protonation of the ruthenacycle intermediate by the alcohol was assumed (Scheme 41), and this sequence is the exact opposite of the former. Presumably, this order was proposed in analogy with a mechanism for previously reported reaction with carboxylic acid.

Scheme 41. Proposed mechanism for [Cp*Ru$^+$]-catalyzed alkoxylative dimerization of arylalkynes.

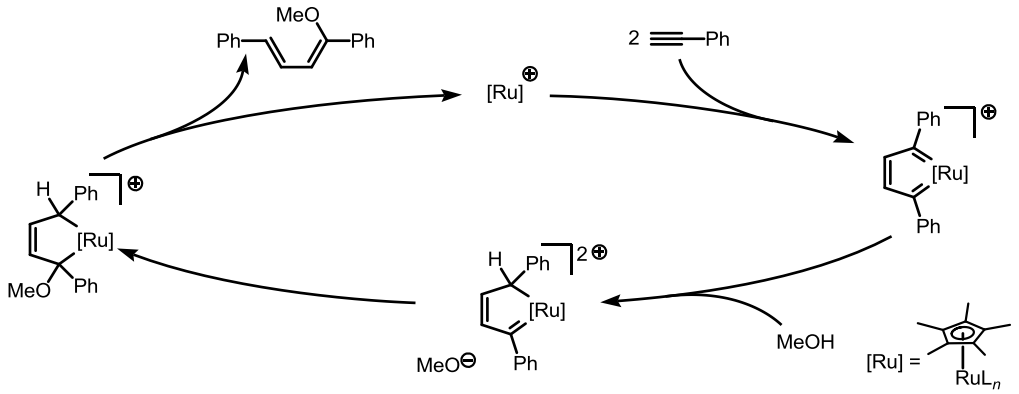

Earlier than these works, Dixneuf and co-worker have reported a ruthenium-catalyzed carboxylative dimerization of alkynes to from dienyl esters **82** (Scheme 42).[56] Interestingly, this reaction is catalyzed by neutral complex Cp*RuCl(cod) (**51a**) although the reaction formally resembles aforementioned alkyne dimerization reactions.

Scheme 42. [Cp*RuCl]-catalyzed carboxylative dimerization of monoynes.

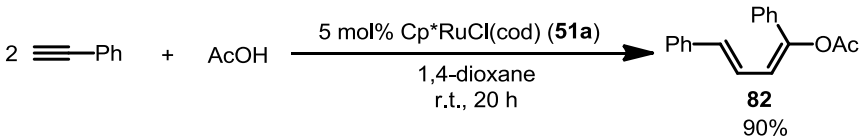

The mechanism of this reaction was well elucidated by means of stoichiometric reaction of an isolable ruthenacyclopentatriene **83** with carboxylic acid, and by DFT study. While **83** is unreactive toward ammonium salt of carboxylate, it readily reacts with carboxylic acid to afford a dienyl ester **82** in a quantitative yield (Scheme 43). This result suggests that in the reaction of neutral ruthenacyclopentadiene and carboxylic acid, the complex is first protonated by the acid. In addition, DFT calculation revealed that the protonation of the ruthenacyclopentatriene occurs preferentially on the α-carbon to generate a cationic intermediate **84**.

Scheme 43. Stoichiometric reaction of isolated ruthenacyclopentatriene complex with carboxylic acid or carboxylate salt.

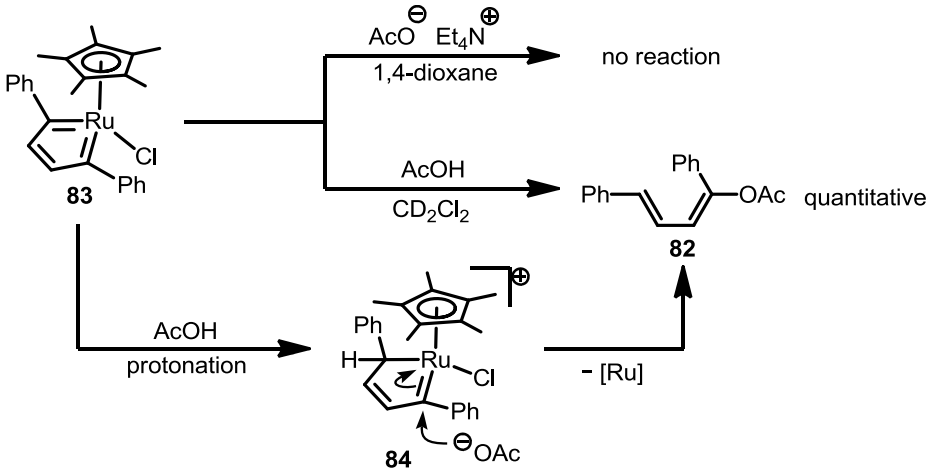

The series of studies on reactivities of the ruthenacyclopentatrienes with oxygen nucleophiles are highly suggestive. It is expected that the electrophilic or nucleophilic nature of the complexes can be easily switched by the charge of the complexes. In other words, the reactivity can be controlled by the presence/absence of an anionic ligand on the ruthenium center. Hence, appropriate combination of catalyst precursor and electrophile/nucleophile will lead to new valuable catalytic transformations of alkynes. In the case of ruthenium–vinylidene or –allenylidene chemistry, as described before, wide variety of nucleophiles were utilized. However, in the realm of ruthenacyclopentatriene chemistry, utilized nucleophiles are virtually limited to oxygen nucleophiles, and they are only three kinds; water, alcohols and carboxylic acids.

5. Objective of this study

As described above, ruthenacyclopentatrienes behave as cyclic biscarbenes and exhibit wide array of reactivities. It was reported or supposed that multiple factor such as presence/absence of anionic ligand or substitution patterns of ligand determine the behavior of these complexes. However, ruthenacyclopentatriene chemistry allows for more developments at present. In addition, accurate tuning of the ruthenium catalyst in conformity with each substrate would augment the utility of the reactions. From this view point, the author sought to obtain a detailed insight into the reactions involving ruthenacyclopentatrienes, and applied it to the development of novel reactions.

In the complexes bearing a frame work [Cp'$RuClL_2$], three coordination site out of six are occupied by the cyclopentadienyl ligands, and the ligand exerts major influence on the nature of the complexes. Hence the modulation of cyclopentadienyl ligand will enable the improvement of the catalytic activity. However, a guideline for the design of efficient Cp'Ru-type catalyst is lacking. To address this issue, the author prepared a series of polymethylcyclopentadienyl ruthenium complexes **51b**–**h** with every possible substitution numbers and positions (Figure 1), and scrutinized their catalytic behaviors in [2+2+2] cycloaddition of alkynes in Chapter 2.

Figure 1. Newly prepared and evaluated complexes in chapter 2.

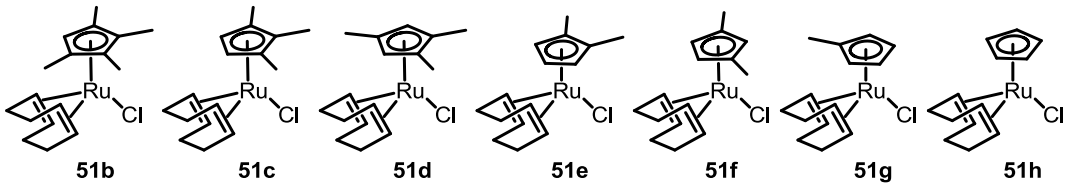

While the reaction mechanism of ruthenacyclopentatrienes with unsaturated compounds has been established, widely accepted interpretation corresponding to reaction with oxygen nucleophiles has yet to be reported. In Chapter 3, the author focused on ruthenium-catalyzed hydrative cyclization of 1,6-diynes and elucidated the reaction mechanism by means of experiments and DFT study.

Exploitation of the bifunctionality that resides in ruthenacyclopentatrienes is intriguing.

Since two carbenes are conjugated by vinylene moiety, they are expected to work cooperatively, and activate a donor–acceptor pair even if it is less reactive (eq 10, Scheme 44). Another possibility is as follows. Even after the transformation of one carbene moiety, another carbene will persist. As shown in Scheme 18, an electrophilic carbene complex might couple with a nucleophile in which both donor and acceptor character coexist on one atom. This step is expected to be followed by electrocyclization to afford five-membered ring (eq 11). Based on these concepts, new catalytic reactions that utilize the interaction between ruthenacyclopentatriene and oxygen nucleophiles were developed and described in Chapters 4 and 5.

Scheme 44. Anticipated expansions of ruthenacyclopentatriene-mediated reactions.

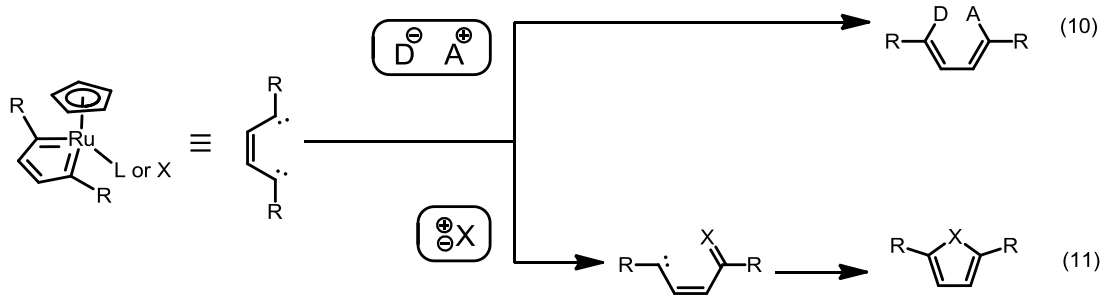

6. References

[1] Doering, W. von E.; Buttery, R. G.; Laughlin, R. G.; Chaudhuri, N. *J. Am. Chem. Soc.* **1956**, *78*, 3224.

[2] Davies, H. M. L.; Hanse, T.; Hopper, D. W.; Panaro, S. A. *J. Am. Chem. Soc.* **1999**, *121*, 6509–6510.

[3] Taylor, T. E.; Hall, M. B. *J. Am. Chem. Soc.* **1984**, *106*, 1576–1584.

[4] Klabunde, U.; Fischer, E. O. *J. Am. Chem. Soc.* **1967**, *89*, 7144–7142.

[5] Case, C. P.; Czerwinski, C. J.; Powell, D. R.; Hayashi, R. K. *J. Am. Chem. Soc.* **1997**, *119*, 5750–5751.

[6] Banks, R. L.; Bailey, G. C. *I & EC Prod. Res. Dev.* **1964**, 170–173.

[7] Natta, G.; Dall'asta, G.; Mazzanti, G. *Angew. Chem. Int. Ed. Engl.* **1964**, *3*, 723–729.

[8] Hérisson, P. J.-L.; Chauvin, Y. *Makromol. Chem.* **1971**, *141*, 161–176. Schrock, R. R. *Angew. Chem. Int. Ed.* **2006**, *45*, 3748–3759

[9] (a) Casey, C. P.; Burkhardt, T. J. *J. Am. Chem. Soc.* **1974**, *96*, 7808–7809; (b) Katz, T. J.; McGinnis, J. *J. Am. Chem. Soc.* **1975**, *97*, 1592–1594; (c) McGinneis, J.; Katz, T. J.; Hurwiz, S. *J. Am. Chem. Soc.* **1976**, *98*, 605–606; (d) Grubbs, R. H.; Carr, D. D.; Burk, H. P. *J. Am. Chem. Soc.* **1976**, *98*, 3478–3483.

[10] (a) Bonge, H. T.; Hansen, T. *J. Org. Chem.* **2010**, *75*, 2309–2310; (b) Nowlan, D. T.; Gregg, T. M.; Davies, H. M. L.; Singleton, D. A. *J. Am. Chem. Soc.* **2003**, *125*, 15902–15911; (c) Hansen, J.; Autschbach, J.; Davies, H. M. L. *J. Org. Chem.* **2009**, *74*, 6555–6563; (d) Fraile, J. M.; García, J. I.; Martínez-Merino, V.; Mayoral, J. A.; Salvatella, L. *J. Am. Chem. Soc.* **2001**, *123*, 7616–7625; (e) Fraile, J. M.; García, J. I.; Gil, M. J.; Martínez-Merino, V.; Mayoral, J. A.; Salvatella, L. *Chem. Eur. J.* **2004**, *10*, 758–765; (f) Suenobu, K.; Itagaki, M.; Nakamura, E. *J. Am. Chem. Soc.* **2004**, *126*, 7271–7280.

[11] (a)Kargel, T. K.; Koch, W. *J. Chem. Soc. Perkin Trans 2* **1996**, 877–881; (b) Bernardi, F.; Bottoni, A.; Miscione, G. P. *J. Am. Chem. Soc.* **1997**, *119*, 12300–12305; (c) Hirai, A.; Nakamura, M.; Nakamura, E. *Chem. Lett.* **1998**, *27*, 927–928; (d) Nakamura, E.; Hirai, A.; Nakamura, M. *J. Am. Chem. Soc.* **1998**, *120*, 5844–5845; (e) Nakamura, M.; Hirai, A.; Nakamura, E. *J. Am. Chem. Soc.* **2003**, *125*, 2341–2350.

[12] (a)Bernardi, F.; Bottoni, A.; Miscione, P. G. *Organometallics* **2001**, *20*, 2751–2758; (b) Berthon-Gelloz, G.; Marchant, M.; Straub, B. F.; Marko, I. *Chem. Eur. J.* **2009**, *15*, 2923–2931.

[13] Yamamoto, Y.; Kitahara, H.; Ogawa, R.; Kawaguchi, H.; Tatsumi, K.; Itoh, K. *J. Am. Chem. Soc.* **2000**, *122*, 4310–4319.

[14] Wang, F.; Meng, Q.; Li, M. *Int. J. Quant. Chem.* **2008**, *108*, 945–953.

[15] (a) Tjaden, E. B.; Stryker, J. M. *J. Am. Chem. Soc.* **1990**, *112*, 6420–6422; (b) Hoffmann, H. M. R.; Otte, A. R.; Wilde, A.; Menzer, S.; Williams, D. J. *Angew. Chem. Int. Ed. Engl.* **1995**, *34*, 100–102.

[16] (a) Park, S.-B.; Sakata, N.; Nishiyama, H. *Chem. Eur. J.* **1996**, *2*, 303–306; (b) Che, C.-M.; Huang, J.-S.; Lee, F.-W.; Li, Y.; Lai, T.-S.; Kwong, H.-L.; Teng, P.-F.; Lee, W.-S.; Lo, W.-C.; Peng, S.-M.; Zhou, Z.-Y. *J. Am. Chem. Soc.* **2001**, *123*, 4119–4129.

[17] Schwab, P.; France, M. B.; Ziller, J. W.; Grubbs, R. H. *Angew. Chem. Int. Ed. Engl.* **1995**, *34*, 2039–2041.

[18] Hugue, J.; Karpf, M.; Dreiding, A. S. *Tetrahedron Lett.* **1983**, *39*, 4177–4180.

[19] (a) Nesmeyanov, A. N.; Aleksandrov, G. G.; Antonova, A. B.; Anisimov, K. N.; Kolbova, N. E.; Struchkov, Yu. T. *J. Organomet. Chem.* **1976**, *110*, C36–C38; (b) Antonova, A. B.; Kolobova, N. E.; Petrosky, P. V.; Lokshin, B. V.; Obezyuk, N. S. *J. Organomet. Chem.* **1977**, *137*, 55–67; (c) Bruce, M. I.; Wallis, R. C. *J. Organomet. Chem.* **1978**, *161*, C1–C4; (d) avison, A.; Solar, J. P. *J. Organomet. Chem.* **1978**, *155*, C8–C12; (e) Davison, A.; Selegue, J. P. *J. Am. Chem. Soc.* **1978**, *100*, 7763–7785.

[20] For a review see: (a) Bruce, M. I. *Chem. Rev.* **1991**, *91*, 197–257; (b) Bruneau, C.; Dixneuf, P. H. *Acc. Chem. Res.* **1999**, *32*, 311–323.

[21] (a) McDonald, F. E.; Olson, T. C. *Tetrahedron Lett.* **1997**, *38*, 7691–7692; (b) Maeyama, K.; Iwasawa, N. *J. Am. Chem. Soc.* **1998**, *120*, 1928–1929; (c) Maeyama, K.; Iwasawa, N. *J. Org. Chem.* **1999**, *64*, 1344-1346; (d) Miura, T.; Iwasawa, N. *J. Am. Chem. Soc.* **2002**, *124*, 518–519.

[22] (a) Iwasawa, N.; Shido, M.; Maeyama, K.; Kusama, H. *J. Am. Chem. Soc.* **2000**, *122*, 10226–10227; (b) Ohe, K.; Miki, K.; Yokoi, T.; Nishino, F.; Uemura, S. *Organometallics* **2000**, *19*, 5525–5528; (c) Miki, K.; Nishino, F.; Ohe, K.; Uemura, S. *J. Am. Chem. Soc.* **2002**, *124*, 5260–5261.

[23] (a) Lo, C.-Y.; Gou, H.; Lian, J.-J.; Shen, F.-M.; Liu, R.-S. *J. Org. Chem.* 2002, *67*, 3930–3932; (b) Madhushaw, R. J.; Lin, M.-Y.; Abu Shoel, S. M.; Liu, R. S. *J. Am. Chem. Soc.* **2004**, *126*, 6895–6899; (c) in, M.-Y.; Maddirala, S. J.; Liu, R.-S. *Org. Lett.* **2005**, *7*, 1745–1748.

[24] (a) McDonald, F. E.; Chatterjee, A. K. *Tetrahedron Lett.* **1997**, *38*, 7687–7690; (b) Gooßen, L. J.; Rauhaus, J. E.; Deng, G.; *Angew. Chem. Int. Ed.* **2005**, *44*, 4042–4045; (c) Fukumoto, Y.; Dohi, T.; Masaoka, H.; Chatani, N.; Murai, S. *Organometallics* **2002**, *21*, 3845–3847.

[25] McDonald, F. E.; Burova, S. A.; Huffman, L. G., Jr. *Synthesis* **2000**, 970–974.

[26] Jérôme, F.; Monnier, F.; Lawicka, H.; Dérien, S.; Dixneuf, P. H. *Chem. Commun.* **2003**, 696–697.

[27] Ruppin, C.; Dixneuf, P. H. *Tetrahedron Lett.* **1986**, *52*, 6323–6324.

[28] Suzuki, T.; Kokunaga, M.; Wakatsuki, Y. *Org. Lett.* **2001**, *3*, 735–737.

[29] For example, see: Wakatsuki, Y.; Hou, Z.; Tokunaga, M. *Chem. Rec.* **2003**, *3*, 144–157.

[30] Bruce, M. I.; Swincer, A. G.; Wallis, R. C. *J. Organomet. Chem.* **1979**, *171*, C5–C8.

[31] (a) Parlier, A.; Rudler, H. *J. Chem. Soc., Chem. Commun.* **1986**, 514–515; (b) Dötz, K. H.; Sturm, W.; Alt, H. G. *Organometallics* **1987**, *6*, 1424–1427; (c) McDonald, F. E.; Connolly, C. B.; Gleason, M. M.; Towne, T. B.; Treiber, K. D. *J. Org. Chem.* **1993**, *58*, 6952–6953.

[32] For example, see: (a) Nishibayashi, Y.; Wakiji, I.; Hidai, M. *J. Am. Chem. Soc.* **2000**, *122*, 1019–11029; (b) Nishibayashi, Y.; Wakiji, I.; Ishii, Y.; Uemura, Y.; Hidai, M. *J. Am. Chem. Soc.* **2001**, *123*, 3393–3394; (c) Nishibayashi, Y.; Inada, Y.; Yoshikawa, M.; Hidai, M.; Uemura, S. *Angew. Chem. Int. Ed.* **2003**, *42*, 1495–1498; (d) Nishibayashi, Y.; Miyake, Y.; Uemura, S. *J. Synth. Org. Chem., Jpn.* **2009**, *67*, 437–450.

[33] Trost, B. M.; Dyker, G.; Klawiec, R. J. *J. Am. Chem. Soc.* **1990**, *112*, 7809–7811.

[34] (a) Trost, B. M.; Rhee, Y. H. *J. Am. Chem. Soc.* **1999**, *121*, 11680–11683; (b) Trost, B. M.; Rhee, Y. H. *J. Am. Chem. Soc.* **2002**, *124*, 2528–2553.

[35] (a) Kornblum, N.; Powers, J. W.; Anderson, G. J.; Jones, W. J.; Larson, H. O.; Levand, O.; Weaver, W. M *J. Am. Chem. Soc.* **1957**, *79*, 6562–6562; (b) Kornblum, N.; Jones, W. J.; Anderson, G. J. *J. Am. Chem. Soc.* **1959**, *81*, 4113-4114.

[36] Casey, C. P.; Burkhardt, T. J.; Bunnell, C. A.; Calabrese, J. C. *J. Am. Chem. Soc.* **1977**, *99*, 2127–2134.

[37] Trost, B. M.; Hashmi, A. S. K. *Angew. Chem. Int. Ed.* **1993**, *32*, 1085–1087.

[38] Chatani, N; Kataoka, K.; Murai, S.; Naoyuki, F.; Seki, Y. *J. Am. chem. Soc.* **1998**, *120*, 9104–9105.

[39] (a) Fürstner, A.; Davies, P. W. *Angew. Chem. Int. Ed.* **2007**, *46*, 3410–3449; (b) Seidel, G.; Mynott, R.; Fürstner, A. *Angew. Chem. Int. Ed.* **2009**, *48*, 2510–2513; (c) Shapiro, N. D.; Toste, F. D. *Synlett* **2009**, 675–691.

[40] For example, see: Senn, H. M.; Blöchl, P. E.; Togni, A. *J. Am. Chem. Soc.* **2000**, *122*, 4098–4107.

[41] (a) Albers, M. O.; de Waal, D. J. A.; Liles, D. C.; Robinson, D. J.; Singleton, E.; Wiege, M. B. *J. Chem. Soc., Chem. Commun.* **1986**, 1680–1682; See also: (b) Gemel, C.; LaPenseé, A.; Mauthner, K.; Mereiter, K. Schmisd, R.; Kirchner. *Monatsh. Chem.* **1997**, *128*, 1189–1199; (c) Yamada, Y.; Mizutani, J.; Kurihara, M.; Nishihara, H. *J.*

Organomet. Chem. **2001**, *80-30*, 637–639.

[42] Yamamoto, Y.; Kitahara, H.; Ogawa, R.; Kawaguchi, H.; Tatsumi, K.; Itoh, K. *J. Am. Chem. Soc.* **2000**, *122*, 4310–4319.

[43] Yoshihiko, Y.; Ogawa, R.; Itoh, K. *Chem. Commun.* **2000**, 549–550.

[44] Reppe, W.; Schlichting, O.; Klager, K.; Toepei, T. *Liebigs Ann. Chem.* **1948**, *560*, 1–92.

[45] For reviews, see: (a) Donohoe, T. J.; Orr, A. J.; Gingham, M. *Angew. Chem. Int. Ed.* **2006**, *45*, 2664–2670; (b) Yoshida, K.; Imamoto, T.; Yanaghisawa, A. *J. Synth. Org. Chem., Jpn.* **2009**, *67*, 876–888.

[46] Lautens, M.; Klute, W.; Tam, W. *Chem. Rev.* **1996**, *96*, 46–92.

[47] [Co]: Hardesty, J. H.; Koerner, J. B.; Albright, T. H.; Lee, G.-Y. *J. Am. Chem. Soc.* **1999**, *121*, 6055–6067; [Rh]: Dachs, A.; Osuna, S.; Roglans, A.; Solá, M. *Organometallics* **2010**, *29*, 562–569.

[48] (a) Yamamoto, Y.; Arakawa, T.; Ogawa, R.; Itoh, K. *J. Am. Chem. Soc.* **2003**, *125*, 12143–12160; (b) Kirchner, K.; Calhorda, M. J.; Schmid, R.; Veiros, L. F. *J. Am. Chem. Soc.* **2003**, *125*, 11721–11729.

[49] Damle, S. V.; Seomoon, D.; Lee, P. H. *J. Org. Chem.* **2003**, *68*, 7085–7087.

[50] Nicolaou, K. C.; Tang, Y.; Wang, J. *Angew. Chem. Int. Ed.* **2009**, *48*, 3449-3453

[51] (a) Mauthner, K.; Soldouzi, K. M.; Mereiter, K.; Schmid, R.; Kirchner, K. *Organometallics* **1999**, *18*, 4681–4683; (b) Rüba, E.; Mereiter, K.; Schmid, R.; Sapunov, V. N.; Kirchner, K.; Schottenberger, H.; Calhorda, M. J.; Veiros, L. F. *Chem. Eur. J.* **2002**, *8*, 3948–3961

[52] Ernst, C.; Walter, O.; Dinjus, E. *J. Organomet. Chem.* **2001**, *627*, 249–254.

[53] Trost, B. M.; Rudd, M. T. *J. Am. Chem. Soc.* **2001**, *123*, 8862–8863.

[54] (a) Trost, B. M.; Rudd, M. T. *Org. Lett.* **2003**, *5*, 4599–4602; (b)Trost, B. M.; Huang, X. *Org. Lett.* **2005**, *7*, 2097–2099; (c) Trost, B. M.; Huang, X. *Chem. Asian J.* **2006**, *1*, 469–478.

[55] (a) Zhan, M.; Jiang, H.; Dixneuf, P. H. *Adv. Synth. Catal.* **2009**, *351*, 1488–1494; (b) Zhang, M.; Jiang, H. -F.; Neumann, H.; Beller, M.; Dixneuf, P. H. *Angew. Chem. Int. Ed.* **2009**, *48*, 1681–1684.

[56] (a) Le Paih, J. L.; Monnier, F.; Dérien, S.; Dixneuf, P. H.; Clot, E.; Eisenstein, O. *J. Am. Chem. Soc.* **2003**, *125*, 11964–11975; (b) Le Paih, J.; Dérien, S.; Dixneuf, P. H *Chem. Commun.* **1999**, 1437–1438.

Chapter 2

Synthesis and Evaluation of Novel Polymethylcyclopentadienylruthenium(II) Complexes For Catalytic Cycloaddition of Diynes

Abstract: A series of η^5-cyclopentadienylruthenium complexes, [(η^5-$C_5Me_nH_{5-n}$)RuCl(cod)] (*n*=0–5, cod=1,5-cyclooctadiene), were synthesized and evaluated as catalysts for the cycloaddition of 1,6-diynes with alkynes. As a result, It was found that the complex bearing the $Cp^{1,2,4\text{-}Me3}$ ligand is the most efficient catalyst in terms of turnover number (TON) for the cycloaddition of a bulky diiododiyne with acetylene, recording the highest TON of 970 with a catalyst loading of 0.1 mol%. To obtain insight into this result, electron richness of all complexes were evaluate the by cyclic voltammetric analyses, which indicate that the electron density of the ruthenium center increases with an increase in methyl substitution on the Cp′ ligands. The initial rate (up to 10% conversion) of the cycloaddition was then measured by using ^{1}H NMR spectroscopy. The initial rate is found to decrease as the number of methyl substituents increases. According to these results, it was suggested that the optimum catalytic performance exhibited by the 1,2,4-trimethylcyclopentadienyl complex can be attributed to its robustness under the catalytic cycloaddition conditions. The steric and electronic effects of the substituted cyclopentadienyl ligands are also investigated in terms of the regioselectivity of the cycloaddition of an unsymmetrical diyne and in terms of the chemoselectivity in the cycloaddition of a 1,6-heptadiyne with norbornene.

1. Introduction

As described in the Chapter 1, the ruthenium-catalyzed [2+2+2] cycloaddition of alkynes has broad functional group tolerability. This feature enables the use of even iodoalkyne, which easily oxidatively adds to low-valent transition-metal centers, as substrates. However, the requirement for large amount of catalyst is unacceptable from the view point of the practical use.

Halobenzenes, including iodobenzenes, are preferable substrates for a series of palladium-catalyzed cross coupling processes, and are useful building blocks in organic synthesis. However, the preparation of halobenzene has had several problems. In the electrophilic halognation of aromatic compounds, the reaction system becomes acidic because of hydrogen halide byproduct. What is worse, when the halogen is less electrophilic iodine, strongly acidic or oxidative condition is required for the activation of iodine is needed. Hence, classical iodination of aromatic ring is not always useful, especially when the substrate has delicate functional groups. In addition, regioselectivity of the halogenation of the substituted benzenes depends on the electronic and steric nature of the originally installed substituents. Therefore, regioselective synthesis of multiply substituted benzenes is difficult, and often, the attempts result in a mixture of several regioisomers.

Ruthenium-catalyzed [2+2+2] cycloaddition can be a solution to this issue. Iodoalkynes can be prepared by treating the terminal alkynes with *N*-iodosuccinimide under a mild condition (in a neutral solution at room temperature) in the presence of silver catalyst.[1] The regio- and chemo-selectivities of the following cyclotrimerization are generally high. Thus, the [2+2+2] cycloaddition of an iododiyne and a monoyne is a rational method for the synthesis of substituted iodobenzenes.

Therefore, to maximize the merits by overcoming the low efficiency, development of a catalyst with a higher efficiency is strongly desired. As 1,5-cyclooctadiene ligand in Cp*RuCl(cod) (**1a**) dissociates in the catalytic cycle, it is predicted that only the cyclopentadienyl ligand is the tunable part of the complex.

The improvement of catalytic activities by means of diversification of Cp′ ligands has been intensively conducted in the area of group IV transition metal catalyst for olefin polymerization.

Although Ziegler-Natta catalyst prepared from titanium chloride and alkylaluminum was revolutionary in that it enabled the production of branchless polyethylene, the problem about it was that the catalyst is heterogeneous and the active sites are not uniform. The diversity of the active sites of the Ziegler-Natta catalyst makes the control of the catalytic character difficult. In contrast, catalysts prepared from group IV metallocenes and methylaluminoxane (MAO) have uniform and unambiguous active center (Kaminsky-Sinn catalysts). By making the most of this point, rational control of catalyst property has been achieved. For example, a zirconocene complex with mirror symmetry (Figure 1) enabled the syndiotactic polymerization of propylene (Scheme 1). [2]

Figure 1. σ–symmetric ziroconocene with a fluorene-derived tethered ligand.

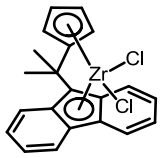

Scheme 1. Syndiotactic polymerization of propylene catalyzed by a σ–symmetric zirconocene complex.

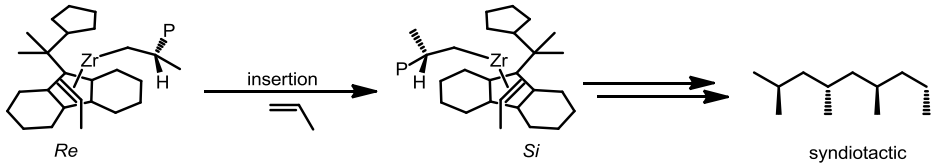

Following these impressive achievements, the relationship between the Cp′ structure and catalyst's property was investigated. In these studies, correlation between between stereo/electronic effects and the catalytic activities are focused on.

Piccolorvazzi and co-worker have revealed that installation of electron withdrawing group on indenyl ligands coordinated to a zirconium(IV) leads to diminished catalytic activities (Table 1).[3] The methoxy-substituted complex exhibits irregularly low activity (entry 1), this was attributed to coordination of the methoxy group to MAO and resultant enhanced σ-electron withdrawing and reduced π-donation from it.

Table 1. Influence of electronic effect on the plymerization catalyst activity.

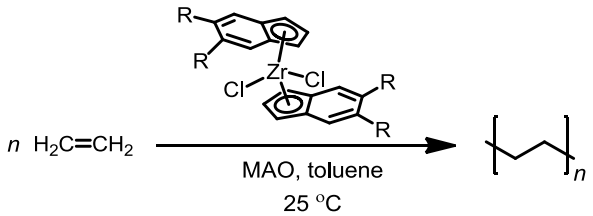

entry	R	productivity Kg PE/mol(Zr)・h
1	OMe	122
2	CH_3	25200
3	H	14000
4	Cl	1900

The relationship between the steric effect of the ligands and the catalytic activity was also studied. Cone angle θ was invented by Tolman and conveniently used to evaluate the steric effects of phosphine ligands. Coville has applied this parameter to describe the steric effects of substituted cyclopentadienyl ligands (Figure 2). [4]

Figure 2. Definition of cone angle θ for substituted cyclopentadienyl ligands.

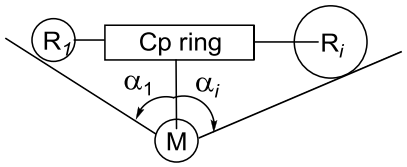

$$\theta = \frac{2}{5}\sum_{i=1}^{5}\alpha_i$$

By using this parameter, they have partially succeeded in correlating the ligand's steric effect and the catalytic activities of the complexes in ethylene polymerization. In that study, the catalytic activity of the substituted titanocenes decreased with the increasing θ, and eventually, the catalyst became inactive when θ was larger than 260°.[5] Similar study on zirconocene catalysts are conducted by Janiak and co-workers. They have compared various zirconocenes bearing two identical Cp′ ligands or two different Cp′, and revealed that the catalytic activity diminished as the substitution numbers on the cyclopentadienyl ligands increased (Figure 3).[6]

Figure 3. The steric effect of the ligand and the ethylene polymerization activity of zirconocenes.

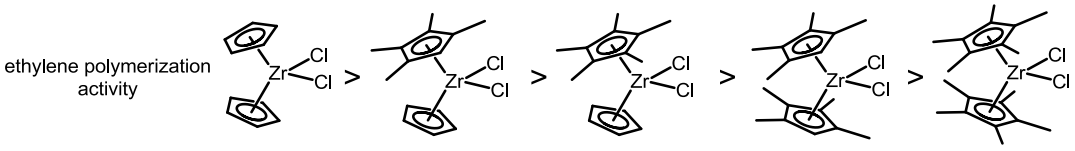

These results come out presumably because steric repulsion between the polysubstituted ligands and the substrate prevents the access to the active metal center. Since the methyl groups are inductively electron donating, increased substitution number on the ligand is expected to make the metal center electron rich. In combination with the study on electronic effect by Piccolorvazzi (Table 1), methyl substituents appear to have contradictory effect on the catalytic activity. However, in the case of group IV metallocene catalysts, above described results suggest

that the steric effect is more influential than the electronic effect.

More dramatic change in the reactivity of metallocene caused by modulation of the cyclopentadienyl ligands can be seen in the activation of molecular nitrogen by low valent zirconocenes. Bercaw and co-workers have discovered that *in situ* generated divalent decamethylzirconocene Cp^*_2Zr (**3a-Zr**) can capture nitrogen molecules to form a N_2-bridged dinuclear complex [{$Cp^*_2Zr(\eta^1\text{-}N_2)$ }$_2(\mu^2,\eta^1,\eta^1\text{-}N_2)$] (**4**). The nitrogen activated by zirconium centers is reduced to give hydrazine on treatment with hydrochloric acid (Scheme 2).[7]

Scheme 2. Activation of nitrogen molecule by low valent zirconocene [Cp^*_2Zr]

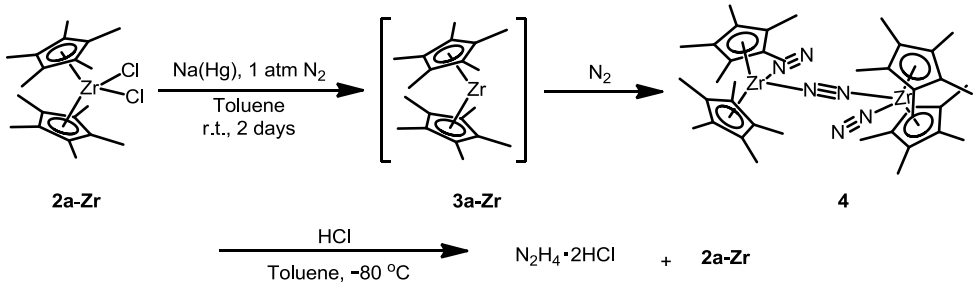

Recently, Chirik and co-workers has used a similar complex with less substituted cyclopentadienyl ligand $(Cp^{Me4})_2ZrCl_2$ (**2b-Zr**) and its hafnium analogue $(Cp^{Me4})_2HfCl_2$ (**2b-Hf**) for the same purpose. Surprisingly, the nitrogen molecule bridged two metals in a side-on manner to form [{$(Cp^{Me4})_2M(\eta^1\text{-}N_2)$ }$_2(\mu^2,\eta^2,\eta^2\text{-}N_2)$] (**5-Zr**: M = Zr; **5-Hf:** M = Hf). When the central metal was zirconium, the nitrogen was finally reduced to afford ammonia on hydrogenation (Scheme 3).[8]

Scheme 3. Side-on coordination of molecular nitrogen to $(Cp^{Me4})_2M$ (M = Zr, Hf).

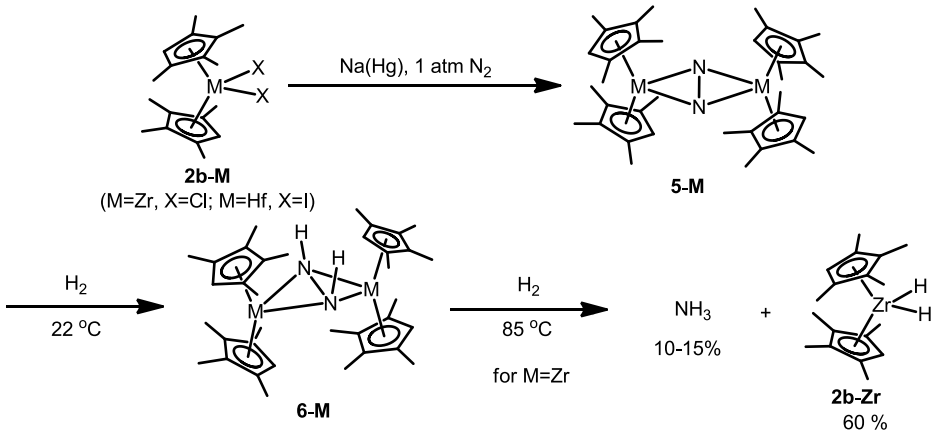

The dramatic change of bridging mode of the nitrogen in the dinuclear complex is attributed to the reduced steric hindrance of the cyclopentadienyl ligand and the eased approximation of two metallocene fragments. Morokuma and co-workers has computationally rationalized relationship between the reactivity of zirconocenes and substitution pattern of the ligands.[9] The study showed that when the substitution number of the cyclopentadienyl ligand is less than or equal to 4, the complex with side-on dinitrogen bridge is energetically favorable than those with end-on dinitrogen bridge.

The studies introduced up to here imply that only a slight change such as elimination of small numbers of methyl substituents can significantly affect the reactivity of the cyclopentadienyl complexes, and as a result, leads to a creation of a new function.

Intrigued by these results, the author attempted to improve the ruthenium-catalyzed alkyne [2+2+2] cycloaddition system by modulating the cyclopentadienyl ligand in Cp′RuCl(cod).

In the [Cp*RuCl]-catalyzed alkyne cyclotrimerization, it is deduced from DFT calculation that the formation of the ruthenacyclopentatriene intermediate is the rate-limiting step.[10] When both alkyne terminals are substituted with small substituents such as proton, the steric repulsion between the diyne and Cp* ligand is presumably negligible. On the other hand, when diyne has large substituents such as iodine, the steric repulsion is expected to be significantly large and might result in an increasingly slower rate-limiting step (Scheme 4).

Scheme 4. The steric repulsion between the Cp* ligand and alkyne terminal substituents

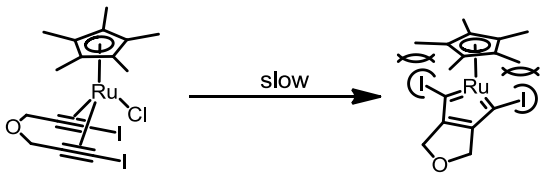

Another step that is possibly affected by the steric effect of the ligand is incorporation of the third alkyne. In the [2+2] addition of the ruthenacyclopentatriene **7** and monoyne component to form ruhtenabicyclo[3.2.0]heptatriene intermediate **8**, the α-carbon shifts its hybridization from sp^2 to sp^3. As a result, the bulky substituent originated from the alkyne terminal will further approach the Cp* ligand and cause an additional steric interaction (Scheme 5). Hence, the steric

bulkiness of the ligand is likely to affect at least two elemental steps of the catalytic cycle.

Scheme 5. Plausible steric interaction in the [2+2] cycloaddition of monoyne component and carbene moiety of the ruthenacyclopentatriene.

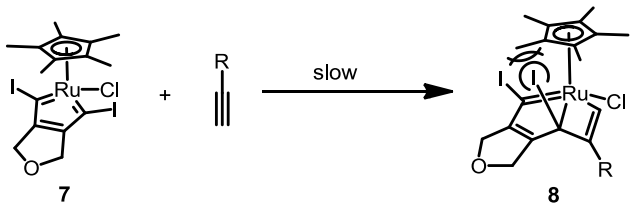

7 8

The author expected that less methyl substitution on the Cp* ligand will lead to a reduced steric hindrance and will result in an improved catalytic efficiency.

At the same time, change of catalytic behavior of the [Cp′RuCl] complexes caused by electronic perturbation accompanying the varied substitution patterns of the ligand is of interest. In the group IV metallocene olefin polymerization catalysts, the electronic effect of the ligands was a subsidiary factor. On the other hand, in the case of transition metal-catalyzed cycloaddition reaction of alkynes mediated by metallacyclopentatrienes or metallacyclopentadienes, the oxidation number of the metal center fluctuates by 2. Therefore, strong electron donation from the ligands to the metal center will facilitate the oxidative cyclization step. Herein, several oxidative cyclization reactions are exemplified.

Lindner and co-workers have reported the formation of 5-memberd ruthenacycles which has $Ru(CO)_3$ or $Ru(CO)_4$ as a central component (Scheme 6).[11] In this example, alkyne component is limited to electron deficient dialkylacetylenedicarboxylates. Although the involved ruthenium complex is zero valent, it seems that the low electron density on the ruthenium center caused by the strong back donation to the carbonyl ligand lowers the reactivity of the metal center.

Scheme 6. Ruthenacycle formation from $[Ru(CO)_3]$ fragment and activated alkyne.

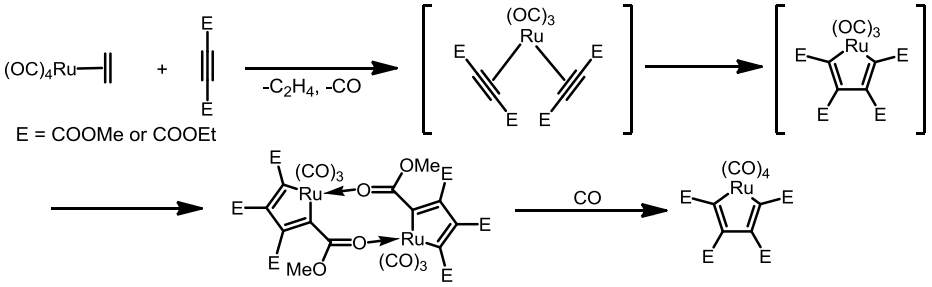

In another cases, group IX and X transition metal complexes that participate in the oxidative cyclization often posses strong donor ligands, e.g. Cp, oxazolines, phosphines, or trispyrazolylborate (Scheme 7).[12]

Scheme 7. Oxidative cyclizations of alkynes and low valent transition metal centers bearing strongly electron donating ligands.

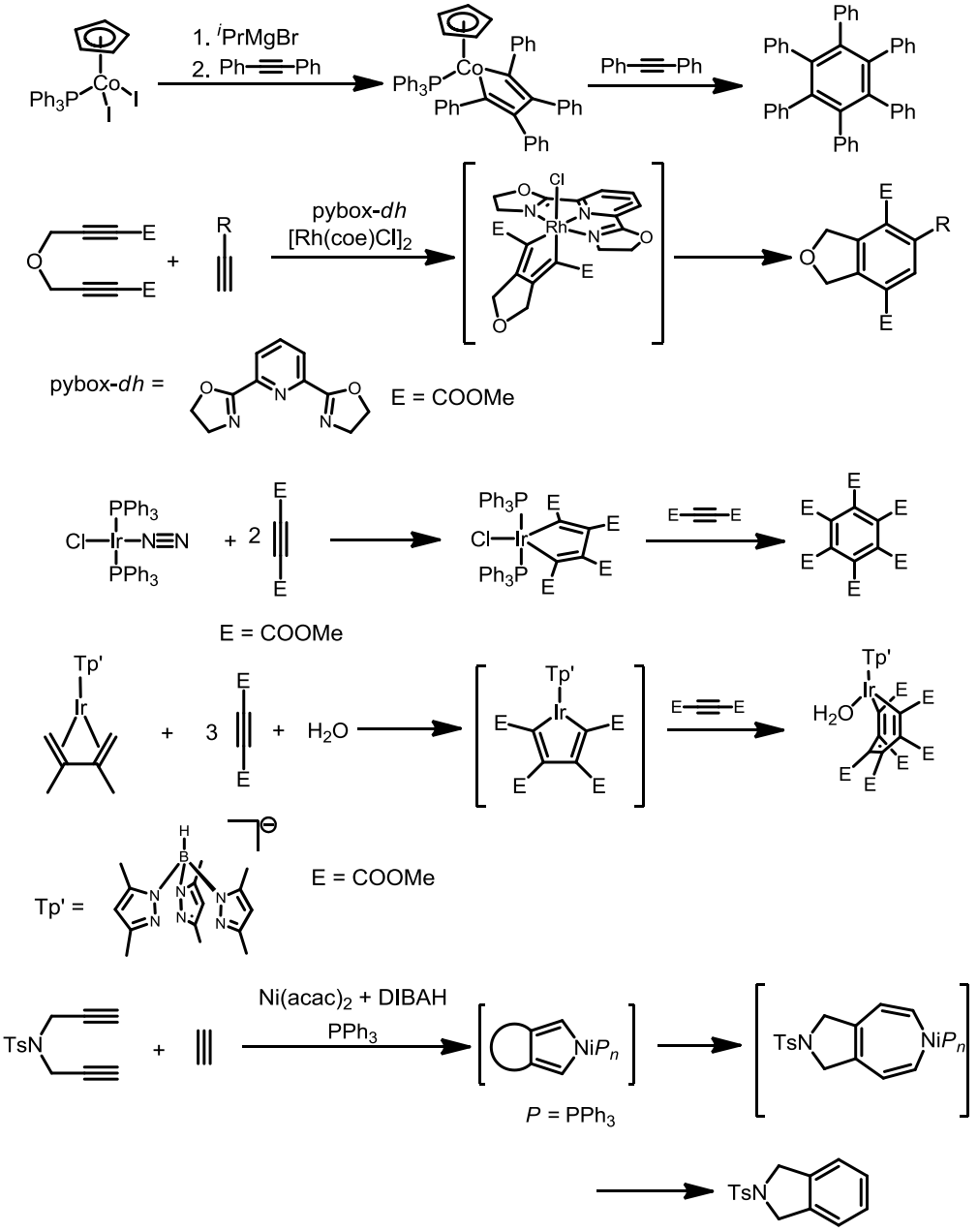

These examples point out the importance of electronic effect of ligand in oxidative cyclization events. Based on this facts, Cp* ligand, which has five inductively electron-donating substituents on it, is likely to contribute to the catalytic activity in terms of electronic effect.

Putting the above discussions together, the elimination of methyl substituents from the ligand is expected to deliver two contradictory effects; the promotion of access to the metal center, and reduced electron density on the metal center. Hence, it is assumed that the a polymethylcyclopentadienyl ligand bearing intermediate methyl substituents between Cp* and Cp would attain a best balance of steric and electronic effects, and would provide better catalytic activity (Figure 4).

Figure 4. Contradictory two effects exerted by methyl substituents and tuning of the substitution patterns.

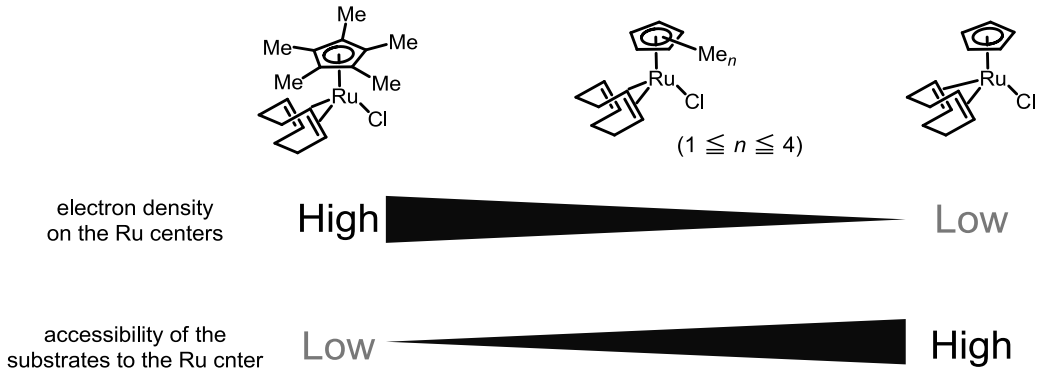

Thus far, the variety of the [Cp′RuCl]-type complexes is practically limited to those having Cp*, Cp, and indenyl as the planer ligand, and the steric and electronic effects of the ligand have not been evaluated in detail. Hence systematic diversification of the ligand substitution pattern and detailed investigation of their behavior in catalysis is of great interest.

Herein, the preparation of the Cp′RuCl(cod) complexes having polymethylcyclopentadienyl ligands with all possible substitution numbers and position will be described first (Figure 5). Then, the electronic effect of the ligand will be discussed on the basis of comparison of electron richness on the ruthenium center. Lastly, catalytic activities and regioselectivities of the complexes in alkyne [2+2+2] cycloaddition will be reported.

Figure 5. Newly prepared and evaluated complexes in this study.

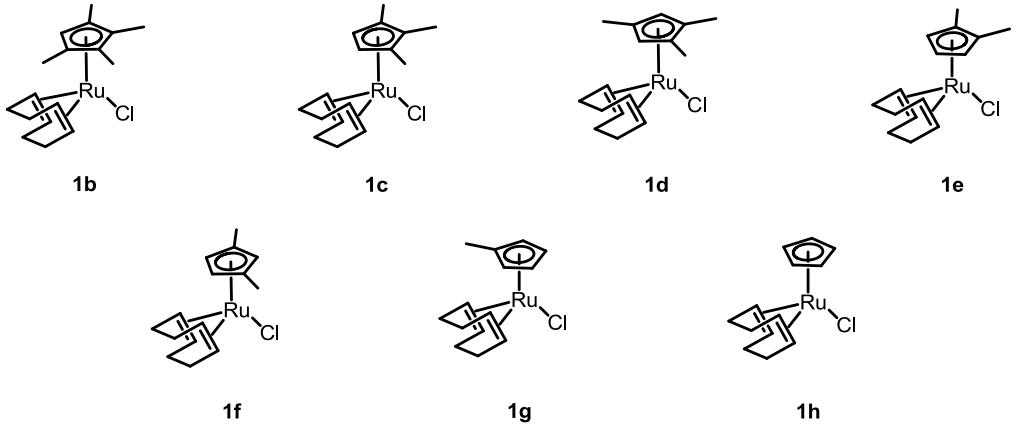

2. Development of Synthetic Route to Novel Polymethylcyclopentadienyl Ruthenium(II) Complexes

In the initial phase of the study, synthesis of (Cp^{Me4})RuCl(cod) (**1b**) through a route applied to Cp*RuCl(cod)[13] was attempted. Even though, the ligand Cp^{Me4} is quite similar to Cp*, yields of a dinuclear complex [$Cp^{Me4}RuCl_2]_2$ (**9b**) and desired **1b** were too low to adopt as standard synthetic procedure (Scheme 8).

Scheme 8. Attempted synthesis of Cp^{Me4}RuCl(cod) through a route applied to the synthesis of **1a**.

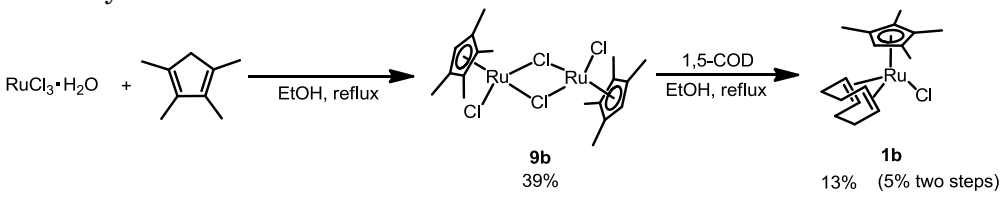

Next, a route that involve diphosphine complexes of type Cp′RuCl(PPh_3)$_2$ was examined. Ito and co-workers have reported that, on oxidative addition of allyl chloride, CpRuCl(PPh_3)$_2$ (**10h**) affords CpRuCl$_2$(η^3-C_3H_5) (**11h**), and the phosphine ligand is removed in the form of phosphonium salt.[14] Treatment of thus obtained tetravalent π-allyl ruthenium complex gives methyl complex **12h**. At elevated temperature (>100 °C), reductive elimination of 1-butene afford divalent [CpRuCl] fragment, and it is capture by added ligand to give isolable complex

CpRuC(cod) (**1h**) (Scheme 9).[15] In the alkylation step, $AlEt_3$ is also useful as well. In this case, the reductive elimination takes place at room temperature.[16]

Scheme 9. Elimination of phosphine ligand and reduction of a Ru(IV) species.

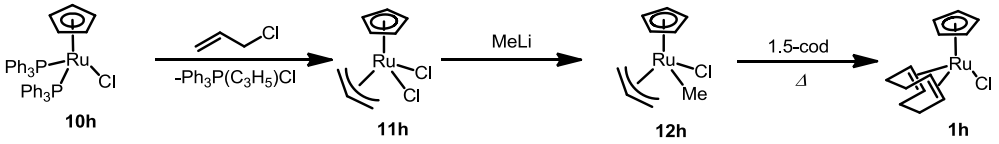

To apply this route for the synthesis of $(Cp^{Me4})RuCl(cod)$ (**1b**), preparation $(Cp^{Me4})RuCl(PPh_3)_2$ (**10b**) was attempted according to Wilkinson's procedure[17], in which $RuCl_3$ is treated with the cyclopentadienyl ligand precursor and phosphine in refluxing ethanol. However, **10b** was not formed in this case, and black crystalline product which was considered to be $RuCl_2(PPh_3)_3$ was obtained instead.

As described above, $[Cp^{Me4}RuCl]$ fragment could not be accessed by simply mimicking existing routes to Cp or Cp*Ru complexes. Next, oxidative addition of Cp^{Me4}–H to zero valent Ru source $Ru_3(CO)_3$[18] was tested, whose applicability was proven for the construction of [Cp′Ru] fragments, where Cp′ = Cp,[18] Cp*,[19a] Cp^{EtMe4},[19b] indenyl[19c]. Mononuclear complex **14** can be obtained by oxidative cleavage of the divalent precursor **13**. In most cases, carbonyl ligand coordinates to the electron rich metal center too strong to be eliminated. In the case of **14**, two carbonyl ligands are known to be removable by treatment with allyl halides (Scheme 10).[15,20] Obtained π–allyl complex **12** is expected to be reduced as shown in Scheme 9.

Scheme 10. Syntheis of $[Cp'Ru(CO)_2]_2$, oxidative cleavage and decarbonylation with by treatment with allylchloride.

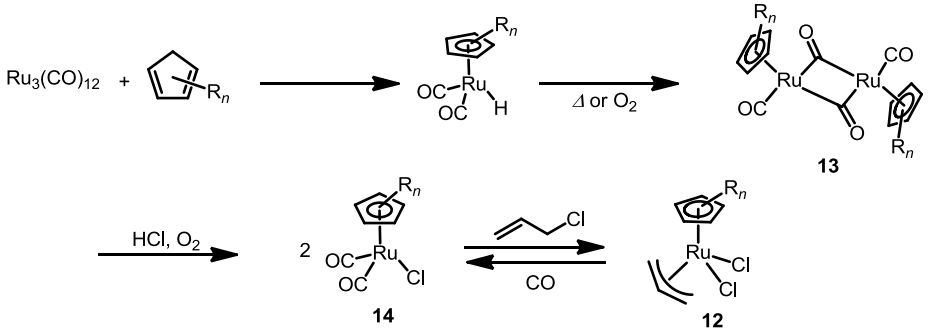

For the preparation of complexes $[Cp^{Men}Ru(CO)_2]_2$ (n = 2–4) (**13b-f**), conditions for $[Cp^*Ru(CO)_2]_2$[19a] was applied (condition A, Scheme 11), and for those with n = 0 or 1 (**13g**, **h**), Humphrie's condition[21] for $[CpRu(CO)_2]_2$ was used (condition B).

Scheme 11. Synthesis of carbonyl bridged dinuclear complex $[Cp^{Men}Ru(CO)_2]_2$ (**13b-h**)

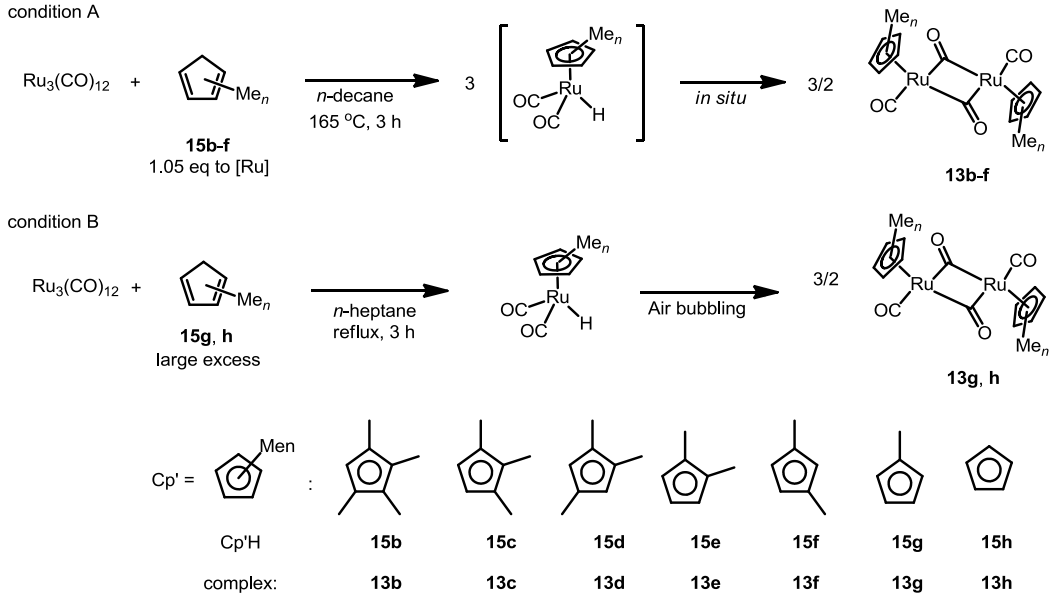

In the method A, excess addition of cyclopentadienyl ligand precursor resulted in low yield of desired intermediate complex **13** For example, excess ratio of **15d** vs. yield of **13d** is shown in Figure 6.

Figure 6. Correlation between mol equivalent of ligand precursor **15d** and yield of dimer complex **13d.**

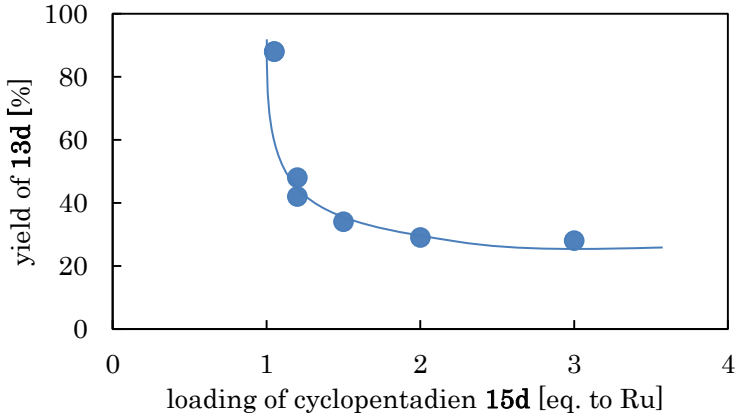

Obtained dimer complexes **13b-h** were oxidatively cleaved by air in the presence of hydrochloric acid to afford dicarbonyl mono nuclear complexes **14b-h** in good yields (Table 2).

Table 2. Yields of dinuclear complexes **13b–h** and their oxidatively-cleaved products **14b–h**.

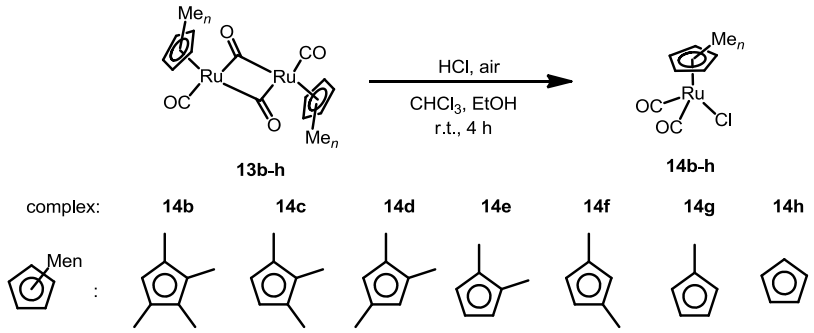

complex	**13b**	**13c**	**13d**	**13e**	**13f**	**13g**	**13h**
(method, eq. of Cp'H)	(A, 1.06)	(A, 1.05)	(A, 1.05)	(A, 1.06)	(A, 1.01)	(B, 44)	(B, 54)
yield [%]	82	88	88	86	87	79	54
complex	**14b**	**14c**	**14d**	**14e**	**14f**	**14g**	**14h**
yield [%]	92	81	91	70	82	83	56

Elimination of CO ligand from carbonyl complexes **14b**–**h** was achieved by a treatment with allyl chloride (**16-H**) as previously reported[15,20] (Table 3). Notably, in the synthesis of **12b**, yield diminished as initial concentration of allyl chloride increased (entries 1–3). According to the report by Ito *et al.*, this oxidative addition step is reversible in the presence of carbon monoxide. However, produced π-allyl complexes are scarcely soluble to decane solvent even at the reaction temperature (140 °C). Hence most of the product precipitates, and does not contribute to the equilibrium. As a result high conversion ratio was achieved. On the other hand, the product is highly soluble to allyl chloride. So, concentration of the product increases as initial concentration of the allyl chloride increases. As CO elimination by gas purge was not done in this system, addition of allyl chloride in large excess results in a decreased yield of the desired π-allyl complexes.

Among the obtained π-allyl complexes, **12**c and **12**e were not soluble to dichloromethane, which is used as solvent in the next reduction step. It was anticipated that solubility of the complexes can be enhanced by increasing the volume ration of organic part in the complexes. For this purpose, methallyl chloride (**16-Me**) was used instead. The η^3-methallyl complexes **17c**, **e** were obtained in comparable yield under the same condition (entries 5, 8). Gratifyingly, as expected, the obtained methallyl complexes **17c**, **e** were soluble in dichloromethane.

Table 3. Results of oxidative addition of allyl or methallyl chloride to Ru(II) dicarbonyl complexes **14b**–**h**.

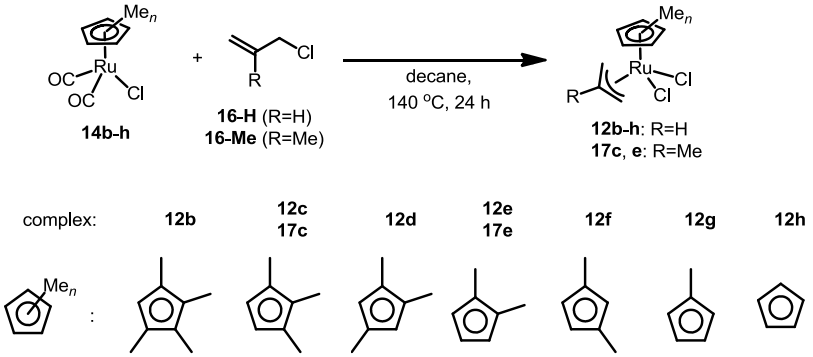

entry	dicarbonyl complex **14**	allyl (**16-H**) or methallyl (**16-Me**) chloride added (eq.)	time [h]	product, yield[%]
1	**14b**	**16-H** (50)	48	**12b**, 92
2	**14b**	**16-H** (100)	15	**12b**, 62 (37 %RSM)
3	**14b**	**16-H** (200)	15	**12b**, 20 (72 %RSM)
4	**14c**	**16-H** (20)	24	**12c**, 90
5	**14c**	**16-Me** (20)	24	**17c**, 76 (14 %RSM)
6	**14d**	**16-H** (20)	24	**12d**, 99
7	**14e**	**16-H** (20)	24	**12e,** 84
8	**14e**	**16-Me** (20)	24	**17e,** 91
9	**14f**	**16-H** (20)	24	**12f**, 75 (11% RSM)
9	**14g**	**16-H** (20)	24	**12g,** 76 (23% RSM)
10	**14h**	**16-H** (20)	8	**12h**, 43 (33% RSM)

Reduction of tetravalent Ru complexes **12b**, **d**, **f**–**h** and **17c**, **e** and capture by 1,5–cyclooctadiene proceeded under same condition for all precursors to give desired complex in moderate yields. Complexes **1b**–**g** could be isolated and purified under ambient atmosphere (Table 4).

Table 4. Reduction of Ru allyl or methallyl complexes with triethylaluminum followed by capture by 1,5-COD.

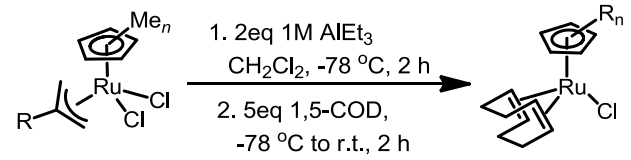

12b, **d**, **f-h**: R = H
17c, **e**: R = Me

1b-h

complex	**1b**	**1c**	**1d**	**1e**	**1f**	**1g**	**1h**
	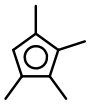	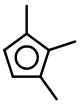	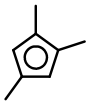		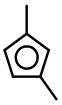		
yield [%]	55	58	58	41	53	44	26

3. Evaluation of Electron Density on the Ruthenium Center

According to the discussion in the chapter 1, the oxidative cyclization between two alkyne moieties and the Ru(II) constitutes the late-limiting step in the alkyne [2+2+2] cycloaddition. This leads to an assumption that higher electron density on the ruthenium center will facilitate the catalytic reaction. Hence the relationship between electronic effect of the cyclopentadienyl ligand and substitution numbers and patterns on it is of interest. In this section, the order of electron density on the ruthenium centers of the newly prepared Ru(II) complexes are determined by means of physicochemical measures.

Carbonyl ligand accepts back donation form a metal center in its π^*-orbital, and exhibits lower C–O stretching frequency than free carbon monoxide. Therefore, by tracing ν_{CO} shift of carbonyl complexes, relative strength of electron donation from a series of ligands can be determined. Keiser *et al.* have compared ν_{CO} of divalent zirconocene dicarbonyl complexes

$Cp'_2Zr(CO)_2$ with various Cp′ ligands.[22] Symmetric and asymmetric stretch of C–O was observed. Wavenumbers of both stretching mode decreased as the number of electron-donating substituents on the cyclopentadienyl group increases. The average wavenumber of the two IR absorption ν_{CO}(av) is sufficiently represented by eq 1, where σ_m is Hammet's meta substituent parameter.

Figure 7. Two C–O stretching of carbonyl ligands in divalent zirconocene

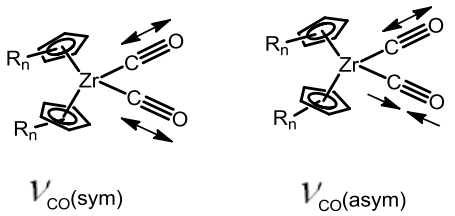

$\nu_{CO(sym)}$ $\nu_{CO(asym)}$

$$\nu_{CO}(av) = 48.3\Sigma\sigma_m + 1932.0 \quad [cm^{-1}] \qquad (1)$$

In the present research, dicarbonyl complexes **14b**–**h** used as synthetic intermediate are suitable for this purpose. IR absorption of Cp*RuCl(CO)$_2$ (**14a**) in CH_2Cl_2 solution was measured (2025, 1975 cm^{-1}) by Ito and co-workers.[14] Complexes **14b**–**h** were tested under the same condition. Wavenumbers correspond to symmetric stretching (ν_{CO}(sym)) and asymmetric stretch (ν_{CO}(asym)) is plotted in Figure 8.

Figure 8. Plot of C–O stretching wavenumber ν_{CO} vs. numbers of methyl substituents *N*.

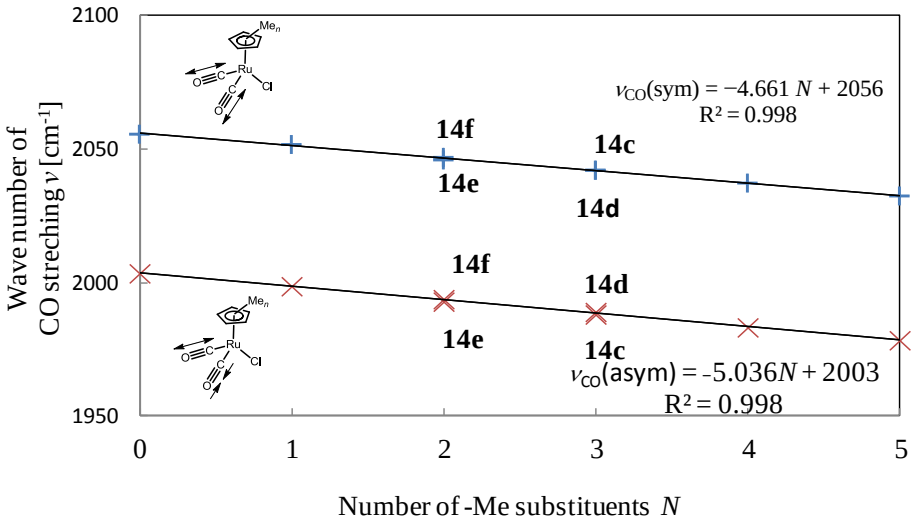

Both ν_{CO}(sym) and ν_{CO}(asym) were in liner relationship with methyl substitution number *N*. The absorbed IR wavenumber decreased with the increase of *N*, indicative of increasing electron density on the ruthenium center. Another notable point is that pared complexes with same substitution numbers but with different substitution positions (pares **14e**, **f** and **14c**, **d**) gave almost identical absorption in both modes.

When the correlation of average wavenumbers of two modes for each complexes and sum of Hammet's parameter of substituents ($\Sigma\sigma_m = N\sigma_m(Me)$) is taken, the result is well approximated with eq 2.

$$\nu_{CO}(av) = 70.3\Sigma\sigma_m + 2030 \ [cm^{-1}] \qquad (2)$$

In comparison with eq 1, the slope is about 1.5 times larger. This result indicates that effect on the electron density on the metal centers exerted by the substituents on the cyclopentadienyl ligand is greater in the ruthenium complexes than in zirconocenes.

Another frequently applied technique for the evaluation of electronic effects on a metal center is oxidation potential measurement, most commonly cyclic voltammetry. Above described method is a rather indirect way which relies on an interaction between a CO and a metal center. On the other hand, the assessment by the oxidation potential is more direct method in which a potential accessible to the frontier orbital of the complex is surveyed.

Previously reported electrochemical studies on Cp′RuL_2X-type complexes have focused on diphosphine complexes of type Cp′RuP_2X, where P_2 represents bidentate phosphine ligands or two monodentate phosphines; X = H or Cl.[23] Hence, optimal conditions for CV measurement of Cp′RuCl(cod)-type complexes were newly screened for the present study.

The CV measurement was performed with standard 3-electrode procedure. Although acetonitrile is a frequently used solvent in electrochemistry, **1a** gave unidentified dark brown precipitate in MeCN. Among the solvents tested, 1,2-dichloroethane was unreactive with the complex, and showed wide potential window on anodic side.

Wide-range cyclic voltammogram of the complex Cp*RuCl(cod) (**1a**) is shown in Figure 9. Two waves corresponds to oxidation and reduction was observed (a and b respectively).

Figure 9. Cyclic voltammogram of **1a** in wide range.

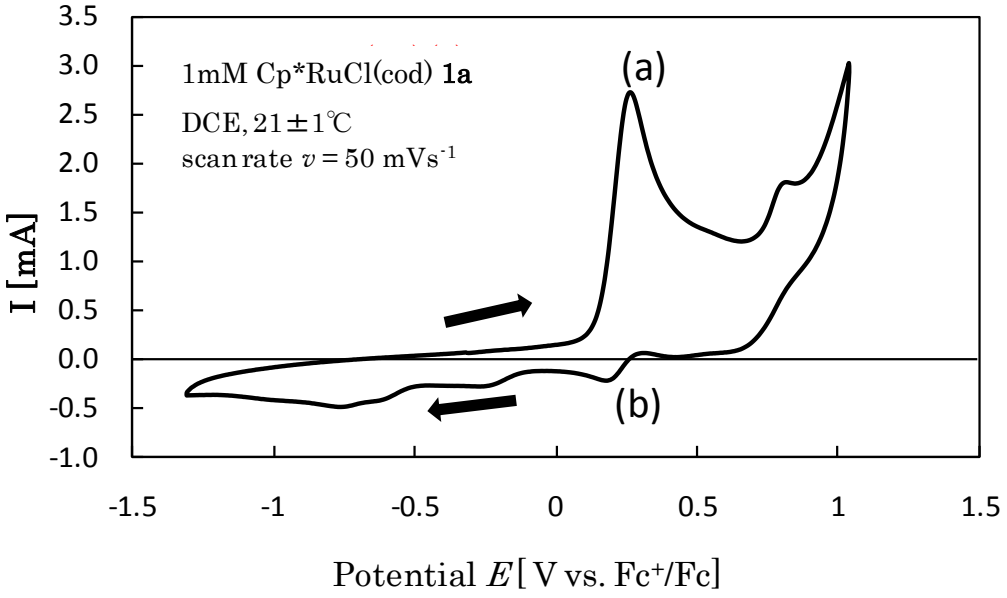

Detailed scanning around the region including the redox waves of **1a** was measured at scanning rate $10 \leq v \leq 500$ [mV/s] (Figure 10, Table 5).

As can be seen in entries 1 and 2, the ratio of reduction current to oxidation current I_{pc} / I_{pa} was small when scan rate was lower than 20 mV/S. This result implies that anodized product is short living. In fact, with the scan rates equal to or faster than 50 mV/s, I_{pc} / I_{pa} were almost equal to unity. (entries 3–8). While v was between 10 and 100 mV/s, peak splitting $\Delta E_p = E_{pa} - E_{pc}$ lies in the range 64–80 mV. These values are larger but sufficiently near to theoretical value of one electron oxidation.[24] Judging from these facts, observed redox event was assigned to 1 electron process depicted in Scheme 12.

Figure 10. Locally scanned voltammogram of **1a** at various rate *v*.

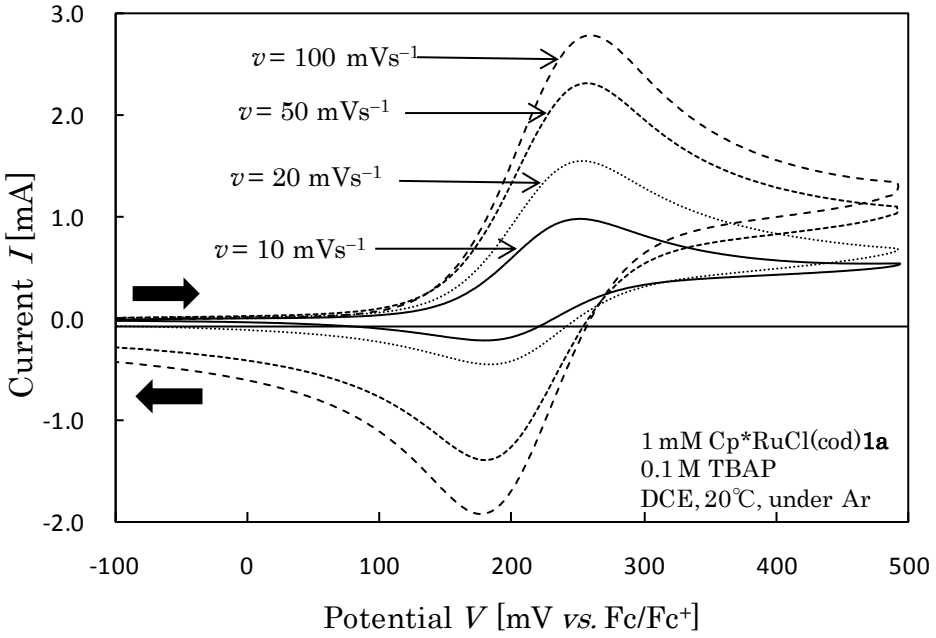

Table 5. Dependence of measured electrochemical parameters of **1a** on scan rate *v*.

entry	v [mVs^{-1}]	E_{pa} [V *vs.* Fc/Fc^+]	E_{pc} [mV *vs.* Fc/Fc^+]	$E_{1/2}$ [mV vs. Fc/Fc^+]	ΔE_p [mV]	I_{pc} / I_{pa}
1	10	251	182	217	69	0.52
2	20	252	188	220	64	0.43
3	50	255	181	218	75	0.82
4	100	259	179	219	80	0.91
5	200	263	175	219	89	0.92
6	300	268	172	220	96	0.92
7	400	273	168	221	105	0.92
8	500	279	162	221	116	0.75

condition: 1 mM Cp*RuCl(cod) (**1a**), 0.1 M TBAP / 1,2-dichloroethane; 20 ± 1 °C; under Ar atmosphere.

Scheme 12. One electron redox process of **1a** observed in the cyclic voltammetry.

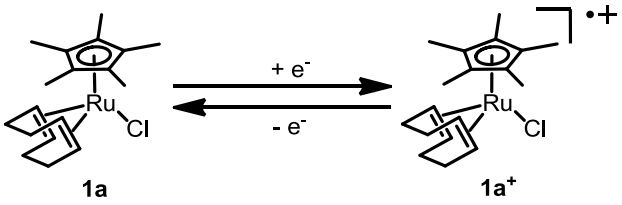

Considering the electrochemical reversibility and the lifetime of the oxidized species, following CV measurements of complexes **1b–h** were carried out at v = 100 mV/s. The results are summarized in Table 6 and plotted in Figure 11. The half-wave potentials of the complexes decreased as the substitution number increased. In addition, the oxidation potential was predominantly determined by substitution numbers while substitution patterns had limited influence on it. This trend was consistent with the one revealed by the IR observation. According to the liner plot of the $E_{1/2}$ vs N, contribution of one methyl group was estimated to −47.0 mV. Keister and co-workers have reported that in $(Cp^{Mem})(Cp^{Men})ZrCl_2$ series, oxidation potential shifted −25.5 mV per one methyl group.

Eventually, these evidences resulted in the same conclusion derived from IR observation, which says that the electron density of the Cp′Ru-type complex is more sensitive to the substitution umbers on the cyclopentadienyl ligand than the zirconocene complexes. At the same time, substitution position exerted little influence on it.

Table 6. Electrochemical parameters obtained for complexes **1a–i**

entry	complex	E_{pa} [mV *vs.* Fc/Fc$^+$]	E_{pc} [mV *vs.* Fc/Fc$^+$]	$E_{1/2}$ [mV *vs.* Fc/Fc$^+$]	ΔE_p
1	Cp*RuCl(cod) (**1a**)	263	179	221	84
2	Cp^{Me4}RuCl(cod) (**1b**)	278	203	241	75
3	Cp$^{1,2,3\text{-}Me3}$RuCl(cod) (**1c**)	317	238	277	79
4	Cp$^{1,2,4\text{-}Me3}$RuCl(cod) (**1d**)	334	260	297	74
5	Cp$^{1,2\text{-}Me2}$RuCl(cod) (**1e**)	363	284	323	79
6	Cp$^{1,3\text{-}Me2}$RuCl(cod) (**1f**)	381	300	340	81
7	Cp^{Me}RuCl(cod) (**1g**)	427	349	388	78
8	CpRuCl(cod) (**1h**)	487	415	451	72
9	IndRuCl(cod) (**1i**)	502	423	462	79

condition: v = 100 mV/s; 1 mM sample, 0.1 M TBAP / 1,2-dichloro ethane; 21 ± 1 °C; under Ar atomosphere

Figure 11. Plot of half-wave potential $E_{1/2}$ and substitution numbers.

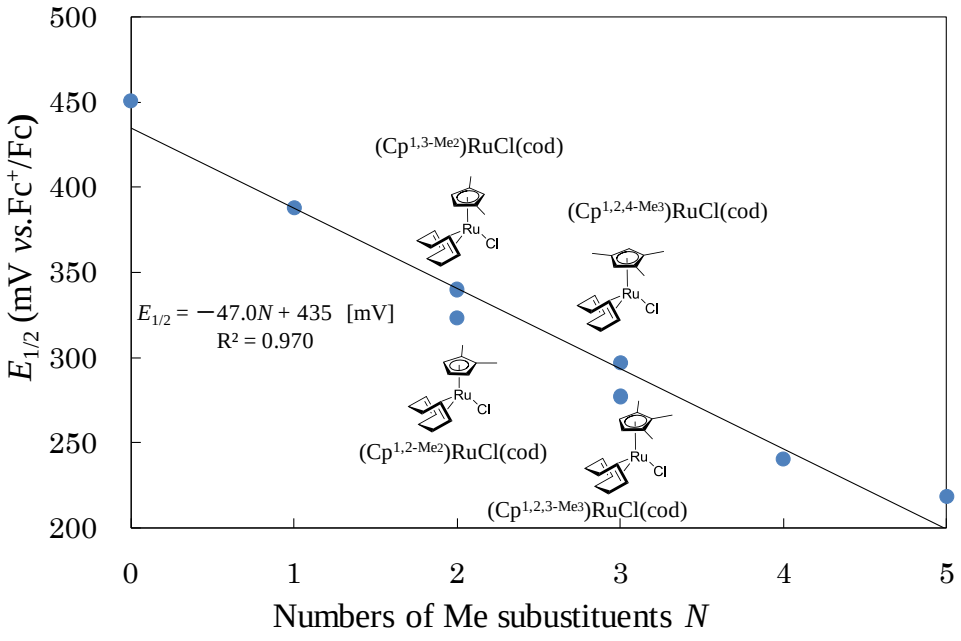

4. Evaluation of Catalytic Activity of Polymethylcyclopentadienyl Ruthenium(II) Complexes

(a) Turnover Numbers

The catalytic activity of the newly prepared complexes Cp´RuCl(cod) in [2+2+2] cycloaddition of 1,7-diiodo-4-oxa-1,6-heptadiyne (**18**) and acetylene was examined. In the test, the turnover numbers of each complexe in up to 3 hours at room temperature were compared. The reaction was trace by TLC analysis. The obtained results are shown in Table 7 and Figure 12.

In the entry 1–6, the reduction of the catalyst loading of **1a-c** from 2 mol% to 1 mol% and extended reaction time did not lead to increased TON, suggesting significant deactivation of the these complexes in the system. On the other hand, the complex ($Cp^{1,2,4\text{-}Me3}$)RuCl(cod) (**1d**) continuously increased its TON when the catalyst loading was reduced from 2 mol% to 0.5 mol% (entry 7–9). The complex with mono-substituted cyclopentadienyl ligand (Cp^{Me})RuCl(cod) (**1g**) exhibited similar trend (entry 13–14), but the results became erratic at low catalyst loading (entry 15).

Figure 12. The TON of complexes summarized in Table 7.

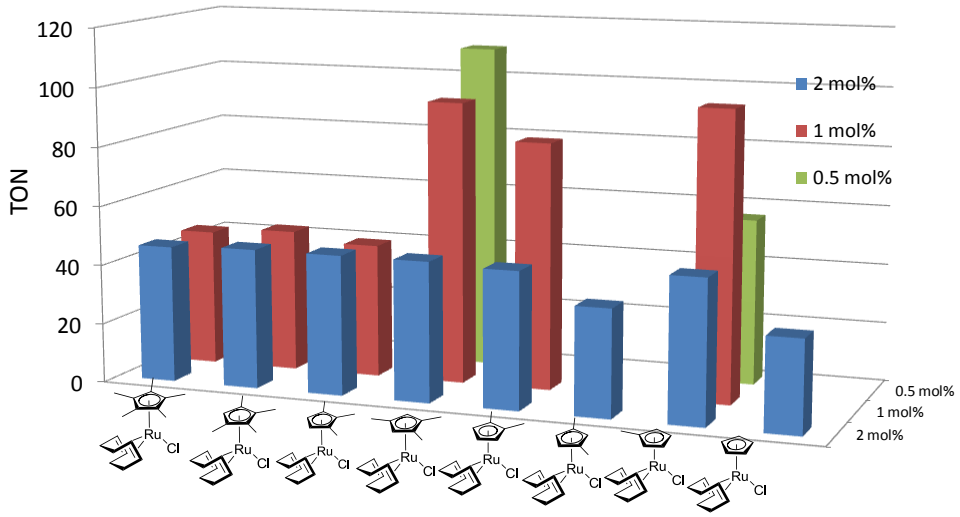

Table 7. TON and TOF of complexes **1a**–**h**.

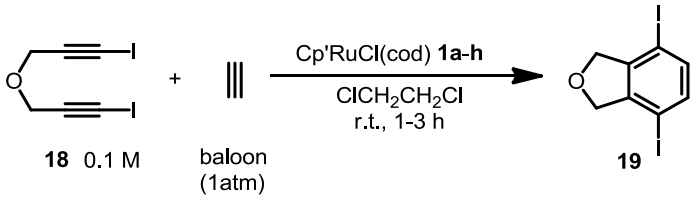

entry	complex	catalyst loading [mol%]	time [h]	**19** yield [%]	TON	TOF [h^{-1}]
1	Cp*RuCl(cod) (**1a**)	2.0	1	91	46	46
2		1.0	3	46 (RSM 53%)	46	15
3	(Cp^{Me4})RuCl(cod) (**1b**)	2.0	1	93	47	47
4		1.0	3	48 (RSM 49%)	48	16
5	($Cp^{1,2,3\text{-}Me3}$)RuCl(cod) (**1c**)	2.0	1	94	47	47
6		1.0	3	45 (RSM 52%)	45	15
7	($Cp^{1,2,4\text{-}Me3}$)RuCl(cod) (**1d**)	2.0	1	94	47	47
8		1.0	1	95	95	95
9		0.50	3	55 (RSM 40%)	110	37
10	($Cp^{1,2\text{-}Me2}$)RuCl(cod) (**1e**)	2.0	1	92	46	46
11		1.0	3	83 (RSM 7.3%)	83	28
12	($Cp^{1,3\text{-}Me2}$)RuCl(cod) (**1f**)	2.0	3	72 (RSM 20%)	36	12
13	(Cp^{Me})RuCl(cod) (**1g**)	2.0	1	96	48	48
14		1.0	1	97	97	97
15		0.50	3	28 (RSM 70%)	56	19
16	CpRuCl(cod) (**1h**)	2.0	3	61 (RSM 30%)	31	10

The potentially robust catalysts **1d** and **1g**, was further tested at lower catalyst loadings and in an extended reaction time (Table 8). Reflecting the expected robustness, both complexes attained improved yield of **19**. Especially, with 0.1 mol% of **1d**, the substrate was completely consumed to afford **19** in 97% yield, and the TON of the catalyst reached 970, which is exceptionally high in a series of [Cp′Ru(II)]-catalyzed transformation of unsaturated compounds.

Table 8. Activity test for complexes **1d** and **1g** at low catalyst loading.

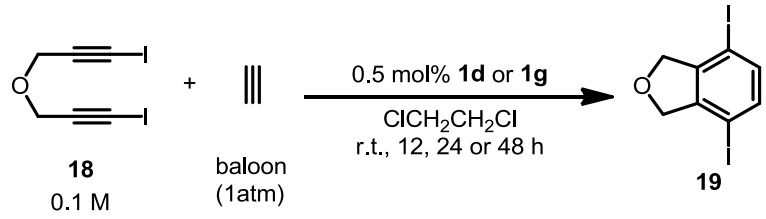

entry	complex	catalyst loading [mol%]	time [h]	**19** yield [%]	TON	TOF [h^{-1}]
1	$(Cp^{1,2,4\text{-}Me_3})RuCl(cod)$ (**1d**)	0.50	12	96	192	16
2		0.10	24	88 (RSM 10%)	880	37
3		0.10	48	97	970	20
4	$(Cp^{Me})RuCl(cod)$ (**1g**)	0.50	12	47 (RSM 50%)	94	7.8

The superior catalytic efficiency of **1d** and **1g** was observed even when the bulkiness of the monoyne component increased. In the [2+2+2] cycloaddition of the diiododiyne **18** and sterically-demanding tolan (**20**), performances of **1d, g** was compared with that of **1a** control specimen (Table 9). In this test reaction, much higher catalyst loading of 5 mol% was required. While, conventionally used **1a** afforded the product in only 26% yield in 12 h (entry 1), **1d** gave **21** in a fairly good yield of 73% in 6 hours, and the reaction completed in 12 hour to afford the product in 82% yield (entry 3). **1g** also showed significant efficiency in comparison with **1a** (entry 4).

Table 9. [2+2+2] cycloaddition of a diiododiyne **19** and tolan (**20**) catalyzed by **1a, d, g**.

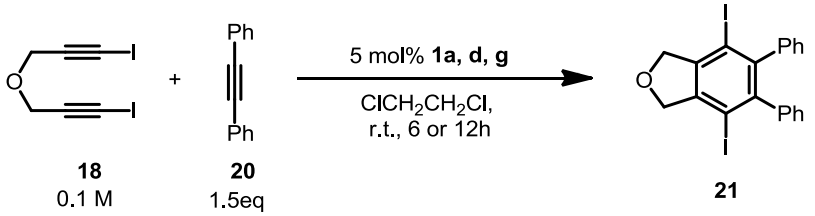

18 0.1 M + **20** 1.5eq → **21**

entry	catalyst	time [h]	**21** yield [%]	RSM **18** [%]
1	Cp*RuCl(cod) (**1a**)	12	26	55
2	($Cp^{1,2,4\text{-}Me3}$)RuCl(cod) (**1d**)	6	73	6.4
3	($Cp^{1,2,4\text{-}Me3}$)RuCl(cod) (**1d**)	12	82	0
4	(Cp^{Me})RuCl(cod) (**1g**)	12	68	5.2

(b) Catalytic Reaction Rates

Above results revealed that the complex **1d** and **1g** are efficient in that very limited amount of these complexes can lead the reaction to completion. Although this fact is of great importance from the view point of practical use of the catalyst, the relationship between the ligand structure and the high performance of these complexes are not elucidated. The turnover numbers of the catalysts depend on both robustness and reaction rate. At this stage, these factors have not been separately evaluated.

To shed light on the influence of the ligands' substitution pattern on the catalytic activity, the rate of the reactions catalyzed by complexes **1a-g** were measured at the initial stage where deactivation of the catalysts can be ignored. The [2+2+2] cycloaddition of the diiododiyne **18** and phenyl acetylene (**22)** was carried out in chloroform-*d*. The reaction was monitored by ^{1}H NMR. The concentration of the product was determined by comparing the peak area of 4 methylene protons and that of TMS protons in *p*-bis(trimethyl)benezene (**24**) added as an internal standard (Scheme 13).

Scheme 13. Test reaction for the comparison of initial reaction rate.

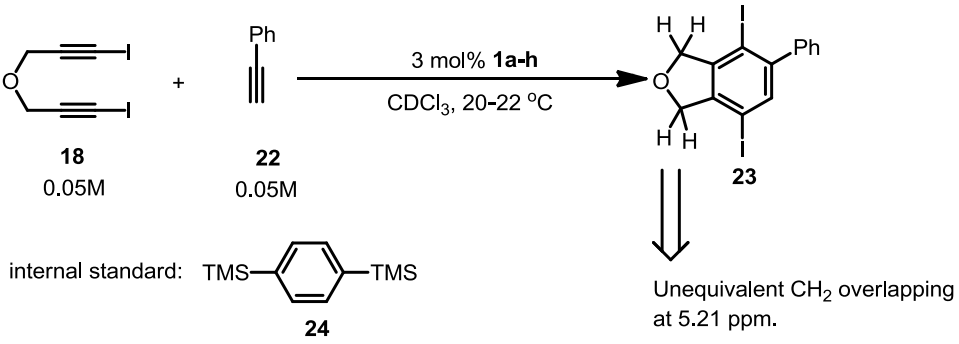

A concentration–time plot of the reaction catalyzed by 3 mol% of CpRuCl(cod) (**1h**) is shown in Figure 13 as an example. While the conversion of the substrate is lower than 10%, the plot is almost linear ($R^2 > 0.99$) (Figure 14).

Figure 13. Development of the concentration of the product **23** in the initial 1 hour of the reaction catalyzed by **1h**.

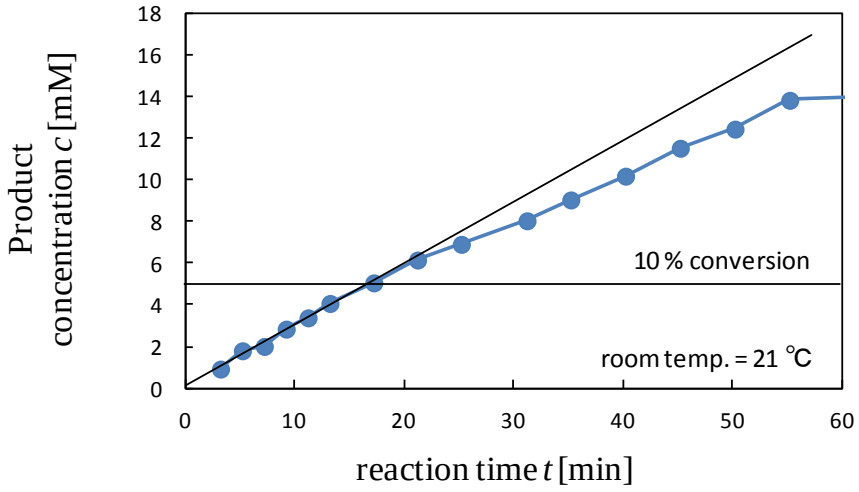

Figure 14. Magnification of Figure 13. During this interval (conversion < 10%), the plot showed a good linearity.

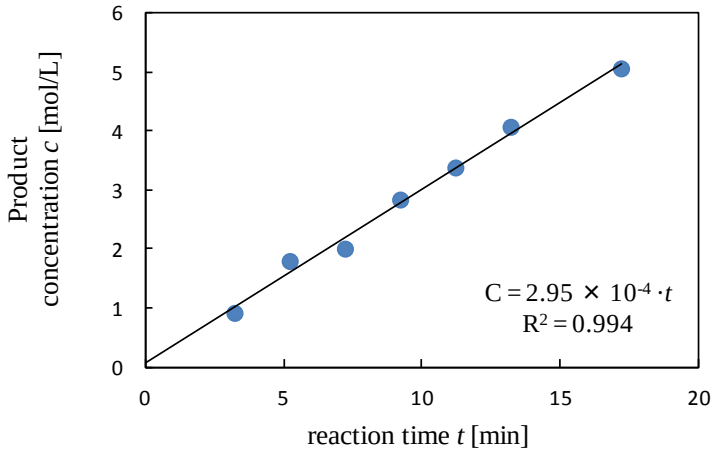

For all complexes, the concentration–time plot exhibited good linearity in the initial stage (where the conversion was less than 10%). The slope of the initial plot is adopted as the reaction rate, and summarized in Table 10 and Figure 15.

Table 10. Observed initial rates of the test reaction in Scheme 13.

entry	catalyst(**1a-h**)	diyne**18** [mM]	monoyne **22** [mM]	temp. [°C]	initial rate [μMmin^{-1}]
1	Cp*RuCl(cod) (**1a**) 1.49 mM	49.6	50	20	5.5 × 10
2	(Cp^{Me4})RuCl(cod) (**1b**) 1.49 mM	49.8	50	22	2.1 × 10^2
3	($Cp^{1,2,3-Me3}$)RuCl(cod) (**1c**) 1.49 mM	50.2	50	20	3.5 × 10^2
4	($Cp^{1,2,4-Me3}$)RuCl(cod) (**1d**) 1.49mM	50.0	50	20	3.4 × 10^2
5	($Cp^{1,2-Me2}$)RuCl(cod) (**1e**) 1.51 mM	50.2	50	21	4.4 × 10^2
6	($Cp^{1,3-Me2}$)RuCl(cod) (**1f**) 1.48 mM	49.8	50	21	4.1 × 10^2
7	(Cp^{Me})RuCl(cod) (**1g**) 1.49 mM	50.3	50	21	5.4 × 10^2
8	CpRuCl(cod) (**1h**) 1.48 mM	50.1	50	21	3.0 × 10^2

Figure 15. Comparison of the initial rates of reactions catalyzed by **1a-h**.

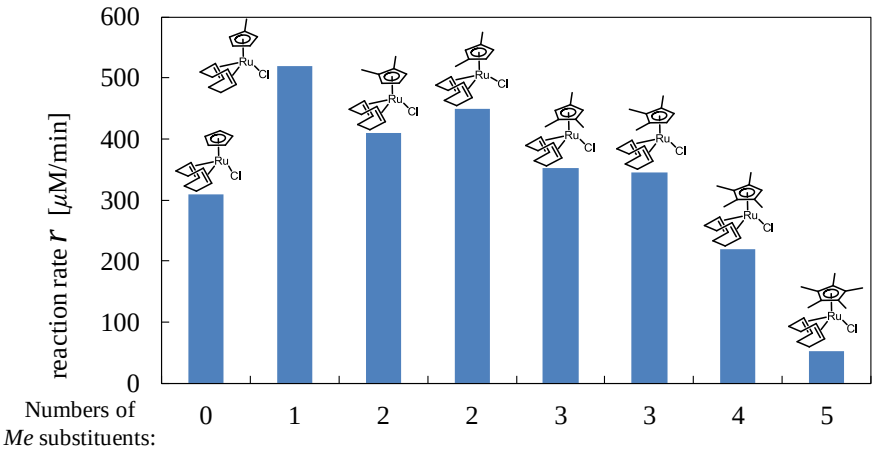

Except for CpRuCl(cod) (**1h**) the reaction rate increased as the substitution numbers on the cyclopentadienyl ligand decreased. Even **1d**, which attained the best record in the TON comparison, is moderate in this series. This general trend suggests that the diminished steric hindrance and easy access to the ruthenium center is the key to the high catalytic activity. The significant deviation of the complex **1h** from this trend is attributable to the lowest electron density on ruthenium among these complexes. With these results in hand, it is most likely that the catalytic activity is mostly determined by steric effect to the ligand, whereas the electronic effect makes a partial contribution.

(c) Regioselectivities

To shed light on the detailed insight into the interaction between the substrates and Cp′ ligands, regioselectivity in [2+2+2] cycloaddition was compared.

When a unsymmetric diyne and a terminal alkyne or unsymmetric internal alkyne undergoes [2+2+2] cycloaddition, two regioisomeric arenes, namely *ortho* and *meta* isomers, are expected (Scheme 14).

Scheme 14. Two expected regioisomeric products produced in [2+2+2] cycloaddition of a dissymmetric diyne and a terminal alkyne.

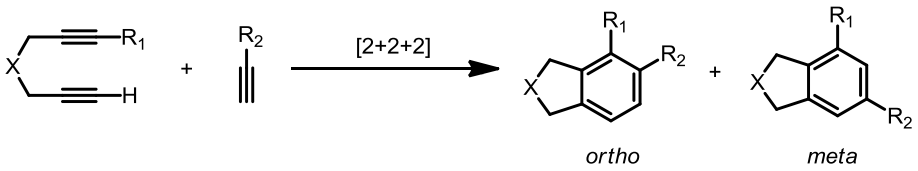

Previous reports on catalytic alkyne [2+2+2] cycloaddition reactions that proceed by way of metallacyclopentatriene or metallacyclopentadiene imply that the orientation of inbounding monoyne component is controlled by several factors. McDonald, Witulski and coworkers have reported regioselective [2+2+2] cycloaddition of unsymmetric diyne and monoyne by employing Wilkinson complex as the catalyst (Scheme 15).[25]

Scheme 15. Metaselective [2+2+2] cycloaddition of dissymmetric diynes and terminal monoynes catalyzed by Wilkinson complex.

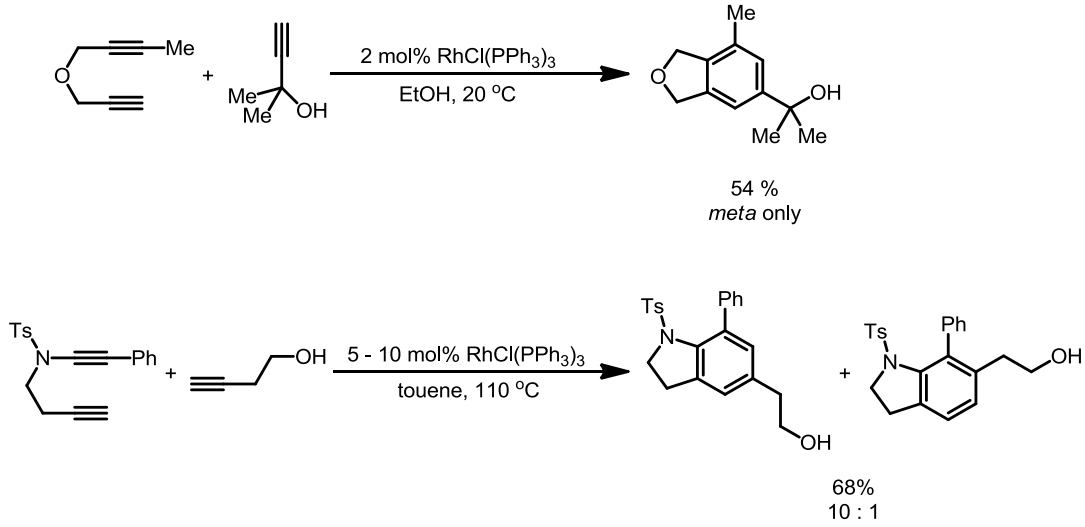

All of Wilkinson complex-catalyzed regioselective [2+2+2] cycloaddition reactions use propargyl or homopropargyl alcohol as monoyne components. Hence, coordination of their hydroxyl group to the metal center appears to play an important role in determining the regioselectivity. However, it is also revealed that a small structural difference of the substrates leads to low regioselectivity (Scheme 16).

Scheme 16. Diminished or reversed regioselectivity of Wilkinson complex-catalyzed [2+2+2] addition.

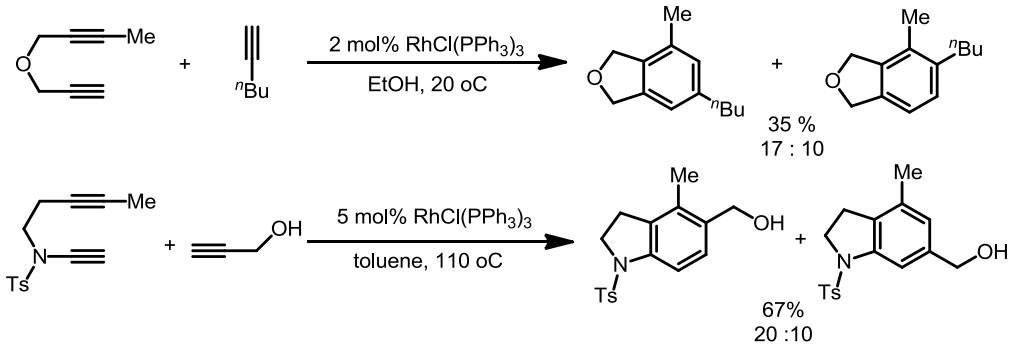

Yamamoto *et al.* have revealed that Cp*Ru-type complexes can catalyze [2+2+2] cycloaddition with high regioselectivity even when the monoyne components do not possess a coordinative directing group (Table 11).[10,26]

Table 11. Comparison of regioselectivity of alkyne [2+2+2] cycloadditions catalyzed by various transition metal complexes.

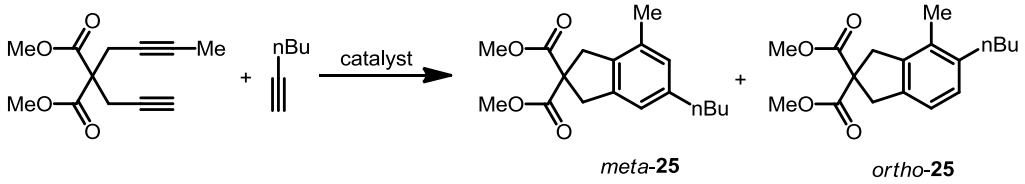

entry	catalyst (mol%)	**25** yield[%] (*meta* : *ortho*)
1	Cp*RuCl(cod) (1)	85 (93:7)
2	$[Cp^*RuCl_2]_2$ (0.5)	81 (94:6)
3	CpRuCl(cod) (1)	76 (87:13)
4	$RhCl(PPh_3)_3$ (5)	61 (63:37)
5	$Ni(cod)_2$/ $2PPh_3$ (15)	83 (30:70)
6	CpCo(cod) (20)	70 (54:46)

Wilkinson complex and $Ni^0/2PPh_3$ exhibit moderate regioselectivities, but as a stark difference from other catalysts, nickel catalyst is *ortho* selective (entry 5). On the other hand, both Cp*RuCl(cod) and $[Cp^*RuCl_2]_2$ shows good *meta* selectivity (entry 1, 2). Although CpRuCl(cod) is less selective than theses two, its selectivity level is still higher than other transition metal catalysts. Judging from these results, it is very likely that cyclopentadienyl-type

planar spectator ligands play a decisive role in realizing high regioselectivities. Hence, Cp′Co complexes are also expected to be regioselective. However, CpCp(cod) shows almost no regioselectivity (entry 6).

According to the proposed mechanism of [Cp'RyCl]-catalyzed [2+2+2] cycloaddition of alkynes, not only the cyclopentadienyl ligands but also chloride ligand on the ruthenium center is supposed to take part in the control of monoyne orientation (Scheme 17). In the [2+2] addition of a ruthenacyclopentatriene with a monoyne, four stereochemical routes are possible. If the [2+2] addition takes place on the substituted side (*cis*), the substituent R inbounds to the bulky pentamethylcyclopentadienyl ligand to give rise to a steric repulsion. Therefore the paths A and B are energetically unfavorable. Next, the reactions *via* path C and path D in which the reaction occurs on the unsubstituted side of the ruthenacyclopentatriene are compared. The monoyne orientations are reversed in two paths. When the monoyne approaches in *syn* fashion, in which the substituent (R′) on the monoyne points to the chloride ligand, there will be a significant repulsion between R′ and Cl. These steric interactions are absent only in the path C (*trans-anti*), and the *meta*-product is selectively formed. Herewith, the stereoselectivity will provide an important insight into the steric interaction between the ligands and substrates.

Scheme 17. The stereoselectivity originates from repulsions between the monoyne substituent R and Cp* ligand, and between R′ and Cl ligand.

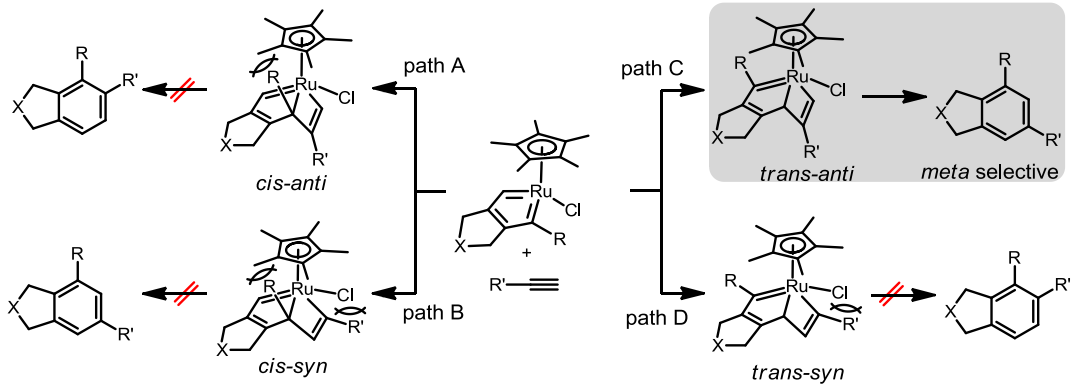

Thus fur, as mentioned in the introduction, parameters such as cone angle have been applied to compare the steric factor of cyclopentadienyl ligands. In this approach, when the substitution numbers of two ligands are same, the obtained steric parameter will be identical even if the substitution position is different (Scheme 18).

Scheme 18. The equivalency of two cyclopentadienyl ligands with a same substitution number but with differed substitution positions.

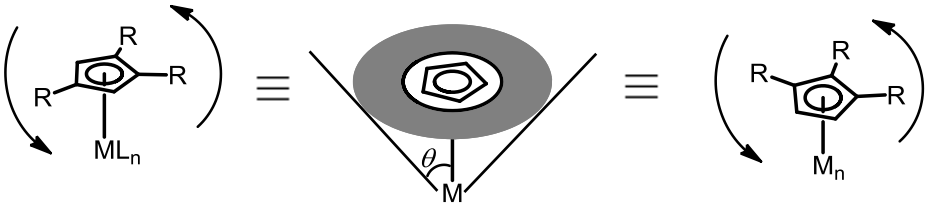

The validity of this approach should be tested. With the ruthenium complexes bearing polymethylcyclopentadienyl ligands with every possible substitution numbers and positions in hand, the author sought to elucidate the insight into the steric effect of the ligands.

In this study, [2+2+2] cycloaddition reaction shown in Table 12 was chosen as a test reaction. Steric interactions between the cyclopentadienyl ligands and bulky TMS group in **26** are expected to be distinctively reflected in the results. Additionally, the use of propargylmethyl ether (**27**) allows the easy purification of the products.

Table 12. The test reaction to examine the regioselctivities of newly prepared Cp'RuCl(cod) complexes.

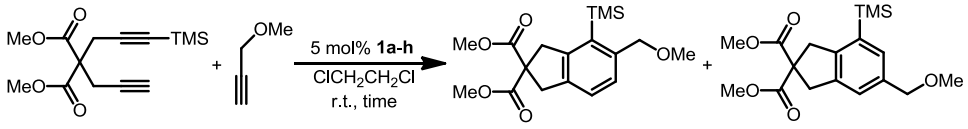

26 0.1 M | **27** 4 eq | *ortho*-**28** | *meta*-**28**

entry	complex	Time [h]	**28** ylield[a] [%] (*meta*:*ortho*)[b]
1	Cp*RuCl(cod) (**1a**)	6	96% (96:4)
2	(Cp^{Me4})RuCl(cod) (**1b**)	2	95% (80:20)
3	($Cp^{1,2,3\text{-}Me3}$)RuCl(cod) (**1c**)	12	45% (72:28) RSM 27%
4	($Cp^{1,2,4\text{-}Me3}$)RuCl(cod) (**1d**)	1	94% (82:18)
5	($Cp^{1,2\text{-}Me2}$)RuCl(cod) (**1e**)	12	41% (74:26) RSM 41%9
6	($Cp^{1,3\text{-}Me2}$)RuCl(cod) (**1f**)	3	79% (77:23)
7	(Cp^{Me})RuCl(cod) (**1g**)	12	53%(75:25) RSM 31%
8	CpRuCl(cod) (**1h**)	12	86% (74:26)

[a] Isolated yield. [b] Ratio determined by ^{1}H NMR analysis of crude mixture

The result shown in Table 12 can be categorized in following three groups: entry 1, entries{2,4}, entries{3,5,6,7,8}. This classification is connected to the maximum sizes of the methyl-deficient site on a cyclopentadienyl ligand (hereafter denoted as "pocket", Scheme 19).

Scheme 19. Definition of the "pocket" and its size.

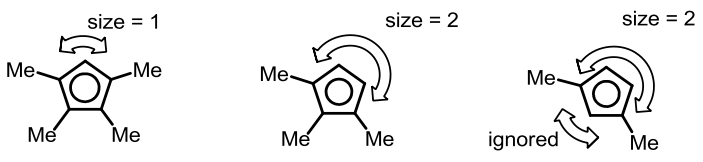

In the first group, the pocket size of Cp* ligand is 0, and selectivity was *meta*:*ortho* = 96:4. In the next group, entries{2,4}, the complexes with pocket size = 1 is employed, and *meta*:*ortho* ≈ 75:25 was observed. Finally, the pocket sizes are more than 2 in the entries{3,5,6,7}. In this case, selectivity was *meta*:*ortho* ≈ 75:25. The relationship between the selectivity for the ortho isomer and pocket size is illustrated in Figure 16.

Figure 16. The relationship between the *ortho* selectivity and the pocket size.

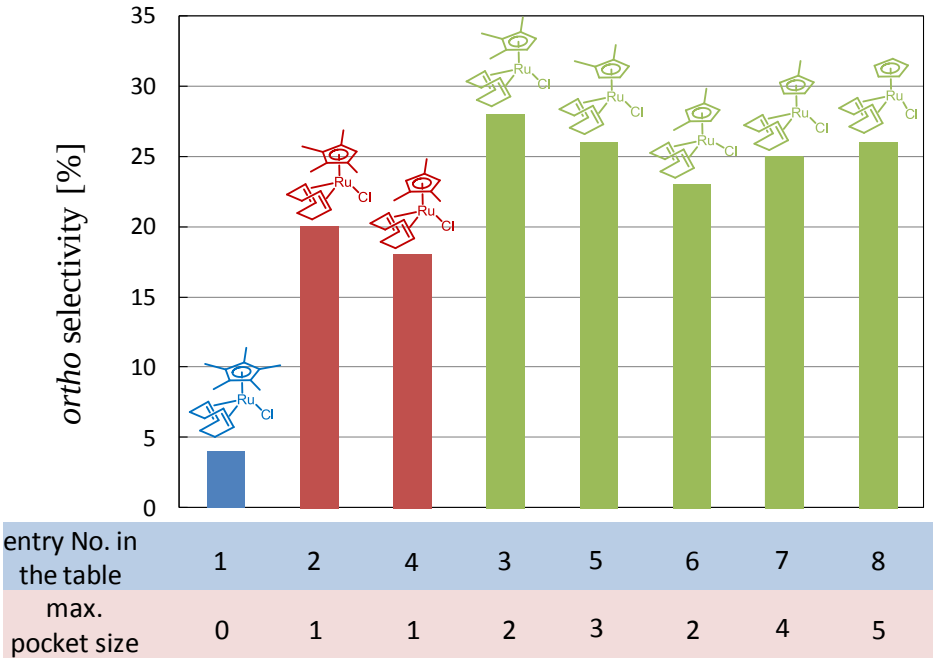

The trend can be accounted for as follows. The steric interaction in the ruthenacyclopentatriene generated from the dissymmetric diynes will be scrutinized below. When the diyne substrate bears a sterically bulky substituent, i.e. TMS, on one of its terminals, the conformation of the cyclopentadienyl ligand is affected by the steric interaction between the ligand and the bulky substituent. That is, the cyclopentadienyl ligand accommodates the bulky substituent in its pocket (Figure 17).

Figure 17. Accommodation of a bulky substituent in the pocket.

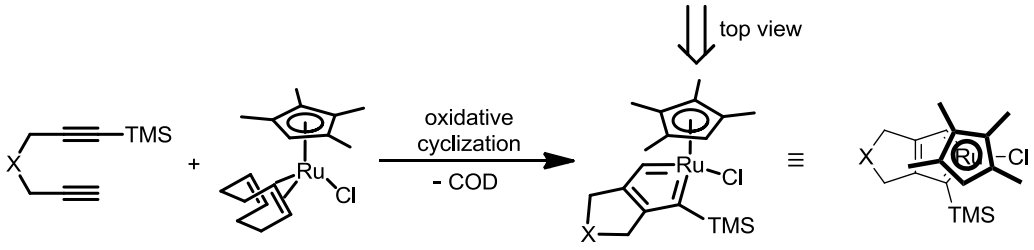

This illustration equivalent with the notion that the conformer **29** is dominant in comparison with other conformers (Scheme 20).

Scheme 20. Equilibrium of conformers in favor of **29**.

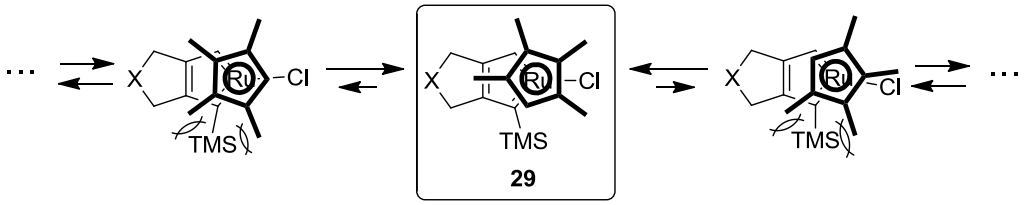

With this predominant conformer, the monoyne component undergoes [2+2] in *anti* manner. Hereafter, in the case of ruthenacyclopentatriene complex bearing the Cp′ ligand with a pocket size *m*, the rate constant of [2+2] addition on the substituted side (*cis*) will be represented by $k_{cis}(m)$ and the one on the unsubstituted side (*trans*) will be denoted as $k_{trans}(m)$ (Scheme 21).

Scheme 21. The definition of $k_{cis}(m)$ and $k_{trans}(m)$.

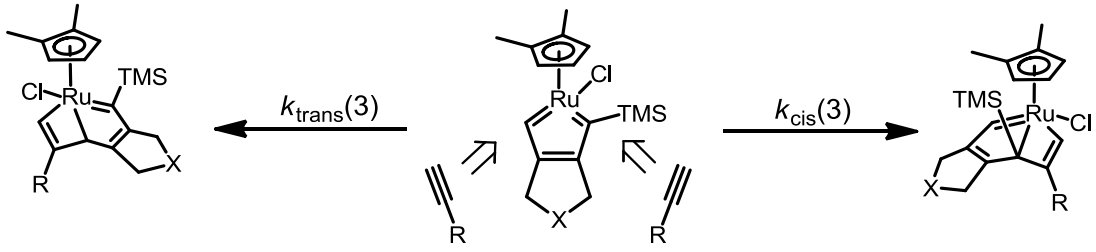

It is highly likely that while the pocket size m is smaller than or equal to 2, the $k_{cis}(m)$ ($0 \leq m \leq 2$) increases as m gets larger. When $m = 0$ (Cp*), because of the reason previously mentioned, the reaction on the *syn* side is virtually prohibited (box A, Scheme 22). When $m = 1$, the steric disadvantage of the reaction on the substituted side would be lowered. In this case, the substituent is expected to approach to an apex of the ligands (box B). As m increase to 2, the steric rigor will be further relaxed. The manner in which the ligand catches the substituent would be significantly different. With a ligand $m \geq 2$, it is reasonable to assume that the ligand reduces the steric repulsion by directing its edge toward the substituent (box C). In this case, only one edge is committed. Presumably, this is the reason why leveling effect in *ortho* selectivity was observed when the complexes bearing ligands with $m \geq 2$ were employed.

Scheme 22. The dependence of $k_{cis}(m)$ on the pocket size.

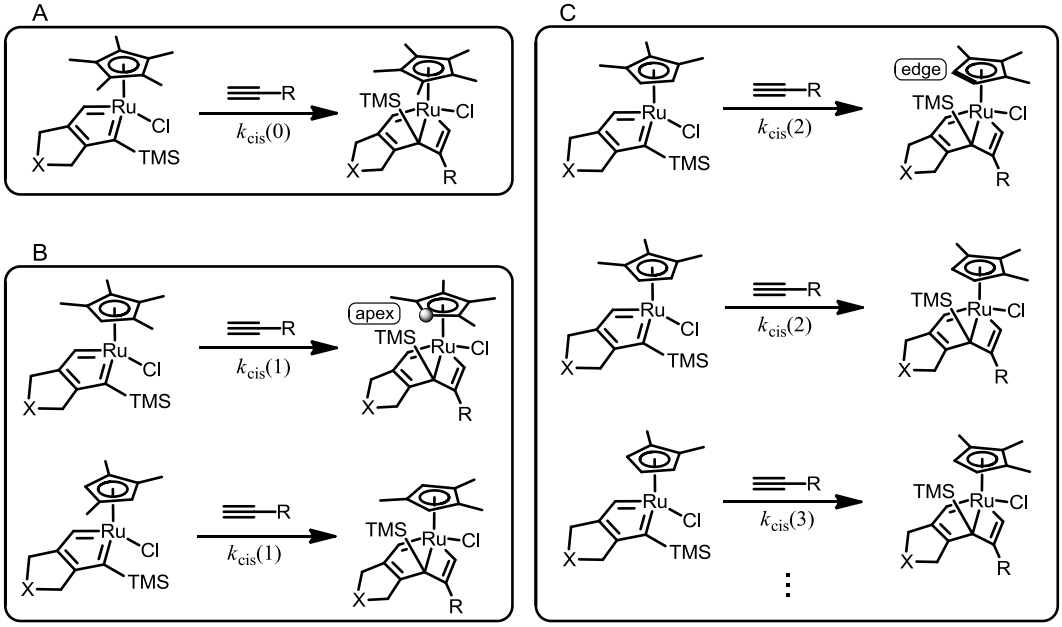

$$k_{cis}(0) < k_{cis}(1) < k_{cis}(2) = k_{cis}(3) = k_{cis}(4) = k_{cis}(5)$$

On the other hand, it is expected the $k_{trans}(m)$ would not enjoy the benefit from the reduced number of methyl substituents on the Cp′. This is simply because hydrogen atom is compact and the influence of the steric repulsion is originally small (Scheme 23).

Scheme 23. Independence of the $k_{trans}(m)$ from the pocket size.

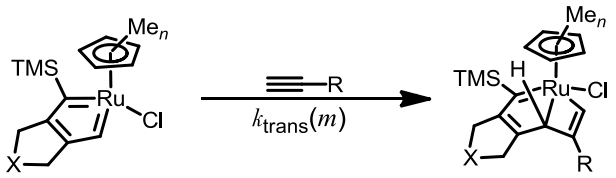

$$k_{trans}(0) = k_{trans}(1) = k_{trans}(2) = k_{trans}(3) = k_{trans}(4) = k_{trans}(5)$$

As mentioned in the outset, the application of cone angle has been extended to the prediction of steric effect of the cyclopentadienyl ligands. In that model, substitution positions on the ligands are not taken into consideration; i.e., the cyclopentadienyl ligands are assumed as isotropic because of the fast rotation around the metal–Cp centroid. The results obtained above suggest a picture which goes against the previously utilized model. At least in the case of [2+2+2] cycloaddition of a dissymmetric diyne and a monoyne, different assumption was required. It appears that the viable approach is the prediction on the interaction between a substrate and a specific site on a ligand.

(d) Tandem Cyclopropanation

As described in chapter 1, Yamamoto and co-workers have reported double cyclopropanation between a diyne and two molecules of norbornene.[27] It was suggested that the ring slippage of the planer ligand from η^5 to η^3 plays an important role in the reaction. This assumption was supported by the fact that a complex with an indenyl ligand, which has high propensity to ring slippage, exhibited higher selectivity for the cyclopropane product than normal [2+2+2] cycloadduct. Based on this point, the propensity of the newly prepared polymethylcyclopentadienyl ligand to the ring slippage was examined.

For abovementioned purpose, the reaction between diyne **30** and norbornene (**31**) was adopted as a probe (Table 13). As expected, (Ind)RuCl(cod) **1i** almost exclusively afforded

bis-cyclopropane **33**, although this catalyst showed much lower reactivity than others at room temperature (entry 9). Cp′ complexes **1a-h** fell into two major groups in terms of the chemoselectivity. Predominant formation of [2+2+2] cycloadduct **32** was observe for **1a–c**, and **1e**, with **1a** and **1c** showing superior (**32**):(**33**) selectivity of over 80:20. Lower selectivity of 73:27 was obtained using **1c** and **1e**. Interestingly, **1c** possessing the $Cp^{1,2,3\text{-}Me3}$ ligand was found to be the best catalyst for the formation of **32** with the highest efficiency. On the other hand, almost no chemoselectivity was observed for **1d**, **1f**, **1g** and **1h**. In these cases, it took several hours for the reaction to reach completion and the total yields were moderate, ranging from 55 to 73%.

Table 13. Selectivities of reaction of a diyne and norbornene catalyzed by **1a-i**.

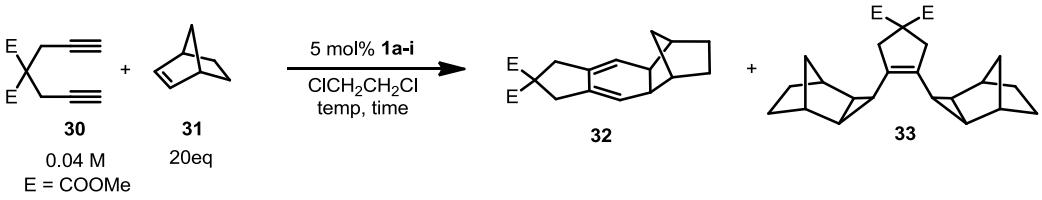

entry	complex	time [h]	**32** + **33** yield [%][a]	**32**:**33**[b]
1	Cp*RuCl(cod) (**1a**)	2	53	86 : 14
2	(Cp^{Me4})RuCl(cod) (**1b**)	1	63	73 : 27
3	$(Cp^{1,2,3-Me3})$RuCl(cod) (**1c**)	1	92	83 : 17
4	$(Cp^{1,2,4-Me3})$RuCl(cod) (**1d**)	4	70	45 : 55
5	$(Cp^{1,2-Me2})$RuCl(cod) (**1e**)	1	87	73 : 27
6	$(Cp^{1,3-Me2})$RuCl(cod) (**1f**)	3	73	43 : 57
7	(Cp^{Me})RuCl(cod) (**1g**)	1	65	50 : 50
8	CpRuCl(cod) (**1h**)	3	55	48 : 52
9	IndRuCl(cod) (**1i**)	24	37	1 : 99

[a] Isolated yields. [b] Ratio determined by ^{1}H NMR analysis of crude mixture.

According to these results, the ease of ligand slippage is roughly estimated as **1i** >> **1d**, **1f**, **1g**, **1h** > **1b**, **1e**> **1a**, **1c**.

The following interpretation of the above results is also justified provide that the mechanism outlined in Scheme 24 is considered. On the bases of DFT calculations, it was proposed that both product **32** and **33** are formed from the common ruthenacycle intermediate **34**. If the

reductive elimination takes place first, the second cyclopropanation of the resultant carbene follows to yield **33**. On the other hand, if the cleavage of the central Ru–C bond prevails, **34** is transformed into ruthenacycloheptadiene **35** and the subsequent reductive elimination occurs to deliver **32**. The product selectivity strongly depends on the nature of the diverging point **34**. It is expected that the reductive elimination producing the cyclopropane prevails when the electron donating ability of the cyclopentadienyl ligand is weak, and **34** bearing a tetra-valent ruthenium center is unstable (path A). On the other hand, if the ligand is highly substituted and electron donating, high oxidation state is stabilized. Hence, the cleavage of the central Ru–C bond in the bicyclic intermediate will occur by retaining the +IV oxidation state on the ruthenium center. The generated ruthenacycloheptadiene intermediate **35** will afford a [2+2+2] cycloaddition product **32** via reductive elimination (path B).

Scheme 24. Plausible mechanisms for the formation of **32** and **33**.

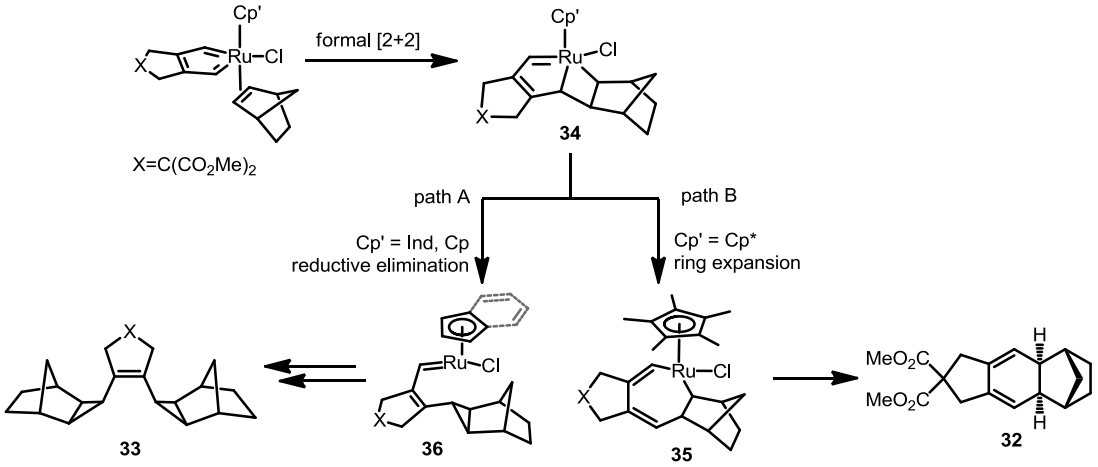

5. Experimental Section

(a) General Considerations.

Column chromatography was performed with silica gel (Cica silica gel 60N or Fuji Silysia FL100D) eluted with hexane or mixed solvents (hexane/ethyl acetate or hexane/CH_2Cl_2). ^1H and ^{13}C NMR spectra were obtained for samples in $CDCl_3$ solution at 25 °C. ^1H NMR chemical shifts are reported in terms of chemical shift (δ, ppm) relative to the singlet at 7.26 ppm for chloroform. Splitting patterns are designated as follows: s, singlet; d, doublet; t, triplet; q, quartet; quint, quintet; sext, sextet; sept, septet; m, multiplet. Coupling constants are reported in Hz. ^{13}C NMR spectra were fully decoupled and are reported in terms of chemical shift (δ, ppm) relative to the triplet at δ = 77.0 ppm for $CDCl_3$. EI mass measurements were performed with a Shimadzu GCMS-QP2010 plus mass spectrometer. Elemental analyses were performed at the Center for Advanced Materials Analysis at the Tokyo Institute of Technology. Melting points were obtained in capillary tubes by Yamato MP-21. Cyclic voltammetric measurements were carried out with Hokuto-Denko potentiostat/galvanostat HSV-100. Standard three-electrode technique was used under dry argon atmosphere in 1,2-dichloroethane containing 0.1 M tetra-*n*-butylammonium perchlorate. The working electrode was 1.6 mm diameter platinum disk and the counter electrode was platinum wire. All potentials were reported relative to the ferrocene half-wave potential. Ruthenium complexes $Ru_3(CO)_{12}$[28], Cp*RuCl(cod) (**1a**)[29], IndRuCl(cod) (**1i**)[30], and cyclopentadienyl ligand precursors[31] were prepared according to the previous report. Ruthenium complexes **1g**,[32] **1h**,[32] **12g**,[32] **12h**,[32] **13g**[33] and **13h**[18] were known compounds. All substrates **18**,[34] **26**,[26] **30**,[35] cycloadducts **19**,[34] **21**,[34] **23**[29b], **35**[27] and **36**[27] were reported previously.

(b) Preparation of CO-Bridged Dimer complexes 13b-h.

Synthesis [(η^5-Cp^{Me4})$Ru(CO)_2]_2$ (13b)–method a: A 30 mL, round-bottom flask was charged with 4.0 mL decane, 117 mg (0.956 mmol) of 1,2,3,4-tetramethylcyclopenta-1,3-diene and 192 mg (0.301 mmol) of $Ru_3(CO)_{12}$. The flask was cooled to −78 °C, degassed and argon was

introduced quickly. Then, the system was warmed to 165 °C and that temperature was maintained. The color of the solution turned dark red then orange. After 3 hours of heating and stirring, the reaction mixture was cooled to room temperature and orange crystals appeared. The crystals were collected on a suction funnel, washed with cold hexane and dried *in vacuo* to yield $[(\eta^5\text{-}Cp^{Me4})Ru(CO)_2]_2$ (**13b**) (204 mg, 82%) as orange crystals (mp. 297.5–299.0 °C); IR (CH_2Cl_2) 1751 (s), 1933 (s), 1981(m) cm^{-1}; ^1H NMR (300 MHz, $CDCl_3$): δ 1.86 (s, 12 H), 1.90 (s, 12 H), 4.65 (s, 2 H); ^{13}C NMR (75 MHz, $CDCl_3$): δ 9.4, 11.0, 86.4, 102.7, 103.7, 229.1; EA calcd (%) for $C_{22}H_{26}O_4Ru_2$ (556.58): C 47.47, H 4.71; found: C 47.55, H 4.48.

Preparation of $[(\eta^5\text{-}Cp^{Me})Ru(CO)_2]_2$ (13g)–method b: A 200 mL, round-bottom flask was charged with 140 ml heptane, 2 mL (*ca*. 20 mmol) of freshly cracked 1-methylcyclopenta-1,3-diene and 0.959 g (1.50 mmol) of $Ru_3(CO)_{12}$. The mixture was then heated to reflux for 2.5 h under argon atmosphere. After cooled to the ambient temperature, air was bubbled through the reaction mixture for 5 min. Solvent was removed *in vacuo* to give dark brown cake. This compound was dissolved in CH_2Cl_2 and passed through a silica gel column with eluent (hexane:CH_2Cl_2 = 1:1). The yellow band was collected and concentrated to give the desired dimer complex (840 mg, 79% yield) as orange crystals. (mp. 136.0–137.5 °C); ^1H NMR (300 MHz, $CDCl_3$): δ 2.04 (s, 6 H), 5.02 ([AA'BB'], $|^3J + {}^4J|$=3.9 Hz, 4 H), 5.19 ([AA'BB'], $|^3J + {}^4J$ =3.9 Hz|, 4 H); ^{13}C NMR (75 MHz, $CDCl_3$): δ 12.9, 88.6, 89.4, 109.4, 222.6.

Analytical data for 13c: Orange crystals; mp. 171.0–173.0 °C; IR (CH_2Cl_2) 1757(s), 1940 (s), 1983 (m) cm^{-1}; ^1H NMR (300 MHz, $CDCl_3$): δ 1.85 (s, 6 H), 1.40 (s, 12 H), 4.86 (s, 4 H); ^{13}C NMR (75 MHz, $CDCl_3$): δ 9.3, 11.6, 86.6, 103.8, 106.0, 226.9; EA calcd (%) for $C_{20}H_{22}O_4Ru_2$ (528.53): C 45.45, H 4.20; found: C 45.62, H 4.02.

Analytical data for 13d: Light orange crystals; mp. 147.0–149.0; IR(CH_2Cl_2) 1758 (s), 1941 (s), 1986 (s), 2065 (w) cm^{-1}; ^1H NMR(300 MHz, $CDCl_3$): δ 1.92 (s, 6 H), 1.94 (s, 12 H), 4.72 (s, 4 H); ^{13}C NMR (75 MHz, $CDCl_3$): δ 11.3, 12.6, 87.9, 104.5, 106.7, 227.2; EA calcd (%) for $C_{20}H_{22}O_4Ru_2$ (528.53): C 45.45, H 4.20; found: C 45.38, H 4.26.

Analytical data for 13e: Yellow needle crystals; mp. 172.5–175.5; IR (CH_2Cl_2) 1762 (s), 1946 (m), 1990 (m), 2065 (w) cm^{-1}; ^1H NMR (300 MHz, $CDCl_3$): δ 1.97 (s, 12 H), 4.97 (d, *J* = 3.0 Hz, 4 H), 5.02 (t, *J* = 3.0 Hz, 2 H) ; ^{13}C NMR (75 MHz, $CDCl_3$): δ 11.2, 88.2, 88.7, 106.1, 225.0; EA calcd (%) for $C_{18}H_{18}O_4Ru_2$ (500.47): C 43.20, H 3.63; found: C 43.04, H 3.96.

Analytical data for 13f: Orange crystals; mp. 153.5–155.5; IR (CH_2Cl_2) 1762 (s), 1947 (s), 1992 (s) cm^{-1}; ^1H NMR (300 MHz, $CDCl_3$): δ 2.00 (s, 12 H), 4.73 (br, 2 H), 4.96 (d, *J* = 1.8 Hz, 4 H); ^{13}C NMR (75 MHz, $CDCl_3$): δ 12.8, 87.1, 87.2, 108.6, 225.5; EA calcd (%) for $C_{18}H_{18}O_4Ru_2$ (500.47): C 43.20, H 3.63; found: C 42.89, H 3.47.

Analytical data for 13h: Orange-yellow crystals; mp. 180.0–183.0 °C; IR (CH_2Cl_2) 1772 (s), 1961 (s), 2002 (s) cm^{-1}; ^1H NMR (300 MHz, $CDCl_3$): d 5.28 (s); ^{13}C NMR (75 MHz, $CDCl_3$): δ 89.1, 216.5.

(c) Synthesis of Cp′RuCl(CO)$_2$ 14b–h by the air oxidation of dinuclear complex 13b–h.

Synthesis of (η ^{5}-Cp^{Me4})RuCl(CO)$_2$ (14b): In a 20 mL, round-bottom flask, 112 mg (0.202 mmol) of dinuclear complex **13b** was dissolved in 2.0 mL of chloroform and 0.7 mL of ethanol. 2N HCl (0.7 ml) and conc. HCl (0.07 ml) were added to form a two layer system. Air was introduced into the reaction mixture stiring magnetically for 4 h. During that time, liquid level was maintained by adding chloroform periodically. After the color of the organic layer turned brown, the organic layer was separated, and the aqueous layer was extracted with chloroform (1 × 2 mL). The combined organic layer was dried over Na_2SO_4, and the solvent was removed. The residual was passed through an alumina column with diethyl ether as eluent. Lemon yellow band was collected. After the evaporation of the solvent, **14b** was obtained as yellow crystals (120 mg, 92 % yield). (mp. 68.5–70.0 °C) ; IR (CH_2Cl_2) 1983 (s), 2037 (s) cm^{-1}; ^1H NMR (300 MHz, $CDCl_3$): δ 1.88 (s, 6 H), 1.90 (s, 6 H), 4.85 (s, 1 H); ^{13}C NMR (75 MHz, $CDCl_3$): δ 9.6, 11.7, 79.8, 101.7, 104.1, 198.1; EA calcd (%) for $C_{11}H_{13}ClO_2Ru$ (313.74): C 42.11, H 4.18;

found: C 42.19, H 4.10.

Analytical data for 14c: Yellow crystals; mp. 138.5–140.0 °C; IR (CH_2Cl_2) 2042 (s), 1988 (s) cm^{-1}; ^1H NMR (300 MHz, $CDCl_3$): δ 1.90–1.95 (m, 9 H), 4.88 (s, 2 H)); ^{13}C NMR (75 MHz, $CDCl_3$): δ 8.9, 11.8, 79.0, 102.6, 108.5, 197.5; EA calcd (%) for $C_{10}H_{11}ClO_2Ru$ (299.72): C 40.07, H 3.70; found: C 40.46, H 3.66.

Analytical data for 14d: Yellow crystals; mp. 91.5–94.0 °C; IR (CH_2Cl_2) 2042 (s), 1989 (s) cm^{-1}; ^1H NMR (300 MHz, $CDCl_3$): δ 1.89 (s, 3 H), 1.91 (s, 6 H), 4.98 (s, 2 H); ^{13}C NMR (75 MHz, $CDCl_3$): δ 11.6, 13.2, 82.54, 103.9, 110.3, 197.3; EA calcd (%) for $C_{10}H_{11}ClO_2Ru$ (299.72): C 40.07, H 3.70; found: C 39.99, H 3.76.

Analytical data for 14e: Yellow crystals; mp. 116.0–117.0 °C; IR (CH_2Cl_2) 1993 (s), 2046 (s) cm^{-1}; ^1H NMR (300 MHz, $CDCl_3$): δ 1.96 (s, 6 H), 4.95 (t, J = 2.7 Hz, 1 H), 5.11 (d, J = 2.7Hz, 2 H); ^{13}C NMR (75 MHz, $CDCl_3$): δ 11.2, 79.6, 83.9, 108.4, 196.9; EA calcd (%) for $C_9H_9ClO_2Ru$ (285.69): C 37.84, H 3.18; found: C 38.23, H 3.06.

Analytical data for 14f: Yellow crystals; mp. 77.5–79.0 °C; IR (CH_2Cl_2) 1994(s), 2047 (s) cm^{-1}; ^1H NMR (300 MHz, $CDCl_3$): δ 1.94 (s, 6 H), 4.94 (d, J =1.8 Hz, 2 H), 5.11 (br, 1 H); ^{13}C NMR (75 MHz, $CDCl_3$): δ 13.4, 80.4, 84.2, 112.5, 196.7; EA calcd (%) for $C_9H_9ClO_2Ru$ (285.69): C 37.84, H 3.18; found: C 37.84, H 2.86.

Analytical data for 14g: Light yellow crystals; mp. 110.0–102.5 °C, IR (CH_2Cl_2) 1999 (s), 2052 (s) cm^{-1}; ^1H NMR (300 MHz, $CDCl_3$): δ 1.97 (s, 3H), 5.13 ([AA'BB'], $|^3J + {}^4J|$=4.2 Hz, 2 H), 5.19 ([AA'BB'], $|^3J + {}^4J|$=4.2 Hz, 2 H); ^{13}C NMR (75 MHz, $CDCl_3$): δ 13.1, 83. 2, 83.7, 118.4, 196.1.

Analytical data for 14h: Light yellow crystals; mp. 98.5–100.0 °C, IR (CH_2Cl_2) 2004 (s), 2056 (s) cm^{-1}; ^1H NMR (300 MHz, $CDCl_3$): δ 5.44 (s); ^{13}C NMR (75 MHz, $CDCl_3$): δ 87.4,

195.5.

(d) Oxidative addition of allyl chloride to a dicarbonyl complex 14b–h to form Cp′RuCl$_2$(η^3-allyl) (12b, d, f, g, h) or Cp′RuCl$_2$(η^3-methallyl) (17c, e)

Synthesis of (η^5-Cp^{Me4})RuCl$_2$(η^3-allyl) 12b: A 50 mL, round-bottomed flask with a reflux condenser was charged with 220 mg (0.702 mmol) of dicarbonyl complex **14b**, 10 mL of decane, and 2.90 mL (35.6 mmol) of 3-chloropropene. The mixture was cooled to −78 °C, degassed and argon was introduced. The whole was heated in an oil bath (140 °C). Several hours after the dissolution of the substrate complex, the orange-brown precipitate appeared. The temperature was maintained for 48 h with stirring magnetically under argon atmosphere. After cooled to the room temperature, the whole reaction mixture was directly mounted on a silica-gel column. Decane and excess 3-chloropropene was removed with hexane as eluent and unreacted **14b** was eluted with Et_2O. Finally, elution with the dichloromethane–methanol (10 : 1) mixed solvent and concentration of a orange band afforded the desired η^3-allyl complex **12b** in 92% yield (216 mg) as orange microcrystals; (mp. > 300 °C) ^{1}H NMR (300 MHz, $CDCl_3$): δ 1.76 (s, 6 H), 1.80 (s, 6 H), 2.93 (d, *J* = 10.2 Hz, 2 H), 4.11 (d, *J* = 6.0 Hz, 2 H), 4.23 (s, 1 H), 5.18 (tt, *J* = 10.2, 6.0 Hz, 1 H); ^{13}C NMR (75 MHz, $CDCl_3$): δ 1.0, 11.1, 66.1, 87.9, 97.7, 100. 4, 114.9; EA calcd (%) for $C_{12}H_{18}Cl_2Ru$ (334.25): C 43.12, H 5.43; found: C 42.93, H 5.61.

Analytical data for 17c: Orange microcrystals; mp. > 300 °C; ^{1}H NMR (300 MHz, $CDCl_3$): δ 1.85(s, 3 H), 1.86 (s, 6 H), 2.35 (s, 3 H), 3.13 (s, 2 H), 3.80 (s, 2 H), 4.48 (s, 2 H); ^{13}C NMR (75 MHz, $CDCl_3$): δ 10.0, 12.0, 18.1, 60.8, 85.3, 109.9, 112.2, 117.6; EA calcd (%) for $C_{12}H_{18}Cl_2Ru$ (334.25): C 43.12, H 5.43; found: C 43.43, H 5.22.

Analytical data for 12d: Orange microcrystals; mp. > 300 °C; ^{1}H NMR (300 MHz, $CDCl_3$): δ 1.86 (s, 6 H), 1.90 (s, 3 H), 3.10 (d, *J* = 10.2 Hz, 2 H), 4.2 1 (d, *J* = 6.0 Hz, 2 H), 4.92 (s, 2 H), 5.15 (tt, *J* = 10.2, 6.0 Hz, 1 H); ^{13}C NMR (75 MHz, CDCl3): δ 11.3, 12.5, 66.7, 95.1, 98.8, 101.5, 109.9; EA calcd (%) for $C_{11}H_{16}C_{l2}Ru$ (320.22): C 41.26, H 5.04; found: C 41.53, H 4.75.

Analytical data for 17e: Orange microcrystals; mp. > 300 °C; ^{1}H NMR (300 MHz, $CDCl_3$): δ 1.95 (s, 6 H), 2.34 (s, 3 H), 3.33 (s, 2 H), 3.91 (s, 2 H), 4.74 (t, *J* = 2.4 Hz, 1 H), 5.07 (d, *J* = 2.4 Hz, 2 H) ; ^{13}C NMR (75 MHz, $CDCl_3$): δ 11.7, 17.9, 61.0, 84.9, 91.3, 112.8, 114.9; EA calcd (%) for $C_{11}H_{16}Cl_2Ru$ (320.22): C 41.26, H 5.04; found: C 41.45, H 4.76.

Analytical data for 12f: Orange microcrystals; mp. > 300 °C; ^{1}H NMR (300 MHz, $CDCl_3$): δ 2.02 (s, 6 H), 3.33 (d, *J* = 10.2 Hz, 2 H), 4.29 (d, *J* = 6.0 Hz, 2 H), 4.84 (d, *J* = 1.8 Hz, 2 H), 5.10 (tt, *J* = 10.2, 6.0 Hz, 1 H), 5.53 (t, *J* = 1.8 Hz, 1 H); ^{13}C NMR (75 MHz, $CDCl_3$): δ 13.1, 65.8, 88. 7, 99.1, 101.1, 110.9; EA calcd (%) for $C_{10}H_{14}Cl_2Ru$ (306.19): C 39.23, H 4.61; found: C 39.29, H 4.48.

Analytical data for 12g: Orange microcrystals; mp. > 300 °C; ^{1}H NMR (300 MHz, $CDCl_3$): δ 2.13 (s, 3 H), 3.56 (d, *J* = 10.2 Hz, 2 H), 4.39 (d, *J* = 6.3 Hz, 2 H), 5.06 (tt, *J* = 10.2, 6.3 Hz, 1 H), 5.22 ([AA'BB'], $|^{3}J + {}^{4}J|$= 3.6 Hz, 2 H), 5.50 ([AA'BB'], $|^{3}J + {}^{4}J|$= 3.6Hz, 2 H); ^{13}C NMR (75 MHz, $CDCl_3$): δ 13.3, 65.4, 88.9, 95.1, 99.4, 116.9.

Analytical data for 12h: Orange microcrystals; mp. > 300 °C; ^{1}H NMR (300 MHz, $CDCl_3$): δ 2.73 (d, ^{3}J = 10.2 Hz, 2 H), 4.47 (d, ^{3}J = 6.0 Hz, 2 H), 5.00 (tt, ^{3}J = 10.2, 6.0Hz, 1 H), 5.70 (s, 5 H); ^{13}C NMR (75 MHz, $CDCl_3$): δ 65.8, 93.9, 100.3.

(e) Preparation of Cp′RuCl(cod) 1b–h.

Synthesis of (η^5-Cp^{Me4})RuCl(cod) (1b): To a stirred dichloromethane (5 mL) solution of η^3-allyl complex **12b** (66.7 mg, 0.199 mmol) was added $AlEt_3$ (1.0 M in hexane, 5.0 mL, 5.0 mmol) dropwise at −78 °C under Ar atmosphere. The reaction mixture was stirred at this temperature for 1.5 h. To this solution, 0.25 mL (2.0 mmol) of 1,5-cyclooctadiene was added. Then, the temperature was raised to r.t. in 2 h. 10 mL of saturated aqueous solution of NH_4Cl was added and stirred. the water layer was extracted with CH_2Cl_2 (10 mL). The combined organic layer was filtered through a pad of Celite. Solvent was removed and the residue was

purified with silica gel column chromatography using CH_2Cl_2 as an eluent. Concentration of the red band gave **1b** as red-brown crystals in 55% yield (39.9 mg). mp. (141.5–144 °C); ^{1}H NMR (300 MHz, $CDCl_3$): δ 1.54 (s, 6 H, overlapping with H_2O), 1.67 (s, 6 H), 1.92–1.94 (m, 2 H), 1.99–2.08 (m, 4 H), 2.58–2.66 (m, 2 H), 3.87–3.95 (m, 2 H), 4.25–4.34 (m, 2 H), 4.28 (s, 1 H, overlapping with the multiplet); ^{13}C NMR (75 MHz, $CDCl_3$): δ 9.3, 11.1, 28.6, 31.5, 81.9, 82.6, 85.1, 96.7, 98.2; EA calcd (%) for $C_{17}H_{25}ClRu$ (365.90): C 55.80, H 6.89; found: C 55.76, H 6.80.

Analytical data for 1c: Brown crystals; mp.124.5–128.0 °C; ^{1}H NMR (300 MHz, $CDCl_3$): δ 1.51 (s, 3 H), 1.69 (s, 6 H), 1.90–1.98 (m, 2 H), 2.02–2.08 (m, 4 H), 2.59–2.64 (m, 2 H), 3.97–4.08(m, 2 H), 4.49 (s, 2 H), 4.53–4.64 (m, 2 H); ^{13}C NMR (75 MHz, $CDCl_3$): δ 8.9, 11.3, 28.4, 32.0, 80.9, 80.9, 84.8, 99.5, 101.0; EA calcd (%) for $C_{16}H_{23}ClRu$ (351.88): C 54.61, H 6.59; found: C 54.34, H 6.85.

Analytical data for 1d: Brown crystals; mp.122.0–124.0 °C; ^{1}H NMR (300 MHz, $CDCl_3$): δ 1.67 (s, 6 H), 1.78 (s, 3 H), 1.92-2.02 (m, 2 H), 2.04–2.06 (m, 2 H), 2.61–2.66 (m, 2 H), 3.98–4.08 (m, 2 H), 4.31 (s, 2 H), 4.46–4.54 (m , 2 H); ^{13}C NMR (75 MHz, $CDCl_3$): δ 10.84, 12.4, 28.5, 31.8, 82.1, 85.2, 86.0, 97.784, 99.0; EA calcd (%) for $C_{16}H_{23}ClRu$ (351.88): C 54.61, H 6.59; found: C 54.34, H 6.76.

Analytical data for 1e: Brown crystals; mp. 182.5–184.5 °C; ^{1}H NMR (300 MHz, $CDCl_3$): δ 1.68 (s, 6 H), 1.89–2.00 (m, 2 H), 2.04–2.06 (m, 4 H), 2.57–2.67 (m, 2 H), 4.11–4.16 (m, 2 H), 4.63 (d, J = 2.4 Hz, 2 H), 4.68 (t, J = 2.4 Hz, 1 H), 4.84–4.92 (m, 2 H) ; ^{13}C NMR (75 MHz, $CDCl_3$): δ 11.0, 28.4, 32.4, 78.9, 79.8, 85.4, 86.3; EA calcd (%) for $C_{15}H_{21}ClRu$ (337.85): C 53.33, H 6.27; found: C 53.31, H 6.15.

Analytical data for 1f: Brown crystals; mp. 93.0–95.0 °C; ^{1}H NMR (300 MHz, $CDCl_3$): δ 1.81 (s, 6 H), 1.92–2.02 (m, 2 H), 2.02–2.09 (m, 4 H), 2.58–2.68 (m, 2 H), 4.12–4.24 (m, 2 H), 4.33 (t, J = 1.8 Hz, 1 H), 4.52 (d, J = 1.8 Hz, 2 H), 4.66–4.78(m, 2 H); ^{13}C NMR (75 MHz,

$CDCl_3$): δ 12.6, 28.3, 31.9, 81.1, 83.72, 86.2, 101.9; EA calcd (%) for $C_{15}H_{21}RuCl$ (337.85): C 53.33, H 6.27; found: C 53.32, H 6.15.

Analytical data for 1g: Yellow-brown crystals; mp. 111.0–112.5 °C; ^{1}H NMR (300 MHz, $CDCl_3$): δ 1.84 (s, 3 H), 1.90–2.02 (m, 2 H), 2.04–2.11 (m, 2 H), 2.54–2.68 (m, 2 H), 4.22–4.34 (m, 2 H), 4.64 ([AA'BB'], $|^3J + {}^4J|$= 3.6 Hz, 2 H), 4.83 ([AA'BB'], $|^3J + {}^4J|$= 3.6 Hz, 2H), 4.98–5.12 (m, 2 H); ^{13}C NMR (75 MHz, $CDCl_3$): δ 12.7, 28.28, 32.3, 79.5, 85.0, 86.1, 86.4, 103.8.

Analytical data for 1g: Orange-brown crystals; mp. 185.0–187.0 °C; ^{1}H NMR (300 MHz, $CDCl_3$): δ 1.91–1.97 (m, 2 H), 1.97–2.16 (m, 4 H), 2.53–2.68 (m, 4 H), 4.34–4.48 (m, 2 H), 4.96 (s, 5 H), 5.26–5.33 (m, 2 H); ^{13}C NMR (75 MHz, $CDCl_3$): δ 30.0, 32.5, 78.5, 85.8, 87.0.

(f) General procedure for ruthenium-catalyzed [2+2+2] cycloaddition of diiododiyne 18 with acetylene.

To a solution of Cp*RuCl(cod) (**1a**) (3.41 mg, 0.00898 mmol, 3.00 mol% to diyne substrate) in dry degassed 1,2-dichloroethane (1.50 mL) was added a solution of bis(3-iodoprop-2-ynyl)ether **18** (103.6 mg, 0.300 mmol) in dry degassed 1,2-dichloroethane (1.5 mL) over 15 min at room temperature under acetylene (balloon, 1 atm) atmosphere. The solution was stirred and the reaction progress was traced by TLC analysis. After 1 h of reaction, the complete consumption of the diyne was confirmed. The solvent was removed *in vacuo*, and the residue was purified by silica-gel column chromatography (eluent: hexane/AcOEt 20:1) to give diiodebenzene **19** (104 mg, 94 %) as colorless solid (mp. 118.0–119.0 °C); ^{1}H NMR ($CDCl_3$, 300 MHz): δ 5.13 (s, 4 H), 7.31 (s, 2 H); ^{13}C NMR ($CDCl_3$, 75 MHz): δ 79.2, 86.9, 137.9, 144.5.

(g) General Procdure for ruthenium-catalyzed [2+2+2] cycloaddition of diiododiyne 18 with tolan.

To a solution of ($Cp^{1,2,4\text{-}Me3}$)RuCl(cod) (5.28 mg, 0.0150 mmol) and tolan (80.2 mg, 0.450 mmol) in dry degassed 1,2-dichloroethane (1.5 mL) was added a solution of bis(3-iodoprop-2-ynyl)ether **18** (103.6 mg, 3.00 mmol) in 1,2-dichloroethane (1.5 mL) over 15 min at room temperature under argon atmosphere. The solution was stirred for 12 h. The solvent was removed *in vacuo* and the residue was purified by silica gel-column chromatography (eluent: hexane/ AcOEt 100 : 1) to give **21** (129.1mg, 82%) as coloress solid (mp. 198.5–200.0 °C): ^{1}H NMR (300 MHz, $CDCl_3$): δ 5.27 (s, 4 H), 6.92 (dd, *J* = 1.8, 7.8 Hz, 4 H), 7.12–7.17(m, 6 H); ^{13}C NMR (75 MHz, $CDCl_3$): δ 80.9, 94.0, 127.2, 127.6, 130.0, 143.3, 144.0.

(h) General procudrure for kinetic study: [2+2+2] cycloaddition reaction of diiododiyne 18 and phenylacetylene.

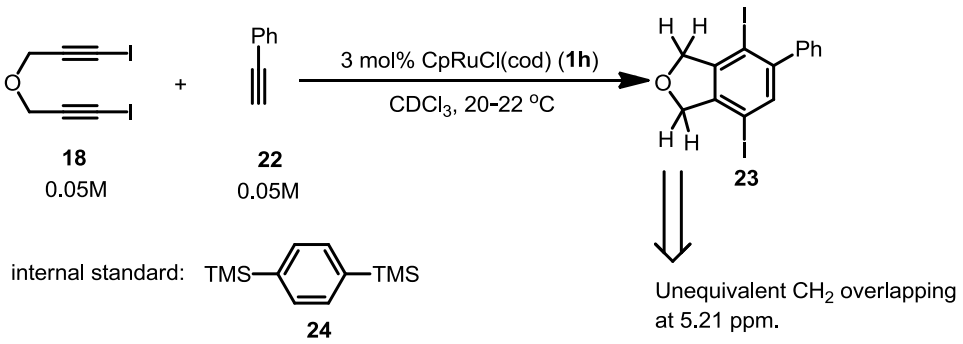

In a 30 mL two necked flask, 1.38 mg (4.45 μmol) of CpRuCl(cod) (**1h**) and 16.5 μL (1.5×10^2 μmol) of phenylacetylene (**22**) was dissolved in 3.00 mL of $CDCl_3$. The solution was cooled to −78 °C and frozen and degassed quickly. Then the solution was warmed to room temperature under argon atmosphere. 0.6 mL of the solution was taken with syringe and mixed with 10.4 mg (3.01×10 μmol) of diiododiyne **18** and a small amount of *p*-bis(trimethylsilyl)benzene (**24**) in Wilmad NMR tube with J Young valve. The whole was frozen at −78 °C, degassed and melted. This degassing process was repeated twice. The concentration of the secondary standard (**24**) was determined by the first NMR measurement in relation to the summed concentration of **18** and atiny amount of **23**. In the first 10 minutes, ^{1}H

NMR was acquired in 2-minutes interval. After that time, the measurement was done once in 5 minutes. Concentrations of the product at each measurement were determined from peak area of TMS group (δ 0.265 ppm, 18 H) of the secondary standard and product **23** − CH_2 – (δ 5.21 ppm, 4 H, inequivalent protons overlapping)

(i) General Procedure for the [2+2+2] cycloaddition of unsymmetrical diyne 26 and terminal monoyne 27.

Under argon atmosphere, to the degassed solution of Cp*RuCl(cod) (**1a**) (5.69 mg, 0.0150 mmol) and 101 μL of methylpropargyl ether (1.20 mmol) in 1.0 mL of 1,2-dichloroethane was added the degassed solution of asymmetric diyne **26** (84.1 mg, 0.300 mmol) In 1.5 mL of 1,2-dichloroethane over 15 min. After the addition, the reaction mixture was stirred magnetically for 12 h. After removal of the solvent the ratio of *meta*-**28 :** *ortho*-**28** was determined by ^{1}H NMR analysis. The crude mixture was purified by silica-gel column chromatography with hexane:AcOEt = 7:1 eluent to give the mixture of minor isomer *ortho*-**69** and major isomer *meta*-**69** in 96% total yield (0.101g). The separation of two regioisomers was achieved by using FL-100D siliga-gel for the chromatographic purification (hexane: AcOEt = 20: 1).

Analytical data for *meta*-28: colorless solid; mp. 61.0–62.5 °C; ^{1}H NMR ($CDCl_3$, 300 MHz): δ 0.31 (s, 9H), 3.39 (s, 3 H), 3.57 (s, 2 H), 3.60 (s, 2 H), 3.74(s, 6 H), 4.40 (s, 2 H), 7.19 (s, 1 H), 7.24 (s, 1 H); ^{13}C NMR ($CDCl_3$, 75 MHz): δ 0.0, 39.9, 41.2, 52.8, 58.1, 60.6, 74.8, 124.6, 132.2, 135.4, 136.1, 139.3, 144.6, 171.9; MS(EI): *m/z*(%) 350 (45) $[M]^+$, 355 (6) $[M-Me]^+$, 319 (5) $[M-OMe]^+$, 290 (100) $[M-H-COOMe]^+$; EA calcd (%) for $C_{18}H_{26}O_5Si$ (350.48): C 61.68, H 7.48; found: C 61.57, H 7.58.

Analytical data for *meta*-28: pale-yellow solid; mp. 56.0–57.5 °C; ^{1}H NMR ($CDCl_3$, 300 MHz): δ 0.39 (s, 9 H), 3.34 (s, 3 H), 3.53(s, 2 H), 3.65 (s, 2 H), 3.74 (s, 6 H), 4.43 (s, 2 H), 7.156–1.190 ([AB], 2 H); ^{13}C NMR ($CDCl_3$, 75 MHz): δ 2.0, 39.7, 42.7, 52.9, 57.7, 60.5, 75.2,

124.8, 128.7, 134.7, 139.0, 142.4, 146.2, 172.0; MS(EI): *m/z* (%) 350 (3) $[M]^+$, 335 (100) $[M-Me]^+$, 319 (7) $[M-OMe]^+$, 291 (21) $[M-COOMe]^+$; EA calcd (%) for $C_{18}H_{26}O_5Si$ (350.48): C 61.68, H 7.48; found: C 61.56, H 7.13.

(j) General procedure for the competing [2+2+2] cyclotrimerization and tandem cyclopropanation of diyne 30 and norbornene

To a stirred solution of Cp*RuCl(cod) (**1a**) (5.68 mg, 0.0150 mmol) in dry degassed 1,2-dichloroethane (6.70 mL) were added norbornene (**31**) (564 mg, 5.99 mmol) and diyne **30** under argon atmosphere at room temperature. The reaction vessel was cooled to −78 °C. The system was degassed and argon was introduced quickly. This degassing was repeated 3 times. The reaction mixture was stirred at room temperature for 2 h. The solvent was removed, and the products were extracted with ethylacetate (3×10 mL). The extract was concentrated, and the residue was purified by siliga-gel column chromatography (eluent hexane: CH_2Cl_2 = 6 : 4) to give tandem cyclopropanation product **33** (9.38 mg, 7.9%) as white solids. Further elution gave [2+2+2] cycloadduct **32** (40.7 mg, 45.0%) as white solid.

Analytical data for 33: White solid; mp. 117.5–118.5 °C; ^{1}H NMR ($CDCl_3$, 300 MHz): δ 0.66 (d, *J* =10.2 Hz, 2 H), 0.92 (d, *J* = 2.1 Hz, 4 H), 1.06 (d, *J* =9.6 Hz, 2 H), 1.18–1.30 (m, 4 H), 1.61–1.66 (m, 2 H), 2.30 (s, 4 H), 2.69 (s, 4 H), 3.70 (s, 6 H); ^{13}C NMR ($CDCl_3$, 75 MHz): δ 12.8, 22.0, 28.2, 29.5, 36.0, 41.3, 57.1, 131.4, 172.5.

Analytical data for 32: White solid; mp. 58.5–60.5 °C; ^{1}H NMR ($CDCl_3$, 300 MHz) δ 1.15 (dt, *J* = 9.9, 1.5 Hz, 1 H), 1.28–1.38 (m, 2 H), 1.46–1.58 (m, 3 H), 1.97 (s, 2 H), 2.43 (s, 2 H), 2.85 (s, 4 H), 3.71 (s, 3 H), 3.72 (s, 3 H); ^{13}C NMR ($CDCl_3$, 75 MHz) δ 30.3, 34.4, 38.9, 43.7, 45.8, 52.7, 58.3, 119.5, 133.7, 171.9.

6. References

[1] Yamamoto, Y. *Chem. Rev.* **2008**, *108*, 3199–3222.

[2] Ewen, J. A.; Elder, M. J.; Jones, R. L.; Razavi, A.; Ferrara, J. *J. Am. Chem. Soc.* **1988**, *110*, 6255–6256.

[3] (a) Piccolrovazzi, N.; Pino, P.; Consiglil, G.; Sironi, A.; Moret, M. *Organometallics* **1990**, *9*, 3098–3105. (b) Lee, I.-M, Gauthier, W. J.; Ball, J. M.; Iyengar, B.; Collins, S. *Organometallics* **1992**, *11*, 2115–2122.

[4] Mohring, P. C.; Coville, N. J. *Coord. Chem. Rev.* **2006**, *250*, 18–35.

[5] Möhring, P. C.; Vlachakis, N.; Grimmer, N. E.; Coville, N. J. *Coord. Chem. Rev.* **1994**, *483*, 159–166.

[6] Janiak, C.; Versteeg, U.; Katharina, C. H. L.; Weimann, R.; Hahn, E. *J. Organomet. Chem.* **1995**, *501*, 219–234

[7] (a) Manriquez, J. M.; Bercaw, J. E. *J. Am. Chem. Soc.* **1974**, *96*, 6229–6230; (b) Sanner, R. D.; Marsh, Manriquez, J. M.; Marsh, R. E.; Bercaw, J. E. *J. Am. Chem. Soc.* **1976**, *98*, 8351–8357.

[8] (a) Pool, J. A.; Lobkovsky, E.; Chirik, P. J. *Nature* **2004**, *427*, 527–529; (b) Hanna, T. E.; Bernskoetter, W. H.; Bouwkamp, M. W.; Lobokovsky, E.; Chirik, P. J. *Organometallics* **2007**, *26*, 2431–2438.

[9] Bobadova-Paranova, P.; Wang, Q.; Morokuma, K.; Musaev, D. G. *Angew. Chem. Int. Ed.* **2005**, *44*, 7101-7103

[10] Yamamoto, Y.; Arakawa, T.; Ogawa, R.; Itoh, K. *J. Am. Chem. Soc.* **2003**, *125*, 12143–12160.

[11] Lindner, E.; Jansen, R. -M.; Mayer, H. A.; Hiller, W.; Fawzi, R. *Organometallics*, **1989**, *8*, 2355–3260.

[12] [Co]: (a) Yamazaki, H.; Hagihara, N. *J. Organomet. Chem.* **1967**, *7*, 22–23; (b) Vollhardt, K. P. C. *Acc. Chem. Res.* **1977**, *10*, 1–8. [Rh]: (c) Nishiyama, H.; Niwa, E.; Inoue, T.; Ishima, Y.; Aoki, K. *Organometallics* **2002**, *21*, 2572–2574; (d) Müller, E. *Synthesis* **1974**, 761–774. [Ir]: (e) Collman, J. P.; Kang, J. W.; Little, W. F.; Sullivan, M. F. *Inorg. Chem.* **1968**, *7*, 1298–1303; (f) Margarita, P.; Posadas, C. M.; Poveda, M. L.; Rendón, N.; Laura, L. S.; Ivarez, E.; Salazar, V.; Mereiter, K.; Oate, E. *Organometallics* **2007**, *26*, 3403–3415; (g) Paneque, M.; Poveda, M. L.; Rendón, N.; Mereiter, K. *Organometallics* **2009**, *28*, 172–180. [Ni]: (h) Sato, Y.; Nishimata, Y.; Mori, M. *J. Org. Chem.* **1994**, *59*, 6133–6135; (i) Sato, Y.; Ohashi, K.; Mori, M. *Tetrahedron Lett.* **1999**, *40*, 5231–5234.

[13] Oshima, N.; Suzuki, H.; Moro-oka, Y. *Chem. Lett.* **1984**, 1161–1164.

[14] Nagashima, H.; Mukai, K.; Shiota, Y.; Yamaguchi, K.; Ara, K.; Fukahori, T.; Suzuki,

H.; Akita, M.; Morooka, Y.; Itoh, K. *Organometallics* **1990**, *9*, 799–807.

[15] Nagashima, H.; Yamaguchi, K.; Mukai, K.; Itoh, K. *J. Organometallic. Chem.* **1985**, *291*, C20–23.

[16] Itoh, K., unpublished result.

[17] Gilbert, J. D.; Wilkinson, G. *J. Chem. Soc.* **1969**, 1749–1751.

[18] Humparies, A. P.; Knox, S. A. R.; *J. Chem. Soc., Dalton Trans.* **1975**, 1710–1714.

[19] (a) King, R. B.; Iqbal, M. Z.; King Jr., A. D. *J. Organomet. Chem.* **1979**, *171*, 53–63; (b) Bailey, N. A.; Radford, S. L.; Sanderson, J. A.; Tabatabaian, K.; White, C.; Worthington, J. M. *J. Organomet. Chem.* **1978**, *154*, 343–351; (c) Ng, S. Y.; Goh, L. Y.; Koh, L. L.; Leong, W. K.; Tan, G. K.; Ye, S.; Zhu, Y. *Eur. J. Inorg. Chem.* **2006**, 663–670.

[20] Nagashima, H.; Muaki, K.; Itoh, K. *Organometallics* **1984**, *3*, 1214–1315.

[21] Humphries, A. P.; Knox, S. A. R. *J. Chem. Soc., Dalton Trans* **1975**, 1710–1714.

[22] Zachmanoglou, C. E.; Docrat, A.; Bridgewater, B. M.; Parkin, G.; Brandow, G.; Bercaw, J. E.; Jardine, C. N.; Lyall, M.; Green, J. C.; Keister, J. B. *J. Am. Chem. Soc.* **2002**, *124*, 9525–9546.

[23] (a) Jia, G.; Morris, R. *J. Am. Chem. Soc.* **1991**, *113*, 875–883; (b) Smith, K. -T.; Tilset, M.; Kristjánsdóttir, S. S.; Norton, J. R. *Inorg. Chem.* **1995**, *34*, 6497–6504; (c) Gutkin, V; Gun, J.; Prikhodchenko, P. V.; Lev, O.; Gonsalvi, J.; Peruzzini, M.; Romerosa, A.; Malpartida, C. T.; Lidrissi, C. *J. Electrochem. Soc.* **2007**, *154*, F7–F15; (d) Shaw, A. P.; Ryland, B. L.; Norton, J. R.; Buccella, D.; Moscatelli, A. *Inorg. Chem.* **2007**, *46*, 5805–5812.

[24] Absaq, M-L.; Saidi, M.; Burgot, J. -L.; Darchen, A. *J. Organomet. Chem.* **2008**, *694*, 36-42.

[25] (a) McDonald, F. E.; Zhu, H. Y. H.; Holmquist, C. R. *J. Am. Chem. Soc.* **1995**, *117*, 6605–6606; (b) Witulski, B.; Stengel, T. *Angew. Chem. Int. Ed.* **1999**, *38*, 2426–2430.

[26] Yoshihiko, Y.; Ogawa, R.; Itoh, K. *Chem. Commun.* **2000**, 549–550.

[27] Yamamoto, Y.; Kitahara, H.; Hattori, R.; Itoh, K. *Organometallics* **1998**, *17*, 1910–1912.

[28] Faure, M.; Saccavini, C.; Lavigne, G. *Chem. Commun.* **2003**, 1578-1579.

[29] (a) Oshima, H.; Suzuki, H.; Moro-oka, Y. *Chem. Lett.* **1984**, 1161-1164; (b) Yamamoto, Y.; Hattori, H. *Tetrahedron* **2008**, *28*, 847-855.

[30] Alvarez, P.; Gimeno, J.; Lastra, E.; García-Granda, S.; Van der Maelen, J. F.; Bassetti, M. *Organometallics* **2001**, *20*, 3762-3771.

[31] Yoshizawa, R.; Matsumoto, T.; Hashimoto, M. *Jpn. Kokai Tokkyo Koho* **1995**, 252168.

[32] Albers, M. O.; Liles, D. C.; Robinson, D. J.; Shaver, A.; Singleton, E. *Organometallics*

1987, *6*, 2347–2354.

[33] (a) Gansow, O. A.; Burke, A. R.; Vernon, W. D. *J. Am. Chem. Soc.* **1976**, *98*, 5817–5826; (b) Byrne, L. T.; Hos, J. P.; Koutsantonis, G. A.; Skelton, B. W.; White, A. H. *J. Organomet. Chem.* **1999**, *592*, 95–102.

[34] Yamamoto, Y.; Hattori, K.; Nishiyama, H. *J. Am. Chem. Soc.* **2006**, *128*, 8336–8340.

[35] Llerena, D.; Aubert, C.; Malacria, M. *Tetrahedron Lett.* **1996**, *37*, 7027–7030.

Chapter 3

Reactivity of Ruthenacyclopentatriene Complex with Water

Abstract: Reactivity of isolable ruthenacyclopentatriene complex with water was examined. It was found that electronically neutral Cp*–ruthenacyclopentatriene complex bearing chloride ligand on the ruthenium center reacts with water slowly under mild conditions to form η^5-oxapentadienyl complex. The reaction was significantly accelerated in the presence of silver salts. With the aid of DFT calculations, it was suggested that the incorporation of water molecule by the ruthenacyclopentatriene starts with the coordination of water molecule to a cationic ruthenium center and deprotonation to form a hydroxo complex. Consecutive 1,2-shift of the hydroxo ligand and intramolecular proton transfer gives the oxapentadienyl complex. The intermediacy of the η^5-oxapentadienyl complex in the previously reported catalytic hydrative cyclization of 1,6-diynes was also demonstrated by elucidating the decomposition behavior of the complex. The η^5-oxapentadienyl complex was stable under neutral or basic condition even at elevated temperature. On the other hand, the complex easily decomposed in the presence of one equivalent of hydrochloric acid. As a result, a cyclic enone, which is the product of the ruthenium-catalyzed hydrative cyclization of diyne, was produced. In this decomposition, the [Cp*RuCl] structure was regenerated and trapped by a diphosphine ligand.

1. Introduction

Ruthenacyclopentatrienes are multifaceted carbene complex. As shown in the previous chapter, neutral ruthenacyclopentatrienes exhibit affinity to unsaturated compounds. Another side of the ruthenacyclopentatrienes is electrophilicity. That reactivity is often possessed by cationic complexes that lack an anionic ligand on the ruthenium center.

Kirchner and co-workers have made a seminal discovery on the electrophilic nature of carbene carbon of ruthenacyclopentatriene complexes. In the study, divalent cationic ruthenium cyclopentadienyl phosphine complexes **1** reacted with 1,6-hexadiyne to form ally carbene complexes **3**.[1,2] This reaction takes place trough the formation of a ruthenacyclopentatriene **2**, followed by 1,2-migration of a phosphine ligand from the metal center to the carbene carbon (Scheme 1).

Scheme 1. Formation of ruthenium ally carbene complex *via* 1,2-migration of phosphine ligand.

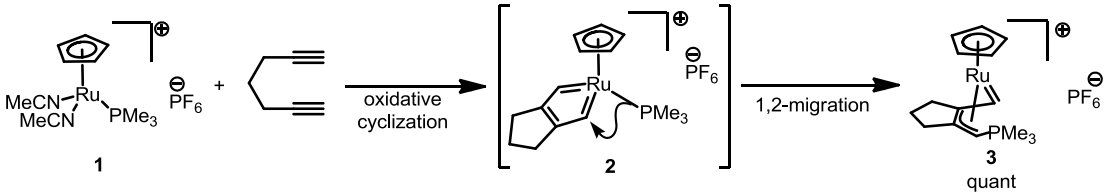

By exploiting the electrophilicity of ruthenacyclopentatriene intermediate, several catalytic reactions have been developed. Trost and co-workers have reported that in the presence of cationic cyclopentadienyl ruthenium complex [CpRu(NCMe)$_3$](PF$_6$) (**4a**), 1,6-diynes cyclyzes by incorporating water or alcohol to afford cyclic enone **5** or dienyl ether **6** respectively (Scheme 2).[3,4]

Scheme 2. Cationic ruthenium complex-catalyzed hydrative and alkoxylative cyclization of diyne.

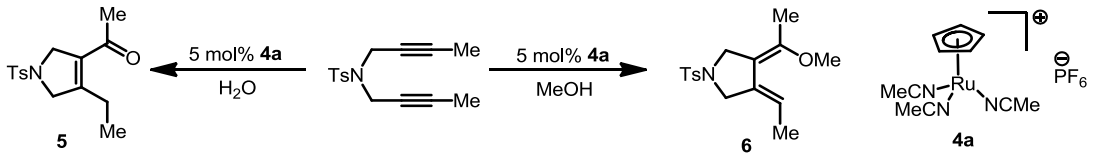

An intermolecular version of Trost's alkoxylative cyclization was reported by Dixneuf, Beller and coworkers (Scheme 3).[5] In this case, two aryl acetylene molecules were combined with a methanol, and 1,3-dienyl ether **7** was produced as a coupling product. The obtained dienyl ether were transformed into 2,5-diarylsubstituted furans **8** through an oxidative process.

Scheme 3. Cationic ruthenium complex catalyzed alkoxylative dimerization of aryl acetylene combined with oxidative furan synthesis.

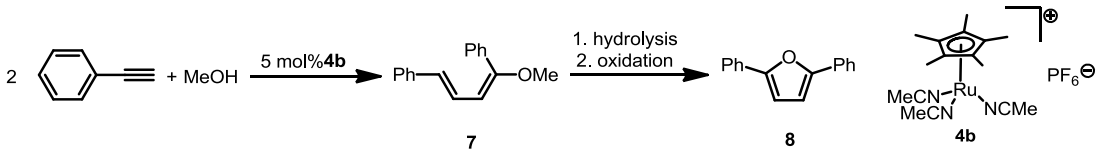

Even though the Dixneuf's reaction is analogous to the Trost's former intramolecular reaction, there was a discrepancy between two reports in terms of proposed reaction mechanism (Scheme 4). The hydrative cyclization reaction or alkoxylative cyclization reported by Trost *et al.* were accounted for by postulating nucleophilic attack to the ruthenacyclopentatriene intermediate by water molecule or alcohol. On the other hand, in Dixneuf's dimerization reaction, protonation of the ruthenacyclopentatriene complex by neutral alcohol was assumed to take place prior to the nucleophilic attack by alkoxylate anion. Taking into account the higher basicity of alcohol than that that of water, two proposed mechanisms are contradictory each other.

Scheme 4. Proposed mechanisms for hydrative cyclization of diynes and alkoxylative dimerization of aryl acetylenes

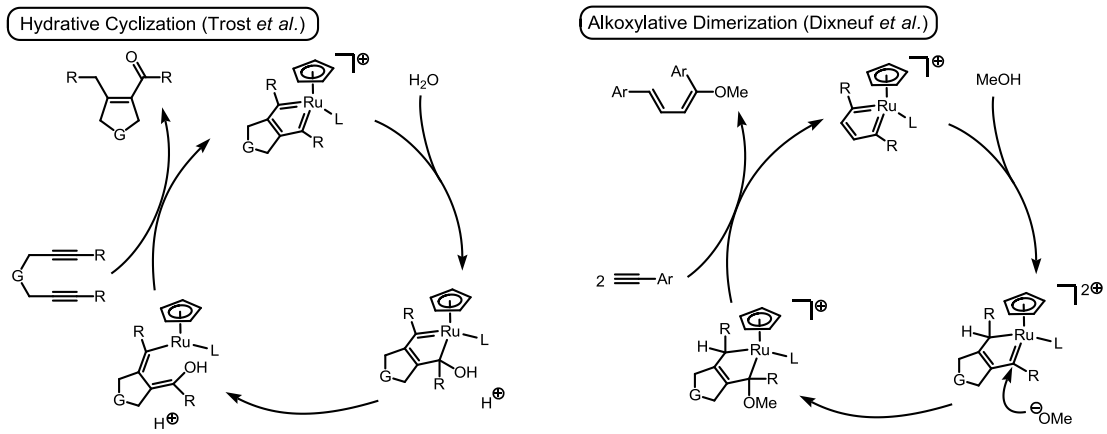

Probably, the mechanism for 1,3-dienyl ether formation was proposed in analogy with previously reported carboxylative dimerization of alkynes (Scheme 5).[6,7] DFT study and stoichiometric reaction of a ruthenacyclopentatriene with carboxylic acid were conducted for the purpose of mechanistic elucidation. These studies revealed that the reaction involves protonation of the neutral ruthenacyclopentatriene intermediate as a key step.

Scheme 5. Carboxylative dimerization of alkyne catalyzed by Cp*RuCl(cod) (**9**) and its mechanism.

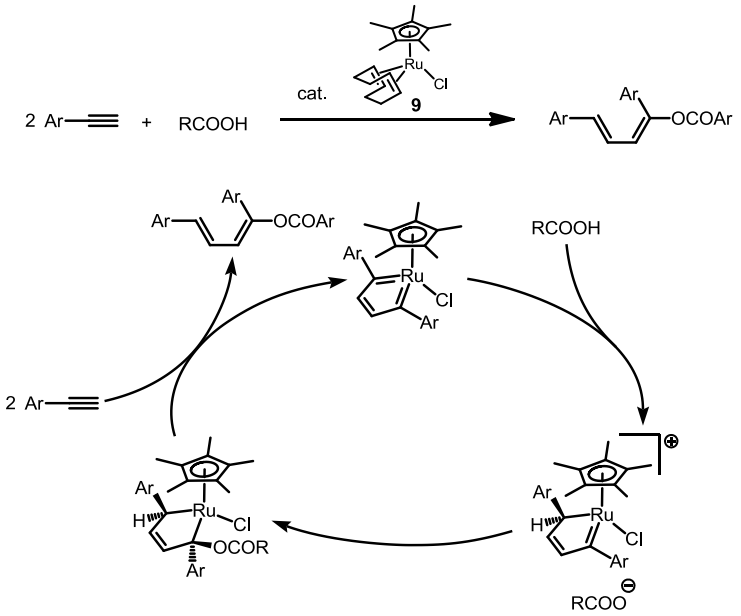

Up to here, several examples of catalytic reactions involving the interaction of ruthenacyclopentatriene and oxygen nucleophiles were introduced. It should be noted that the oxygen nucleophiles used in the ruthenacyclopentatriene chemistry is virtually limited to above mentioned 3; water, alcohols and carboxylic acids. To expand the realm of this chemistry, deep understanding on the existing reactions is essential. In contrast to the reaction with carboxylic acids, the absence of examination on stoichiometric basis is an obstacle to the understanding of the reaction with neutral oxygen nucleophiles. The cause of this issue should be attributed to absence of isolable cationic ruthenacyclopentatriene which has an appropriate level of reactivity.[8] Hence the second best resort should be generation of cationic species from a neutral precursor.

2. Hydration of Ruthenacyclopentatriene

The initial study on the reactivity of ruthenacyclopentatriene complex started with an unexpected observation of water incorporation by isolable ruthenacyclopentatriene complex. In an attempt to purify crude **10** by neutral alumina column chromatography, expected **10** disappeared and new complex **11** was obtained (Scheme 6).

Scheme 6. Incorporation of a water molecule by a ruthenacyclopentatriene to form an oxapentadienyl complex.

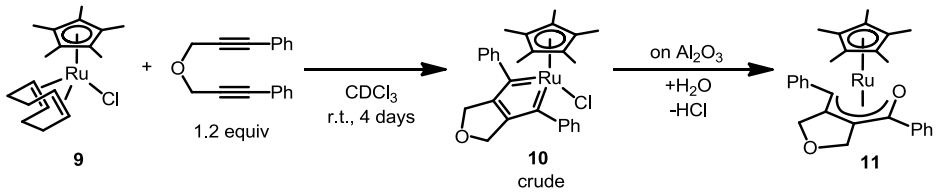

In ^{1}H NMR spectrum, all four protons of the methylene unit adjacent to the furan oxygen atom were observed as inequivalent geminal doublets at δ = 4.58–4.32 ppm, indicating the loss of symmetry. In HRMS (FAB) measurement, peak at *m/z* = 500.1300 was found, which corresponds to $C_{28}H_{30}O_2Ru$ with a deviation of $+2.2\times10^{-3}$ mass unit. This composition is indicative of replacement of Cl^- by OH^-. Finally, single crystal X-ray diffraction study unambiguously established a half-open oxaruthenocene structure of complex **11** as shown in Figure 1.

Figure 1. ORTEP-drawing of the Cp*Ru–η^5oxapentadienyl complex **11**, shown as 50% ellipsoids. All hydrogen atoms are omitted for clarity.

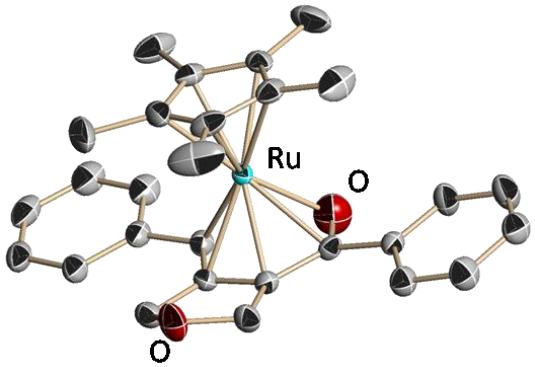

Related complexes without fused 5-membered cyclic structure have already been reported by several groups.[9] The η^5-oxapentadienyl ligand takes almost complete planar form in **11**, and C–O and C–C bond lengths are comparable to those of previously known complexes.

It should be noted that this is the first example of the synthesis of the ruthenium–oxapentadienyl complex from a ruthenacyclopentatriene, which features new C−O bond formation in the coordination sphere of the ruthenium center. In most of existing cases, oxapentadienyl complexes were synthesized through straightforward methods; i.e., reaction of Cp*Ru-source and enones in the presence of a base. Intrigued by this point, we tried to reveal the mechanistic insight into the generation of complex **11**.

Reactions of **10** and water under various conditions are summarized in Table 1. **10** reacted with water slowly in THF solution at room temperature to give **11** (entry 1). Although the extended reaction time (6 hours) improved the conversion, ketone **12** and furan **13** were also detected (entry 2). If the reaction proceeds through Trost's mechanism (Scheme 4), abstraction of chloride will facilitate the reaction. To distinguish the previously proposed two pathways, the author next intended to abstract the chloride anion with silver(I) salts. Addition of the Ag^+ significantly accelerated the reaction rate, and the yield of **11** reached 44% in 1 h when $AgBF_4$ was used (entry 3). Notably, use of silver salts other than Ag_2O significantly increased formation of furan by-product, especially when $AgNO_3$ was employed (entry 5). In the reaction with Ag_2O, the complex **11** was produced in a higher yield of 50% together with 32% of unreacted substrate and trace amount of **13** (entry 6). On extending the reaction time to 2 h, **10** was completely consumed to give **11** in 71% yield (entry 7). Judging from the fact that elimination of Cl^- accelerated the reaction, Trost's mechanism is supported as the pathway to **11**. Additionally, neutral alumina (Merck, Aluminum Oxide 90 standardized) was tested as an additive to reproduce the transformation occurred during the chromatographic purification. Eventually, the alumina enhanced the reaction rate moderately (entry 8). The reaction was led to completion in four hours to afford **11** in the best yield of 79% (entry 9). In contrast to the reaction with Ag^+, neither **12** nor **13** were detected in crude mixture. This reaction condition was scalable, and complex **11** necessary for the following investigation was synthesized with this procedure.

Table 1. Reaction of a ruthenacyclopentatriene **10** and water under various conditions

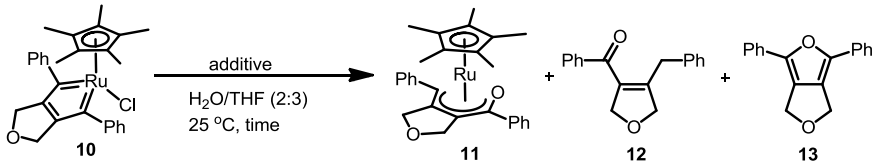

entry	additive	time [h]	conversion [%]	yields[a] **11** / **12** / **13** [%]
1	none	1	48	26 / 0 / 0
2	none	6	84	54 / 5 / 3
3	$AgBF_4$ [b]	1	> 99	44 / 0 / 30
4	AgF [b]	1	> 99	38 / 0 / 0
5	$AgNO_3$ [b]	1	> 99	7 / 0 / 52
6	Ag_2O [b]	1	68	50 / 0 / 3
7	Ag_2O [b]	2	> 99	71(60)[c] / 0 / 1
8	Al_2O_3	1	54	42 / 0 / 0
9	Al_2O_3	4	>99	79(73)[c] / 0 / 0

[a]Yields determined by ^{1}H NMR analysis of crude reaction mixture. [b]1.1 equivalent of Ag^+. [c]Isolated yields.

As described in the introduction, two mechanisms for the incorporation of neutral oxygen nucleophiles have been proposed. Since water (pK_a = 15.7) is much less acidic than carboxylic acids (e.g. acetic acid: pK_a = 4.8), it is unnatural to assume that the ruthenacycle is protonated by water, let alone by alcohol. In fact, the formation of the ruthenacyclopentatriene proceeded more favorably in the presence of basic Ag_2O than other silver salts which generate acid as byproduct.

3. Mechanistic Study

To find a reasonable mechanism of the water incorporation, DFT calculation on a model complex composed of $[CpRu]^+$ fragment and unsaturated C4 unit was carried out. The DFT calculation suggested that the protonation of the cationic ruthenacyclopentatriene **A** by water to give **C** is rather unfavorable, because the activation barrier was as high as 27.6 kcal/mol (Figure 2).

Figure 2. Reaction profile for the protonation of cationic ruthenacyclopentatriene intermediate.

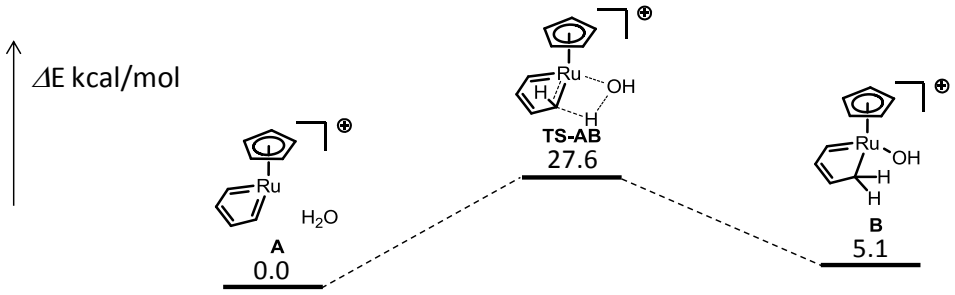

It is anticipated that the nucleophilic attack of water to the cationic ruthenacyclopentatriene would be advantageous. Both carbene carbon and coordinatively unsaturated ruthenium center are both potential electrophilic sites. However, no stationary point for the water adduct **C** could be located. Thus, intramolecular 1,2-migration of hydroxo ligand was investigated. Kirchner and co-workers have reported 1,2-migration of phosphine ligand from the metal center to the carbene carbon. Because the reaction takes place in the presence of base (oxide anion of Ag_2O) in the real system, the reaction from hydroxo complex **E** rather than directly from an aquo complex **D** appears reasonable (Scheme 7).

Scheme 7. Formation of hydroxo complex and 1,2-migration of hydroxo ligand.

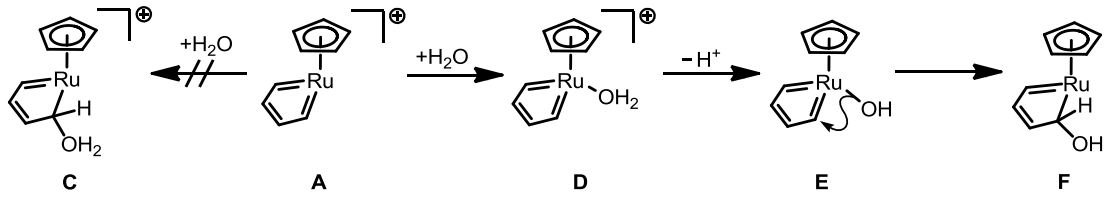

The DFT calculation suggested that 1,2-migration of the hydroxo ligand takes place with an activation barrier of 16.9 kcal/mol (TS-EF, Figure 3), indicating that the hydroxo migration takes place much easier than the protonation (Figure 2). The formation of the hydroxylated ruthenacycle **F** is estimated to be endothermic by 6.2 kcal/mol. Subsequently, the β-H abstraction took place through a late transition state, **TS-FG**, with an activation barrier of 18.8 kcal/mol. The Ru–H and O–H distances are 1.72 and 1.34 Å respectively. The formation of hydride complex **G** is estimated as exothermic by 8.1 kcal/mol. The subsequent 1,2-hydride

shift was found to be very facile. This process was estimated to proceed *via* an early transition state **TS-GH**: the Ru–H bond was elongated by only 0.06 Å when compared with **G**. The activation energy was estimated to be very small (2.4 kcal/mol). The formation of σ-allyl complex **H** bearing a side-on bound formyl ligand from **G** was found to be exothermic by 6.6 kcal/mol.

Figure 3. Reaction profile for transformation of hydroxo complex **E** into σ-allyl complex **J**

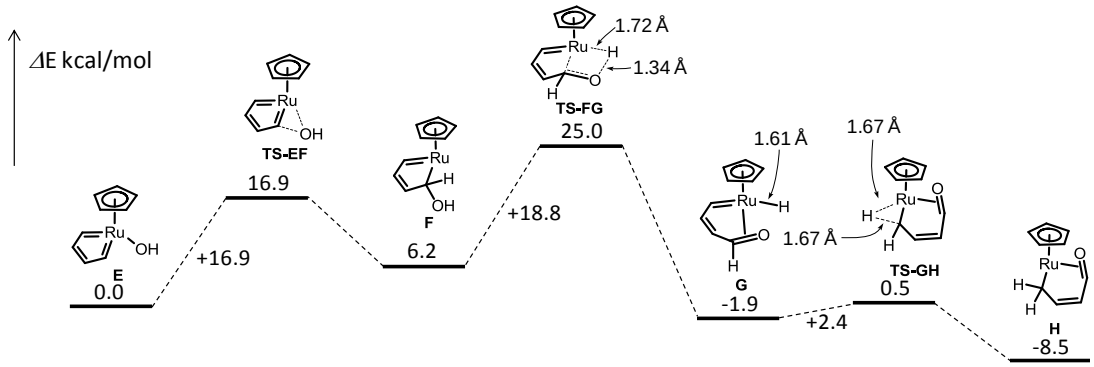

The haptotropic rearrangement from the γ-formylallyl complex to an η^5-oxapentadienyl complex was investigated by using higher model including a 2,5-dihydro furan moiety (Figure 4). This modification helps to simplify further investigation by avoiding the *s-cis*/*s-trans* conformational change of the diene moiety at the expense of computational efficiency. As a result, we could find that the γ-formyl complex **I** was transformed into the final η^5-oxapentadienyl complex **K** through an intermediate σ-allyl complex **J** with an end-bound formyl group (the Ru–O and Ru–C bond distance are 2.06 and 3.04 Å, respectively). The initial side-on to end-on isomerization of **I** was estimated to occur with almost no barrier via an early transition state (**TS-IJ**). The formation of **J** is thermodynamically favorable because of relatively large exothermicity of −21.0 kcal/mol. Subsequent rearrangement to **K** took place with the dissociation of formyl group. This process was estimated to require activation energy of 11.8 kcal/mol the thermodynamically favorable formation of η^5-oxapentadienyl complex **K** is estimated to proceed with an exothermicity of 14.9 kcal/mol. The entire rearrangement path way was found to be downhill process with a considerable exothermicity of 35.9 kcal/mol.

Figure 4. Reaction profile for haptotropic rearrangement.

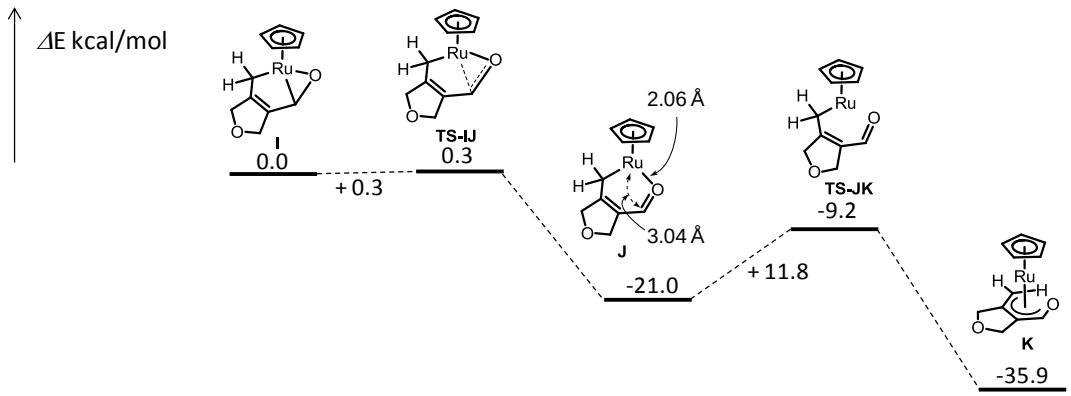

4. Catalytic Hydrative Cyclization of 1,6-diyne

It is anticipated that the release of the oxapentadienyl ligand form **11** will give conjugated enone. In fact, **12** was observed as a by-product in the hydration of **10** as shown above. Hence, examining the reactivity of the oxapentadienyl complex will deliver a key to the mechanism of ruthenium-catalyzed hydrative cyclization of diynes. To evaluate the role of the oxapentadienyl complex in the hydrative cyclization, **11** was subjected to an examination in stoichiometric reactions (Table 2). In the presence of base or acid, decomposition behavior of **11** was studied in THF–water solution at 70 °C. As might be expected for 18e complexes, **11** was inert to nucleophilic attack, and it remained intact after 6 hours of refluxing in neutral or basic aqueous THF solutions (entries 1 and 2). On the contrary, even under weakly acidic condition (4.2 mM HCl, 1 equiv), **11** decomposed to give **12** in 52% yield (entry 3) along with intractable materials. The Cp*Ru fragment was captured with bidentate ligands L_2 (L_2: cod, nbd = 2,5-norbornadiene, dppe = 1,2-diphenylphoshinoethane), and piano-stool type complexes **14** were formed in moderate yields (entries 4–6). This result indicates that acid serves as an indispensable promoter in the ruthenium-catalyzed hydrative cyclization.

Table 2. Hydration of η^5–oxapentadienyl complex **11** in the presence/absence of base or acid, and capture of [Cp*Ru] fragment by bidentate ligands.

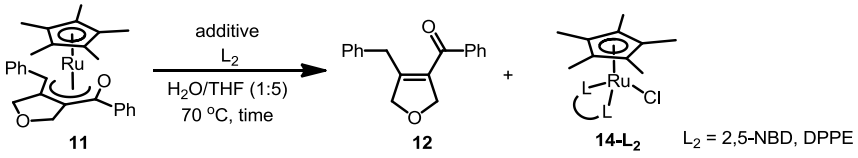

entry	additive	L	time [h]	conversion [%]	yields[a] **12** / **14-L$_2$** [%]
1	none	none	6	0	0 / 0
2	NaOH (40 equiv)[b]	none	6	0	0 / 0
3	HCl (1.0 equiv)[c]	none	1.5	>99	52 / 0
4	HCl (1.0 equiv)[c]	COD (10 equiv)	1.5	77	68 / **14**-cod (**9**), 54
5	HCl (1.0 equiv)[c]	NBD (10 equiv)	6	88	80 / **14**-nbd, 81
6	HCl (1.0 equiv)[c]	DPPE (10 equiv)	12	86	85 / **14**-dppe, 86

[a]Yields determined by ^{1}H NMR analysis of crude reaction mixture. [b] 0.17 M. [c]4.2 mM.

Based on these results, the catalytic activities of **9** and **11** in hydrative cyclization of diyne **15** were examined (Table 3). While **9** showed an activity and produced **12** in moderate yield (entry 1), **11** alone did not promoted the reaction at all (entry 2). In good agreement with the stoichiometric study, addition of a small amount of HCl (1 equiv to **11**) activate the catalyst and **12** was obtained in high yield (entry 3). This result further supports the intermediacy of **11** in the ruthenium-catalyzed hydrative cyclization of diynes.

Table 3. Hydrative cyclization of diyne **15** catalyzed by 9 or **11**+HCl.

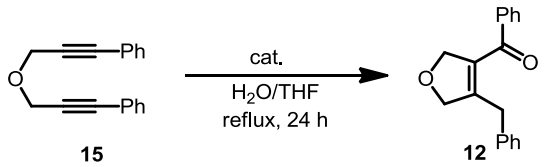

entry	catalyst	conversion	**12** yield
1	**9**	91	64
2	**11**	0	0
3	**11**+HCl	99	87

With the results obtained above, the mechanism of ruthenium-catalyzed hydrative cyclization can be described as shown in Scheme 8. Ruthenacyclopentatriene **10** generated from a diyne component and divalent cyclopentadienylruthenium fragment incorporate one molecule of water with the loss of HCl, and forms a hydroxo complex **16**. The 1,2-migration of OH ligand and consecutive proton transfer afford a η^5-oxapentadienyl complex **11**. Whilst the neutral condition has to be sustained to isolate the oxapentadienyl complex in good yield, the acid generated in the prior step is essential to decompose the oxapentadienyl complex to afford the product enone, and to accomplish the catalytic cycle.

Scheme 8. Deduced mechanism for ruthenium-catalyzed hydrative cyclization reaction of 1,6-diyne.

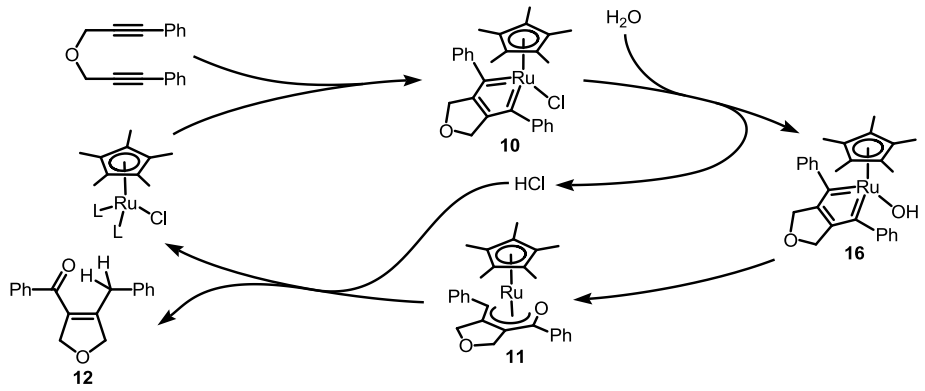

In conclusion, the intermediacy of the half-sandwich-type η^5-oxapentadienylruthenium complex in the ruthenium-catalyzed hydrative cyclization was confirmed. The formation of the oxapentadienyl complex was elucidated by means of stoichiometric hydration reaction of neutral ruthenacyclopentatriene and DFT study. It was strongly suggested that the incorporation of water by ruthenacyclopentatriene is initiated by coordination of water molecule to the cationic ruthenium center followed by deprotonation to afford a neutral hydroxo complex. Importantly, the C–O bond formation step in the intermediate takes place as 1,2-migration of the hydroxo ligand from the ruthenium center to a α-carbon. Subsequent β-H elimination followed by 1,2-hydride migration produces the γ-formylallyl complex. Finally, *via* haptotropic rearrangement sequence, the intermediate evolves into the η^5-oxapentadienyl complex.

5. Experimental Section

(a) General Considerations.

Column chromatography was performed on silica gel (Cica silica gel 60N) with solvents specified below. ^{1}H and ^{13}C NMR spectra were obtained for samples in $CDCl_3$ solution at 25 °C. ^{1}H NMR chemical shifts are reported in terms of chemical shift (δ, ppm) relative to the singlet at 7.26 ppm for chloroform. Splitting patterns are designated as follows: s, singlet; d, doublet; t, triplet; q, quartet; quint, quintet; sext, sextet; sept, septet; m, multiplet. Coupling constants are reported in Hz. ^{13}C NMR spectra were fully decoupled and are reported in terms of chemical shift (δ, ppm) relative to the triplet at δ = 77.0 ppm for $CDCl_3$. Mass measurements and elemental analyses were performed by the Instrumental Analysis Facility of Nagoya University. Melting points were obtained in capillary tubes. [Cp*RuCl(cod)] (**9**)[10] and ruthenacyclopentatriene **10**[11] were prepared according to the reports. Diyne **15,**[12] ketone **12**,[13] and [Cp*RuCl(dppe)] (**14-dppe**)[14] were known compounds. Diphenylphosphinoethane, all silver salts, and solvents were purchased and used as received.

(b) Genral procedure for Reaction of Ruthenacycle 10 with H_2O.

Reaction in the absence of additives: To a vigorously stirred solution of **10** (25.8 mg, 0.0498 mmol) in degassed THF (1.5 mL) was added degassed H_2O (1.0 mL) under argon atmosphere. The mixture was stirred at 25 °C for 6 h. The solution was diluted with 20 mL of THF, dried over K_2CO_3, and filtrated. The residue was washed with THF and $CHCl_3$ (10 mL each). The combined filtrate was concentrated *in vacuo* to give a mixture of **10**, η^5-oxapentadienyl complex **11**, ketone **12**, and furan **13**. Crude yields were determined as unreacted **10** (0.00782 mmol, 16%), **11** (0.0268 mmol, 54%), **12** (0.00233 mmol, 5%), and **13** (0.00137 mmol, 3%) by ^{1}H NMR analysis with ethylbenzene (5.0 μL, 0.0410 mmol) as internal standard.

Reaction in the presence of a silver salt: To a vigorously stirred solution of $AgNO_3$ (9.35 mg, 0.0550 mmol) in degassed H_2O (1.0 mL) was added a solution of **10** (25.9 mg, 0.0500 mmol) in degassed THF (1.5 mL) under Ar atmosphere. The reaction mixture was stirred for 1 h at 25 °C. After diluted with THF (20 mL), the solution was dried over K_2CO_3, and filtrated. The residue

was washed with THF and $CHCl_3$ (10 mL each). The combined organic layer was concentrated i*n vacuo* to give a mixture of **11** (0.00371 mmol, 7%) and furan **6** (0.0261 mmol, 52%) as analyzed by ^{1}H NMR analysis with ethylbenzene (5.0 mL, 0.0410 mmol) as internal standard. The crude mixture was purified with silica gel column chromatography (elution with hexane/CH_2Cl_2 1:1 ~ 1:2) to give **13** (6.20 mg, 0.0236 mmol, 47 %) as colorless crystals (mp. 167.5–169.5 °C): ^{1}H NMR (300 MHz, CDCl3) δ 5.08 (s, 4 H), 7.26 (tt, *J* = 1.2, 7.4 Hz, 2 H), 7.38–7.44 (m, 4 H), 7.49–7.53 (m, 4 H); ^{13}C NMR (75 MHz, $CDCl_3$) δ 66.5, 123.6, 126.8, 128.3, 128.7, 130.1, 141.3; HRMS (FAB) *m/z* calcd for $C_{18}H_{14}O_2$ 262.0994, found 262.0994 $[M]^+$.

Reaction in the presence of neutral alumina: To a solution of **10** (25.9 mg, 0.0500 mmol) in degassed THF (1.5 mL) was added degassed water (1.0 mL) and Al_2O_3 (64.8 mg, 636 mmol). The reaction mixture was flushed with argon. The mixture was stirred at 25 °C for 4 h. Then the mixture was diluted with THF (20 mL), dried over K_2CO_3, and filtrated. The residue was washed with THF and $CHCl_3$ (10 mL each). The combined solution was concentrated *in vacuo*. The crude mixture was purified with alumina column chromatography. The yellow band eluted with a mixed solvent (hexane/CHCl3 1:1 ~ 0:1) was concentrated *in vacuo* to give **11** (18.1 mg, 73%) as orange micro crystals (mp 228.0–229.5 °C): ^{1}H NMR (300 MHz, $CDCl_3$) δ 1.30 (s, 15 H), 3.93 (s, 1 H), 4.57 (d, *J* = 11.1 Hz, 1 H), 4.90 (d, *J* = 10.2 Hz, 1 H), 5.01 (d, *J* = 11.1 Hz, 1 H), 5.32 (d, 10.2 Hz, 1 H), 7.16–7.22 (m, 1 H), 7.27–7.47(m, 7 H), 7.56–7.61 (m, 2 H); ^{13}C NMR (75 MHz, $CDCl_3$) δ 9.2, 69.4, 71.5, 72.7, 87.6, 91.4, 103.9, 124.3, 125.3, 127.1, 127.7, 128.1, 128.3, 128.6, 138.1, 141.7; HRMS (FAB) *m/z* calcd for $C_{28}H_{30}O_2Ru$ 500.1289, found 500.1300 $[M]^+$.

(c) Acid-promoted Decomposition of η^4-Oxapentadienyl Complex 11 with Diphenylphosphinoethane.

To a solution of **11** (24.9 mg, 0.0498 mmol) and diphenylphosphinoethane (20.9 mg, 0.0523 mmol) in degassed THF (10 mL) was added aqueous HCl (0.025 M, 2.0 mL, 0.050 mmol). The mixture was cooled to –78 °C, degassed, and backfilled with argon. This step was repeated twice. The solution was stirred at 70 °C for 12 h. After cooled to room temperature, the mixture was evaporated under reduced pressure to give a mixture of unreacted **11** (0.00680 mmol, 14%),

ketone **12** (0.0421 mmol, 85%), and [Cp*RuCl(dppe)] (**14-dppe**) (0.0430 mmol, 86%) as analyzed by ^{1}H NMR with *p*-xylene (10.0 μL, 0.0810 mmol) as an internal standard. The following spectral data of **14-dppe** were in good agreement with those of an authentic sample prepared according to the report[14]: ^{1}H NMR (300 MHz, $CDCl_3$) δ 1.44 (s, 15 H), 2.05–2.20 (m, 2 H), 2.57–2.78 (m, 2 H), aromatic protons were obscure because of overlapping with those of **11**, **12**, and excess dppe. Spectral data for the authentic sample: ^{1}H NMR (300 MHz, $CDCl_3$) δ 1.46 (s, 15 H), 2.05–2.30 (m, 2 H), 2.50–2.90 (m, 2 H), 7.14–7.74 (m, 20 H).

(d) Catalytic Hydrative Cyclization of Diyne 15.

With Cp*RuCl(cod) (9): To a solution of **15** (73.8 mg, 0.300 mmol) and **9** (5.74 mg, 0.0151 mmol) in degassed THF (3.0 mL) was added degassed H_2O (0.6 mL) under Ar atmosphere. The mixture was stirred at 70 °C for 24 h. After cooled to room temperature, the mixture was diluted with AcOEt (20 mL), dried over $MgSO_4$, and filtered. The residue was washed with AcOEt (10 mL), and combined filtrate was concentrated *in vacuo*. The crude product was purified with silica gel column chromatography (elution with hexane/EtOAc 17:1) to give recovered **15** (5.67 mg, 0.023 mmol, 8%). Further elution (hexane/EtOAc 15:1 ~ 13:1) afforded **12** (50.9 mg, 0.193 mmol, 62 %) as colorless oil. Following spectral data are in good accordance with those previously reported[13]: ^{1}H NMR (300 MHz, $CDCl_3$) δ 3.52 (s, 2 H), 4.68 (t, *J* = 4.8 Hz, 2 H), 5.01–5.05 (m, 2 H), 7.07–7.10 (m, 2 H), 7.16–7.29 (m, 3 H), 7.45–7.51 (m, 2 H), 7.55–7.62 (m, 1 H), 7.81–7.85 (m, 2 H); ^{13}C NMR (75 MHz, $CDCl_3$) δ 33.3, 77.7, 78.6, 126.5, 128.3, 128.45, 128.49, 132.8, 132.9, 136.8, 138.1, 146.4, 192.8; IR (KBr): 1644 cm^{-1} (C=O); HRMS (FAB) *m/z* calcd for $C_{l8}H_{17}O_2$ 265.1229, found 165.1221 $[M+H]^+$.

With η^4-oxapentadienyl complex 11: To a solution of **15** (73.9 mg, 0.300 mmol) and **11** (7.48 mg, 0.0150 mmol) in degassed THF (3.0 mL) was added aqueous HCl (0.025 M, 0.6 mL, 0.0150 mmol) under Ar atmosphere. The mixture was stirred at 70 °C for 24 h. After cooled to room temperature, the solvent was removed under reduced pressure. The crude product was purified with silica gel column chromatography (elution with $CHCl_3$/hexane 3:1 then 1:0) to afford **5** (73.3 mg, 0.278 mmol, 88% based on **12** + **15**).

(e) Crystallographic Structural Determinations.

A single crystal of **11** suitable for X-ray analysis was mounted on a glass fiber, and diffraction data were collected at 153 K on a Brucker SMART APEX CCD diffractometer with graphite monochromated Mo-Kα radiation (λ = 0.71073 Å). The absorption correction was made using SADABS. The structure was solved by direct methods and refined by the full-matrix least-squares on *F2* by using SHELXTL.[15] All non-hydrogen atoms were refined with anisotropic displacement parameters. All hydrogen atoms were placed in calculated positions.

Table S 1 Selected crystallographic data and collection parameters for **11**.

	11
Formula	$C_{28}H_{30}O_2Ru$
Fw	499.59
Crystal system	Monoclinic
Space group	$P2_1/n$ (#14)
a [Å]	8.2716(8)
b [Å]	23.868(2)
c [Å]	11.4379(11)
β [°]	93.401(2)
V [Å^3]	2254.1(4)
Z	4
D_{calc} [g cm^{-3}]	1.472
μ [mm^{-1}]	0.718
F(000)	1032
Crystal size [mm^3]	0.5 × 0.3 × 0.3
Reflections collected	16230
Independent reflections	5576 (R_{int} = 0.0312)
GOF on F^2	1.106
R_1 [I>2σ(I)][a]	0.0554
wR_2 (all data)[b]	0.1514
Largest diff. peak and hole [e Å^{-3}]	0.506 / −1.023

[a] $R_1 = \Sigma|(F_o-F_c)|/\Sigma(F_o)$. [b] $wR_2 = \{\Sigma[(w(F_o^2-F_c^2)^2)]/\Sigma[w(F_o^2)^2]\}^{1/2}$.

(f) Theoretical Calculations.

The Gaussian 03 program package was used for all geometry optimizations.[16] The geometries of stationary points **A**–**K** and transition states **TS-AB**–**TS-JK** were fully optimized by means of the Becke's three-parameter hybrid density functional method (B3LYP)[17] with the basis set, consisting of a double-ζ basis set with the relativistic effective core potential of Hay and Wadt (LanL2DZ)[18] for Ru and the 6-31G(d)[19] basis sets for other elements (BS-I). The vibrational frequencies, zero-point energy (ZPE) and thermal correction to Gibbs free energy (TCGFE) were calculated at the same level of theory. The obtained structures were characterized by the number of imaginary frequencies (one or zero for transition or ground states, respectively). The connectivity of each step was further confirmed by IRC calculation[20] from the transition states **TS-AB**–**TS-JK** followed by optimization of the resulted geometries. Single-point energies for geometries obtained by the above method were calculated at the same level using the basis sets consisting of a [6s5p3d2f1g] contracted valence basis set with the Stuttgart-Dresden-Bonn energy-consistent pseudopotential (SDD) [21,22] for Ru and the 6-311++G(2d,p) basis sets[23] for other elements. Relative energies were corrected with unscaled ZPE obtained at the B3LYP/BS-I level. The obtained results are summarized in Table S 2

Table S 2. Summary of Theoretical Calculations

Model	Energy/au	ZPE/au	IF/cm^{-1}
A	–519.57026878	0.173944	
TS-AB	–519.52150090	0.169190	1267.24i
B	–519.56302775	0.174840	
E	–519.17709823	0.161484	
TS-EF	–519.14992458	0.161241	365.02i
F	–519.17000366	0.164301	
TS-FG	–519.14479230	0.158489	1476.54i
G	–519.18976710	0.160578	
TS-GH	–519.18476799	0.159476	752.60i
H	–519.20313838	0.163538	
I	–671.87401769	0.203908	
TS-IJ	–671.87295542	0.203390	111.74i
J	–671.90769958	0.204152	
TS-JK	–671.88832376	0.203525	130.61i
K	–671.93334603	0.206048	

6. References and Notes

1 (a) Mauthner, K.; Soldouzi, K. M.; Mereiter, K.; Schmid, R.; Kirchner, K. *Organometallics* **1999**, *18*, 4681–4683; (b) Rüba, E.; Mereiter, K.; Schmid, R.; Sapunov, V. N.; Kirchner, K.; Schottenberger, H.; Calhorda, M. J.; Veiros, L. F. *Chem. Eur. J.* **2002**, *8*, 3948–3961; (c) Becker, E.; Mereiter, K.; Puchberger, M.; Schmid, R.; Kirchner, K. *Organometallics* **2003**, *22*, 2124–2133.

2 See also: (a) Becker, E.; Rüba, E.; Mereiter, K.; Schmid, R.; Kirchner, K. *Organometallics* **2001**, *20*, 3851–3853; (b) Rüba, E.; Mereiter, K.; Schmid, R.; Kirchner, K. *Chem. Commun.* **2001**, 1996–1997; (c) Rüba, E.; Mereiter, K.; Schmid, R.; Kirchner, K. *Organometallics* **2002**, *21*, 2912–2920.

3 (a) Trost, B. M.; Rudd, M. T. *J. Am. Chem. Soc.* **2003**, *125*, 11516–11517; (b) Trost, B. M.; Rudd, M. T. *Org. Lett.* **2003**, *5*, 4599–4602; (c) Trost, B. M.; Huang, X. *Org. Lett.* **2005**, *7*, 2097–2099; (d) Trost, B. M.; Huang, X. *Chem. Asian J.* **2006**, *1*, 469–478.

4 For a prototype of hydrative cyclization, see: Trost, B. M.; Rudd, M. T. *J. Am. Chem. Soc.* **2002**, *124*, 4178–4179.

5 Zhang, M.; Jiang, H. -F.; Neumann, H.; Beller, M.; Dixneuf, P. H. *Angew. Chem. Int. Ed.* **2009**, *48*, 1681–1684.

6 (a) Le Paih, J.; Dérien, S.; Dixneuf, P. H. *Chem. Commun.* **1999**, 1437–1438; (b) Le Paih, J.; Monnier, F.; Dérien, S.; Dixneuf, P. H.; Clot, E.; Eisenstein, O. *J. Am. Chem. Soc.* **2003**, *125*, 11964–11975.

7 For closely related systems, see: (a) González-Dodríguez, C.; Varela, J. A.; Saá, C. *J. Am. Chem. Soc.* **2007**, *129*, 12916–12917; (b) Tanaka, K.; Saitoh, S.; Hara, H.; Shibata, Y. *Org. Biomol. Chem.* **2009**, *7*, 4817–4820; (c) Kim, H.; Goble, S. D.; Lee, C. *J. Am. Chem. Soc.* **2007**, *129*, 1030–1031.

8 A stable cationic ruthenacyclopentatriene complex bearing an NHC ligand has been reported: Becker, E.; Stingl, V.; Mereiter, K.; Kirchner, K. *Organometallics* **2006**, *25*, 4166–4169.

9 (a) Crocker, M.; Froom, S. F. T.; Green, M.; Nagle, K. R.; Orpen, A. G.; Thomas, D. M. *J. Chem. Soc., Dalton Trans.* **1987**, 2803–2814; (b) Traarnpruk, W.; Arif, M. A.; Erunst, R. D. *Organometallics* **1992**, *11*, 1686–1692; (c) Trakarnpruk, W.; Arif, A. M. Ernst, R. D. *Organometallics* **1994**, *13*, 2423–2429; (d) Clemente, M .E. N.; Saavedra, P. J.; Vásquez, M. C.; Paz-Sandoval, M. A; Arif, A. M.; Ernst, R. D. *Organometallics* **2002**, *21*, 592–605; (e) Rajapakshe, S.; Paz-Sandoval, M. A.; Gutierrez, J. A.; Navarro-Clemente, M .E.; Saaavedra, P. J.; Gruhn, N. E.; Lichtenberger, D. L. *Organometallics* **2006**, *25*, 1914–1923.

10 (a) Oshima, N.; Suzuki, H.; Moro-oka, Y. *Chem. Lett.* **1984**, 1161–1164; (b) Yamamoto, Y.; Hattori, H. *Tetrahedron* **2008**, *28*, 847–855.

[11] Yamamoto, Y.; Arakawa, T.; Ogawa, R.; Itoh, K. *J. Am. Chem. Soc.* **2003**, *125*, 12143–12160.

[12] Scheller, A; Winter, W.; Müller, E. *Liebigs Ann. Chem.*, **1976**, 1448–1454.

[13] Yacoub, B.; Blunm, J.; Ibrahin, A.; Vollhardt, K. P. C. *J. Mo. Cat.* **1991**, *66*, 295–312.

[14] (a) Bruce, M. I.; Ellis, B. G.; Low, P. J.; Skelton, B. W.; White, A. H. *Organometallics* **2003**, *22*, 3184–3198; (b) Singh, K. S.; Thöne, K.; Kollipara, M. R. *J. Organomet. Chem.* **2005**, *690*, 4222–4231.

[15] G. M. Sheldrick, SHELXTL 5.1, Bruker AXS Inc., Madison, Wisconsin, 1997.

[16] Gaussian 03, Revision C.02, Frisch, M. J.; Trucks, G. W.; Schlegel, H. B.; Scuseria, G. E.; Robb, M. A.; Cheeseman, J. R.; Montgomery, J. A. Jr.; Vreven, T.; Kudin, K. N.; Burant, J. C.; Millam, J. M.; Iyengar, S. S.; Tomasi, J.; Barone, V.; Mennucci, B.; Cossi, M.; Scalmani, G.; Rega, N.; Petersson, G. A.; Nakatsuji, H.; Hada, M.; Ehara, M.; Toyota, K.; Fukuda, R.; Hasegawa, J.; Ishida, M.; Nakajima, T.; Honda, Y.; Kitao, O.; Nakai, H.; Klene, M.; Li, X.; Knox, J. E.; Hratchian, H. P.; Cross, J. B.; Bakken, V.; Adamo, C.; Jaramillo, J.; Gomperts, R.; Stratmann, R. E.; Yazyev, O.; Austin, A. J.; Cammi, R.; Pomelli, C.; Ochterski, J. W.; Ayala, P. Y.; Morokuma, K.; Voth, G. A.; Salvador, P.; Dannenberg, J. J.; Zakrzewski, V. G.; Dapprich, S.; Daniels, A. D.; Strain, M. C.; Farkas, O.; Malick, D. K.; Rabuck, A. D.; Raghavachari, K.; Foresman, J. B.; Ortiz, J. V.; Cui, Q.; Baboul, A. G.; Clifford, S.; Cioslowski, J.; Stefanov, B. B.; Liu, G.; Liashenko, A.; Piskorz, P.; Komaromi, I.; Martin, R. L.; Fox, D. J.; Keith, T.; Al-Laham, M. A.; Peng, C. Y.; Nanayakkara, A.; Challacombe, M.; Gill, P. M. W.; Johnson, B.; Chen, W.; Wong, M. W.; Gonzalez, C.; Pople, J. A. Gaussian, Inc., Wallingford CT, 2004.

[17] (a) Kohn, W.; Becke, A. D.; Parr, R. G. *J. Phys. Chem.* **1996**, *100*, 12974−12980; (b) Stephen, P. J.; Devlin, F. J.; Chabalowski, C. F.; Frisch, M. *J. Phys. Chem.* **1994**, *98*, 11623−11627; (c) Becke, A. D. *J. Chem. Phys.* **1993**, *98*, 1372−1377; (d) Lee, C.; Yang, W.; Parr, R. G. *Phys. Rev. B* **1988**, *37*, 785−789.

[18] Hay, P. J.; Wadt, W. R. *J. Chem. Phys.* **1985**, *82*, 299−310.

[19] (a) Hehre, W. J.; Ditchfield, R.; Pople, J. A. *J. Chem. Phys.* **1972**, *56*, 2257−2261; (b) Hariharan, P. C.; Pople, J. A. *Theor. Chim. Acta* **1973**, *28*, 213−222; (c) Fracl, M. M.; Pietro, W. J.; Hehre, W. J.; Binkley, J. S.; Gordon, M. S.; DeFrees, D. J.; Pople, J. A. *J. Chem. Phys.* **1982**, *77*, 3654−3665.

[20] (a) Fukui, K. *Acc. Chem. Res.* **1981**, *14*, 363−368; (b) Gonzalez, C.; Schlegel, H. B. *J. Chem. Phys.* **1989**, *90*, 2154−2161; (c) Gonzalez, C.; Schlegel, H. B. *J. Phys. Chem.* **1990**, *94*, 5523−5527.

[21] Martin, J. M. L.; Sundermann, A. *J. Chem. Phys.* **2001**, *114*, 3408−3420.

[22] Andrae, D.; Häussermann, U.; Dolg, M.; Stoll, H.; Preuß, H. *Theor. Chim. Acta* **1990**, *77*, 123−131.

[23] (a) Krishnan, R.; Binkley, J. S.; Seeger, R.; Pople, J. A. *J. Chem. Phys.* **1980**, *72*, 650−654; (b) McLean, A. D.; Chandler, G. S. *J. Chem. Phys.* **1980**, *72*, 5639−5648; (c) Frisch, M. J.; Pople, J. A.; Binkley, J. S. *J. Chem. Phys.* **1984**, *80*, 3265−3269; (d) Clark, T.; Chandrasekhar, J.; Spitznagel, G. W.; Schleyer, P. v. R. *J. Comp. Chem.* **1983**, *4*, 294−301.

Chapter 4

Ruthenium-Catalyze Transfer-Hydrogenative Reduction/Cyclization of 1,6-Diynes

Abstract: Novel transfer-hydrogenation/cyclization reaction of 1,6-diyne to give exocyclic diene was developed. The reaction is catalyzed by Cp*RuCl(cod) and utilizes MeOH as hydrogen surrogate. The reaction exhibited tolerability toward wide variety of functional groups. Mechanistic studies by means of stoichiometric reaction of ruthenium complex, kinetic study, isotope-effect study and DFT calculations were conducted. The reaction proceed through ruthenacyclopentatriene intermediate which is generated from a divalent ruthenium catalyst and a 1,6-diyne substrate, and it accepts hydrogen from methanol. The hydrogen transfer from methanol to the ruthenacyclopentatriene proceeds *via* stepwise mechanism in which proton and hydride are transferred in discrete steps. Abovementioned studies showed that transfer of protonic hydrogen from alcohol is the rate-determining step.

1. Introduction

Transition metal-catalyzed semi-reduction of alkynes is attracting increasing attention because it allows rational route to geometrically defined alkenes. For instance, Elsevier and co-workers have developed Pd(NMC)-catalyzed transfer semi-reduction of alkynes (Scheme 1).[1]

Scheme 1. Pd-catalyzed transfer hydrogenative semireduction of alkyne.

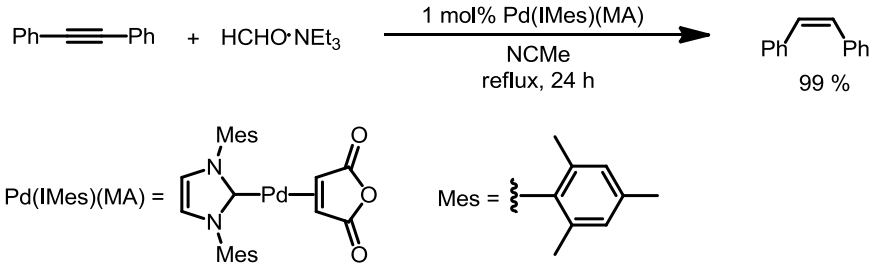

If an alkyne reduction process and C–C bond formation can be combined, it will be synthetically intriguing. Such a process is expected to enable selective coupling between two alkyne parts without affecting other unsaturated moieties. In this respect, several transition metal complex-catalyzed reductive cyclization of 1,6-diynes have been reported (Scheme 2). The pioneering work was achieved by Trost and Lee (eq 1). In their report, in the presence of palladium catalyst, 1,6-diynes were reduced and cyclyzed to afford exocyclic 1,3-dienes by using triethylsilane and acetic acid as hydride and proton source respectively.[2] Krische and co-workers have developed rhodium-catalyzed reductive cyclization of 1,6-diynes by using gaseous hydrogen (eq 2).[3] Similar transformation catalyzed by iron catalyst was reported by Sylvester and Chirik (eq 3).[4]

Scheme 2. Transition metal-catalyzed reductive cyclization of 1,6-diynes.

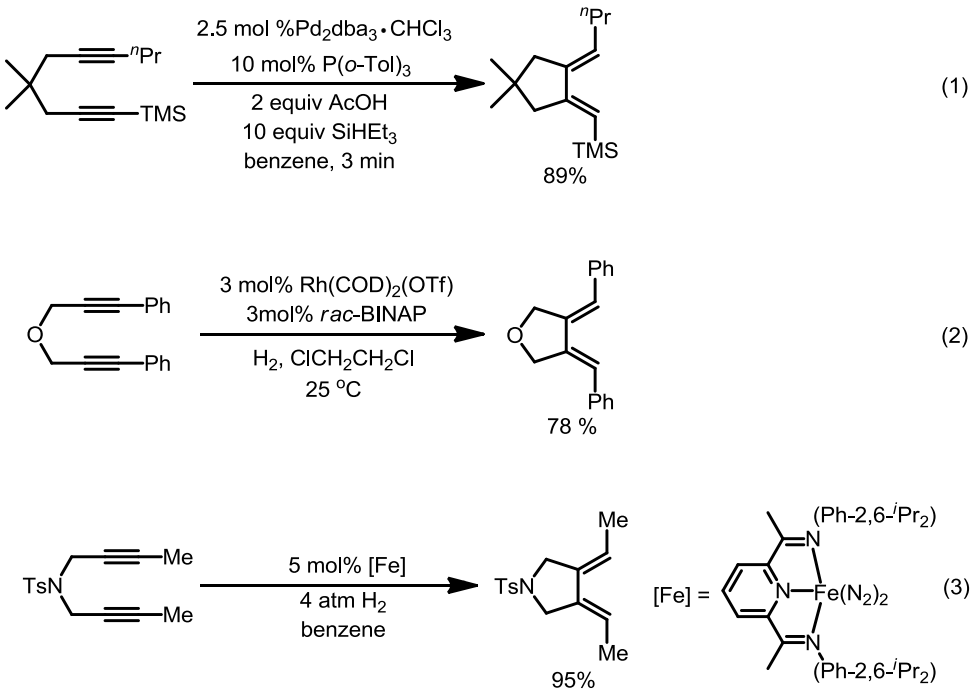

If a lower alcohol such as methanol, ethanol or isopropanol can be used in place of silanes or gaseous hydrogen, it will be advantageous in terms of both cost and safety. However, the reductive transformation of alkynes employing alcohols as hydrogen surrogate is quite limited. Tani and co-workers have developed a rhodium-catalyzed reductive coupling of electron-deficient alkynes (Scheme 3). Interestingly, while (*E*,*E*)- and (*Z*,*Z*)-hydrodimers **1** are formed, (*E*,*Z*) dimer was not observed. To the best of author's knowledge, transfer hydrogenative alkyne dimerization that uses alcohol as a hydrogen surrogate has not been reported other than this.

Scheme 3. Rhodium-catalyzed transfer hydrogenative dimerization of electron-deficient alkynes.

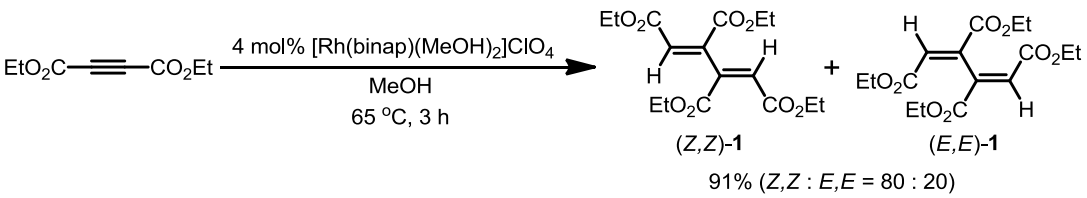

Catalyzed semi-reductions of alkynes employing alcohol as hydrogen source have been reported by Tani[5a] (eq 4, Scheme 4), García[5b] (eq 5) and their respective co-workers. In spite of their synthetic potential, these reactions face problems about chemoselectivity. In Tani's case, alkane was observed as over-reduction product. In the case of García's nickel-catalyzed transfer hydrogenative reduction, addition of an alcohol across the alkyne hampers the reaction.

Scheme 4. Transfer hydrogenative semireduction of alkynes catalyzed by Ir or Ni.

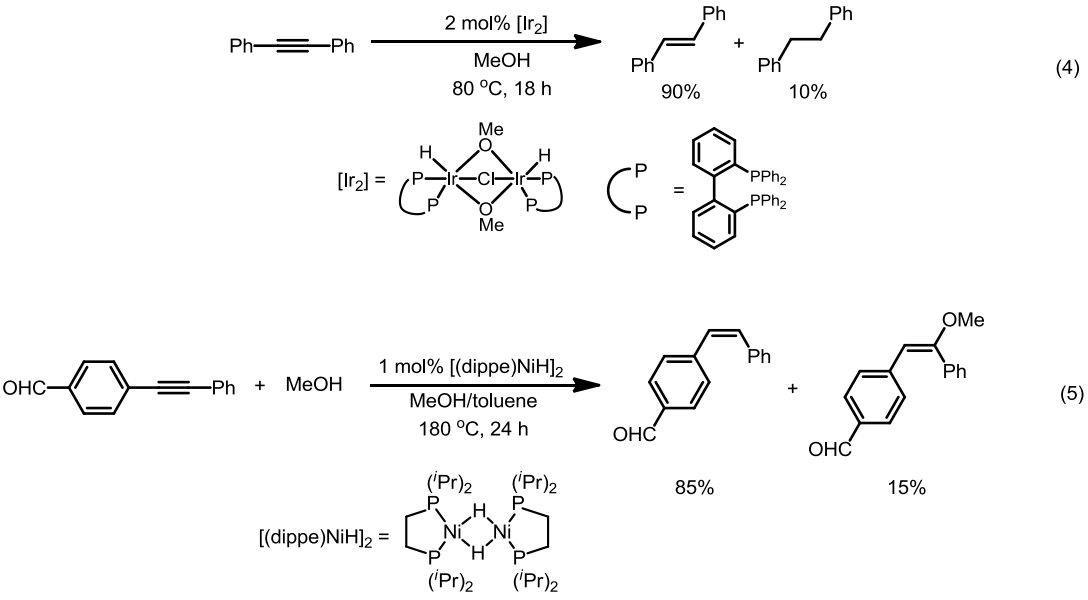

Generally, hydrido complex is generated prior to the activation of alkyne substrate in the reductive transformations of alkynes. It is likely that the hydride complexes can react also with the primarily produced alkene to cause isomerization or over-reduction. If the activation of alkyne takes place first and formation of hydride complex is not required, that reaction may pave the way for the highly selective transfer-hydrogenative reduction of alkynes. Among several possibilities, formation of carbenic intermediate is worth considering as an activation mode of alkynes.

Hydrogen transfer from alcohol to carbene complex has scarcely been reported. Among the limited examples, Mol and co-workers have studied on the reductive decomposition of 1st generation Grubbs' complex (**2**) by using primary alcohols as hydrogen source (Scheme 5).[6] In the reaction, benzylidene moiety was reduced, and a ruthenium hydrido carbonyl complex **3** and

toluene were formed. It should be noted that at least the first hydride transfer from the methoxo group to the benzylidene moiety was rationally presumed to takes place without forming hydrido complex.

Scheme 5. Reductive decomposition of 1st generation Grubbs complex **2**.

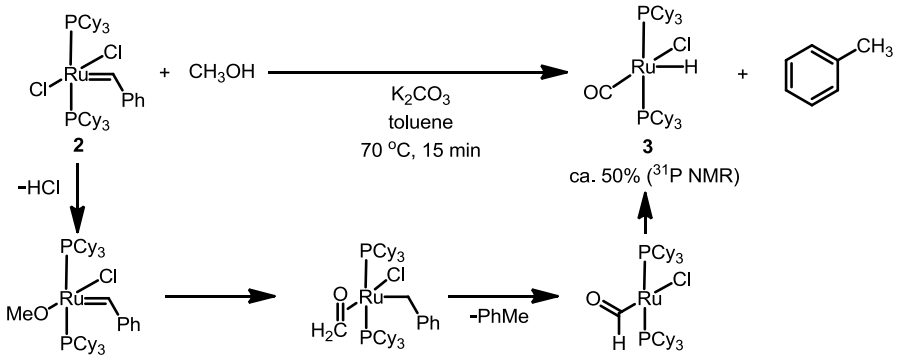

Bruce and co-workers have reported a reductive coupling reaction of electron deficient alkynes mediated by five-membered ruthenacycle **4** (Scheme 6).[7] In the original report, the ruthenacycle was considered as ruthenacyclopentadiene (**4**) rather than a ruthenacyclopentatriene. It appears that the hydrogen originated form methanol, but added salt NH_4PF_6 was proposed to be the reductant. Regrettably, this reaction has not been developed to a catalytic reaction.

Scheme 6. Formation of η^4-1,3-diene complex *via* reductive coupling of electron deficient dienes.

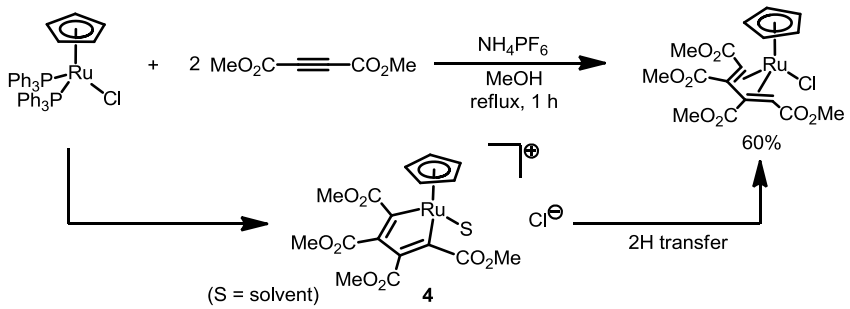

Inspired by these backgrounds, the author sought to develop a new catalytic system.

2. Catalytic Study

In the previous chapter, the reactivity of the ruthenacyclopentadiene complex with water was described. It was attested that the first step of the formation of oxapentadienyl complex was an intake of water molecule by the cationic ruthenacyclopentatriene complex. Naturally, alcohols are expected to behave similarly. Actually, in the presence of silver salt, the ruthenacyclopentatriene complex **5** reacted with methanol to undergo C–O bond formation (Table 1). Although a product corresponding to the η^5-oxapentadienyl complex was not observed, dienyl ether **6** was obtained in 43% yield instead (entry 1). When the counter anion of the silver was tetrafluoroborate, the ether **6** was obtained in comparable yield, and small amount of the diene **7** and furane **8** were also formed (entry 2). Here again, when silver nitrate was added, furan **8** became the major product, and **6**, **7** were not obtained at all (entry 3).

Table 1. The reaction of ruthenacyclopentatriene complex with methanol in the presence of silver salts.

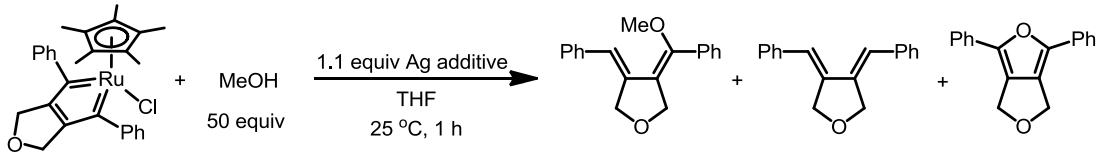

5 **6** **7** **8**

entry	additive	conversion [%]	yields[a] **6** / **7** / **8** [%]
1	$AgPF_6$	> 99	43 / 0 / trace
2	$AgBF_4$	> 99	40 / 11 / 6
3	$AgNO_3$	> 99	0 / 0 / 44

In the absence of Ag^{+}, the ruthenacyclopentatriene exhibited completely different reactivity with methanol. In this case, **5** was reduced, and η^4-1,3-diene complex **9** was formed in 30% yield, while dienyl ether **6** was not formed at all (Scheme 7).

Scheme 7. Formation of η^4-1,3-diene complex **9** from the ruthenacyclopentatriene **5**.

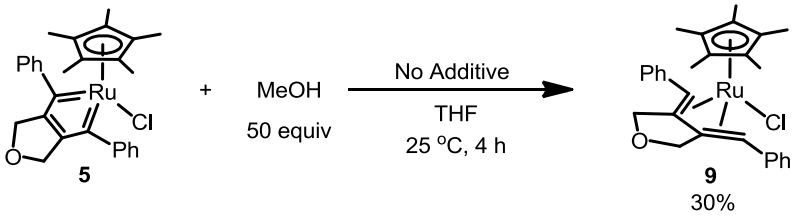

The structure of **9** was unambiguously determined by X-ray crystallography, and shown in Figure 1. The newly incorporated hydrogen atoms occupy the *endo* position of the 1,3-diene moiety.

Figure 1. ORTEP-drawing of the Cp*RuCl–η^4-1,3-diene complex **9**, shown as 50% ellipsoids. All hydrogen atoms are omitted for clarity.

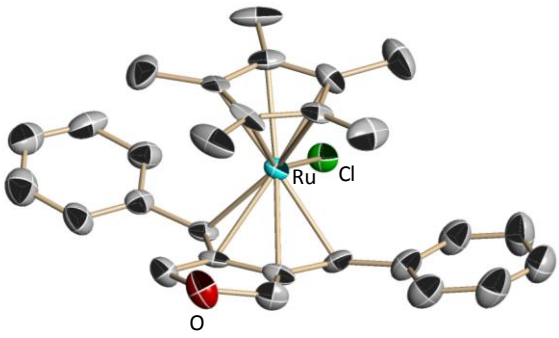

It is natural to think that the hydrogen is originated from methanol. The [Cp*RuCl] structure derived from the precursor complex was retained in the newly formed complex **9**. Hence, it was anticipated that release of the 1,3-diene moiety and formation of a new ruthenacyclopentatriene complex will allow for a catalytic transfer-hydrogenation/cyclization of 1,6-diynes.

In the initial attempt (Scheme 8), ether-tethered diyne **11a** was treated with excess amount of methanol in refluxing THF in the presence of 10 mol% of Cp*RuCl(cod) (**10**). Eventually,

the diyne was completely consumed in 4 hours to afford desired *exo*-diene **12a** in 72 % yield as an exclusive stereoisomer.

Scheme 8. First transfer-hydrogenative reduction/cyclization of 1,6-diyne using methanol as a hydrogen surrogate.

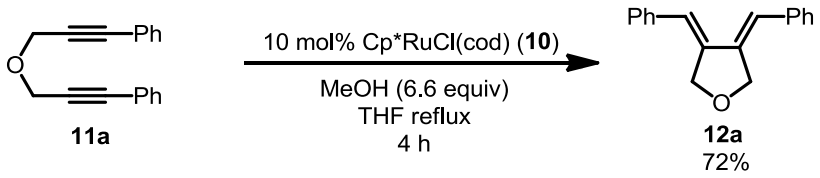

The generality of this new method was investigated by using diyne substrates bearing various functional groups (Table 2). When the diyne (**11b**) contains tosylamide as a heteroatom tether, the reaction gave a complex mixture in refluxing THF. To suppress the side reactions, the temperature was lowered to 50 °C to afford heterocyclic **12b** in 78% yield (entry 1). On the other hand, with quaternary carbons as the tethers, the reaction proceeded cleanly (entries 2–6). In addition, the required catalyst loading was reduced to 1 mol%. In these cases, ester, ketone, nitrile remained intact. Substrates bearing substituted aromatic rings, such as *p*-methoxyphenyl, *p*-fluorophenyl or even reactive *p*-bromophenyl group, were also reductively cyclyzed under established condition with ease (entries 7–9). In terms of electronic effect, electron withdrawing halogen substituents slightly accelerated the reaction. Contrarily to successful reactions employing 1,6-diaryldiynes, substrates bearing alkyl, alkenyl or heteroaryl terminal substituents gave intractable complexes.

Table 2. Scope of the newly developed ruthenium-catalyzed transfer hydrogenation.

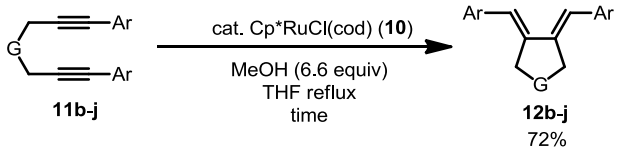

entry	diyne **11**	cat. (loading [mol%])	time [h]	**12** yield [%]
1	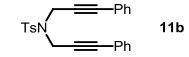 **11b**	10	9[a]	**12b**, 78
2	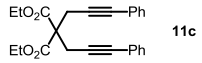 **11c**	10	3	**12c**, 90
		1	21	**12c**, quant
3	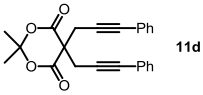 **11d**	1	8	**12d**, 98
4	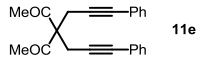 **11e**	1	10	**12e**, 97
5	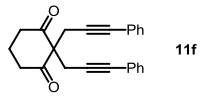 **11f**	1	18	**12f**, quant
6	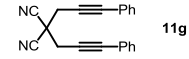 **11g**	1	13	**12g**, 92
7	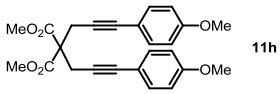 **11h**	3	11	**12h**, 88
8	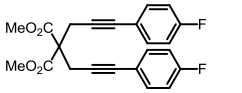 **11i**	2	4	**12i**, 95
9	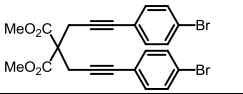 **11j**	3	4	**12j**, 87 (90[b])

[a] The reaction was carried out at 50 °C. [b] The reaction was carried out at 12.9 g scale (25 mmol of **11j**). The product was isolated by 4 times of recrystallization.

The present reaction enables the construction of a configurationally defined 1,4-diphenyl-1,3-diene framework, which is a key component in π-conjugated materials.[8] In this regard, *p*-bromophenyl derivative **12j** is a potentially useful building block, which is easily derivatized by cross couplings at the C–Br bonds. For example, double Sonogashira coupling of **12j** with phenyl acetylene afforded **13**, which has an expanded π-conjugation system, in high yield (Scheme 9). The synthesis of the building block **12j** could be easily scalable; the reductive cyclization of 12.9 g (25 mmol) of **11j** under the same condition as described above afforded **12j** in 90% yield after four times of recrystallization (Table 2, entry 9, in parenthesis).

Scheme 9. Expansion of π-conjugation system by Sonogashira coupling.

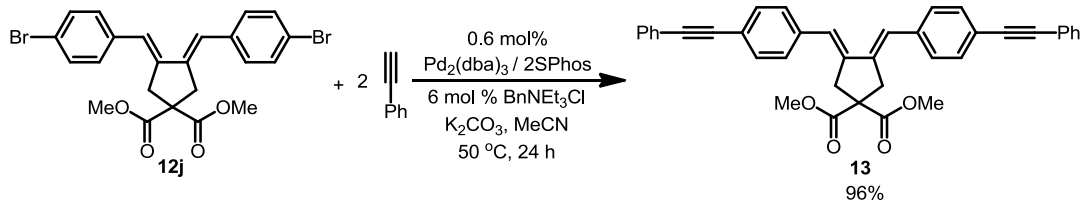

To further demonstrate the synthetic utility of the novel method, double reductive cyclization of tetrayne **14** was performed. With 5 mol catalyst loading at 70 °C for 5 h, tetraene **15** was obtained in quantitative yield (Scheme 10).

Scheme 10. Double reductive cyclization of tetrayne **14**.

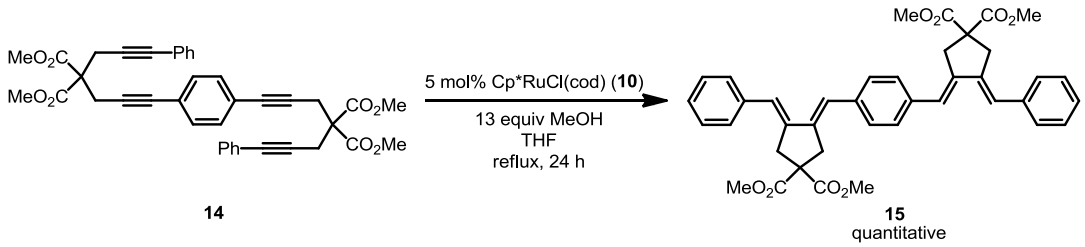

3. Mechanistic Study

Next, experiments to confirm the origin of the hydrogen were conducted. To detect the alcohol oxidation product, heavier benzyl alcohol (**16**) was used with diyne **11c′** in place of methanol (Scheme 11). The reaction proceeded smoothly, and ^{1}H NMR analysis of the crude mixture showed that benzaldehyde (**16**) was formed in 96% yield (based on the diyne **11c′**) together with the expected diene product **11c′** (99% yield).

Scheme 11. Reductive cyclization using benzyl alcohol as hydrogen source.

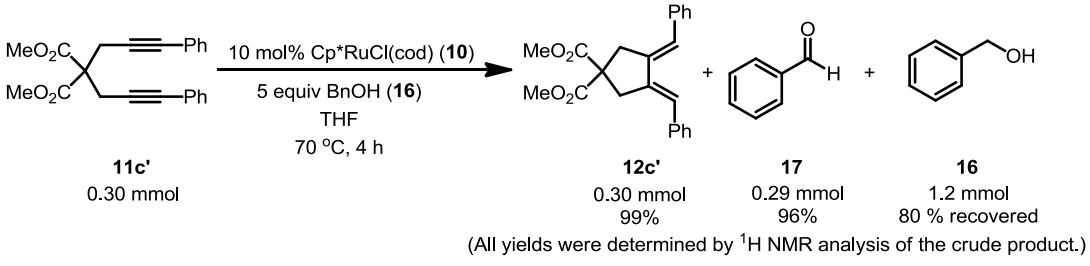

When **11c** was treated with deuterated methanol CD_3OH under the above-established condition, mono-deuterated product **12c**-d_1 was exclusively formed (Scheme 12). The isotopological uniformity was guaranteed by FAB-MS analysis (Figure 2).

Scheme 12. HD transfer from CD_3OH.

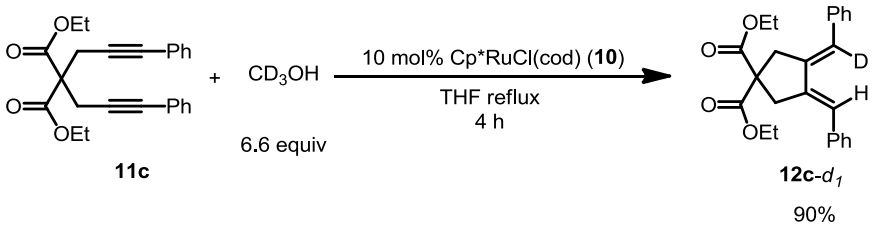

Figure 2. FAB-MS analysis of **12c**-d_1.

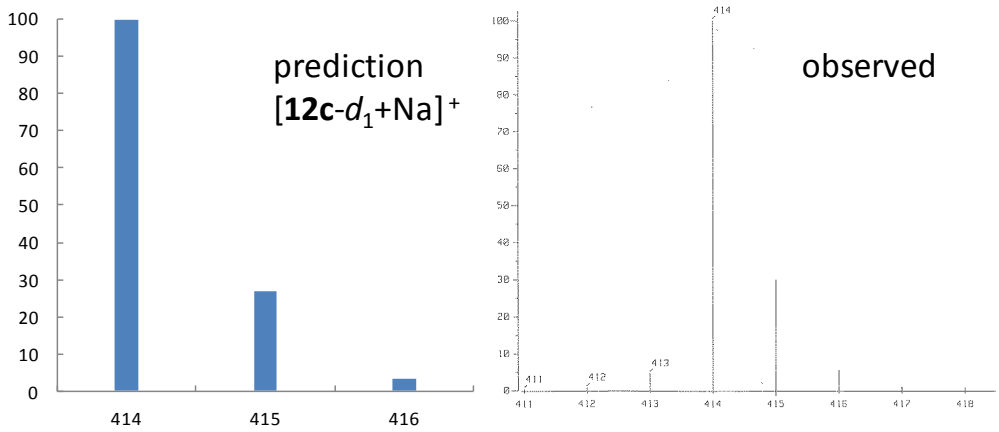

These facts clearly indicate that two hydrogen atoms originated from the primary alcohols. In addition, almost complete 1:1 incorporation of H and D from CD_3OH implies that a ruthenium hydride species is not generated. Ruthenium hydride species are prone to hydride exchange with alcoholic hydroxyl group,[9] and diminished deuterium incorporation is predicted.

To obtain further insight into the reaction mechanism, kinetic studies were carried out. As a preliminary investigation, time–concentration relationship was inspected (Figure 3). 0.21 M of diyne **11c′** was treated with 1.8 M of methanol in the presence of 5 mol% of Cp*RuCl(cod) (**10**). The concentration of substrate **11c′** and product **12c′** was determined by ^{1}H NMR analysis by using 0.12 M of dioctyl ether as an internal standard. As shown, the obtained plot exhibited very good linearity ($R^2 > 0.99$). Since excessive methanol was added, this result implies that the reaction rate is independent of concentration of the diyne.

Figure 3. Concentration-time plot at 60 °C.

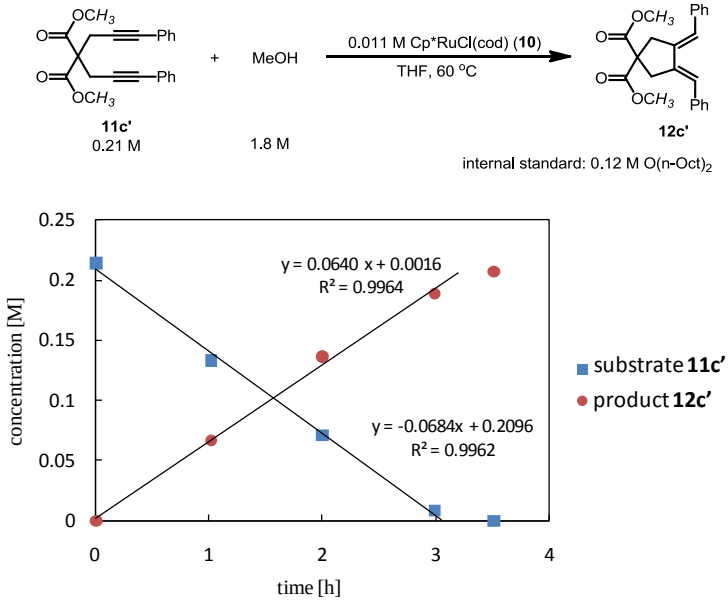

In fact, when the initial concentration of the diyne **11c′** was higher than 0.1 M, the reaction rate was almost constant (A, Figure 4). In contrast, obvious dependence of the reaction rate on methanol concentration was observed (B, Figure 4). These results imply that the late-limiting step involves the activation of methanol.

Figure 4. Dependence of the reaction rate on the concentration substrate concentrations.

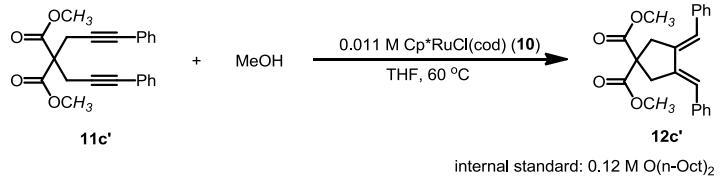

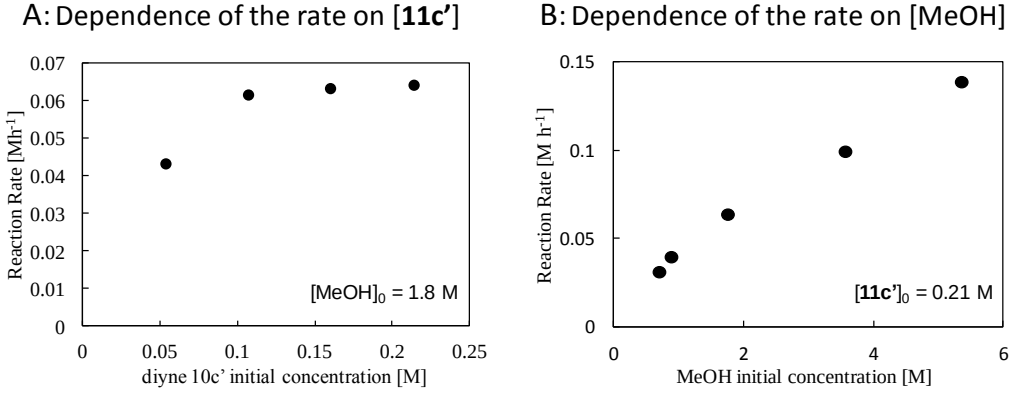

Next, in an attempt to gain a further insight into the hydrogen abstraction step, kinetic studies with deuterated methanol was conducted as shown in Figure 5. Interestingly, the reactions employing CH_3OH and CD_3OH exhibited virtually same reaction rate (k = 0.062 ± 0.002 and 0.063 ± 0.002 M/h respectively). On the other hand, the reaction with CH_3OD showed a significantly low reaction rate (k = 0.039 ± 0.005 M/h). Therefore, it is highly likely that the transfer of protonic hydrogen atom (–OH) rather than hydridic one (–CH_3) consists the rate-limiting step.

Figure 5. Comparison of reaction rate by using deuterated methanol.[a]

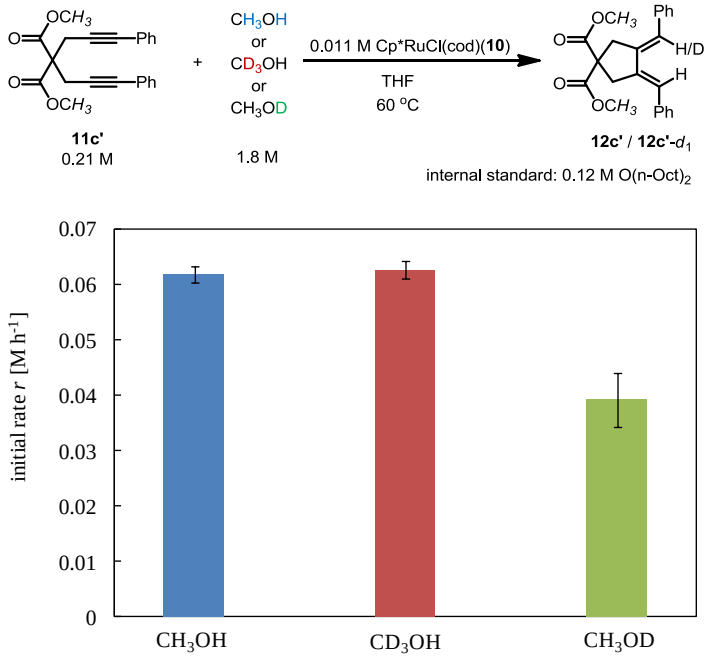

[a] Average of three measurements. Err bars correspond to standard deviations.

With above kinetic information in hand, catalytic cycle is proposed (Scheme 13). Since the stoichiometric transfer-hydrogenation of a ruthenacyclopentatriene have been examined (Scheme 7), it is most likely that the reaction is mediated by a ruthenacyclopentatrienes. As it is known that Cl^- anion can dissociate from the ruthenium center in a polar medium,[10] **18** is presumably in equilibrium with methoxo analogue **19**. **19** will undergo reversible protonation with by concomitantly produced HCl. Subsequently, hydride abstraction from the methoxo

ligand by an electrophilic carbene center occurs *via* transition state **21**, giving rise to ruthenacyclopentene **22** and one molecule of formaldehyde. The isomerization of **22** must occur in disrotatory fashion to furnish thermodynamically more stable η^4-1,3-diene complex **23**. The intermediacy of **23** again supported by the isolation of **9** (Scheme 7). Finally, the displacement of the resultant 1,3-diene ligand with a 1,6-diyne substrate is followed by oxidative cyclization to produce **12**.

Scheme 13. Proposed catalytic cycle of ruthenium-catalyzed reductive cyclization of diynes.

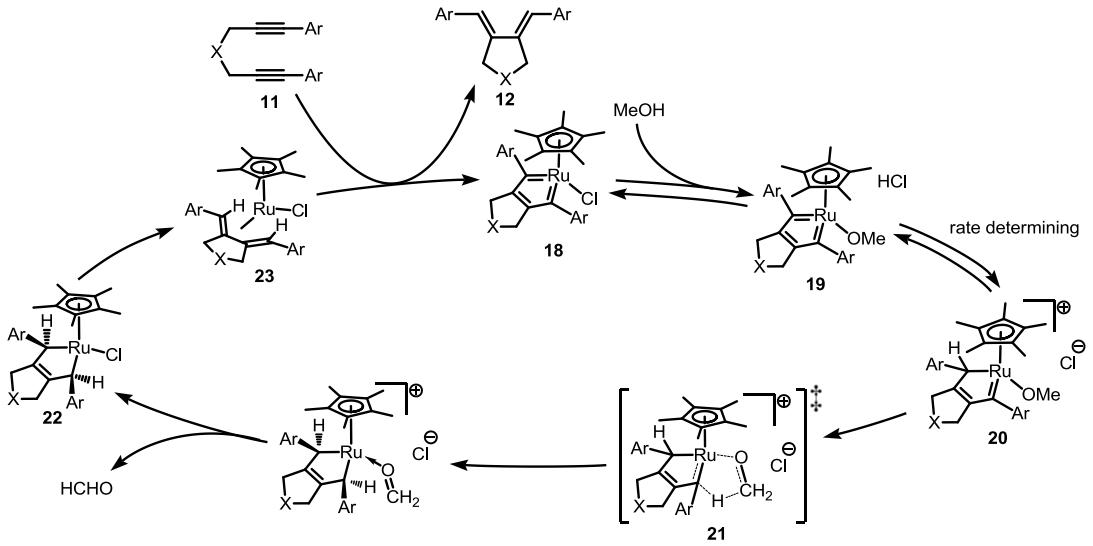

The proposed catalytic cycle involves an unprecedented elementary step where **19** evolves into **22** through transition state **22**. Although metallacyclic mechanisms were proposed in the previous examples of reductive cyclizations,[3,4] this is the first experimental evidence for hydrogen transfer from MeOH to a metallacyclopentatriene. Moreover this novel hydride transfer mechanism is well corroborated by a preliminary theoretical study on model system. A transition state for normal β-hydride elimination of a methoxo complex could not be located. On the other hand, a transition state (**TS-AB**) for hydride transfer from the methoxo ligand onto one of the carbene carbon could be located (path A, Figure 6). However, this process was estimated to take place with an activation energy of $\Delta G^{\ddagger}$ = 20.3 kcal/mol, and is thermodynamically unfavorable with an endothermicity of ΔG = 4.7 kcal/mol.

Figure 6. DFT calculation on hydrogen transfer step.

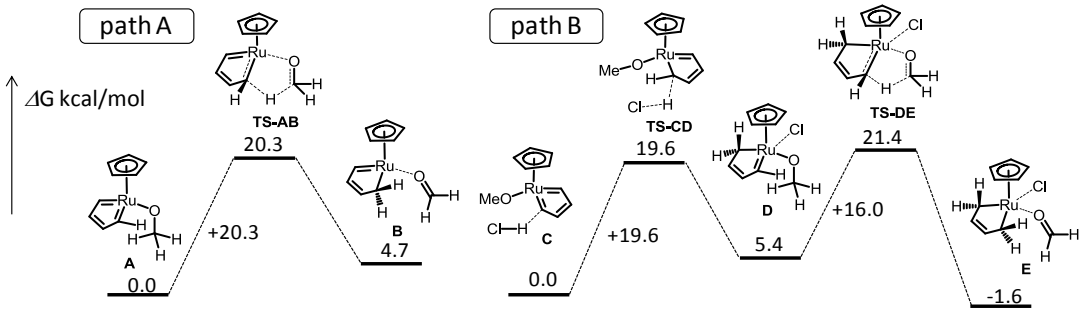

Next, an alternative route was sought (path B, Figure 6). Since the protonation of ruthenacyclopentatriene intermediate and subsequent nucleophilic attack of conjugate base onto the remaining carbene carbon have been proposed in a series of studies by Dixneuf's group.[11] The protonation of the model ruthenacycle methoxo complex with HCl was estimated to occur with an activation barrier of $\Delta G^{\ddagger}$ = 19.6 kcal/mol (**TS-CD**), which is smaller than that of **TS-AB**. Although the protonation is endothermic (ΔG = 5.4 kcal/mol), a further lower activation barrier of $\Delta G^{\ddagger}$ = 16.0 kcal/mol was calculated for the subsequent hydride transfer process *via* **TS-DE**. As a result, the protonation/hydride transfer mechanism is favorably supported by these DFT calculations. In addition, the subsequent isomerization of the resultant ruthenacyclopentene into a η^4-diene complex is estimated to be facile and thermodynamically favorable owning to a small activation barrier of $\Delta G^{\ddagger}$ = 2.2 kcal/mol (**TS-FG**) and large exothermicity of 31.2 kcal/mol.

Figure 7. Isomerization of a ruthenacyclopentene complex **E** to a η^4-1,3-dene complex **G**.

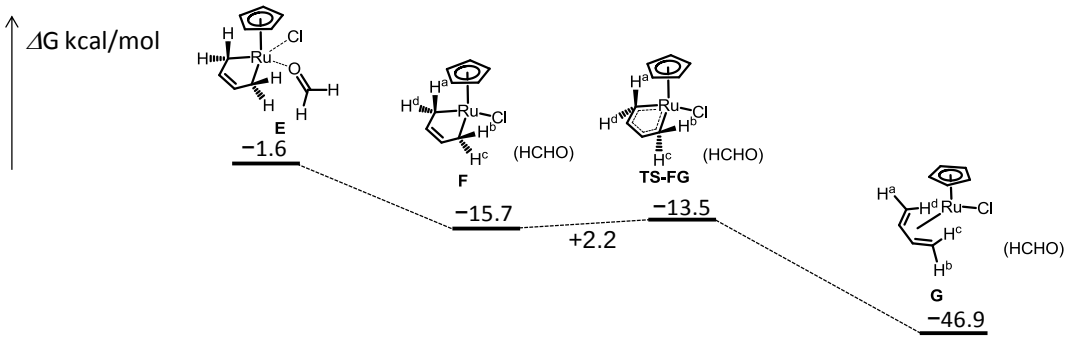

Therefore, the step of the highest barrier in the overall process is the reversible protonation (between **19** and **20**), and this is in good agreement with the significant rate decrease observed when CH_3OD was used in place of CH_3OH.

In conclusion, the author developed a novel transfer hydrogenation/cyclization process that employs methanol as a hydrogen surrogate. The novel reaction has wide functional group tolerability and generality toward 1,7-diaryl-1,6-diynes. Based on a stoichiometric reaction between an isolable ruthenacyclopentatriene **5** and methanol, it was revealed this reaction is the first confirmed example of reductive coupling of alkyne moieties that proceed through a metallacyclopentatriene. Kinetic and DFT studies suggest that the hydrogen transfer from methanol to ruthenacyclopentatriene intermediate proceeds through a step wise mechanism, in which protonic and hydridic hydrogen atoms are transferred in discrete steps.

4. Experimental Section

(a) General Considerations.

Column chromatography was performed on silica gel (Cica silica gel 60N) with solvents specified below. ^{1}H and ^{13}C NMR spectra were obtained for samples in $CDCl_3$ solution at 25 °C. ^{1}H NMR chemical shifts are reported in terms of chemical shift (δ, ppm) relative to the singlet at 7.26 ppm for chloroform. Splitting patterns are designated as follows: s, singlet; d, doublet; t, triplet; q, quartet; quint, quintet; sext, sextet; sept, septet; m, multiplet. Coupling constants are reported in Hz. ^{13}C NMR spectra were fully decoupled and are reported in terms of chemical shift (δ, ppm) relative to the triplet at δ = 77.0 ppm for $CDCl_3$. Mass measurements and elemental analyses were performed by the Instrumental Analysis Facility of Nagoya University. Melting points were obtained in capillary tubes. Ruthenacyclopentatriene (**5**), [12] and Cp*RuCl(cod) (**10**)[13] were prepared according the reports. Diynes **11a**,[14] **11b**,[15] **11c**,[16] **11c′**,[3] **11d**,[16] **11e**,[17] **11f**,[16] and **11i**,[16] and dienes **12a**,[16] **12c′**,[16] **12d**[16] and **12f**[16] are known compounds.

(b) Preparations of Substrates

Synthesis of diyne 11g: To a solution of malononitrile (0.20 g, 3.0 mmol), triethylamine (0.84 mL, 6.0 mmol) and sodium iodide (0.99 g, 6.6 mmol) in dry DMSO (9 mL) was added dropwise a solution of 3-phenylprop-2-ynyl 4-methylbenzenesulfonate (1.7 g, 6.0 mmol) in dry DMSO (3.0 mL) under an argon atmosphere. The reaction mixture was stirred at room temperature for 10 h. The solution was diluted with Et_2O (20 mL) and quenched with H_2O (40 mL). The aqueous layer was extracted with Et_2O (2 × 20 mL). The combined organic layer was washed with H_2O (50 mL) and brine (50 mL), and dried over $MgSO_4$. The organic layer was concentrated in vacuo to obtain dark brown solids. After short-column chromatography on silica gel, the crude product was purified by recrystallization from hexane/Et_2O to afford **11g** (0.82 g, 47% yield) as colorless crystals (mp 83.5–85.5 °C): IR (KBr) 2238 (CN) cm^{-1}; ^{1}H NMR (300 MHz, CDCl3, 25 °C): δ 3.35 (s, 4 H), 7.30–7.42 (m, 6 H), 7.45–7.53 (m, 4 H); ^{13}C NMR (75 MHz, CDCl3, 25 °C): δ 28.6, 36.9, 79.1, 87.2, 113.8, 121.3, 128.2, 128.9, 131.8; HRMS (FAB) m/z calcd for $C_{21}H_{15}N_2$ 295.1230, found 295.1237 $[M+H]^+$.

Synthesis of diyne 11j: A solution of dimethyl dipropargylmalonate (6.0 g, 29 mmol), 1-bromo-4-iodobenzene (17 g, 60 mmol), $Pd(PPh_3)_4$ (70 mg, 0.060 mmol), and CuI (0.023 g, 0.12 mmol) in diisopropylamine (104 mL) was stirred at room temperature under an argon atmosphere for 5 h. The resultant mixture was diluted with AcOEt (100 mL), and quenched with H_2O (100 mL). The aqueous layer was extracted with AcOEt (100 mL). The combined organic layer was washed with H_2O (2 × 100 mL) and with brine (100 mL), and dried over $MgSO_4$. The solvents were evaporated under reduced pressure to give a brown solid. After filtration through a pad of silica gel (solvent: hexane/AcOEt = 5:1), a crude product was purified by recrystallization form hot hexane/AcOEt to give **11j** (14 g, 92 %) as colorless crystals (mp 75.5–77.5 °C); IR (KBr): 1740 (C=O) cm^{-1}; ^1H NMR (300 MHz, $CDCl_3$, 25 °C): δ 3.23 (s, 4 H), 3.80 (s, 6 H), 7.23 (ddd, *J* = 8.7, 2.4, 2.1 Hz, 4 H), 7.41 (ddd, *J* = 8.7, 2.4, 2.1 Hz, 4 H); ^{13}C NMR (75 MHz, $CDCl_3$, 25 °C): δ 24.0, 53.3, 57.1, 82.8, 85.0, 121.7, 122.2, 131.3, 132.9, 168.9; HRMS (FAB) *m/z* calcd for $C_{25}H_{18}Br_2NaO_4$ 539.9464, found 538.9471 $[M+Na]^+$.

Synthesis of diyne 11h: **11h** was prepared from dimethyl dipropargylmalonate and *p*-iodoanisole according a similar procedure for **10j**; colorless crystals (mp 80.0–82.0 °C); IR (KBr): 1741 (C=O) cm^{-1}; ^1H NMR (300 MHz, $CDCl_3$, 25 °C): δ 3.25 (s, 4 H), 3.80 (s, 12 H), 6.80 (ddd, *J* = 9.0, 2.7, 2.7 Hz, 4 H), 7.31 (ddd, *J* = 9.0, 2.7, 2.7 Hz, 4 H); ^{13}C NMR (75 MHz, $CDCl_3$, 25 °C): δ 24.0, 53.1, 55.3, 57.4, 82.3, 83.5, 113.6, 115.0, 132.8, 159.0, 169.1; HRMS (FAB) *m/z* calcd for $C_{25}H_{24}NaO_6$ 443.1465, found 443.1470 $[M+Na]^+$.

Synthesis of Tetrayne 14: A solution of dimethyl 2-(3-phenylprop-2-ynyl)-2-(prop-2-ynyl)-malonate (0.59 g, 2.1 mmol), 1,4-diiodobenzene (0.34 g, 1.0 mmol), $Pd(PPh_3)_4$ (1.2 mg, 0.0010 mmol), and CuI (0.66 mg, 0.0035 mmol) in degassed diisopropylamine (4.0 mL) was stirred at room temperature under an argon atmosphere for 12 h. The resultant reaction mixture was diluted with AcOEt (20 mL) and quenched with H_2O (20 mL). The aqueous layer was extracted with AcOEt (20 mL). The combined organic layer was washed with H_2O (50 mL) and then with brine (50 mL) and dried over $MgSO_4$. The solvents were removed under reduce pressure to give brown oil. The crude product was purified with column chromatography on silica gel (elution

with hexane/AcOEt = 10:1–2:1) to give **14** (0.58 g, 87 % yield) as off-white solids (mp 121.5–122.5 °C); IR (KBr): 1741 (C=O) cm^{-1}; ^1H NMR (300 MHz, $CDCl_3$, 25 °C): δ 3.25 (s, 4 H), 3.27 (s, 4 H), 3.81 (s, 12 H), 7.26–7.32 (m, 10 H), 7.34–7.40 (m, 4 H); ^{13}C NMR (75 MHz, $CDCl_3$, 25 °C): δ 24.0, 24.1, 53.2, 57.2, 83.4, 83.7, 83. 8, 85.6, 122.5, 122.8, 127.9, 128.0, 131.3, 131.4, 169.0; HRMS (FAB) *m/z* calcd for $C_{40}H_{34}O_8Na$ 665.2146, found 655.2153 $[M+Na]^+$.

(c) Reactions of Ruthenacyclopentatriene 5 with MeOH.

Reaction in the presence of a silver salt: To a stirred solution of **5** (26 mg, 0.050 mmol) and dry MeOH (0.10 mL, 2.5 mmol) in dry THF (0.5 mL) was added a solution of $AgPF_6$ (14 mg, 0.055 mmol) in dry THF (1.0 mL) under an argon atmosphere. The crude yield of **6** (0.022 mmol, 43%) was determined by ^1H NMR analysis with ethylbenzene (10.0 μL, 0.082 mmol) as internal standard. Purification of **6** by means of chromatography on silica gel or alumina led to extensive decomposition, and ultimately to only low-yield isolation as a colorless oil; ^1H NMR (300 MHz, $CDCl_3$) δ 3.59 (s, 3 H), 4.45 (s, 2 H), 4.81 (d, *J* = 2.4 Hz, 2 H), 7.19–7.26 (m, 2 H), 7.31–7.46 (m, 8 H), 7.57 (t, *J* = 2.4 Hz, 1 H); ^{13}C NMR (75 MHz, $CDCl_3$) δ 57.3, 70.9, 72.5, 119.7, 123.4, 126.4, 128.0, 128.22, 128.26, 128.32, 128.5, 134.9, 137.4, 138.1, 149.6; HRMS (FAB) *m/z* calcd for $C_{19}H_{19}O_2$ 279.1385, found 279.1387 $[M+H]^+$.

Reaction in the absence of additives: To a stirred solution of **1** (26.0 mg, 0.050 mmol) in degassed dry THF (1.5 mL) was added degassed dry MeOH (0.1 mL, 2.5 mmol) under an argon atmosphere. The mixture was stirred at 25 °C for 4 h. The solvent and excess MeOH was removed under reduced pressure. The crude yield of **9** (0.025 mmol, 50%) was determined by ^1H NMR analysis with ethylbenzene (10.0 μL, 0.082 mmol) as internal standard. The crude material was purified with silica gel column chromatography (elution with hexane/AcOEt 10:1 ~ 5:1) to give **9** (7.90 mg, 0.015 mmol, 30%) as red micro crystals (mp. 174 °C decomp.); ^1H NMR (300 MHz, $CDCl_3$) δ 1.09 (s, 15 H), 3.97 (s, 2 H), 4.84 (d, *J* = 11.5 Hz, 2 H), 5.44 (d, *J* = 11.5 Hz, 2 H), 7.15–7.40 (m, 6 H), 7.52 (d, *J* = 7.2 Hz, 4 H); ^{13}C NMR (75 MHz, $CDCl_3$) δ 8.3, 64.6, 71.9, 94.3, 102.6, 125.7, 126.8, 128.0, 139.5; HRMS (FAB) *m/z* calcd for $C_{28}H_{31}ClORu$ 520.1107, found 520.1107 $[M]^+$.

(d) Crystallographic Structural Determinations.

A single crystal of **9** suitable for X-ray analysis was mounted on a glass fiber, and diffraction data were collected at 153 K on a Brucker SMART APEX CCD diffractometer with graphite monochromated Mo-Kα radiation (λ = 0.71073 Å). The absorption correction was made using SADABS. The structure was solved by direct methods and refined by the full-matrix least-squares on *F2* by using SHELXTL.[18] All non-hydrogen atoms were refined with anisotropic displacement parameters. All hydrogen atoms were placed in calculated positions.

Table S 1. Selected crystallographic data and collection parameters for **9**.

	9
Formula	$C_{28}H_{31}ClORu$
Fw	520.05
Crystal system	Orthorhombic
Space group	$P2_12_12_1$ (#19)
a [Å]	7.2976(5)
b [Å]	14.8834(11)
c [Å]	23.5529(17)
V [Å^3]	2558.2(3)
Z	4
D_{calc} [g cm^{-3}]	1.350
μ [mm^{-1}]	0.734
F(000)	1072
Crystal size [mm^3]	0.8 × 0.5 × 0.15
Reflections collected	6358
Independent reflections	6358 (R_{int} =0.0000)
GOF on F^2	1.128
R_1 [I>2σ(I)][a]	0.0567
wR_2 (all data)[b]	0.1339
Absolute structure parameter	0.16(6)
Largest diff. peak and hole [e Å^{-3}]	0.899 / −1.439

[a] $R_1 = \Sigma | (F_o - F_c) | / \Sigma (F_o)$. [b] $wR_2 = \{\Sigma[(w(F_o^2 - F_c^2)^2)]/\Sigma[w(F_o^2)^2]\}^{1/2}$.

(e) Cp*RuCl-Catalyzed Cyclization/Transfer Hydrogenation.

General procedures – Cyclization of 11a: To a solution of Cp*RuCl(cod) (23 mg, 0.060 mmol) and MeOH (0.16 mL, 4.0 mmol) in dry degassed THF (1.2 mL) was added a solution of **11a** (0.15 g, 0.60 mmol) in THF (1.2 mL) under an argon atmosphere. The reaction mixture was stirred at 70 °C for 4 h. The reaction was traced by TLC analysis. After concentration in vacuo, the crude product was purified by column chromatography on silica gel (hexane/AcOEt = 15:1 – 8:1) to give **12a** (0.11 g, 72% yield) as colorless crystals (mp 157.5–158.5 °C); ^{1}H NMR (300 MHz, $CDCl_3$, 25 °C): δ 4.86 (d, *J* = 2.4 Hz, 4 H), 6.98 (t, *J* = 2.4Hz, 2 H), 7.23–7.29 (m, 6 H), 7.36–7.42 (m, 4 H); ^{13}C NMR (75 MHz, $CDCl_3$, 25 °C): δ 71.1, 118.5, 127.0, 128.4, 128.5, 136.7, 138.8; HRMS (FAB) *m/z* calcd for $C_{18}H_{16}O$ 248.1201, found 248.1199 $[M]^+$.

Analytical data for 12b: Colorless crystals (mp 199.5–201.0 °C); ^{1}H NMR (300 MHz, $CDCl_3$, 25 °C): δ 2.43 (s, 3 H), 4.35 (d, *J* = 2.4 Hz, 4 H), 6.90 (t, *J* = 2.4 Hz, 2 H), 7.23–7.44 (m, 12 H), 7.72–7.76 (m, 2 H); ^{13}C NMR (75 MHz, CDCl3, 25 °C): δ 21.8, 51.3, 120.7, 127.4, 127.5, 128.5, 128.6, 129.7, 132.8, 135.5, 136.1, 143.6; HRMS (FAB) *m/z* calcd for $C_{25}H_{23}NO_2S$ 401.1449, found 401.1448 $[M]^+$.

Analytical data for 12c: Colorless crystals (mp 88.0–88.5 °C); IR (KBr): 1723 (C=O) cm^{-1}; ^{1}H NMR (300 MHz, $CDCl_3$, 25 °C): δ 1.20 (t, *J* = 7.2 Hz, 6 H), 3.39 (d, *J* = 2.1 Hz, 4 H), 4.17 (q, *J* = 7.2 Hz, 4 H), 6.99 (t, *J* = 2.1 Hz, 2 H), 7.20–7.30 (m, 2 H), 7.30–7.46 (m, 8 H); ^{13}C NMR (75 MHz, $CDCl_3$, 25 °C): δ 14.2, 39.0, 59.0, 61.8, 120.4, 126.6, 128.2, 128.7, 137.2, 139.5, 170.9; HRMS (FAB) *m/z* calcd for $C_{25}H_{26}NaO_4$ 413.1723, found 413.1717 $[M+Na]^+$.

Analytical data for 12c′: Colorless crystals (mp 146.5–148.0 °C); IR (KBr): 1723 (C=O) cm^{-1}; ^{1}H NMR (300 MHz, $CDCl_3$, 25 °C): δ 3.41 (d, *J* = 2.1 Hz, 4 H), 3.72 (s, 6 H), 7.00 (t, *J* = 2.1 Hz, 2 H), 7.22–7.28 (m, 2 H), 7.33–7.44 (m, 8 H); ^{13}C NMR (75 MHz, $CDCl_3$, 25 °C): δ 39.1, 53.1, 58.9, 120.4, 126.7, 128.2, 128.8, 137.2, 139.2, 171.3; HRMS (FAB) *m/z* calcd for $C_{23}H_{22}NaO_4$ 385.1410, found 385.1414 $[M+Na]^+$.

Analytical data for 12d: Colorless crystals (mp 235.5–238.0 (dec.) °C); IR (KBr): 1740 (C=O) cm^{-1}; ^1H NMR (300 MHz, $CDCl_3$, 25 °C): δ 1.77 (s, 6 H), 3.48 (d, *J* = 2.1 Hz, 4 H), 7.12 (t, *J* = 2.1 Hz, 2 H), 7.23–7.28 (m, 2 H), 7.33–7.40 (m, 8 H); ^{13}C NMR (75 MHz, CDCl3, 25 °C): δ 29.2, 43.2, 52.4, 105.0, 120.8, 126.9, 128.3, 128.7, 136.9, 138.5, 169.7; HRMS (FAB) *m/z* calcd for $C_{24}H_{22}NaO_4$ 397.1410, found 397.1410 $[M+Na]^+$.

Analytical data for 12e: Colorless crystals (mp 132.0–133.5 °C); IR (KBr): 1702 (C=O) cm^{-1}; ^1H NMR (300 MHz, $CDCl_3$, 25 °C): δ 2.13 (s, 6 H), 3.30 (d, *J* = 2.1 Hz, 4 H), 6.99 (t, *J* = 2.1 Hz, 2 H), 7.22–7.32 (m, 2 H), 7.34–7.46 (m, 8 H); ^{13}C NMR (75 MHz, $CDCl_3$, 25 °C): δ 27.0, 36.5, 73.1, 120.8, 126.9, 128.3, 128.8, 137.0, 139.3, 204.5; HRMS (FAB) *m/z* calcd for $C_{23}H_{22}O_2$ 330.1620, found 330.1616 $[M]^+$.

Analytical data for 12f: Colorless crystals (mp 211.5–212.0 °C); IR (KBr): 1695 (C=O) cm^{-1}; ^1H NMR (300 MHz, $CDCl_3$, 25 °C): δ 1.98 (quint, *J* = 6.6 Hz, 2 H), 2.71 (t, *J* = 6.6 Hz, 4 H), 3.25 (d, *J* = 2.4 Hz, 4 H), 6.98 (t, *J* = 2.4 Hz, 2 H), 7.20–7.30 (m, 2 H), 7.32–7.46 (m, 8 H); ^{13}C NMR (75 MHz, $CDCl_3$, 25 °C): δ 18.0, 37.6, 37.9, 71.2, 120.4, 126.7, 128.2, 128.8, 137.3, 139.6, 206.7; HRMS (FAB) *m/z* calcd for $C_{24}H_{22}O_2$ 342.1620, found 342.1617 $[M]^+$.

Analytical data for 12g: Colorless crystals (mp 168.0–169.0 °C); IR (KBr): 2251 (CN) cm^{-1}; ^1H NMR (300 MHz, $CDCl_3$, 25 °C): δ 3.54 (d, *J* = 2.4 Hz, 4 H), 7.18 (t, *J* = 2.4 Hz, 2 H), 7.28–7.35 (m, 6 H), 7.38–7.46 (m, 4 H); ^{13}C NMR (75 MHz, $CDCl_3$, 25 °C): δ 33.2, 42.7, 115.5, 123.6, 127.8, 128.6, 128.7, 133.6, 135.8; HRMS (FAB) *m/z* calcd for $C_{21}H_{16}N_2$ 296.1313, found 296.1308 $[M]^+$.

Analytical data for 12h: Colorless crystals (mp 155.5–159.0 °C); IR (KBr): 1744 (C=O) cm^{-1}; ^1H NMR (300 MHz, $CDCl_3$, 25 °C): δ 3.37 (d, *J* = 2.4 Hz, 4 H), 3.72 (s, 6 H), 3.84 (s, 6 H), 6.86–6.94 (m, 6 H), 7.34 (d, *J* = 8.7 Hz, 4 H); ^{13}C NMR (75 MHz, $CDCl_3$, 25 °C): δ 39.1, 53.0, 55.3, 59.0, 113.7, 119.2, 130.0, 130.1, 137.3, 158.1, 171.5; HRMS (FAB) *m/z* calcd for $C_{25}H_{26}O_6$ 422.1729, found 422.1733 $[M]^+$.

Analytical data for 12i: Colorless crystals (mp 161.0–163.5 °C); IR (KBr): 1735 (C=O) cm^{-1}; ^1H NMR (300 MHz, $CDCl_3$, 25 °C): δ 3.35 (d, *J* = 2.1 Hz, 4 H), 3.72 (s, 6 H), 6.93 (t, *J* = 2.1 Hz, 2 H), 7.05–7.12 (m, 4 H), 7.30–7.39 (m, 4 H); ^{13}C NMR (75 MHz, $CDCl_3$, 25 °C): δ 39.0, 53.1, 58.9, 115.3 (d, *J* = 21.0 Hz), 119.3, 130.3 (d, *J* = 7.4 Hz), 133.2 (d, *J* = 3.4 Hz), 138.7, 161.3 (d, *J* = 245.3 Hz), 171.2; HRMS (FAB) *m/z* calcd for $C_{23}H_{20}F_2O_4$ 398.1330, found 398.1332 $[M]^+$.

Analytical data for 12j: Off-white crystals (mp 207.5–209.5 °C); IR (KBr): 1718 (C=O) cm^{-1}; ^1H NMR (300 MHz, $CDCl_3$, 25 °C): δ 3.34 (d, *J* = 1.8 Hz, 4 H), 3.72 (s, 6 H), 6.91 (t, *J* = 1.8 Hz, 2 H), 7.26 (d, *J* = 8.4 Hz, 4 H), 7.49 (d, *J* = 8.4 Hz, 4 H); ^{13}C NMR (75 MHz, $CDCl_3$, 25 °C): δ 39.1, 53.2, 58.8, 119.7, 120.7, 130.2, 131.4, 135.9, 139.8, 171.1; HRMS (FAB) *m/z* calcd for $C_{23}H_{20}Br_2NaO_4$ 540.9621, found 540.9616 $[M+Na]^+$.

Large-scale procedures – Cyclization of 11j: To a solution of **11j** (13.0 g, 25.0 mmol) and Cp*RuCl(cod) (0.285 g, 0.750 mmol) in dry degassed THF (100 mL) was added MeOH (6.70 mL, 165 mmol) under an argon atmosphere. The reaction mixture was stirred at 70 °C for 4 h. The reaction mixture was cooled to room temperature, filtered through a celite pad. After concentration in vacuo, the crude product was purified by recrystallization from hot AcOEt to afford **12j** (11.6 g, 90%) as pale-yellow micro crystals.

Cyclization of tetrayne 14: A solution of tetrayne **14** (0.19 g, 0.30 mmol), Cp*RuCl(cod) (5.7 mg, 0.015 mmol), and MeOH (0.16 mL, 4.0 mmol) in dry degassed THF (1.8 mL) was stirred at 70 °C for 5 h under an argon atmosphere. After concentration in vacuo, the crude product was purified by column chromatography on silica gel ($CHCl_3$) to give **15** (0.19 g, quantitative yield) as yellow crystals (mp 243.5–247.0 °C); IR (KBr): 1734 (C=O) cm-1; ^1H NMR (300 MHz, $CDCl_3$, 25 °C): δ 3.42 (d, *J* = 2.1 Hz, 4 H), 3.44 (d, *J* = 2.1 Hz, 4 H), 3.74 (s, 12 H), 7.00 (t, *J* = 2.1 Hz, 2 H), 7.02 (t, *J* = 2.1 Hz, 2 H), 7.21–7.29 (m, 2 H), 7.34–7.46 (m, 12 H); ^{13}C NMR (75 MHz, $CDCl_3$, 25 °C): δ 39.1, 39.4, 53.1, 59.0, 120.1, 120.5, 126.7, 128.2, 128.8, 128.9, 135.8, 137.1, 139.3, 139.4, 171.3; HRMS (FAB) *m/z* calcd for $C_{40}H_{38}O_8$ 646.2567, found 646.2571

$[M]^+$.

Cyclization of 11c with CD_3OH:

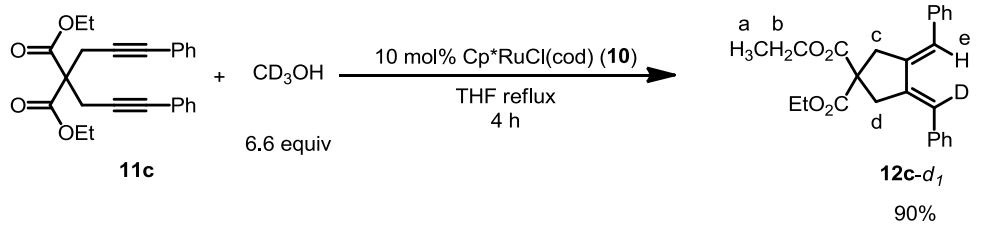

A solution of **11c** (0.12 g, 0.30 mmol), Cp*RuCl(cod) (11 mg, 0.030 mmol), and CD_3OH (0.080 mL, 2.0 mmol) in THF (1.2 mL) was stirred at 70 °C under an argon atmosphere for 4 h. After the concentration in vacuo, the crude product was purified by column chromatography on silica gel (elution: toluene) to give **12c**-d_1 (0.11 g, 90 % yield). In its ^{1}H NMR specrum, the peak areas are as follows: δ 1.21 (t, H^a, area = 6.15), 3.39 (s, H^c and H^d, area = 4.01), 4.17 (q, H^b, area = 4.00), and 6.99 (t, H^e, area = 1.00) indicating that the ratio of the newly incorporated H and D in the diene moiety is H : D = 1.01 : 1.00. The product was analyzed by FAB-MS spectroscopy with the aid of NaI in NBA matrix. The peak intensity calculated for [**12c**-d_1+Na]$^+$ was *m/z*: 414 (100%), 415 (27%), 416 (4%), while the observation was *m/z*: 414 (100%), 415 (30%), 416 (6%). This consistency shows that the product was a single isotopologue rather than a mixture with statistical H/D distribution (Figure 2).

Cyclization of 11c′ with benzyl alcohol: A solution of **11c′** (0.11 g, 0.30 mmol), Cp*RuCl(cod) (11 mg, 0.030 mmol) and benzyl alcohol (0.16 mL, 1.5 mmol) in dry degassed THF (1.2 mL) was stirred at 70 °C under Ar atmosphere for 2 h. The reaction was traced by TLC analysis. THF was carefully removed under reduced pressure to concentrate the solution to approximately quarter of the original volume. To thus obtained crude mixture was added ethyl benzene (50.0 μL, 0.410 mmol) as a internal standard. The molar ratio of the compounds in the crude mixture was determined with ^{1}H NMR by comparing the peak area of following signals: **12c′**: δ 3.41 (d, 4 H), 7.01 (d, 2 H), benzaldehyde: δ 10.01 (s, 1 H), unreacted benzyl alcohol: δ 4.69 (s, 2 H), ethylbenzene: δ 2.66 (q, 2 H). The ratio was [**12c′**] : [benzaldehyde] : [benzyl alcohol] : [ethylbenzene] = 1.0 : 0.98 : 4.0 : 1.4. This corresponds to 0.30 mmol (99% yield) of

12c′, 0.29 mmol (96% yield) of benzaldehyde, and 1.2 mmol of benzyl alcohol.

(f) Sonogashira coupling of 12j.

A mixture of **12j** (0.42 g, 0.81 mmol), ethynylbenzene (0.27 mL, 2.45 mmol), $Pd_2(dba)_3$•$CHCl_3$ (5.2 mg, 0.0050 mmol), SPhos (4.1 mg, 0.010 mmol), finely ground K_2CO_3 (0.28 g, 2.0 mmol), and benzyltriethylammonium chloride (13.9 mg, 0.050 mmol) was stirred in acetonitrile (4.0 mL) at 50 °C under an argon atmosphere for 24 h. After cooled to room temperature, the mixture was filtered through a pad of celite, and the solvent was removed under reduced pressure to give a yellow brown solid. The crude product was purified by column chromatography on silica gel (toluene/$CHCl_3$ = 1:1) to give **13** (0.44g, 96% yield) as light-yellow solid (mp 245.5–249.0 °C); IR (KBr): 1735 (C=O) cm^{-1}; ^1H NMR (300 MHz, $CDCl_3$, 25 °C): δ 3.42 (d, *J* = 2.1 Hz, 4 H), 3.74 (s, 6 H), 7.00 (t, *J* = 2.1 Hz, 2 H), 7.32–7.44 (m, 10 H), 7.51–7.62 (m, 8 H); ^{13}C NMR (75 MHz, $CDCl_3$, 25 °C): δ 39.2, 53.2, 59.0, 89.5, 90.3, 120.4, 121.5, 123.0, 128.1, 128.2, 128.7, 131.4, 131.5, 136.9, 140.1, 171.2; HRMS (FAB) *m/z* calcd for $C_{39}H_{30}NaO_4$ 585.2036, found 585.2043 $[M+Na]^+$.

(g) Mechanistic Studies.

Dependence of reaction rates on [Diyne] and [MeOH]: In a Schlenk tube equipped with septum and stirring bar, diyne **11c′** (0.22 g, 0.60 mmol), methanol (0.20 mL, 4.9 mmol) and di-*n*-octyl ether as an internal standard (0.10 mL, 0.33 mmol) were dissolved in THF (1.5 mL), and the solution was heated to 50 °C. To this solution was added a stock solution of Cp*RuCl(cod) in THF (0.30 M, 1.0 mL, 0.3 mmol). Aliquots were taken out periodically, concentrated in vacuo, and analyzed as a $CDCl_3$ solution by ^1H NMR spectroscopy. The ratios of the compounds were determined by monitoring the peak areas at δ 0.89 (t, *J* = 6.9 Hz, 6 H, di-*n*-octyl ether), 3.72 (s, 6 H, **12c′**), and 3.81(s, 6 H, **11c′**). Since the quantitation of **11c′** is most accurate among those of the compounds, the precise concentration of the internal standard was determined relative to that of **11c′** in the initial sampling. The concentrations of **11c′** and **12c′** ([**11c′**] and [**12c′**], respectively) are plotted against the reaction time (*t*/h). The material balance was good and both plots showed good linearity within 3 h. The reaction rates were

determined by referring to the linear part of the [**12c′**] vs. *t* plot (Figure 3).

The dependence of the reaction rate on the diyne concentration [**11c′**] was examined at $[\mathbf{11c'}]_0$ = 0.054, 0.11, 0.16, and 0.21 M (A, Figure 4). In a similar manner, the effect of MeOH was studied by performing the reactions at five methanol concentrations, $[MeOH]_0$ = 0.71, 0.89, 1.8, 3.6, and 5.4 M (B, Figure 4). The obtained results are summarized in Table S 2.

Table S 2. Summary of kinetic studies

#	$[\mathbf{11c'}]_0$ [M]	$[MeOH]_0$ [M]	numbers of points	decision coefficient R^2		−d[**11c′**]/dt [Mh^{-1}]	d[**12c′**]/dt [Mh^{-1}]
				[**11c′**] *vs. t*	[**12'**] vs *t*.		
1	0.0536	1.76	3	0.968	0.976	0.0449	0.0431
2	0.107	1.76	4	0.991	0.997	0.0589	0.0614
3	0.16	1.76	5	0.999	0.998	0.0639	0.0631
4	0.214	1.76	4	0.996	0.996	0.0684	0.064
5	0.214	0.705	6	0.986	0.993	0.0341	0.0314
6	0.214	0.89	7	0.991	0.999	0.0407	0.0399
7	0.214	3.57	5	0.984	0.998	0.105	0.0996
8	0.214	5.36	4	0.998	0.998	0.145	0.139

Kinetic isotope effects: By employing 1.8 M of CH_3OH, CD_3OH or CH_3OD as hydrogen surrogates, the rates of the cyclization/transfer hydrogenation of diyne **11c′** ($[\mathbf{11c'}]_0$ = 0.21 M) was measured in a similar manner as described above. To cancel the experimental error, the measurements were repeated 3 times for each alcohol. The concentrations of **12c′** or **12c′**-d_1 in each experiment are shown in Figures S1–S3. The obtained results are summarized in Table S 3.

Figure S 1. Time course of the cyclization/transfer hydrogenation of **11c′** with CH_3OH.

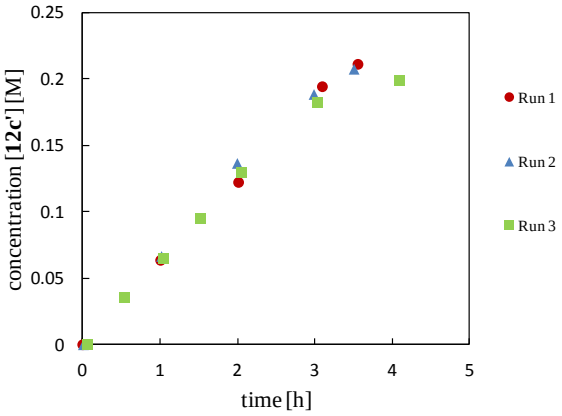

Figure S 2. Time course of the cyclization/transfer hydrogenation of **11c′** with CD_3OH.

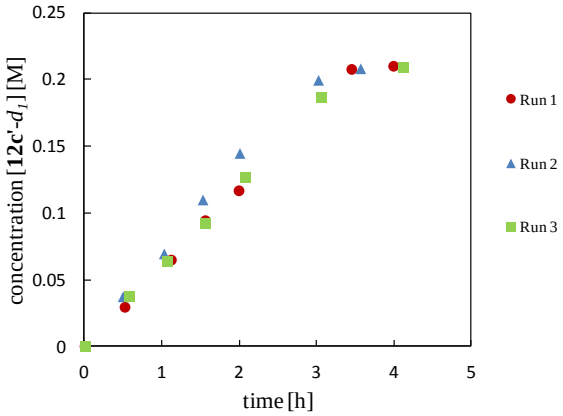

Figure S 3. Time course of the cyclization/transfer hydrogenation of **11c′** with CH_3OD

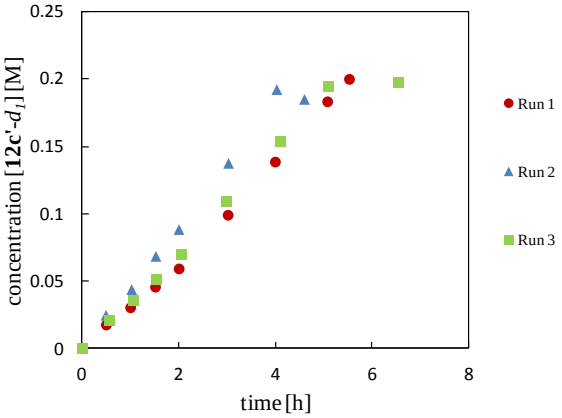

Table S 3. Summary of initial rates (Mh^{-1}) of reactions using CH_3OH, CD_3OH, and CH_3OD.

run	CH_3OH	CD_3OH	CH_3OD
1	0.0603	0.0603	0.0365
2	0.0640	0,0670	0.0432
2	0.0613	0.0606	0.0383
average rate	0.062±0.002	0.063±0.002	0.039±0.005

(h) Theoretical Calculations.

The Gaussian 03 program package was used for all geometry optimizations.[19] The geometries of stationary points and transition states were fully optimized by means of the Becke's three-parameter hybrid density functional method (B3LYP)[20] with the basis set, consisting of a double-ζ basis set with the relativistic effective core potential of Hay and Wadt (LanL2DZ)[21] for Ru and the 6-31G(d)[22] basis sets for other elements (BS-I). The vibrational frequencies, zero-point energy (ZPE) and thermal correction to Gibbs free energy (TCGFE) were calculated at the same level of theory. The obtained structures were characterized by the number of imaginary frequencies (one or zero for transition or ground states, respectively). The connectivity of each step was further confirmed by IRC calculation[23] from the transition states followed by optimization of the resulted geometries. The obtained geometry of η^4-diene complex **G** was in good agreement with those of an X-ray structure of **9** (Table S 4). Single-point energies for geometries obtained by the above method were calculated at the same level using the basis sets consisting of a [6s5p3d2f1g] contracted valence basis set with the Stuttgart-Dresden-Bonn energy-consistent pseudopotential (SDD) [24, 25] for Ru and the 6-311++G(2d,p) basis sets[26] for other elements. Relative energies were corrected with unscaled ZPE obtained at the B3LYP/BS-I level. The obtained results are summarized in Table S5.

Table S 4. Comparison of selected bond distances of **9** and **G**.

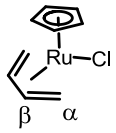

G

	9 (X-ray)	**G**
Ru–Cl [Å]	2.4544(14)	2.48
Ru–Cα [Å]	2.240(5), 2.249(6)	2.25, 2.26
Ru–Cβ [Å]	2.216(6)	2.21
Cα–Cβ [Å]	1.422(8), 1.403(8)	1.41
Cβ–Cβ [Å]	1.424(9)	1.44
Cα–Cβ–Cβ [°]	122.9(5), 123.3(5)	121.7, 121.9

Table S 5. Summary of theoretical calculations.

Model	Energy/au	ZPE/au	TCGFE/au	IF/cm^{-1}
A	–558.49947218	0.190611	0.151864	
TS-AB	–558.45898596	0.185968	0.148335	1112.2089i
B	–558.48422448	0.187941	0.146837	
C	–1019.33675981	0.198689	0.152940	
TS-CD	–1019.31293919	0.200114	0.158994	102.1790i
D	–1019.34270237	0.203641	0.162531	
TS-DE	–1019.31109623	0.200116	0.159954	1032.2411i
E	–1019.35214680	0.203265	0.161244	
F	–904.80630105	0.171998	0.133942	
TS-FG	–904.79961402	0.170452	0.132214	338.3980i
G	–904.86077935	0.174389	0.136356	
HCHO	–114.54178832	0.026841	0.005177	

5. References and Notes

[1] (a) Sprengers, J. W.; Wassenaar, J.; Clement, N. D.; Cavell, K. J.; Elsevier, C. J. *Angew. Chem. Int. Ed.* **2005**, *44*, 2026–2029; (b) Hauwert, P.; Maestri, G.; Sprengers, J. W.; Catellani, M.; Elsevier, C. J. *Angew. Chem. Int. Ed.* **2008**, *47*, 3223–3226; (c) Hauwert, P.; Boerleider, R.; Warsink, S.; Weigand, J. J.; Elsevier, C. J. *J. Am. Chem. Soc.* **2010**, *132*, 16900–16910.

[2] Trost, B. M.; Lee, D. C. *J. Am. Chem. Soc.* **1988**, *110*, 7255–7258.

[3] Jan, H.-Y.; Krische, M. J. *J. Am. Chem. Soc.* **2004**, *126*, 7875–7880.

[4] Sylvester, K. T.; Chirik, P. J. *J. Am. Chem. Soc.* **2009**, *131*, 8772–8774.

[5] (a) Tani, K.; Iseki, A.; Yamagata, T. *Chem. Commun.* **1999**, 1821–1822; (b) Barrios-Francisco, R.; García, J. J. *Inorg. Chem.* **2009, *48*,** 386–393.

[6] Dinger, M. B.; Mol, J. C. *Organometallics* **2003**, *22*, 1089–1095.

[7] Bruce, M. I.; Koutosantonis, G. A.; Tieknik, E. R. T.; Nicholson, B. K. *J. Organomet. Chem.* **1991**, *420*, 271–288.

[8] (a) Lucht, B. L.; Mao, S. S. H.; Tilley, T. D. *J. Am. Chem. Soc.* **1998**, *120*, 4354–4364; (b) Fabin, W. M. F.; Kauffman, J. M. *J. Lumin.* **1999**, *85*, 137–148.

[9] For example, see: Grüdemann, S.; Ulrich, S.; Limbach, H.-H.; Golubev, N. S.; Denisov, G. S.; Epstein, L. M.; Sabo-Etienne, S.; Chaudret, B. *Inorg. Chem.* **1999**, *38*, 2550–2551.

[10] Saito, N.; Tanaka, Y.; Sato, Y. *Org. Lett.* **2009**, *11*, 4124–4126.

[11] (a) Le Paih, J.; Sylvie Dérien and Pierre H. Dixneuf *Chem. Commun.* **1999**, 1437–1438; (b) Le Paih, J. L.; Monnier, F.; Dérien, S.; Dixneuf, P. H.; Clot, E.; Eisenstein, O. *J. Am. Chem. Soc.* **2003**, *125*, 11964–11975; (c) Zhan, M.; Jiang, H.; Dixneuf, P. H. *Adv. Synth. Catal.* **2009**, *351*, 1488–1494.

[12] Yamamoto, Y.; Arakawa, T.; Ogawa, R.; Itoh, K. *J. Am. Chem. Soc.* **2003**, *125*, 12143–12160.

[13] (a) Oshima, N.; Suzuki, H.; Moro-oka, Y. *Chem. Lett.* **1984**, 1161–1164; (b) Yamamoto, Y.; Hattori, H. *Tetrahedron* **2008**, *28*, 847–855.

[14] Scheller, A; Winter, W.; Müller, E. *Liebigs Ann. Chem.*, **1976**, 1448–1454.

[15] Jung, I. G.; Seo, J.; Lee, S. I.; Choi, S. Y.; Chung, Y. K. *Organometallics* **2006**, *25*, 4240–4242.

[16] Hu, Y.; Hu, J.; Zhu, T.; Yu, T.; Zhao, Q. *Chem. Asian. J.* **2011**, *6*, 797–800.

[17] Schulte, K. E.; Reisch, J.; Mock, A. *Arch. Pharm.* **1962**, *295*, 627–639.

[18] G. M. Sheldrick, SHELXTL 5.1, Bruker AXS Inc., Madison, Wisconsin, 1997.

[19] Gaussian 03, Revision C.02, Frisch, M. J.; Trucks, G. W.; Schlegel, H. B.; Scuseria, G.

E.; Robb, M. A.; Cheeseman, J. R.; Montgomery, J. A. Jr.; Vreven, T.; Kudin, K. N.; Burant, J. C.; Millam, J. M.; Iyengar, S. S.; Tomasi, J.; Barone, V.; Mennucci, B.; Cossi, M.; Scalmani, G.; Rega, N.; Petersson, G. A.; Nakatsuji, H.; Hada, M.; Ehara, M.; Toyota, K.; Fukuda, R.; Hasegawa, J.; Ishida, M.; Nakajima, T.; Honda, Y.; Kitao, O.; Nakai, H.; Klene, M.; Li, X.; Knox, J. E.; Hratchian, H. P.; Cross, J. B.; Bakken, V.; Adamo, C.; Jaramillo, J.; Gomperts, R.; Stratmann, R. E.; Yazyev, O.; Austin, A. J.; Cammi, R.; Pomelli, C.; Ochterski, J. W.; Ayala, P. Y.; Morokuma, K.; Voth, G. A.; Salvador, P.; Dannenberg, J. J.; Zakrzewski, V. G.; Dapprich, S.; Daniels, A. D.; Strain, M. C.; Farkas, O.; Malick, D. K.; Rabuck, A. D.; Raghavachari, K.; Foresman, J. B.; Ortiz, J. V.; Cui, Q.; Baboul, A. G.; Clifford, S.; Cioslowski, J.; Stefanov, B. B.; Liu, G.; Liashenko, A.; Piskorz, P.; Komaromi, I.; Martin, R. L.; Fox, D. J.; Keith, T.; Al-Laham, M. A.; Peng, C. Y.; Nanayakkara, A.; Challacombe, M.; Gill, P. M. W.; Johnson, B.; Chen, W.; Wong, M. W.; Gonzalez, C.; Pople, J. A. Gaussian, Inc., Wallingford CT, 2004.

[20] (a) Kohn, W.; Becke, A. D.; Parr, R. G. *J. Phys. Chem.* **1996**, *100*, 12974−12980; (b) Stephen, P. J.; Devlin, F. J.; Chabalowski, C. F.; Frisch, M. *J. Phys. Chem.* **1994**, *98*, 11623−11627; (c) Becke, A. D. *J. Chem. Phys.* **1993**, *98*, 1372−1377; (d) Lee, C.; Yang, W.; Parr, R. G. *Phys. Rev. B* **1988**, *37*, 785−789.

[21] Hay, P. J.; Wadt, W. R. *J. Chem. Phys.* **1985**, *82*, 299−310.

[22] (a) Hehre, W. J.; Ditchfield, R.; Pople, J. A. *J. Chem. Phys.* **1972**, *56*, 2257−2261; (b) Hariharan, P. C.; Pople, J. A. *Theor. Chim. Acta* **1973**, *28*, 213−222; (c) Fracl, M. M.; Pietro, W. J.; Hehre, W. J.; Binkley, J. S.; Gordon, M. S.; DeFrees, D. J.; Pople, J. A. *J. Chem. Phys.* **1982**, *77*, 3654−3665.

[23] (a) Fukui, K. *Acc. Chem. Res.* **1981**, *14*, 363−368; (b) Gonzalez, C.; Schlegel, H. B. *J. Chem. Phys.* **1989**, *90*, 2154−2161; (c) Gonzalez, C.; Schlegel, H. B. *J. Phys. Chem.* **1990**, *94*, 5523−5527.

[24] Martin, J. M. L.; Sundermann, A. *J. Chem. Phys.* **2001**, *114*, 3408−3420.

[25] Andrae, D.; Häussermann, U.; Dolg, M.; Stoll, H.; Preuß, H. *Theor. Chim. Acta* **1990**, *77*, 123−131.

[26] (a) Krishnan, R.; Binkley, J. S.; Seeger, R.; Pople, J. A. *J. Chem. Phys.* **1980**, *72*, 650−654; (b) McLean, A. D.; Chandler, G. S. *J. Chem. Phys.* **1980**, *72*, 5639−5648; (c) Frisch, M. J.; Pople, J. A.; Binkley, J. S. *J. Chem. Phys.* **1984**, *80*, 3265−3269; (d) Clark, T.; Chandrasekhar, J.; Spitznagel, G. W.; Schleyer, P. v. R. *J. Comp. Chem.* **1983**, *4*, 294−301.

Chapter 5

Straightforward [2+2+1] Pathway to Furans *via* Oxygen Transfer from Sulfoxide to Diynes

Abstract: Novel transfer oxygenative [2+2+1]-type cyclization of diynes that affords bicyclic furans was developed. The reaction is catalyzed by cationic ruthenium complexes $[Cp'Ru(NCMe)_3](PF_6)$ (Cp′ = Cp or Cp*, vide infra), and safe and inexpensive dimethylsulfoxide is utilized as oxygen atom donor. The reaction makes use of the combination of electrophilicity of cationic ruthenacyclopentatriene complex and oxygen atom-donating ability of the sulfoxide. As the substrate, both aryl- and alkyl-substituted 1,6-diynes could be used. With the substrate choice, a contrasting effect of the catalyst was seen; $[CpRu(NCMe)_3](PF_6)$ was suitable for the reaction with aryl-substituted diynes, while the reaction with alkyl-substituted diyne was efficiently catalyzed by its Cp* analogue. Stoichiometric reaction of ruthenacyclopentatriene and dimethyl sulfoxide was conducted. As a result, intermediacy of the cationic ruthenacyclopentatriene was shown.

1. Introduction

Catalytic [2+2+1]-type cyclization between two unsaturated compounds and one atom component is one of the most powerful methods to construct five membered rings. Among them, carbocyclization reactions, representatively Pauson-Khand-type CO or isonitrile insertion, have been extensively studied. On the other hand, [2+2+1]-type hetero cyclization reaction is rarely known. Since hetero five-membered rings are ubiquitously found in natural products, pharmaceutical compounds and electronic materials, simple and straightforward [2+2+1] cyclization would be of great use.

Difficulty in direct construction of five-membered heterocycles *via* transition metal catalyzed [2+2+1] cycloaddition reaction is attributed to general vulnerability of low valent metal complexes. For instance, when an oxygen atom is considered as a component in [2+2+1] cycloaddition, it is an electron deficient oxygen species. In general, electron deficient oxygen species, e.g. peracids, dioxilanes, peroxides or molecule oxygen, are strong oxidant. Thus they are less compatible with reactions catalyzed by low valent transition metal complexes or complexes bearing easily oxidized ligands. For example, Maitlis and co-workers have reported that a pentamethylcyclopentadienyl ruthenium complex $[Cp^*RuCl_2]_2$ ($Cp^* = \eta^5$-C_5Me_5) (**1**) is readily oxidized by a molecular oxygen in a chloroform solution to form a tetramethylfulvene complex $[(C_5Me_4CH_2)RuCl_2]_2$ (**2**) (Scheme 1).[1]

Scheme 1. Oxidation of $[Cp^*RuCl_2]_2$ by molecular oxygen.

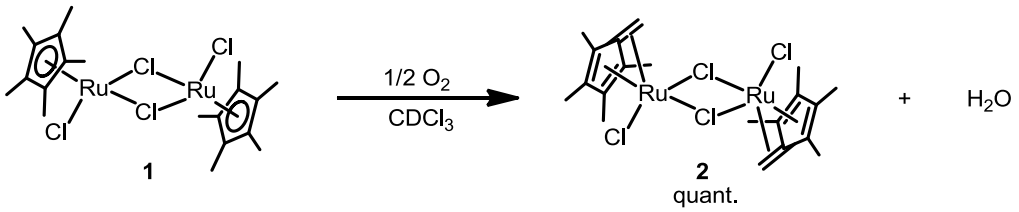

The author anticipated that sulfoxide might act as an oxygen atom source in [2+2+1] cycloaddition. Among the oxidants, sulfoxiside is known to have little oxidizing activity toward low valent transition metal complexes including divalent ruthenium complexes.[2,3] Meanwhile, as known for Kornblum (or Swern) type oxidation processes, oxygen atom-donating ability of

sulfoxides appears on *O*–alkylation.[4] By replacing the *O*–alkylating reagent with electrophilic carbene complex, a new type of oxidation is anticipated. In fact, oxygenation of electrophilic carbene by dimethylsulfoxide (DMSO) was reported by Casey and co-workers (Scheme 2).[5] In the report, an electrophilic tungsten carbene complex **3** was oxidized by DMSO at room temperature to give benzophenone in high yield.

Scheme 2. Oxidation of electrophilic tungsten carbene complex by dimethylsulfoxide.

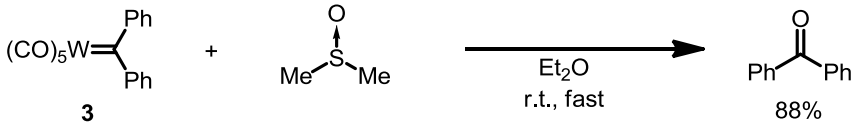

The oxidation of carbene complexes had been studied on stoichiometric basis,[6] but it has not been employed as an elemental step in a catalytic cycle for a long period. Pioneering work on the use of oxidation of carbene complexes in catalytic chemistry was achieved by Trost and Rhee.[7] In their work, a Fischer-type carbene complex **7** generated from a homopropargyl alcohol and a divalent ruthenium complex **4a** is oxidized by *N*-hydroxysuccinimide (**6**) to afford a butylo lactone **8**.

Scheme 3. The first catalytic process that proceeds through oxidation of a carbene intermediate.

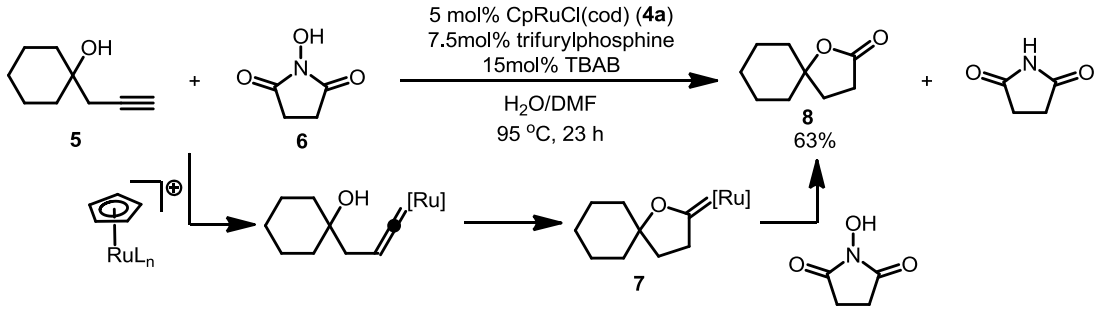

Toste, Zhang and their respective co-workers conducted studies on gold-catalyzed intermolecular oxygen atom transfer reaction of alkynylsulfoxides (Scheme 4).[8] Since then, intermolecular versions of these reactions have been developed,[9] and also oxygen atom donor

such as amine-*N*-oxides,[10] nitorons,[11] and nitro compounds[12] are utilized.

Scheme 4. Gold-catalyzed intramolecular oxygen atom transfer reaction.

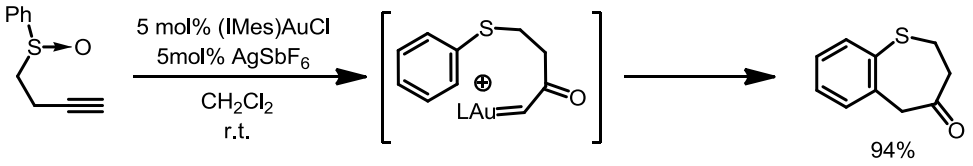

Based on these results, it is expected that sulfoxide may serve as a good oxygen atom donor in catalytic hetero [2+2+1] cyclization processes (Scheme 5).

Scheme 5. Concept of hetero [2+2+1] cyclization using sulfoxide as mild oxygen donor.

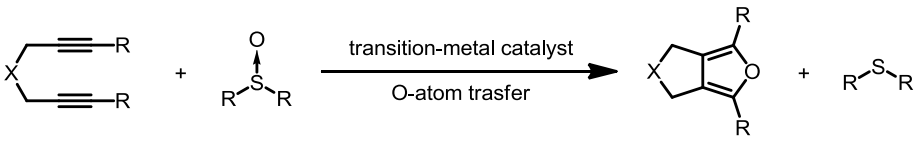

2. Catalytic Study

To realize abovementioned concept, screening of the reaction condition was conducted by using ether tethered 1,6-diyne **10a** with terminal phenyl substituent as the substrate. Examined Ru-catalyst candidates were electronically neutral Ru-complex Cp*RuCl(cod) (**4b**), cationic complex [CpRu(NCMe)$_3$](PF$_6$) (**9a**) and [Cp*Ru(NCMe)$_3$](PF$_6$) (**9b**) (Figure 1). The results are summarized in Table 1.

Figure 1. Catalysts examined in this study.

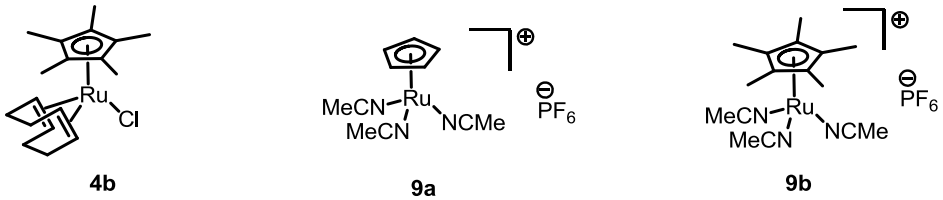

4b **9a** **9b**

Initial attempted was carried out with neutral **4b** in THF only to observe predominant

self-dimerization of diyne **10a**, and yield of the desired furan product **11a** was as low as 4% (entry 1). In contrast, when 20 mol% of methanesulfonic acid was added, conversion of the diyne **10a** was significantly improved, and also [2+2+2] cycloaddition was suppressed. As a consequence, the yield of the desired furan **11a** jumped up to 51 % (entry 2). With further optimization such as doubled volume of THF (entry 3), reduced amount of DMSO (entry 4), and use of 1,4-dioxiane as the solvent, the yield of **11a** reached 78% (entry 5). Glyme (1,2–dimethoxyethane) was not as suitable as 1,4-dioxane (entry 6).

A problem with [2+2+1] cyclization system catalyzed by neutral complex **4b** was concomitant [2+2+2] cycloaddition of alkynes. As long as the author knows, cationic cyclopentadienylruthenium complexes do not promote the cyclotrimerization of alkynes. In addition, ruthenacyclopentatriene intermediates generated from the cationic precursors and diyne substrates are expected to have higher electrophilicity owing to their positive charge. In accordance with this assumption, $[CpRu(NCMe)_3]PF_6$ (**9a**) and $[Cp^*Ru(NCMe)_3]PF_6$ (**9b**) catalyzed oxygen transfer reaction without forming **12** in THF solution (entries 7 and 8). Although **9a** showed higher catalytic activity than **9b**, its TON (5.0 in 24 hours) was inferior to that of the combination of **4b** and MsOH in dioxane (7.8 in 3 hours).

The catalytic activity of **9a** was drastically improved by carrying out the reaction in DMF solution, and catalyst loading could be reduced to 5 mol% (entry 9). As reaction temperature was raised, reaction rate increased (entries 11 and 12). Eventually, at 140 °C, the substrate was completely consumed within an hour to afford the furan **11a** in satisfactory 80% yield. Furthermore, 3 mol% of **9a** was sufficient to accomplish the reaction at that temperature to give **11a** in a good yield (entry 13). The reaction mixture was bubble with nitrogen gas in an attempt to remove highly volatile Me_2S at 100 °C (entry 11). In this case, consumption of the diyne **10** was significantly accelerated, and the yield of **11a** reached to 80% in 6 hours, while the reaction without bubbling took 10 hours to reach the completion.

With regard to solvent effect, DMF was specifically suitable for this reaction. Attempted oxidation/cyclization of the same diyne in other amide solvent such as DMAc or DMI resulted in a rather sluggish crude product and reduced yield of the furans **11a**.

Table 1. Ruthenium-catalyzed oxygen atom transfer/cyclization of diyne **10a**.

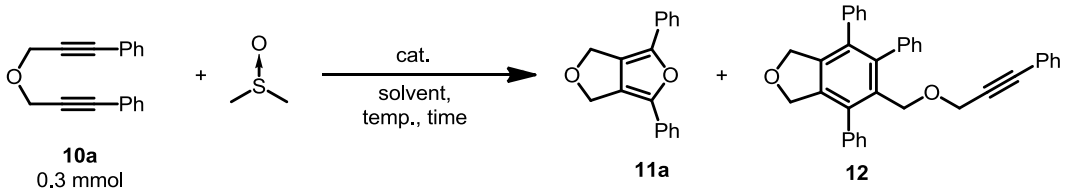

entry	cat. (loading [mol%])	DMSO [equiv.]	solvent	temp. [°C]	time [h]	yield **11a/12/10a**
1	**4b** (10)	10	THF[a]	70[b]	12	4 / 36 / 37[c]
2	**4b** (10) + MsOH (20)	10	THF[a]	70[b]	12	51 / 3 / 6
3	**4b** (10) + MsOH (20)	10	THF[d]	70[b]	5	69 / 6 / 0
4	**4b** (10) + MsOH (20)	5	THF[d]	70[b]	4	71 / trace / 0
5	**4b** (10) + MsOH (20)	5	1,4-dioxane[c, d]	70	3	78 / trace / 0
6	**4b** (10) + MsOH (20)	5	glyme[d]	70	3	60 / 4 / 0[c]
7	**9b** (10)	5	THF[d]	70[b]	24	19 / 0 / 57[c]
8	**9a** (10)	5	THF[d]	70[b]	24	50 / 0 / 30[c]
9	**9a** (5)	5	DMF[d]	70	24	73 / 0 / 1
10	**9a** (5)	5	DMF[d]	100	10	79 / 0 / 0
11	**9a** (5)	5	DMF[d]	100[e]	6	81 / 0 / 0
12	**9a** (5)	5	DMF[d]	140	1	80 / 0 / 0
13	**9a** (3)	5	DMF[d]	140	4	90 / 0 / 0
13	**9a** (5)	5	DMAc[d]	140	6	49 / 0 / 18[c]
14	**9a** (5)	5	DMI[e, f]	140	6	13 / 0 /45[c]

[a]1.5 mL. [b]reflux. [c]Yields determined by ^{1}H NMR analysis of crude products. [d]3.0 mL. [e] Bubbled with N_2 (ca. 5 mL/min). [f]1,3-dimethyl-2-imidazolidinone.

Currently, furan synthesis from alkyl-substituted alkynes *via* [2+2+1] cycloaddition remains challenging. The authors intended to expand the applicability of the novel ruthenium-catalyzed [2+2+1] cyclization system. In this attempt, malonate-derived diyne **13a** was selected as a specimen.

Interestingly, the contrasting effect of the ligand choice was seen (Table 2, entries 1 and 2). In the cyclization of the diyne **13a**, complex **9b** which has bulkier but more electron-donating Cp* ligand exhibited high activity. With only 3 mol% of **9b**, desired furan **14a** was formed in 85% isolated yield in 1 h. On the other hand, in the case of the complex **9a**, which was suitable for the transformation of diphenyldiyne **10a**, the result was poorer even with increased catalyst loading and longer reaction time. Choice of solvent was also important (entries 2−4). The reaction proceeded well in ether solvents such as THF or 1,4-dioxane, and an attempt in DMF resulted in a low conversion and the yield of the product was only 6 %. When the catalyst loading was reduced to 1 mol%, reversed concentration effect of DMSO was observed (entries 5−7). This result arose presumably from poisoning of the catalyst by the sulfoxide. Therefore, the product yield increased as sulfoxide concentration decreased. Although the reaction with 1.2 equivalents of DMSO gave the best result among entries 5−7, 2.5 equivalent of the sulfoxide was chosen as the optimal condition from the view point of redundancy of the system and operational ease.

Table 2. Ruthenium-catalyzed oxygen atom transfer/cyclization of alkyl-substituted diyne **13a**.

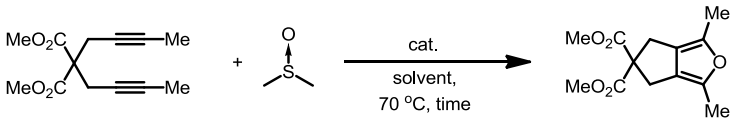

entry	cat. (loading [mol%])	solvent	DMSO [equiv.]	time [h]	yield **14a** / **13a**[%]
1	**9b** (10)	THF	5	2	5 / 89[a]
2	**9a** (3)	THF	5	1	85 / 0
3	**9a** (3)	1,4-dioxane	5	1	60 / 26[a]
4	**9a** (3)	DMF	5	1	6 / 73[a]
5	**9a** (1)	THF	5	6	22 / 67[a]
6	**9a** (1)	THF	2.5	6	65 / 16[a]
7	**9a** (1)	THF	1.2	6	74 / 18[a]

[a]Yields determined by ^{1}H NMR analysis of crude products.

Having surveyed the reaction conditions, the author started to investigate the scope of the ruthenium-catalyzed oxygen atom transfer/cyclization reaction (Table 3). In general, methods for diynes with aryl or alkyl terminal groups established above could be applied without special amendment except for catalyst loadings.

First, to investigate the functional group compatibility, 1,6-diynes with phenyl terminal and variously functionalized tether groups were subjected to the reaction. Substrates **10b**–**e** bearing ester, ketone, nitrile and tosylamide were easily transformed into corresponding furans in high yields (entries 1−4). In the case of sulfone-tethered 1,6-diyne **10f**, increased catalyst loading was required to complete the reaction in a short reaction time (entry 5). The product **11f** has good crystallinity, and its structure was unambiguously determined by X-ray crystallography (Figure 2).

Next, to shed light on the influence of alkyne terminal groups, reactions with dimethyl malonate-derived diynes **10g**–**k** possessing various aryl terminal groups were performed (entries 6−9). Substrates with both electron-donating and withdrawing groups were cleanly transformed into corresponding furans in high yield within a few hours catalyzed by 5 mol% of **9a**. Among

them, the effect of electron withdrawing *p*-fluorophenyl group was obvious, and **10h** was completely converted to **11h** within an hour (entry 7). The effect of a fluorine substituent was valid even when electron donating *p*-methoxyphenyl group was located on the other terminal (entry 8). This method was also applicable to a transformation of a substrate with *p*-bromophenyl group, which is expected to be a favorable scaffold for palladium-catalyzed cross coupling reactions, and the C−Br bond remained intact (entry 9).

Other than benzene rings, aromatic parts such as thienyl or ferrocenyl groups were also useful (entries 10, 11). Thienyl-substituted diyne **10k** was fully converted in an hour under the standard condition to afford hetero aromatic array **11k** in 90 % yield. Bis(ferrocenyl) diyne **10l** was converted into corresponding 1,5-bis(ferrocenyl)furane although significantly increased amount of the catalyst was necessary and the yield was moderate. In the light of steric bulkiness and strong electron-donating nature of the Fc group, this result is acceptable.

Interestingly, the optimized condition for the oxidation of diaryldiynes was compatible with transformation of **13m**, which lacks an aryl group on one alkyne terminal (entry 12). This result is parallel to the one obtained with the diyne **10i**. These results imply that the reactivity of a diyne substrate in this reaction is determined by one substituent which has stronger electronic effect.

Usefulness of the condition optimized for diynes with alkyl terminal (condition B, Table 3) was investigated. As expected, reaction of malonate-derived diyne with 2.5 equivalent of DMSO gave a little improved yield than the one with 5 equivalents of sulfoxide (entry 13 in Table 3 and entry 2 in Table 2). Conversion of a tosylamide analogue required 5 mol% of catalyst, and corresponding product was produced in a good yield in 30 minutes (entry 14). Furthermore, the oxygenative cyclization could be performed with a substrate bearing secondary carbon on the alkyne terminal (entry 15). 15 mol% of **9b** catalyzed oxygen transfer to a sterically hindered cyclopentyl substituted diyne **13c**, and also applicability of this condition toward ether-tethered diyne was demonstrated at the same time.

Table 3. Substrate scope of the ruthenium-catalyzed oxygen-atom transfer/ cyclization of 1,6-diynes.

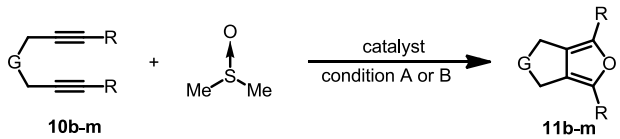

10b-m
13a-c
0.3 mmol

11b-m
14a-c

entry	diyne		cat. (loading [mol%])	conditions	time [h]	furan yield [%]
1	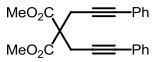	**10b**	**9a** (5)	A	4	**11**b, 90
2	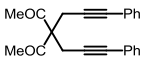	**10c**	**9a** (5)	A	4	**11c**, 87
3	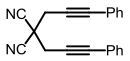	**10d**	**9a** (5)	A	5	**11d**, 94
4	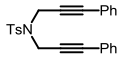	**10e**	**9a** (5)	A	2	**11e**,89
5	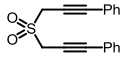	**10f**	**9a** (10)	A	4	**11f**, 87
6	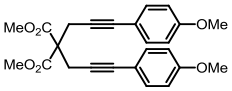	**10g**	**9a** (5)	A	3	**11g**, 92
7	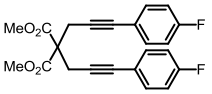	**10h**	**9a** (5)	A	1	**11h**, 94
8	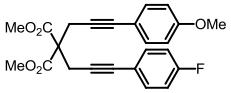	**10i**	**9a** (5)	A	1	**11i**, 93
9	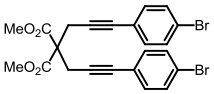	**10j**	**9a** (5)	A	2	**11j**, 93
10	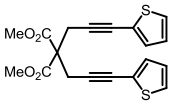	**10k**	**9a** (5)	A	1	**11k**, 90
11	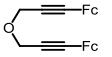	**10l**	**9a** (20)	A	2	**11l**, 57
12	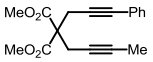	**10m**	**9a** (5)	A	1	**11m**, 81
13	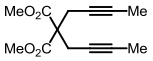	**13a**	**9b** (3)	B	1	**14a**, 90
14	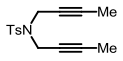	**13b**	**9b** (5)	B	0.5	**14b**, 74
15	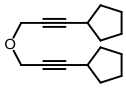	**13c**	**9b** (15)	B	6	**14c**, 61

condition A: diyne (0.3 mmol), DMSO (5 equiv), DMF (3 mL), 140 °C.
condition B: diyne (0.3 mmol), DMSO (2.5 equiv), THF (3 mL), 70 °C (reflux).
[a]Yields determined by ^{1}H NMR analysis of crude products.

Figure 2. ORTEP drawing of the furan **11f**, shown as 50% ellipsoids. All hydrogen atoms are omitted for clarity.

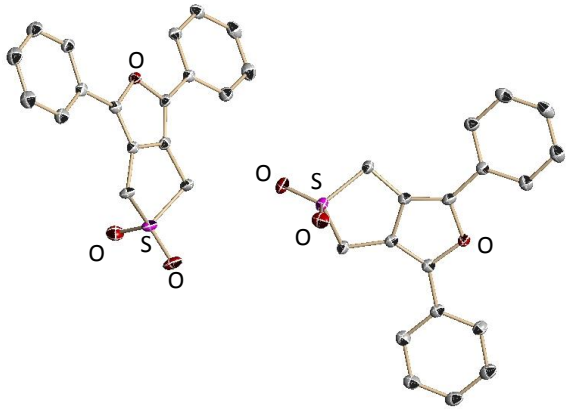

Gratifyingly, 1,7-diyne **10n** could also be used as a substrate to give 6-membered-ring-annulated furan **11n** in good yield, although required catalyst loading increased (Scheme 6).

Scheme 6. Oxygenative cyclization of a 1,7-diyne **10n**.

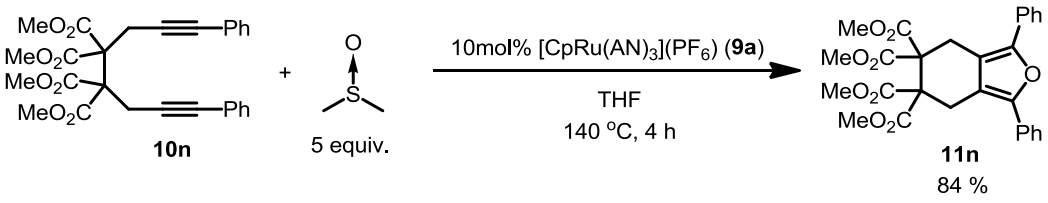

Previously, Beller, Dixneuf, and co-workers have reported that dienyl ethers, which are formed via *the* ruthenium-catalyzed alkoxylative dimerization of arylacetylenes undergo cyclization to afford 2,5-diarylfurans in the presence of copper(II) catalyst and TsOH in air (eq 1, Scheme 7).[13a] A similar transformation of diarylacetylenes into tetraarylfurans has been achieved using a palladium catalyst and zinc Lewis acid under an oxygen atmosphere (eq 2).[13b,c] The scope of these furan formation was almost limited to aryl substituted monoalkynes.

Scheme 7. Previously reported transition metal-catalyzed oxidative furan synthesis form monoaokynes.

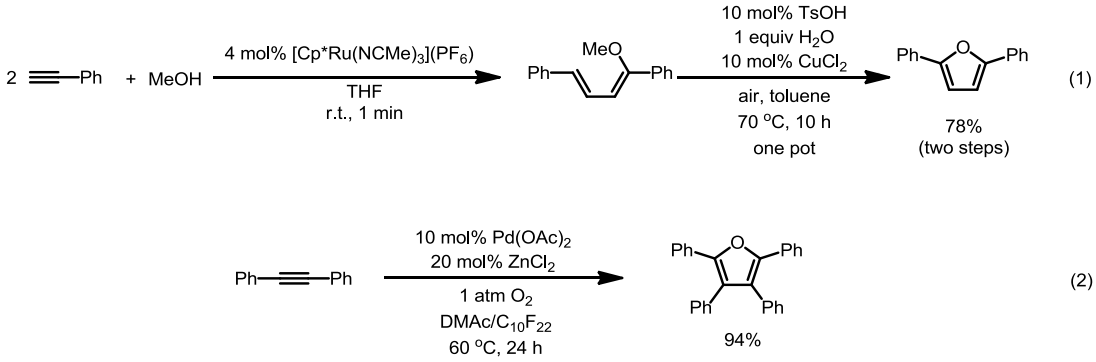

In contrast to these precedents, the newly established method catalytically convert a wide variety of α,ω-diyne substrate, having both aryl and alkyl terminal groups to bicyclic furans in good yields.

With the result of substrate screening, the author further sought to present a synthetic utility of the new method. Wu, Luh and co-workers have demonstrated that oligoaryls based on phenyl–(2,5-furylene)–(*p*-phenylene)–(2,5-furylene)–phenyl framework (**15**) are useful for organic electroluminescence devices.[14] According to the report, the oligoaryls work as efficient hole-transporting materials, or serve as blue-light emitter in themselves. The device containing the oligoaryl hole-transporting material in combination with PEDOT:PSS conduction layer exhibited higher efficiency than the devices with commonly used triarylamine hole transporter. (Scheme 8). The author anticipated that the basic frame work of this material could be constructed more atom-economically by using the new catalytic process.

Scheme 8. Hole-transporting oligoaryl compounds with an Ar–furylene–arylene–furylene–Ar sequence.

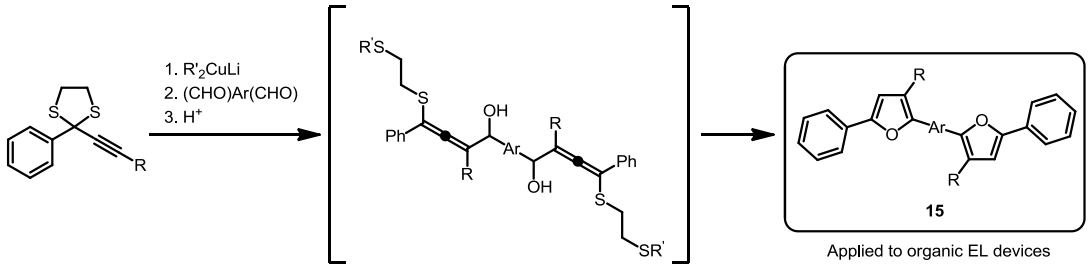

The phenyl-(2,5-furylene)-(*p*-phenylene)-(2,5-furylene)-phenyl array could be easily constructed by tandem oxygen-transfer cyclization of readily accessible phenylene-containing tetrayne **16** (Scheme 9). As established for aryl diynes, **16** was treated with dimethylsulfoxide in DMF solution in the presence of 10 mol% of $[CpRu(AN)_3](PF_6)$ (**9a**), desired diyne **17** was cleanly produced and easily isolated in high yield.

Scheme 9. Tandem transfer oxygenative cyclization of tetrayne **16** to form fruan-containing oligoaryl **17**.

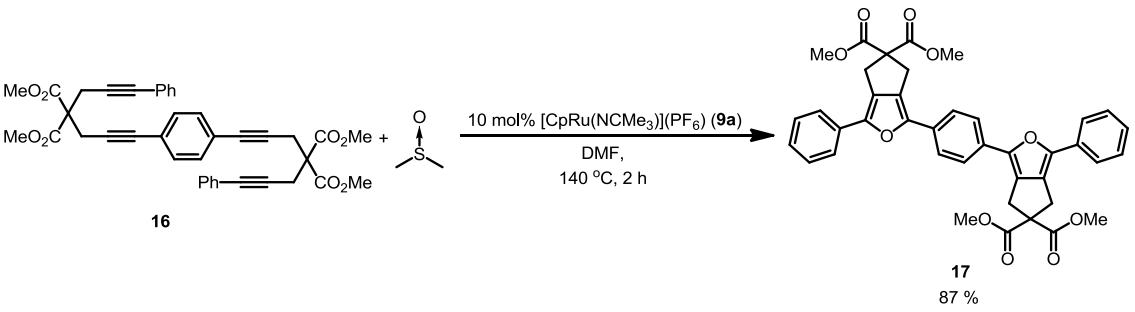

Even though the catalytic system has been developed, insight into its mechanism had not been revealed. The author postulated two plausible reaction mechanisms (Scheme 10). The mechanism A involves initial oxidative cyclization step between a Ru(II) and a diyne. Meanwhile, a mechanism which begins with C–O bond formation between DMSO and an alkyne moiety activated by cationic ruthenium complex is also possible (mechanism B).

Since, as shown in the chapter 2, ruthenacyclopentatriene derived from cationic cyclopentadienyl ruthenium complex is expected to be highly electrophilic, nucleophilic attack of DMSO oxygen to the ruthenium center will occur to form DMSO–complex **18**. Dimethyl sulfide is expelled from the generated adduct to give ketonic intermediate **19**. Following ring

closure between the ketone oxygen and carbene carbon will give rise to the furan product. Considering the high propensity of Cp′Ru(II) to form ruthenacyclopentatriene with diyne, this possibility seems convincing.

However, as mentioned in the introduction of this chapter, precedent transition metal-catalyzed oxygen transfer reactions from organic oxide to alkynes are known to be initiated by the formation of α-ketocarbene intermediates **20**. If nucleophilic attack of sulfoxide oxygen to the alkyne activated by Ru is very facile, this mechanism is feasible. Indeed, the acceleration effect of *p*-fluorophenyl group was seen even when only one terminal was substituted with this group (Table 3, entry 9). In addition, another unsymmetrical diyne **10m** that possesses methyl and phenyl groups on each terminal was smoothly transformed under the condition optimized for diaryldiyne substrate. These facts may support the mechanism B, in which only one alkyne moiety is involved in the oxygen transfer step.

Scheme 10. Proposed mechanisms for ruthenium-catalyzed oxygen-transfer/ cyclization reaction.

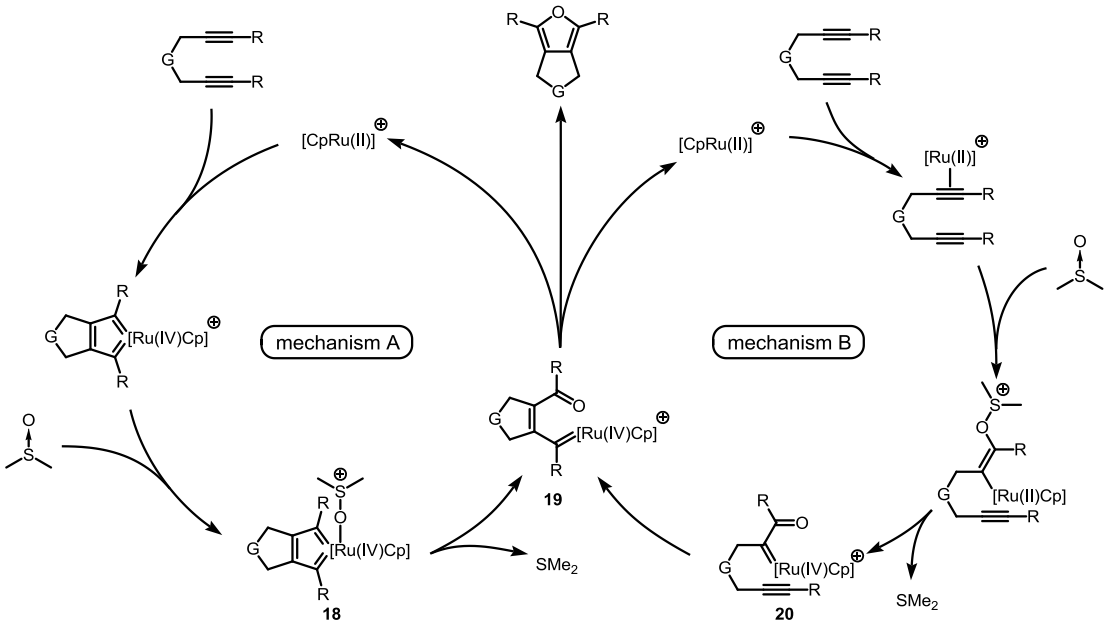

To test the first postulation, stoichiometric reaction between isolable ruthenacyclopentatriene **21** and dimethylsulfoxide was conducted in the presence or absence of activators ($AgPF_6$, MsOH) at 25 °C in THF solution (Table 4).

The result supported the mechanism A. Without an activator, **21** scarcely reacted with DMSO (entry 1). This result was parallel to the inactivity of neutral complex **4b**. Next, $AgPF_6$ was added to generate cationic ruthenacyclopentatriene complex in order to mimic the catalytic reaction condition. As a result, **21** was consumed within a short period of time to afford the furan **11a** in 65% yield (entry 2). Same as the catalytic reaction, MsOH (1.0 equiv) was also tested as an activator. Expected oxygen atom transfer took place and bicyclic furan **11a** was produced in 34% NMR yield (entry 3) along with 44% of unreacted starting **21**. Extending the reaction time resulted in a moderately improved yield of the furan (entry 4).

Table 4. Stoichiometric oxidation of ruthenacyclopentatriene complex **21** with DMSO in the presence/absence of activators.

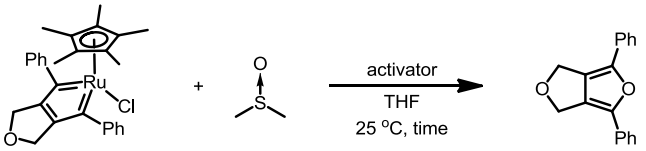

21 0.050 mmol | 0.10 mmol | **11a**

entry	activator	time[h]	yield **11a**/**21** [%][a]
1	none	1	<1/99
2	$AgPF_6$[c]	0.5	65/0
3	MsOH[b]	0.5	34/42
4	MsOH[b]	1	43/25

[a]yields determined by ^1H NMR analysis of crude products. [b]0.050 mmol. [c]0.055 mmol.

In combination with above mentioned experimental result, a feasible reaction mechanism was proposed with the aid of DFT calculation (Figure 3). Oxygen transfer from the sulfoxide to the carbene carbon takes place through two steps. At the outset, it was suggested that, the coordination of DMSO by oxygen atom (**A**) is more favorable than coordination by sulfur (**A′**). From the O-bound complex, the dimethyl sulfide moiety is expelled to form an oxocomplex **B**

through a rate-determining transition state with an activation barrier of 17.2 kcal/mol (**TS-AB**). Then, the oxygen atom on the ruthenium center undergoes 1,2-migration to form a oxaruthenacyclohexatriene intermediate **C**. The activation barrier corresponds to the transition state of this step was 12.3 kcal/mol. It was predicted that this intermediate evolves into cationic η^5-furan complex **E** through following two steps; isomerization of the ruthenacyclic moiety into envelope-like structure and ring closure of ketonic intermediate. Both steps were estimated to proceed smoothly through transition states **TS-CD** (2.6 kcal/mol) and **TS-DE** (2.8 kcal/mol).

Figure 3. Reaction profile for oxygen atom-transfer/cyclization of ruthenacyclopentatriene.

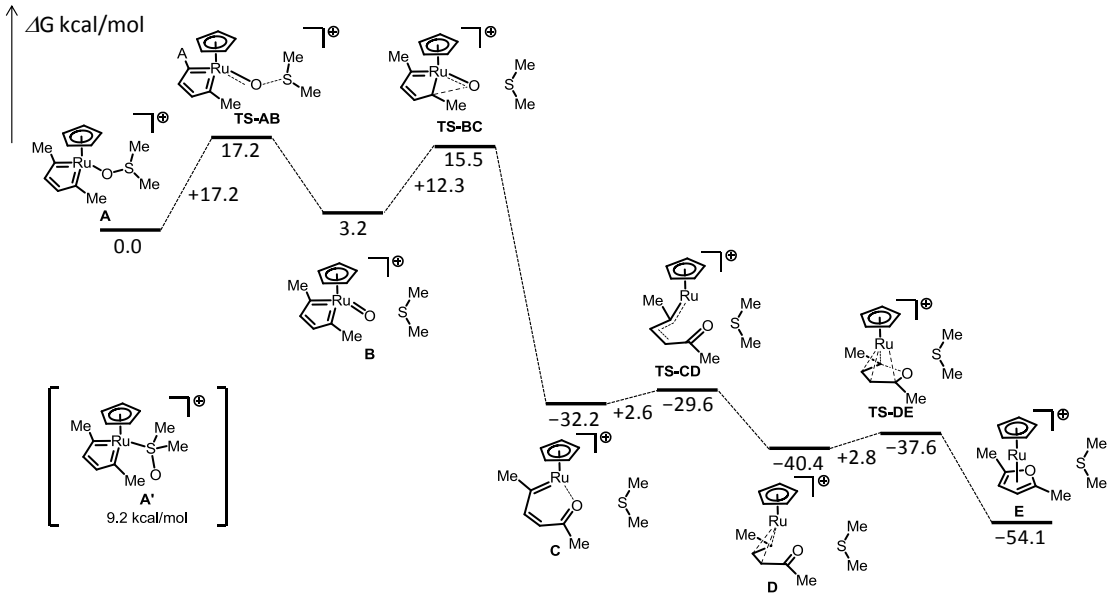

In summary, a novel transfer oxygenative cyclization of diynes with DMSO catalyzed by cyclopentadienyl ruthenium complexes was developed. The new reaction has a broad substrate scope, and highly useful for the synthesis of bicyclic furans. For diynes with aryl terminal groups, $[CpRu(AN)_3](PF_6)$ was the optimal catalyst, while those with alkyl terminal groups were effectively catalyzed by corresponding Cp* complex. The mechanism of the formation of bicyclic furans was proposed on the basis of the results obtained by carrying out the stoichiometric reaction of a ruthenacyclopentatriene. As a result, intermediacy of cationic ruthenacyclopentatriene was demonstrated. In addition, with the aid of DFT calculation, it was

predicted that the oxygen atom-transfer from DMSO proceeds through two steps; formation of ruthenium oxocomplex bearing a ruthenacyclopentatriene structure, and 1,2-migration of the oxygen atom from the ruthenium to the carbene carbon to generate a ketonic intermediate. Following isomerization and ring closure of the intermediate is predicted to form a η^5-furan complex.

3. Experimental Section

(a) General Considerations.

Column chromatography was performed on silica gel (Cica silica gel 60N) with solvents specified below. ^{1}H and ^{13}C NMR spectra were obtained for samples in $CDCl_3$ solution at 25 °C. ^{1}H NMR chemical shifts are reported in terms of chemical shift (δ, ppm) relative to the singlet at 7.26 ppm for chloroform. Splitting patterns are designated as follows: s, singlet; d, doublet; t, triplet; q, quartet; quint, quintet; sext, sextet; sept, septet; m, multiplet. Coupling constants are reported in Hz. ^{13}C NMR spectra were fully decoupled and are reported in terms of chemical shift (δ, ppm) relative to the triplet at δ = 77.0 ppm for $CDCl_3$. Mass measurements and elemental analyses were performed by the Instrumental Analysis Facility of Nagoya University. Melting points were obtained in capillary tubes. Cp*RuCl(cod) (**4b**),[15] $[CpRu(NCMe)_3](PF_6)$ (**9a**),[16] $[Cp^*Ru(NCMe)_3](PF_6)$ (**9b**)[17] and ruthenacyclopentatriene **21**[18] were prepared according to the reports. Diynes **10a**,[19] **10b**,[20] **10c**,[21] **10d**,[22] **10e**,[23] **10f**,[24] **10g**,[22] **10h**,[25] **10j**,[22] **10l**,[26] **13a**,[20] **13b**,[20] and **12**[27] are known compounds.

(b) Preparations of Substrates.

Synthesis of diyne 10i: To a dispersion of NaH (ca. 60 wt% in mineral oil, washed with hexane prior to use, 170 mg, 4.2 mmol) in THF (6.6 mL) was added dropwise a solution of 2-(3-(*p*-methoxyphenyl)prop-2-ynyl)malonic acid dimethyl ester[28] (1.1 g, 3.9 mmol) in THF(4.0 mL) at 0 ℃, and the solution was stirred for 30 min. To the reaction mixture was added dropwise a solution of 3-(*p*-fluorophenyl)prop-2-ynylmethanesulfonate (960 mg, 4.2 mmol) in THF (4.0 mL) at 0 °C. The reaction mixture was allowed to warm to room temperature in 4 hours. The reaction mixture was diluted with Et_2O (20 mL) and quenched with H_2O (20 mL). The aqueous phase was extracted with Et_2O (2 × 20 mL). The combined organic layer was washed with H_2O (20 mL) and brine (20 mL), dried over $MgSO_4$, and the solvents were evaporated *in vacuo*. The crude product was purified by column chromatography on silica gel (hexane : AcOEt = 5:1–5:2) to afford **10i** (0.90 g, 55 % yield) as colorless crystals (mp 97.0–99.5 °C); IR (KBr): 1740 (C=O) cm^{-1}; ^{1}H NMR (300 MHz, $CDCl_3$, 25 °C): δ 3.24 (s, 2 H), 3.25 (s, 2 H), 3.80 (two s overlap, 9 H), 6.78–6.83 (m, 2 H), 6.93–7.00 (m, 2 H), 7.28–7.38 (m,

2 H); ^{13}C NMR (75 MHz, $CDCl_3$, 25 °C): δ 23.9, 24.0, 53.2, 55.3, 57.3, 82.1, 82.7, 83.6, 113.6, 114.9, 115.1, 115.4, 118.9 (d, *J* = 3.3 Hz), 132.8, 133.3 (d, *J* = 8.0 Hz), 159.1, 162.0 (d, *J* = 246.3 Hz), 169.1; HRMS (FAB) *m/z* calcd for $C_{24}H_{21}O_5FNa$ 431.1265, found 431.1273 $[M+Na]^+$.

Synthesis of diyne 10k: To a dispersion of NaH (ca. 60wt% in mineral oil, washed with hexane prior to use, 0.64 g, 16 mmol) in THF (18 mL) was added dropwise dimethylmalonate (0.82 mL, 7.2 mmol) at 0 °C, and the solution was stirred for 30 min. To the reaction mixture was added dropwise a solution of 3-thienyl-prop-2-ynylmethansulfonate[29] (3.4 g, 16 mmol) in THF (18 mL) at 0 °C. The reaction mixture was stirred at room temperature for 9 hours. The reaction mixture was diluted with Et_2O (50 mL) and quenched with H_2O (50 mL). The aqueous phase was extracted with Et_2O (2 × 50 mL). The combined organic layer was washed with H_2O (2 × 50 mL) and brine (50 mL), dried over $MgSO_4$, and the solvents were evaporated *in vacuo*. The crude product was purified by silica gel chromatography (hexane / toluene = 1:2 – 1:6) to yield **10k** (1.3 g, 50 % yield) as yellow crystals (mp 42.0–44.5 °C); IR (KBr): 1741 (C=O) cm^{-1}; ^{1}H NMR (300 MHz, $CDCl_3$, 25 °C): δ 3.27 (s, 4 H), 3.81 (s, 6 H), 6.94 (dd, *J* = 5.4, 3.6 Hz, 2 H), 7.14 (dd, *J* = 3.6, 0.9 Hz, 2 H), 7.20 (d, *J* = 4.8, 0.9 Hz, 2 H); ^{13}C NMR (75 MHz, $CDCl_3$, 25 °C): δ 24.3, 53.3, 57.1, 77.0, 87.8, 122.7, 126.5, 126.6, 131.6, 168.8; HRMS (FAB) *m/z* calcd for $C_{19}H_{16}O_4NaS_2$ 395.0382, found 395.0382 $[M+Na]^+$.

Synthesis of diyne 10m: A solution of 2-(3-phenylprop-2-ynyl)-2-(but-2-ynyl)malonic acid dimethyl ester (0.79 g, 3.6 mmol), iodobenzene (0.44 mL, 3.9 mmol), CuI (1.9 mg, 10 μmol) and $Pd(PPh_3)_4$ (4.0 mg, 3.6 μmol) in $^iPr_2NH$ (6.2 mL) was stirred at room temperature for 9 hours. After that time, the solution was diluted with AcOEt (20 mL) and quenched with H_2O (20 mL). The aqueous layer was extracted with AcOEt (2×20 mL). The combined organic layer was successively washed with H_2O (20mL) and brine (20 mL), and dried over $MgSO_4$. The solutions were evaporated *in vacuo*. The obtained crude product was purified with silica gel column chromatography to give diyne **10m** as pale yellow oil (0.84 g, 79%); IR (liquid film): 1740 (C=O) cm^{-1}; ^{1}H NMR (300 MHz, $CDCl_3$, 25 °C): δ 1.78 (t, *J* = 2.7 Hz, 3 H), 2.99 (q, *J* = 2.7 Hz,

2 H), 3.19 (s, 2 H), 3.78 (s, 6 H), 7.24-7.30 (m, 3 H), 7.33-7.39 (m, 2 H); ^{13}C NMR (75 MHz, $CDCl_3$, 25 °C): δ 3.8, 23.4, 23.8, 53.1, 57.2, 73.0, 79.2, 83.5, 84.0, 122.9, 127.8, 128.0, 131.5, 169.2; HRMS (FAB) *m/z* calcd for $C_{18}H_{18}O_4Na$ 321.1103, found 321.1093 $[M+Na]^+$.

Synthesis of diyne 10m: To a dispersion of NaH (ca. 60wt% in mineral oil, washed with hexane prior to use, 0.46 g, 11 mmol) in THF (24 mL) was added .dropwise tetraethyl-1,1,2,2-ethanecarboxylate (1.3 g, 4.2 mmol) in two portions at room temperature, and the solution was stirred for 1 h at room temperature. After that time, solution of 1-phenyl-3-bromoprop-1-yne (2.2 g, 11 mmol) in THF (5 mL) was added dropwise. The reaction mixture was heated to reflux and stirred for 6 h at that temperature. The reaction mixture was diluted with Et_2O (30 mL) and quenched with saturated aqueous solution of NH_4Cl (10 mL) and H_2O (10 mL). The aqueous phase was extracted with Et_2O (2 × 30 mL). The combined organic layer was washed with H_2O (50 mL) and brine (50 mL), dried over $MgSO_4$, and the solvents were evaporated *in vacuo*. The crude product was purified by silica gel chromatography (hexane / AcOEt = 10:1 – 3:1) to yield **10m** (1.8 g, 77 % yield) as yellow oil; IR (liquid film): 1733 (C=O) cm^{-1}; ^{1}H NMR (300 MHz, $CDCl_3$, 25 °C): δ (300 MHz, CDCl3, 25 ℃): δ 1.29 (t, *J* = 7.2 Hz, 12 H), 4.25 (dq, *J* = 10.8, 7.2 Hz, 4H), 4.29 (qd, *J* = 10.8, 7.2 Hz, 4H) 7.33-7.38 (m, 4H); ^{13}C NMR (75 MHz, $CDCl_3$, 25 °C): δ 14.0, 23.7, 61.93 62.1, 82.7, 85.8, 123.3, 127.6, 127.9, 131.3, 168.3; HRMS (FAB) *m/z* calcd for $C_{32}H_{34}O_8$ 546.2248, found 546.2255 $[M]^+$.

Synthesis of diyne 10n: To a dispersion of NaH (ca. 60wt% in mineral oil, washed with hexane prior to use, 0.46 g, 11 mmol) in THF (24 mL) was added dropwise tetraethyl-1,1,2,2-ethanecarboxylate (1.3 g, 4.2 mmol) in two portions at room temperature, and the solution was stirred for 1 h at that temperature. After that time, solution of 1-phenyl-3-bromoprop-1-yne (2.2 g, 11 mmol) in THF (5 mL) was added dropwise. The reaction mixture was heated to reflux and stirred for 6 h at that temperature. The reaction mixture was diluted with Et_2O (30 mL) and quenched with saturated aqueous solution of NH_4Cl (10 mL) and H_2O (10 mL). The aqueous phase was extracted with Et_2O (2 × 30 mL). The

combined organic layer was washed with H_2O (50 mL) and brine (50 mL), dried over $MgSO_4$, and the solvents were evaporated *in vacuo*. The crude product was purified by silica gel chromatography (hexane / AcOEt = 10:1 – 3:1) to yield **10n** (1.8 g, 77 % yield) as yellow oil; IR (liquid film): 1733 (C=O) cm^{-1}; ^1H NMR (300 MHz, $CDCl_3$, 25 °C): δ (300 MHz, $CDCl_3$, 25 °C): δ 1.29 (t, *J* = 7.2 Hz, 12 H), 4.25 (dq, *J* = 10.8, 7.2 Hz, 4H), 4.29 (qd, *J* = 10.8, 7.2 Hz, 4H) 7.33-7.38 (m, 4H); ^{13}C NMR (75 MHz, $CDCl_3$, 25 °C): δ 14.0, 23.7, 61.93 62.1, 82.7, 85.8, 123.3, 127.6, 127.9, 131.3, 168.3; HRMS (FAB) *m/z* calcd for $C_{32}H_{34}O_8$ 546.2248, found 546.2255 $[M]^+$.

Synthesis of diyne 13c: To a dispersion of NaH (ca. 60wt% in mineral oil, washed with hexane prior to use, 141 mg, 3.5 mmol) in glyme (3 mL) was added dropwise a solution of 3-Cyclopentylprop-2-yn-1-ol (399 mg, 3.2 mmol) in glyme (5.0 mL) at 0 ℃, and the solution was stirred for 20 min at the temperature, and another 20 min at room temperature. To the reaction mixture was added dropwise a solution of above obtained 3-cyclopentylprop-2-ynyl-*p*-toluenesulfonate (840 mg, ca. 95%, 2.9 mmol) in glyme (3.0 mL) at 0 ℃. The solution was stirred at room temperature for 30 h. Then the reaction mixture was quenched with H_2O and extracted with Et_2O (2 × 30 mL). The combined organic layer was washed with H_2O (50 mL) and with brine (20 mL), dried over $MgSO_4$, and concentrated *in vacuo*. Obtained crude product was purified by silica gel column chromatography (hexane/toluene = 1:1–1:2) to give diyne **13c** as colorless oil (540 mg, 81 % yield); ^1H NMR (300 MHz, $CDCl_3$, 25 °C): δ 1.48-1.68 (m, 8 H), 1.69-1.76 (m, 4 H), 1.86-1.98 (m, 4 H), 2.641 (m, 2H), 4.21 (d, *J* = 1.8 Hz, 4H); ^{13}C NMR (75 MHz, $CDCl_3$, 25 °C): δ 25.1, 30.2, 33.8, 57.1, 74.8, 91.5; HRMS (FAB) *m/z* calcd for $C_{16}H_{21}O$ 229.1587, found 229.1591 $[M-H]^+$.

(c) Ruthenium-Catalyzed Reaction of Diynes with Aryl Terminal Groups.

General procedures – Cyclization of 10a: solution of a diyne **10a** (74 mg, 0.30 mmol), $CpRu(AN)_3PF_6$ (**9a**) (3.9 mg, 9.0 μmol) and dimethylsulfoxide (110 μL, 1.5 mmol) in dry degassed DMF (3.0 mL) was stirred at 140 °C for 4 h under an argon atmosphere. The reaction was traced by TLC analysis. After cooled to room temperature, the reaction mixture was diluted

with 10 mL of hexane-AcOEt (10:1) and quenched with 20 mL of distilled water. The aqueous phase was extracted with hexane–AcOEt (2 x 10 mL). The combined organic layer was washed with H_2O (20 mL) and brine (10 mL), and dried over $MgSO_4$. After a removal of solvent under reduced pressure, the pale brown crystalline product was purified with silica gel column chromatography (toluene) to give **11a** (71 mg, 90% yield) as colorless crystals (mp 171.5–173.5 °C, lit[22] mp 167.5–169.5 °C). Following analytical data were in good agreement with those reported; ^{1}H NMR (300 MHz, $CDCl_3$, 25 °C): δ 5.08 (s, 4 H), 7.26 (tt, *J* = 1.2 , 7.4 Hz, 2 H), 7.42 (t, *J* = 7.5 Hz, 4 H), 7.51 (d, *J* = 7.2 Hz); ^{13}C NMR (75 MHz, $CDCl_3$, 25 °C): δ 66.5, 123.6, 126.8, 128.3, 128.6, 130.1, 141.2.

Analytical data for 11b: Colorless crystals (mp 191.5–193.0 °C); IR (KBr): 1737 (C=O) cm^{-1}; ^{1}H NMR (300 MHz, $CDCl_3$, 25 °C): δ 3.61 (s, 4 H), 3.80 (s, 6 H), 7.24 (t, *J* = 7.5 Hz, 2 H), 7.41 (dd, *J* = 7.8, 7.8 Hz, 4 H), 7.64 (d, *J* = 7.8 Hz, 4 H); ^{13}C NMR (75 MHz, $CDCl_3$, 25 °C): δ 33.5, 53.3, 67.4, 123.6, 126.5, 127.1, 128.5, 130.6, 142.9 171.1; HRMS (FAB) *m/z* calcd for $C_{23}H_{20}O_5$ 399.1203, found 399.1208 $[M+Na]^+$.

Analytical data for 11c: Colorless crystals (mp 170.0–173.0 °C); IR (KBr): 1702 (C=O) cm^{-1}; ^{1}H NMR (300 MHz, $CDCl_3$, 25 °C): δ 2.25 (s, 6 H), 3.51 (s, 4 H), 7.22-7.28 (m, 2 H), 7.38–7.46 (m, 4 H), 7.63–7.69 (m, 4 H); ^{13}C NMR (75 MHz, $CDCl_3$, 25 °C): δ 26.7 30.4, 82.2, 123.6, 126.6, 128.5, 130.5, 143.1, 203.5; HRMS (FAB) *m/z* calcd for $C_{23}H_{20}O_3Na$ 367.1305, found 367.1310 $[M+Na]^+$.

Analytical data for 11d: Colorless crystals (mp 235.0–236.0 °C); IR (KBr): 2252 (C≡N) cm^{-1}; ^{1}H NMR (300 MHz, $CDCl_3$, 25 °C): δ 3.77 (s, 4 H), 7.32 (tt, *J* = 7.5, 1.5 Hz, 2 H), 7.45 (dd, *J* = 7.5, 7.5 Hz, 4 H), 7.59 (dd, *J* = 7.5, 1.8 Hz, 4 H); ^{13}C NMR (75 MHz, $CDCl_3$, 25 °C): δ 38.1, 39.7, 115.5, 122.8, 123.9, 127.7, 128.8, 129.4, 144.4; HRMS (FAB) *m/z* calcd for $C_{21}H_{14}N_2O$ 310.1101, found 310.1099 $[M]^+$.

Analytical data for 11e: colorless crystals (mp 258.5–260.5 °C); IR (KBr): 1162(S=O), 1348(S=O) cm^{-1}; 1H NMR (300 MHz, $CDCl_3$, 25 °C): δ 2.42 (s, 3 H), 4.63 (s, 4 H), 7.23–7.30 (m, 2 H), 7.34 (d, *J* = 8.4 Hz, 2 H), 7.37–7.44 (m, 4 H), 7.47–7.53 (m, 4 H), 7.83 (d, *J* = 8.4 Hz, 2 H); ^{13}C NMR (75 MHz, $CDCl_3$, 25 °C): δ 21.7, 47.50, 123.3, 123.6, 127.2, 127.2, 128.7, 129.6, 129.8, 133.7, 142.6, 143.7; HRMS (FAB) *m/z* calcd for $C_{25}H_{21}O_3NS$ 415.1237, found 415.1226 $[M]^+$.

Analytical data for 11f: Colorless crystals (mp 233.0–236.5 °C); IR (KBr): 1144(S=O), 1302(S=O) cm^{-1}; ^1H NMR (300 MHz, $CDCl_3$, 25 °C): δ 4.38 (s, 4 H), 7.31–7.38 (m, 2 H), 7.42–7.50 (m, 4 H), 7.55–7.63 (m, 4 H); ^{13}C NMR (75 MHz, $CDCl_3$, 25 °C): δ 52.8, 113.6, 124.0, 128.0, 128.8, 129.1, 146.6; HRMS (FAB) *m/z* calcd for $C_{18}H_{14}O_3S$ 310.0658, found 310.0658 $[M]^+$.

Analytical data for 11g: Colorless crystals (mp 180.5–182.5 °C); IR (KBr): 1750 (C=O) cm^{-1}; ^1H NMR (300 MHz, $CDCl_3$, 25 °C): δ 3.55 (s, 4 H), 3.79 (s, 6 H), 3.85 (s, 6 H), 6.94 (d, *J* = 8.7 Hz, 4 H), 7.54 (d, *J* = 8.7 Hz, 2 H); ^{13}C NMR (75 MHz, $CDCl_3$, 25 °C): δ 33.4, 53.2, 55.4, 67.5, 114.0, 124.0, 124.9, 125.2, 142.2, 158.0, 171.2; HRMS (FAB) *m/z* calcd for $C_{25}H_{24}O_7Na$ 459.1414, found 459.1408 $[M+Na]^+$.

Analytical data for 11h: Colorless crystals (mp 185.0–186.5 °C); IR (KBr): 1733 (C=O) cm^{-1}; ^1H NMR (300 MHz, $CDCl_3$, 25 °C): δ 3.56 (s, 4 H), 3.80 (s, 6 H), 7.09 (m, 4 H), 7.05–7.16 (m, 4 H), 7.53–7.63 (m, 4 H); ^{13}C NMR (75 MHz, $CDCl_3$, 25 °C): δ 33.4, 53.3, 67.4, 115.5, 115.8, 125.2 (d, *J* = 8.0 Hz), 126.5, 126.9 (d, *J* = 3.5 Hz), 142.0, 161.3 (d, *J* = 244.7 Hz), 171.0; HRMS (FAB) *m/z* calcd for $C_{23}H_{18}O_5F_2Na$ 435.1015, found 435.1017 $[M+Na]^+$.

Analytical data for 11i: Colorless crystals (mp 135.0–137.0 °C); IR (KBr): 1732 (C=O) cm^{-1}; ^1H NMR (300 MHz, $CDCl_3$, 25 °C): δ 3.56 (s, 4 H), 3.79 (s, 6 H), 3.85 (s, 3 H), 6.94 (d, *J* = 8.7 Hz, 2 H), 7.05–7.12 (m, 2 H), 7.52–7.60 (m, 4 H); ^{13}C NMR (75 MHz, $CDCl_3$, 25 °C): δ 33.30, 33.33, 53.2, 55.3, 67.4, 114.0, 115.4, 115.7, 123.6, 124.97, 125.00 (d, *J* = 8.0 Hz), 125.19, 126.5,

127.1 (d, *J* = 2.9 Hz), 141.3, 142.8, 158.2, 161.1 (d, *J* = 244.1 Hz), 171.1; HRMS (FAB) *m/z* calcd for $C_{24}H_{21}O_6F$ 424.1317, found 424.1321 $[M]^+$.

Analytical data for 11j: Colorless crystals (mp 229.5–231.5 °C); IR (KBr): 1721 (C=O), 1746 (C=O) cm^{-1}; ^1H NMR (300 MHz, $CDCl_3$, 25 °C): δ 3.56 (s, 4 H), 3.80 (s, 6 H), 7.43–7.49 (m, 4 H), 7.49–7.55 (m, 4 H); ^{13}C NMR (75 MHz, $CDCl_3$, 25 °C): δ 33.4, 53.4, 67.3, 120.4, 125.0, 127.8, 129.2, 131.6, 142.2, 170.9; HRMS (FAB) *m/z* calcd for $C_{23}H_{18}O_5Br_2$ 531.9516, found 531.9525 $[M]^+$.

Analytical data for 11k: Pale yellow crystals (mp 155.0–158.0 °C); IR (KBr): 1744 (C=O) cm^{-1}; ^1H NMR (300 MHz, $CDCl_3$, 25 °C): δ 3.49 (s, 4 H), 3.80 (s, 6 H), 7.06 (dd, *J* = 5.1, 3.9 Hz, 2 H), 7.18 (dd, *J* = 3.6, 0.9 Hz, 2 H), 7.24 (dd, *J* = 4.8, 1.2 Hz, 2 H); ^{13}C NMR (75 MHz, $CDCl_3$, 25 °C): δ 33.0, 53.3, 67.2, 121.9, 123.8, 126.1, 127.5, 133.1, 138.8, 170.9; HRMS (FAB) *m/z* calcd for $C_{19}H_{16}O_5S_2$ 388.9434, found 388.0439 $[M+Na]^+$.

Analytical data for 11l: Reddish brown crystals (mp 154.5–157.5 °C); ^1H NMR (300 MHz, $CDCl_3$, 25 °C): δ 4.16 (s, 10 H), 4.27–4.32 (m, 4 H), 4.51-4.56 (m, 4 H), 4.87 (s, 4 H); ^{13}C NMR (75 MHz, $CDCl_3$, 25 °C): δ 65.0, 66.0, 68.5, 69.2, 76.2, 125.4, 139.9; HRMS (FAB) *m/z* calcd for $C_{26}H_{22}Fe_2O_2$ 478.0313, found 478.0308 $[M]^+$.

Analytical data for 11m: Colorless solid (mp 123.0–125.5 °C); IR (KBr): 1726(C=O), 1740 (C=O) cm^{-1}; ^1H NMR (300 MHz, $CDCl_3$, 25 °C): δ 3.28 (s, 3 H), 3.25 (d, *J* = 1.5 Hz, 2 H), 3.52 (s, 2H), 3.77 (s, 6 H), 7.17 (t, *J* = 7.2 Hz, 1 H), 7.35 (dd, *J* = 7.2, 7.2 Hz, 2 H), 7.50 (d, *J* = 7.2 Hz, 2 H); ^{13}C NMR (75 MHz, $CDCl_3$, 25 °C): δ 12.9, 31.6, 33.7, 53.1, 67.2, 123.1, 125.3, 125.7, 125.8, 128.3, 131.0, 141.3, 141.8, 171.2; HRMS (FAB) *m/z* calcd for $C_{18}H_{18}O_5Na$ 337.1046, found 337.1049 $[M+Na]^+$.

Analytical data for 11n: pale yellow oil; IR (liquid film): 1734 (C=O) cm^{-1}; ^1H NMR (300 MHz, $CDCl_3$, 25 °C): δ 1.13–1.32 (m, 12 H), 3.62 (s, 4 H), 4.08–4.40 (m, 8 H), 7.26 (dd, *J* = 7.8 Hz, 2 H), 7.43 (dd, *J* = 7.8, 7.2 Hz, 4 H), 7.70 (d, *J* = 7.2 Hz, 4 H); ^{13}C NMR (75 MHz, $CDCl_3$, 25 °C): δ 14.0, 28.9, 57.9, 62.0, 116.9, 124.4, 126.5, 128.4, 131.0, 145.6, 169.6 (br); HRMS (FAB) *m/z* $C_{32}H_{34}O_9$ 562.2197, found 562.2194 $[M]^+$.

Cyclization of 16: solution of tetrayne **16** (97 mg, 0.15 mmol), $[CpRu(NCMe)_3](PF_6)$ (**9a**) (6.6 mg, 15 μmol) and DMSO (110 μL, 1.5 mmol) in dry degassed DMF (3.0 mL) was stirred at 140 °C under an argon atmosphere for 2 h. The reaction progress was traced by TLC analysis. After cooled to room temperature, the reaction mixture was diluted with $CHCl_3$ (10 mL) and quenched with distilled water (20 mL). The aqueous phase was extracted with $CHCl_3$ (2 × 10 mL). The combined organic layer was washed with H_2O (20 mL) and brine (10 mL), and dried over $MgSO_4$. After concentration *in vacuo*, the brown solid was purified with silica gel column chromatography (hexane:$CHCl_3$:AcOEt = 20:20:1−20:20:5) to afford **17** (88 mg, 87% yield) as yellow solid (mp 296.0–299.5 °C); IR (KBr): 1737 (C=O) cm^{-1}; ^1H NMR (300 MHz, $CDCl_3$, 25 °C): δ 3.61 (s, 4 H), 3.62 (s, 4 H), 3.81 (s, 12 H), 7.22–7.28 (m, 2 H), 7.38–7.46 (m, 4 H), 7.62–7.68 (m, 8 H); ^{13}C NMR (75 MHz, CDCl3, 25 °C): δ 33.5, 33.6, 53.3, 67.4, 123.6, 123.9, 126.6, 127.3, 127.4, 128.5, 128.7, 130.5, 142.7, 143.0, 171.1; HRMS (FAB) *m/z* calcd for $C_{40}H_{34}O_{10}$ 674.2146, found 674.2144 $[M]^+$.

(d) Crystallographic Structural Determinations.

A single crystal of **11f** suitable for X-ray analysis was mounted on a glass fiber, and diffraction data were collected at 153 K on a Brucker SMART APEX CCD diffractometer with graphite monochromated Mo-Kα radiation (λ = 0.71073 Å). The absorption correction was made using SADABS. The structure was solved by direct methods and refined by the full-matrix least-squares on F^2 by using SHELXTL.[30] All non-hydrogen atoms were refined with anisotropic displacement parameters. All hydrogen atoms were placed in calculated positions.

Table S 1. Selected crystallographic data and collection parameters for **11f**.

11f (2 molecules)	
Formula	$C_{36}H_{28}O_6S_2$
Fw	620.70
Crystal system	Monoclinic
Space group	$P2_1/C$ (#14)
a [Å]	21.6727(18)
b [Å]	7.9317(6)
c [Å]	18.6280(16)
β [°]	93.401(2)
V [Å^3]	2900.5(4)
Z	4
D_{calc} [g cm^{-3}]	1.421
μ [mm^{-1}]	0.233
F(000)	1296
Crystal size [mm^3]	0.30 × 0.15 × 0.15
Reflections collected	20913
Independent reflections	7198 (R_{int} =0.0433)
GOF on F^2	0.983
R_1 [I>2σ(I)][a]	0.459
wR_2 (all data)[b]	0.1135
Largest diff. peak and hole [e Å^{-3}]	0.499 / −0.349

[a] $R_1 = \Sigma \mid (F_o - F_c) \mid / \Sigma(F_o)$. [b] $wR_2 = \{\Sigma[(w(F_o^2 - F_c^2)^2)]/\Sigma[w(F_o^2)^2]\}^{1/2}$.

(e) Ruthenium-Catalyzed Reaction of Diynes with Alkyl Terminal Groups.

General procedures–Cyclization of 13a: A solution of 13a (70 mg, 0.30 mmol), [Cp*Ru(NCMe)$_3$](PF$_6$) (9b) (4.5 mg, 8.9 μmol) and dimethylsulfoxide (53 μL, 0.75 mmol) in dry degassed THF (3.0 mL) was stirred at 70 °C for 1 h. The reaction mixture was cooled to room temperature, diluted with $CHCl_3$ (10 mL), and quenched with H_2O (20 mL). The aqueous phase was extracted with $CHCl_3$ (2 × 10 mL). The combined organic layer was washed with H_2O (20 mL) and brine (10 mL), dried over $MgSO_4$, and the solvents were removed *in vacuo*. The crude brown oil was purified with silica gel column chromatography (hexane/AcOEt = 5 : 1) to afford **14a** (68 mg, 90% yield) as colorless solid (mp 60.5–63.0 °C); IR (KBr): 1734 (C=O) cm^{-1}; ^{1}H NMR (300 MHz, $CDCl_3$, 25 °C): δ 2.15 (s, 6 H), 3.16 (q, *J* = 0.9 Hz, 4 H), 3.75 (s, 6 H); ^{13}C NMR (75 MHz, $CDCl_3$, 25 °C): δ 12.7, 31.9, 53.0, 67.0, 123.6, 139.5, 171.4; HRMS (FAB) *m/z* calcd for $C_{13}H_{16}O_5Na$ 275.0890, found 275.0890 $[M+Na]^+$.

Analytical data for 13b: Colorless solid (mp 165.0–167.5 °C); IR (KBr): 1161 (S=O), 1341 (S=O) cm^{-1}; ^{1}H NMR (300 MHz, $CDCl_3$, 25 °C): δ 2.13 (s, 6 H), 2.42 (s, 3 H), 4.22 (s, 4 H), 7.32 (d, *J* = 1.5 Hz, 2H), 7.74 (d, *J* = 1.5 Hz, 2 H); ^{13}C NMR (75 MHz, $CDCl_3$, 25 °C): δ 12.8, 21.7, 46.3, 120.7, 127.3, 129.6, 133.7, 139.4, 143.3; HRMS (FAB) *m/z* calcd for $C_{15}H_{17}O_3NNaS$ 314.0821, found 314.0823 $[M+Na]^+$.

Analytical data for 13c: Colorless oil; ^{1}H NMR (300 MHz, $CDCl_3$, 25 °C): δ 1.49–1.74 (m, 12 H), 1.89–2.03 (m, 4 H), 2.94–3.07 (m, 2 H), 4.71 (d, *J* = 0.6 Hz, 2 H); ^{13}C NMR (75 MHz, $CDCl_3$, 25 °C): δ 25.2, 31.6, 38.3, 65.4, 123.6, 145.2; HRMS (FAB) *m/z* calcd for $C_{16}H_{21}O_2$ 246.1536 found 246.1541 $[M-H]^+$.

(f) Reactions of Ruthenacyclopentatriene 21 with DMSO.

To a solution of **21** (26 mg, 50 μmol) in dry degassed THF (1.5 mL) was successively added a solution of DMSO in THF (0.20 M, 0.50 mL, 0.10 mmol) and a solution $AgPF_6$ in THF (0.11 M, 0.50 mL, 0.057 mmol). The reaction mixture was stirred at 25 °C for 30 min. After the solvent was removed *in vacuo*, ethylbenzene (10.0 μL, 0.0820 mmol) was added as an internal standard.

The composition of the crude mixture was determined with ^{1}H NMR by comparing the peak area of following signals; **11a**: δ 5.09 (s, 4 H), ethyl benzene δ 1.25 (t, 3 H). The ratio was [**11a**] : [ethylbenzene] = 3.97 : 10.0. This result corresponds to 0.0325 mmol (65% yield) of **11a**.

(g) Theoretical Calculations.

The Gaussian 03 program package was used for all geometry optimizations.[31] The geometries of stationary points and transition states were fully optimized by means of the Becke's three-parameter hybrid density functional method (B3LYP)[32] with the basis set, consisting of a double-ζ basis set with the relativistic effective core potential of Hay and Wadt (LanL2DZ)[33] for Ru and the 6-31G(d)[34] basis sets for other elements (BS-I). The vibrational frequencies, zero-point energy (ZPE) and thermal correction to Gibbs free energy (TCGFE) were calculated at the same level of theory. The obtained structures were characterized by the number of imaginary frequencies (one or zero for transition or ground states, respectively). The connectivity of each step was further confirmed by IRC calculation[35] from the transition states followed by optimization of the resulted geometries. Single-point energies for geometries obtained by the above method were calculated at the same level using the basis sets consisting of a [6*s*5*p*3*d*2*f*1*g*] contracted valence basis set with the Stuttgart-Dresden-Bonn energy-consistent pseudopotential (SDD) [36,37] for Ru and the 6-311++G(2d,p) basis sets[38] for other elements. Relative energies were corrected with unscaled ZPE obtained at the B3LYP/BS-I level. The obtained results are summarized in Table S 2.

Table S 2. Summary of theoretical calculations.

Model	Energy/au	ZPE/au	TCGFE/au	IF/cm^{-1}
A'	–1075.04722309	0.286730	0.238492	
A	–1075.05868610	0.286095	0.235956	
TS-AB	–1075.03007543	0.284830	0.235970	247.4128i
B	–596.96771459	0.208256	0.168830	
TS-BC	–596.94619691	0.207361	0.168194	311.7914i
C	–597.02430646	0.209433	0.168193	
TS-CD	–597.01989528	0.208991	0.168376	137.6189i
D	–597.03765747	0.209351	0.168517	
TS-DE	–597.03355529	0.209006	0.169199	163.4921i
E	–597.06828376	0.212099	0.174590	
Me_2S	–478.06683270	0.076325	0.049265	

4. References and Notes

[1] (a) Fan, L.; Turner, M. L.; Hursthouse, M. B.; Malik, K. M. A.; Gusev, O. V.; Maitlis, P. M. *J. Am. Chem. Soc.* **1994**, *116*, 385–386; (b) Fan, L.; Turner, M. L.; Adams, H.; Bailey, N. A.; Baitlis, P. M. *Organometallics* **1995**, *14*, 676–684; (c) Fan, L.; Wei, C.; Aigbirhio, F. I.; Turner, M. L.; Gusev, O. V.; Morozova, L. N.; Knowles, D. R. T.; Maitlis, P. M. *Organometallics* **1996**, *15*, 98–104.

[2] For example, see: (a) James, B. R.; Ochiai, E.; Rampel, G. L. *Inorg. Nucl. Chem. Lett.* **1971**, *7*, 781–784; (b) Evans, I. P.; Spencer, A.; Wilkinson, G. J. *J. Chem. Soc., Dalton Trans.* **1973**, 204–; (c) Mercer, A.; Trotter, J. *J. Chem. Soc., Dalton Trans.* **1975**, 2480–2483; (d) Oliver, J. D.; Riley, D. P. *Inorg. Chem.* **1984**, *23*, 156-158; (e) Alessio, E.; Mestroni, G.; Nardin, G.; Attia, W. M.; Galligaris, M.; Sava, G.; Zorzet, S. *Inorg. Chem.* **1988**, *27*, 4099–4106.

[3] For a review, see: Allesio, E. *Chem. Rev.* **2004**, *104*, 4203–4242.

[4] (a) Kornblum, N.; Powers, J. W.; Anderson, G. J.; Jones, W. J.; Larson, H. O.; Levand, O.; Weaver, W. M *J. Am. Chem. Soc.* **1957**, *79*, 6562–6562; (b) Kornblum, N.; Jones, W. J.; Anderson, G. J. *J. Am. Chem. Soc.* **1959**, *81*, 4113–4114.

[5] Casey, C. P.; Burkhardt, T. J.; Bunnell, C. A.; Calabrese, J. C. *J. Am. Chem. Soc.* **1977**, *99*, 2127–2134.

[6] (a) Fischer, E. O.; Riedmüller, S. *Chem. Ber.* **1974**, *107*, 915–919; (b) Hill,, A. F.; Roper, W. R.; Waters, J. M.; Wright, A. H. *J. Am. Chem. Soc.* **1983**, *105*, 5939–5940; (c) Alcaide, B.; Casarrubios, L.; Domínguez, G.; Sierra, M. A. *J. Org. Chem.* **1993**, *58*, 3886–3894; (d) Quayle, P.; Rahman, P.; Ward, E. L. M.; Herbert, J. *Tetrahedron Lett.* **1994**, *35*, 3801–3804; (e) Quayle, P.; Rahman, S. *Tetrahedron Lett.* **1995**, *36*, 8087–8088; (f) Gibert, M.; Ferrer, M.; Lluch, A.-M.; Sánchez-Baeza, F.; Messeguer, A. *J. Org. Chem.* **1999**, *64*, 1591–1595; (g) Werner, H.; Schwab, P.; Bleuel, E.; Mahr, N.; Windmüller, B.; Wolf, J. *Chem. Eur. J.* **2000**, *6*, 4461–4470.

[7] (a) Trost, B. M.; Rhee, Y. H. *J. Am. Chem. Soc.* **1999**, *121*, 11680–11683; (b) Trost, B. M.; Rhee, Y. H. *J. Am. Chem. Soc.* **2002**, *124*, 2528–2553.

[8] (a) Shapiro, N. D.; Toste, F. D. *J. Am. Chem. Soc.* **2007**, *129*, 4160–4161; (b) Li, G.; Zhang, L. *Angew. Chem. Int. Ed.* **2007**, *46*, 5156–5159.

[9] (a) Witham, C. A.; Mauleón, P.; Shapiro, N.; Sherry, B. D.; Toste, F. D. *J. Am. Chem. Soc.* **2007**, *129*, 5838–5839; (b) Cuenca, A. B.; Montserrat, S.; Hossain, K. M.; Mancha, G.; Lledós, A.; Medio-Simón, M.; Ujaque, G.; Asensio, G. *Org. Lett.* **2009**, *11*, 4906–4909; (c) Li, C.-W.; Pati, K.; Lin, G.-Y.; Sohel, S. M. A.; Hung, H.-H.; Liu, R.-S. *Angew. Chem. Int. Ed.* **2010**, *49*, 9891–9894.

[10] (a) Cui, L.; Peng, Y.; Zhang, L. *J. Am. Chem. Soc.* **2009**, *131*, 8394–8395; (b) Cui, L.;

Zhang, G.; Peng, Y.; Zhagn, L. *Org. Lett.* **2009**, *11*, 1225–1228; (d) Ye, Y.; Cui, L.; Zhang, G.; Zhang, L. *J. Am. Chem. Soc.* **2010**, *132*, 3258–3259; (e) Ye, L.; He, W.; Zhang, L. *J. Am. Chem. Soc.* **2010**, *132*, 8550–8551; (f) He, W.; Li, C.; Zhang, L. *J. Am. Chem. Soc.* **2011**, *133*, 8482–8485.

[11] (a) Yeom, H.-S.; Lee, J.-E.; Shin, S. *Angew. Chem. Int. Ed.* **2008**, *47*, 7040–7043; (b)Yeom, H.-S.; Lee, Y.; Lee, J.-E.; Shin, S. *Org. Biomo. Chem.* **2009**, *7*, 4744–475; (c) Pati, K.; Liu, R.-S. *Chem. Commun.* **2009**, 5253–5235; (c) Yeom, H.-S.; Lee, Y.; Jeong, J.; So, E.; Hwang, S.; Lee, J.-E.; Lee, S. S.; Shin, S. *Angew. Chem. Int. Ed.* **2010**, *49*, 1611–1614.

[12] (a) Asao, N.; Sato, K.; Yamamoto, Y. *Tetrahedron Lett.* **2003**, *44*, 5675–5677; (b) Jadhav, A. M.; Bhunia, S.; Liao, H.-Y.; Liu, R.-S. *J. Am. Chem. Soc.* **2011**, *133*, 1769–1771.

[13] (a) Zhang, M.; Jiang, H.-F.; Neumann, H.; Beller, M.; Dixneuf, P. H. *Angew. Chem. Int. Ed.* **2009**, *48*, 1681−1684; (b) Wang, Z.; Jiang, H.; Xu, Q. *Synlett* **2009**, 929−932; (c) Wen, Y.; Zhu, S.; Jiang, H.; Wang, A.; Chen, Z. *Synlett* **2011**, 1023−1027.

[14] Zhang, L.-Z.; Chen, C.-W.; Lee, C.-F.; Wu, C.-C.; Luh, T.-Y. *Chem. Commun.* **2002**, 2336–2337.

[15] (a) Oshima, N.; Suzuki, H.; Moro-oka, Y. *Chem. Lett.* **1984**, 1161–1164; (b) Yamamoto, Y.; Hattori, H. *Tetrahedron* **2008**, *28*, 847–855.

[16] Kündig, E. P.; Monnier, F. R. *Adv. Synth. Catal.* **2004**, *346*, 901–904.

[17] Mbaye, D. M.; Demerseman, B.; Renaud, J.-L.; Toupet, L.; Bruneau, C. *Adv. Synth. Catal.* **2004**, *346*, 835–841.

[18] Yamamoto, Y.; Arakawa, T.; Ogawa, R.; Itoh, K. *J. Am. Chem. Soc.* **2003**, *125*, 12143–12160.

[19] Scheller, A; Winter, W.; Müller, E. *Liebigs Ann. Chem.*, **1976**, 1448–1454.

[20] Jan, H.-Y.; Krische, M. J. *J. Am. Chem. Soc.* **2004**, *126*, 7875–7880.

[21] Schulte, K. E.; Reisch, J.; Mock, A. *Arch. Pharm.* **1962**, *295*, 627–639.

[22] Yamashita, K.; Nagashima, Y.; Yamamoto, Y.; Nishiyama, H. *Chem. Commun.* **2011**, *47*, 11552–11554.

[23] Jung, I. G.; Seo, J.; Lee, S. I.; Choi, S. Y.; Chung, Y. K. *Organometallics* **2006**, *25*, 4240–4242.

[24] Braverman, S.; Zafrani, Y.; Gottlieb, H. E. *Tetrahedron* **2001**, *57*, 9177–9185.

[25] Hu, Y.; Sun, Y.; Hu, J.; Zhu, T.; Yu,T.; Zhao, Q. *Chem. Asian. J.* **2011**, *6*, 797–800.

[26] Yamamoto, Y.; Kataoka, H.; Kinprara, K.; Nishiyama, H.; Itoh, K. *Lett. Org. Chem.* **2005**, *2*, 219–221.

[27] Yacoub, B.; Blunm, J.; Ibrahin, A.; Vollhardt, K. P. C. *J. Mo. Cat.* **1991**, *66*, 295–312.

[28] Jiménez-Núñez, E.; Claverie, C. K.; Bour, C.; Cárdenas, D. J.; Echavarren, A. M. *Angew. Chem. Int. Ed.* **2008**, *47*, 7892–7895.

[29] Bargar, T. M.; Creemer, L. C.; McCarthy, J. R., U.S. Patent 4,743,617 (1988-5-10).

[30] G. M. Sheldrick, SHELXTL 5.1, Bruker AXS Inc., Madison, Wisconsin, 1997.

[31] Gaussian 03, Revision C.02, Frisch, M. J.; Trucks, G. W.; Schlegel, H. B.; Scuseria, G. E.; Robb, M. A.; Cheeseman, J. R.; Montgomery, J. A. Jr.; Vreven, T.; Kudin, K. N.; Burant, J. C.; Millam, J. M.; Iyengar, S. S.; Tomasi, J.; Barone, V.; Mennucci, B.; Cossi, M.; Scalmani, G.; Rega, N.; Petersson, G. A.; Nakatsuji, H.; Hada, M.; Ehara, M.; Toyota, K.; Fukuda, R.; Hasegawa, J.; Ishida, M.; Nakajima, T.; Honda, Y.; Kitao, O.; Nakai, H.; Klene, M.; Li, X.; Knox, J. E.; Hratchian, H. P.; Cross, J. B.; Bakken, V.; Adamo, C.; Jaramillo, J.; Gomperts, R.; Stratmann, R. E.; Yazyev, O.; Austin, A. J.; Cammi, R.; Pomelli, C.; Ochterski, J. W.; Ayala, P. Y.; Morokuma, K.; Voth, G. A.; Salvador, P.; Dannenberg, J. J.; Zakrzewski, V. G.; Dapprich, S.; Daniels, A. D.; Strain, M. C.; Farkas, O.; Malick, D. K.; Rabuck, A. D.; Raghavachari, K.; Foresman, J. B.; Ortiz, J. V.; Cui, Q.; Baboul, A. G.; Clifford, S.; Cioslowski, J.; Stefanov, B. B.; Liu, G.; Liashenko, A.; Piskorz, P.; Komaromi, I.; Martin, R. L.; Fox, D. J.; Keith, T.; Al-Laham, M. A.; Peng, C. Y.; Nanayakkara, A.; Challacombe, M.; Gill, P. M. W.; Johnson, B.; Chen, W.; Wong, M. W.; Gonzalez, C.; Pople, J. A. Gaussian, Inc., Wallingford CT, 2004.

[32] (a) Kohn, W.; Becke, A. D.; Parr, R. G. *J. Phys. Chem.* **1996**, *100*, 12974–12980; (b) Stephen, P. J.; Devlin, F. J.; Chabalowski, C. F.; Frisch, M. *J. Phys. Chem.* **1994**, *98*, 11623–11627; (c) Becke, A. D. *J. Chem. Phys.* **1993**, *98*, 1372–1377; (d) Lee, C.; Yang, W.; Parr, R. G. *Phys. Rev. B* **1988**, *37*, 785–789.

[33] Hay, P. J.; Wadt, W. R. *J. Chem. Phys.* **1985**, *82*, 299–310.

[34] (a) Hehre, W. J.; Ditchfield, R.; Pople, J. A. *J. Chem. Phys.* **1972**, *56*, 2257–2261; (b) Hariharan, P. C.; Pople, J. A. *Theor. Chim. Acta* **1973**, *28*, 213–222; (c) Fracl, M. M.; Pietro, W. J.; Hehre, W. J.; Binkley, J. S.; Gordon, M. S.; DeFrees, D. J.; Pople, J. A. *J. Chem. Phys.* **1982**, *77*, 3654–3665.

[35] (a) Fukui, K. *Acc. Chem. Res.* **1981**, *14*, 363–368; (b) Gonzalez, C.; Schlegel, H. B. *J. Chem. Phys.* **1989**, *90*, 2154–2161; (c) Gonzalez, C.; Schlegel, H. B. *J. Phys. Chem.* **1990**, *94*, 5523–5527.

[36] Martin, J. M. L.; Sundermann, A. *J. Chem. Phys.* **2001**, *114*, 3408–3420.

[37] Andrae, D.; Häussermann, U.; Dolg, M.; Stoll, H.; Preuß, H. *Theor. Chim. Acta* **1990**, *77*, 123–131.

[38] (a) Krishnan, R.; Binkley, J. S.; Seeger, R.; Pople, J. A. *J. Chem. Phys.* **1980**, *72*, 650–654; (b) McLean, A. D.; Chandler, G. S. *J. Chem. Phys.* **1980**, *72*, 5639–5648; (c) Frisch, M. J.; Pople, J. A.; Binkley, J. S. *J. Chem. Phys.* **1984**, *80*, 3265–3269; (d) Clark, T.; Chandrasekhar, J.; Spitznagel, G. W.; Schleyer, P. v. R. *J. Comp. Chem.* **1983**, *4*, 294–301.

Chapter 6

Conclusion

In this study, the author surveyed the reactivity of ruthenacyclopentatriene complex, and developed new catalytic transformations of alkynes that proceed through the ruthenacyclopentatriene intermediates.

Owing to valence deficiency, carbene species show high activity toward synthetically useful reactions such as cyclopropanation and C–H insertion. However, the extremely high reactivity of free carbenes leads to serious drawbacks; i.e. the loss of selectivity. One solution to this problem is the combination with transition metal complexes. The reactivity of the carbene can be controlled by modulating the electronic or steric factors of its complex. This strategy also enables the development of new reactions which are difficult to be realized without the aid of transition metals.

Alkynes have intrinsic carbenic reactivity and carbene complexes can be generated from them in combination with appropriate transition metal complexes. This method is highly useful in synthetic chemistry. Among the alkyne-derived carbene complexes, the author focused on ruthenacyclopentatrienes, which is formed *via* oxidative cyclization of a divalent ruthenium center and two alkyne moieties. The carbene part of the complex has affinity for a variety of species. It undergoes [2+2] cyclization with unsaturated compounds, is protonated by acids, and accepts nucleophilic attack (Scheme 1). To exploit this multifaceted reactivity, the author sought to develop novel ruthenium-catalyzed transformations of 1,6-diynes.

Scheme 1. Formation and representative reactivities of the ruthenacyclopentariene.

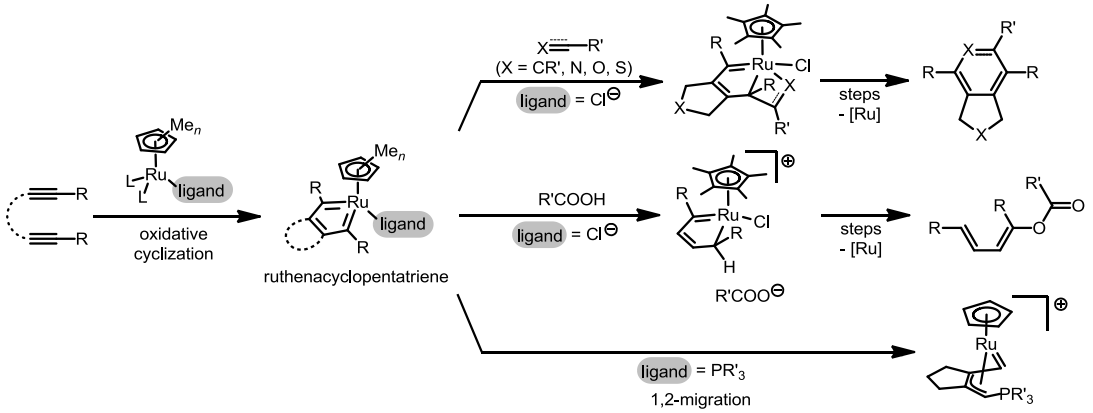

In the chapter 1, the chemistry of carbene complexes was reviewed, and the formation and reactivity of representative carbene complexes are described. Especially, the carbene complexes formed from alkynes and transition metal complexes were focused on. In the 4th section of the chapter, previously reported catalytic reactions that proceed *via* ruthenacyclopentatriene intermediate is dealt with. This part includes the features of those reactions, mechanistic uncertainty and issues to be addressed. Based on theses points, the author described the goal of the research.

In the chapter 2, improvement of the divalent ruthenium complex for alkyne [2+2+2] cycloaddition was described. The [2+2+2] cycloaddition of alkynes catalyzed by Cp*RuCl(cod) (**1a**) has previously been shown to have wide functional group tolerability, and is one of the best method for the regioselective synthesis of multiply substituted benzenes including iodobenzenes. However, the catalytic efficiency significantly decreases when the substrate alkynes are sterically demanding. It was assumed that the steric repulsion between the bulky Cp* ligand and the substrate was the main cause of the low catalytic efficiency (steric effect). However, it has also been implied that strongly electron-donating pentasubstituted Cp* ligand plays an important role in facilitating the ruthenacyclopentatriene formation *via* oxidative cyclization (electronic effect). Hence the author postulated that a polymethylcyclopentadienyl ligand with intermediate substitution numbers between 5 and 0 will have the best balance of the steric and electronic effects, and furnishes highly active catalyst. To test this hypothesis, divalent ruthenium complexes with the formula [(η^5-$C_5Me_nH_{5-n}$)RuCl(cod)] (**1a**–**h**, n = 0–5) were prepared, characterized and their catalytic behavior was compared. Prior to catalytic study, the electron richness on the ruthenium center was compared by means of cyclic voltammetry and IR spectroscopy of [(η^5-$C_5Me_nH_{5-n}$)RuCl$(CO)_2$]. It was revealed that the oxidation potential linearly increased as the substitution number on the cyclopentadienyl ligand increased. In addition, the oxidation potential was affected only by the substitution number, and the substitution position on the ligand exerted no influence. The same trend was revealed also by IR measurement. The catalytic behavior of the complexes was compared in terms of catalytic reaction rate and turnover numbers. With a complex bearing the trisubstituted ligand ($Cp^{1,2,4\text{-}Me3}$)RuCl(cod) (**1d**), the best turnover number of 970 was observed in the cycloaddition

of acetylene and 1,6-diyne **2** bearing iodine substituents on two alkyne terminals (Table 1).

Table 1. Dramatically improved TON of ($Cp^{1,2,4\text{-}Me3}$)RuCl(cod) (**1d**) compared with Cp* analogue **1a**.

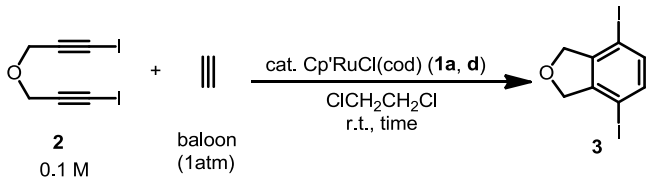

entry	Cp′	catalyst loading [mol%]	time [h]	**3** yield [%]	TON
1		1.0	3	91	46
2		0.5	3	93	110
3		0.1	48	48 (RSM 49%)	970

The initial rate (up to 10% conversion) of the cycloaddition was then compared. The initial rate is found to increase as the number of methyl substituents decreased (Figure 1).

Figure 1. The relationship between the catalytic activities of [Cp′RuCl] complexes and substitution patterns of Cp′ ligand.

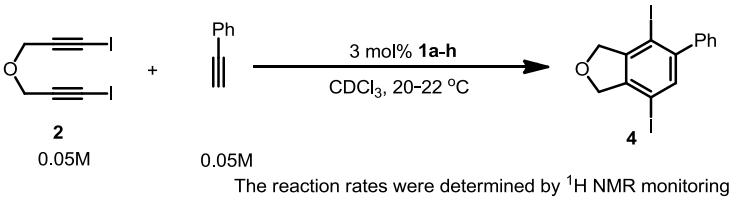

The reaction rates were determined by ^{1}H NMR monitoring.

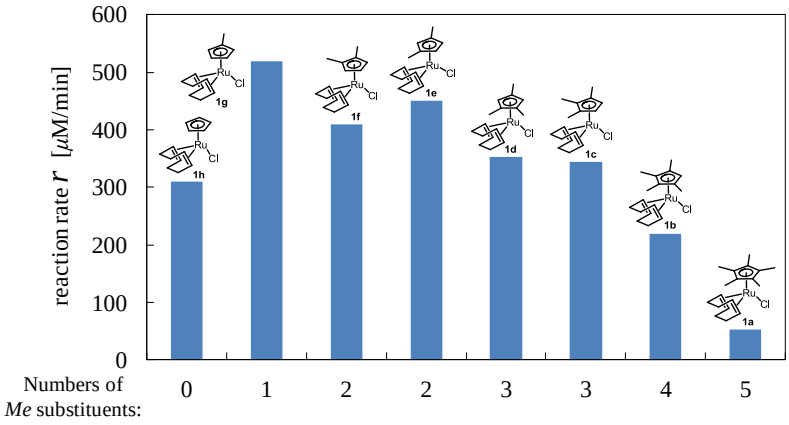

This result indicates two points. First, the steric effect of the cyclopentadienyl ligand has predominant influence on the catalytic activity. Second, the high catalytic efficiency of the complex bearing $Cp^{1,2,4\text{-}Me3}$ ligand originates from the robustness of the complex. The insight into the steric interaction between the cyclopentadienyl ligand and the substrates was obtained by comparing the regioselectivity of [2+2+2] cycloaddition between an unsymmetric 1,6-diyne **5** and a terminal alkyne **6**. The regioselectivity (*ortho* and *meta*) of the cycloaddition product **7** depends on the largest substituent-vacant site on the cyclopentadienyl ligand (Table 2). This result implies that a bulky substituent on the alkyne terminal is accommodated by the vacant site on the ligand.

Table 2. The relationship between the *ortho* selectivity and the maximum size of unsubstituted site on the Cp′ ligand.

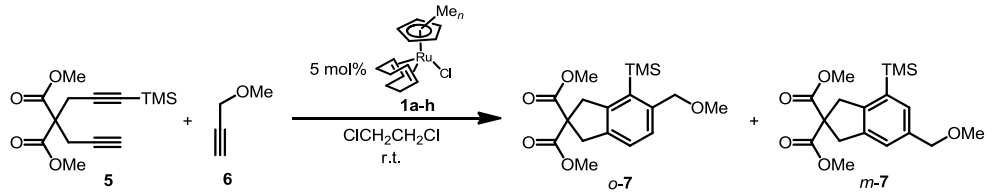

Me$_n$ =	0	1	1	2	2	3	4	5
o-**7** : *m*-**7**	4 : 96	20 : 80	18 : 82	28 : 72	23 : 77	26 : 74	25 : 75	26 : 74

In the chapter 3, the reactivity of the ruthenacyclopentatriene with water was described. This study was initiated by a discovery of the fact that an isolable neutral ruthenacyclopentatriene complex **8** bearing a chloride ligand accepts oxygen and hydrogen atoms on each carbene carbons from a molecule of water with a loss of chloride ligand to afford an η^5-oxapentadienyl complex **9**. It was also predicted that the ruthenium oxapentadienyl complex is an intermediate of previously reported hydrative cyclization of 1,6-diynes, whose mechanism was not fully elucidated. The formation of the oxapentadienyl complex was significantly accelerated in the presence of silver oxide under a neutral condition to give the complex **9** in high yield (Table 3).

Table 3. Reaction of an isolable ruthenacyclopentatriene and water.

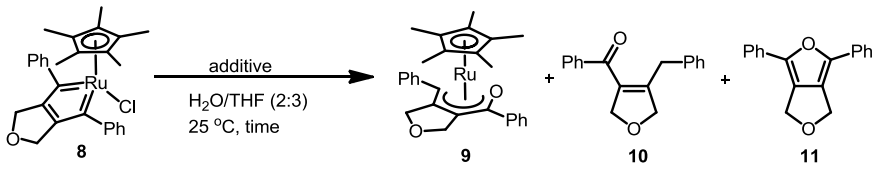

entry	additive	time [h]	conversion [%]	yields[a] **9** / **10** / **11**[%]
1	none	6	84	54 / 5 / 3
2	Ag_2O (0.55 equiv)	2	>99	71 / 0 / 1

[a]Yields were determined by ^1H NMR analysis of crude reaction mixture.

A DFT study in combination with the experimental evidence indicates that the first step of the reaction is the coordination of oxygen atom of the water molecule to the ruthenium center. This is followed by deprotonation to generate a neutral hydroxo complex. The C–O bond formation takes place as 1,2-migration of the hydroxo ligand from the ruthenium center to a carbene carbon (Scheme 2).

Scheme 2. Proposed mechanism for the formation of η^5-oxapentadienyl ruthenium complex from a ruthenacyclopentatriene complex.

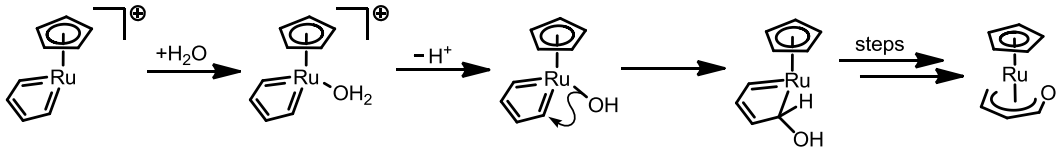

These results indicate that the vacant site on the ruthenium center plays an essential role in the incorporation of oxygen nucleophiles. Thus formed oxapentadienyl complex **9** readily decomposed under an acidic condition to afford an enone product **10**. In addition, the complex in combination with HCl showed a catalytic activity in hydrative cyclization of 1,6-diynes, indicating the intermediacy of the oxapentadienyl complex in the catalytic cycle (Scheme 3).

Scheme 3. Deduced mechanism for ruthenium-catalyzed hydrative cyclization reaction of 1,6-diyne.

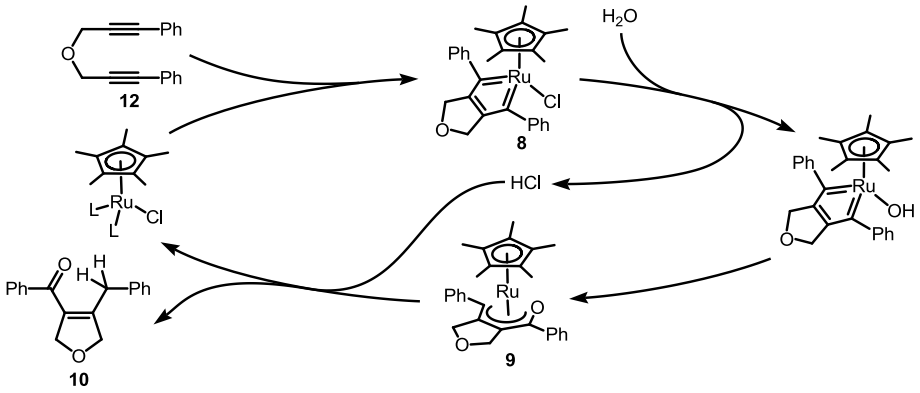

In the chapter 4, development of the ruthenium-catalyzed reductive cyclization of 1,6-diynes that utilizes primary alcohols as hydrogen source was described. When a charge-neutral ruthenacyclopentatriene **8** bearing a chloride ligand on the ruthenium center was treated with methanol in THF, the C_4 unit of the ruthenacycle was reduced to afford a 1,3-diene complex **13**. This result is in contrast with the reaction of alcohol with *in situ*-generated cationic ruthenacyclopentatriene, in which C–O bond formation between the carbene carbon and alcohol oxygen takes place to give a butadienyl ether **14** (Scheme 4).

Scheme 4. Reactivities of ruthenacyclopentatriene with methanol in the presence/absence of silver salt.

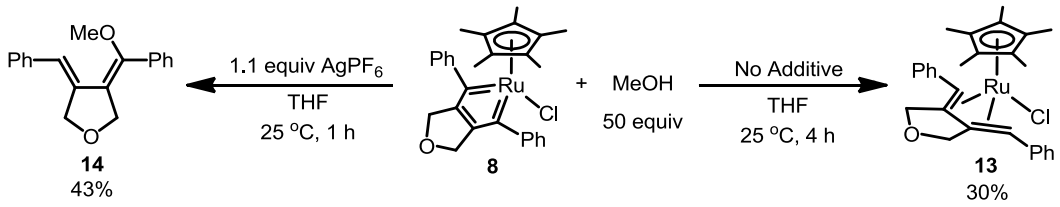

Inspired by this stoichiometric reaction, [Cp*Ru]-catalyzed chemo- and stereoselective reductive cyclization of 1,6-diyne was developed. In the reaction, hydrogen is transferred from methanol to a 1,7-diaryl-1,6-diyne to afford a 1,3-diene in the presence of neutral complex Cp*RuCl(cod) (**1a**) in refluxing THF (Scheme 5).

Scheme 5. Novel [Cp*Ru]-catalyzed transfer-hydrogenation/cyclization of 1,6-diyne.

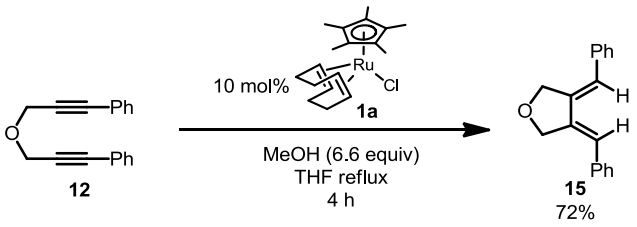

The reaction system exhibited tolerability toward wide range of functional groups including ketone, ester, ether, sulfonamide and C–Br bond. When CD_3OH was used as an alcohol component, equal amount of H and D were newly introduced to the vinyl position of the product. This result indicates that the hydrido intermediate, which can undergo H/D exchange with alcohol hydroxyl proton, is not formed in the reaction system. In addition, rates of the reactions with deuterated methanol isotopologues were compared. As a result, the ratio CH_3OH : CD_3OH : CH_3OD = 1.0 : 1.0 : 0.63 was found. This result indicates that protonic and hydridic hydrogen atoms are transferred from the alcohol to the ruthenacyclopentatriene intermediate in distinctive steps, and the transfer of the protonic hydrogen is the rate-determining step. Based on these points, the mechanism of the transfer hydrogenative cyclization was proposed as in Scheme 6.

Scheme 6. Proposed catalytic cycle of ruthenium-catalyzed reductive cyclization of diynes.

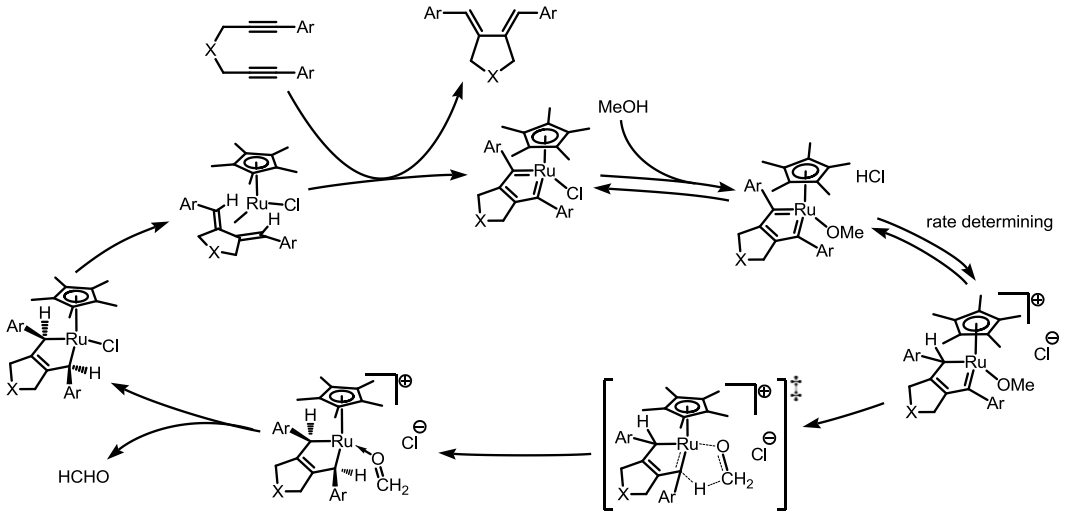

It is proposed that the methoxy group of methanol and chloride in the ruthenacyclopentatriene undergoes ligand exchange to form a methoxo complex by releasing HCl. The proton transfer step can be considered as a protonation of the carbene carbon by this HCl. Then, a hydride is transferred from the methoxo ligand to another carbene carbon to accomplish the hydrogen transfer.

In the chapter 5, novel ruthenium-catalyzed oxygen atom-transfer [2+2+1] cyclization of 1,6-diynes that affords furans were described. The reaction utilizes the coexistence of donor and acceptor nature on the oxygen atom of dimethyl sulfoxide. In the presence of catalytic amount of cationic complex $[CpRu(AN)_3](PF_6)$, 1,7-diaryl-1,6-diyne **12** accepted oxygen atom from the sulfoxide to afford bicyclic furan product **11**.

Scheme 7. Cationic ruthenium complex-catalyzed novel oxygen-transfer/cyclization of diyne to afford a bicyclic furan.

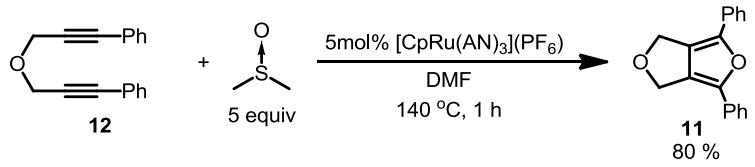

The newly discovered reaction possessed a wide range of functional group tolerability, i.e. ketone, ester, ether, sulfonamide and C–Br bond remained intact. In addition, sulfone group in a substrate did not serve as an oxygen source, while sulfoxide was a good oxidant. Diynes with alkyl terminal substituents were also transformed into corresponding 2,5-dialkyl furans. Mechanistic study was carried out by examining the reactivity of ruthenacyclopentatriene with dimethyl sulfoxide. A charge-neutral ruthenacyclopentatriene complex **8** bearing a chloride ligand did not react with the sulfoxide in THF at 25 °C. On the other hand, the complex immediately reacted with the sulfoxide to afford the furan when the chloride ligand is removed with silver salt. Based on this result, it was proposed that the oxygen-transfer from sulfoxide begins with nucleophilic attack of the sulfoxide to a cationic ruthenacyclopentatriene intermediate. DFT calculation suggested that the oxygen atom of the sulfoxide coordinates to

the cationic ruthenium center, and the sulfide moiety is released from the intermediate to generate an oxocomplex. The oxygen atom undergoes 1,2-migration from the ruthenium center to the carbenic carbon to form a C–O bond. Following isomerization and ring closure of the intermediate were predicted to afford a cationic η^5-furan complex (Scheme 8).

Scheme 8. Proposed mechanisms for ruthenium-catalyzed oxygen-transfer/ cyclization reaction.

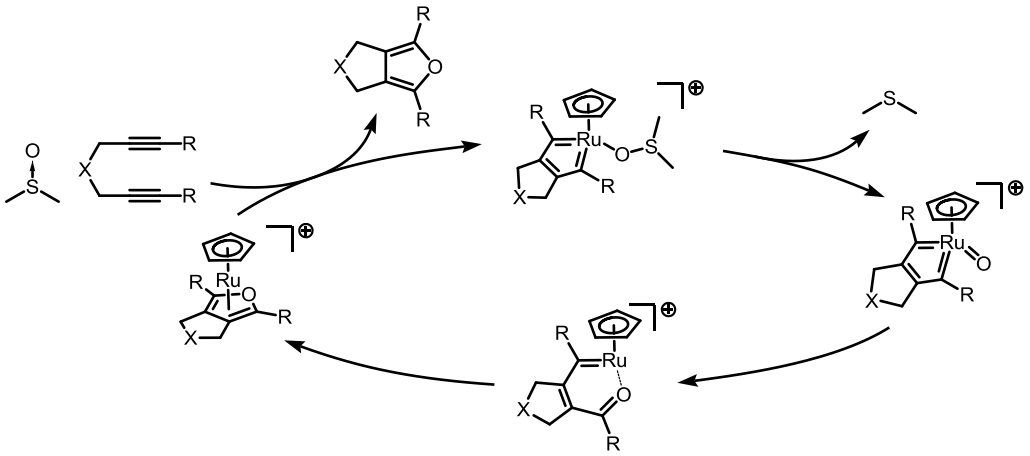

In conclusion, the author shed light on the factors that control the reactivity of ruthenacyclopentadiene complex. It was found that the reactivity of the complex with unsaturated substrate was mainly controlled by the steric effect of substituted cyclopentadienyl ligand. On the other hand, presence/absence of an anionic ligand exerts a major influence on the reactivity of the ruthenacyclopentatriene complex with oxygen nucleophiles. Based on the latter discovery, two novel ruthenium-catalyzed cyclization of 1,6-diynes were developed. In these reactions, atoms are transferred from stable and inexpensive reagents with the aid of the interactions between oxygen nucleophiles and ruthenacyclopentatrienes.

List of Publications

Papers

(1) "Systematic Evaluation of Substituted Cyclopentadienyl Ruthenium Complexes, [(η^5-$C_5Me_nH_{5-n}$)RuCl(cod)], for Catalytic Cycloaddition of Diynes" Yamamoto, Y.; Yamashita, K.; Harada, Y. *Chem. Asian J.* **2010**, *5*, 946–952.

(2) "Activation of a water molecule under mild conditions by ruthenacyclopentatriene: mechanism of hydrative cyclization of diynes" Yamamoto, Y.; Yamashita, K.; Nishiyama, H. *Chem. Commun.* **2011**, *47*, 1556–1558.

(3) "Ruthenium-catalyzed cyclization/transfer hydrogenation of 1,6-diynes: unprecedented mode of alcohol activation *via* metallacyclopentatriene" Yamashita, K.; Nagashima, Y.; Yamamoto, Y.; Nishiyama, H. *Chem. Commun.* **2011**, *47*, 11552–11554.

(4) "Ruthenium-Catalyzed Transfer Oxygenative Cyclization of α,ω-Diynes: Unprecedented [2+2+1] Route to Bicyclic Furans via Ruthenacyclopentatriene" Yamashita, K.; Yamamoto, Y.; Nishiyama, H. (submitted).

Acknowledgement

The author would like to express his grateful acknowledgment to Associate Professor Yoshihiko Yamamoto whose encouragements and helpful suggestions have been indispensible to the completion of the present thesis. The author is also deeply indebted to Professor Hisao Nishiyama and Assistant Professor Jun-ichi Ito for their pertinent and practical advices. It is pleasure to express his appreciation to the colleagues Mr. Yu Harada, Mr. Yuki Nagashima, Mr. Shota Mori and Mr. Kosuke Fukatsu for valuable contributions.

He is very grateful to the Fellowship of the Japan Society for the Promotion of Science for Japanese Junior Scientists during 2011–2012, and the Nagoya University Global COE Program "Elucidation and Design of Materials and Molecular functions" during 2009–2011.

Finally, he would like to express special thanks to Professor Masato Kitamura and Professor Hiroshi Shinokubo for serving on his dissertation committee.

January, 2012

Ken Yamashita